

**RADIOPACITY AND CHEMICAL RESISTANCE OF
ELASTOMER-BARIUM SULPHATE NANOCOMPOSITES**
*WITH SPECIAL REFERENCE TO NATURAL RUBBER,
ETHYLENE PROPYLENE RUBBER AND ISOBUTYLENE ISOPRENE RUBBER*

Thesis submitted to
Cochin University of Science and Technology
in partial fulfilment of the requirements
for the award of the degree of
Doctor of Philosophy

Nisha Nandakumar



Department of Polymer Science and Rubber Technology
Cochin University of Science and Technology
Kochi- 682 022, Kerala, India

December 2013

Radiopacity and Chemical resistance of Elastomer-Barium sulphate nanocomposites
with special reference to Natural Rubber, Ethylene Propylene Rubber and Isobutylene Isoprene Rubber

Ph. D Thesis

Author

Nisha Nandakumar
Department of Polymer Science and Rubber Technology
Cochin University of Science and Technology
Cochin- 682 022, Kerala, India
E-mail: nisha84nandu@gmail.com

Guide:

Dr. Philip Kurian
Professor
Department of Polymer Science and Rubber Technology
Cochin University of Science and Technology
Cochin- 682 022, Kerala, India
E-mail: pkurian@cusat.ac.in

December 2013



Department of Polymer Science and Rubber Technology
Cochin University of Science and Technology

Cochin- 682 022, Kerala, India

#

Dr. Philip Kurian
Professor

Mob: +91 9447662790
E-mail: pkurian@cusat.ac.in

Certificate

This is to certify that this thesis entitled **“Radiopacity and Chemical resistance of Elastomer-Barium sulphate nanocomposites with Special Reference to Natural Rubber, Ethylene Propylene Rubber and Isobutylene Isoprene Rubber”** is a report of the original work carried out by **Mrs. Nisha Nandakumar** under my supervision and guidance in the Department of Polymer Science and Rubber Technology, Cochin University of Science and Technology, Cochin-22. No part of the work reported in this thesis has been presented for any other degree from any other institution.

Cochin-22
11/12/13

Dr. Philip Kurian
(Supervising Guide)

Declaration

I hereby declare that the thesis entitled **“Radiopacity and Chemical resistance of Elastomer-Barium sulphate nanocomposites with special reference to Natural Rubber, Ethylene Propylene Rubber and Isobutylene Isoprene Rubber”** is the original work carried out by me under the supervision of **Prof. Philip Kurian**, Department of Polymer Science and Rubber Technology, Cochin University of Science and Technology, Cochin-22 and has never been included in any other thesis submitted previously for the award of any degree.

Cochin – 22
11/12/2013

Nisha Nandakumar

Dedicated to
My Parents, Teachers, Husband Jayesh
& Daughter Sreegowri

Acknowledgement

I would like to thank all those who were material in this journey at this great moment of realisation of my Ph.D thesis. First and foremost I would like to bow before god almighty for having granted me with wisdom, health and strength to undertake this research task and enabling me to its completion.

I would like to express my profound debt of gratitude to my supervising guide Prof. Philip Kurian for proper guidance and freedom throughout my research work,

All faculty members of the Institute have been very kind enough to extend their help at various phases of this research, whenever I approached them, and I do hereby acknowledge all of them. I am grateful to the Head of the department Prof. Sunil K Narayanan Kutty, former Heads of the department, Prof. Eby Thomas Thachil, and Prof. Thomas Kurian for giving necessary facilities and support during the research.

I would like to express my sincere thanks to Prof. Rani Joseph for her support, Prof. K. E George and Jaya Teacher for the whole hearted cooperation throughout my research work, I express my gratitude to all the teaching and non-teaching staff of Department of Polymer Science & Rubber Technology for their support during these years.

I am grateful to STIC, and friends at DOP and DAC CUSAT for assisting me in characterisation. Dr. Sobhanadevi and Dr. Jaydeep needs a special mention for all the interest they have invested in my research and for their enthusiastic support in X-ray analysis at Medical college tripunithura & TVM, Dr. Rajeev and Sobha teacher for introducing me into this possibility of research and Brindha for TEM studies.

I am very thankful to my dear friend Sona for being with me to share my pains and her concern during the days in Athulya hostel and in my life. At this

moment I remember Uma and Laina for their love and caring . There are no words to express my gratitude to Preetha teacher and Dennymol teacher for their sincere guidance, timely help and their motherly affection, without which I would not have completed my Ph.D. They have always lifted me up whenever I was in trouble and felt desperate.

It is a pleasure to thank all those who made this thesis possible, my seniors and colleagues Abhilash.G, Jabin teacher, Sreejesh for their friendship, Dr.Pramila devi, Dr. Vidya Francis, Dr.Vidya.G and Dr. Nimmi K P for their valuable help, support, motivation, love and caring. I will cherish the days spent with Dr.Saisy, Asha, Remya, Aiswarya, Bindhu teacher, Reshmi chechi. Readiness of Nishad and Teena in rendering me a helping hand without any hesitation despite their busy schedule is appreciable. I thank Neena, Neethu, Bhagyesh, for their sincere friendship and support extended to me. At this moment. I thank all my friends in Athulya hostel for their help and love.

I am immensely thankful to Renju chechi and family for their love, motivation and care. I great fully acknowledge Bipin sir, for his valuable help, support, encouragement, advices and suggestions and for his presence that has always acted as a strong pillar of support for me when ever I used to feel depressed at each and many stages of my work. I am also thankful to Sinto chettan, Suma teacher, Zeena chechi and Jenish Paul for their care, love and support especially during their stay in this department. I am grateful to Dr. Anna Dilfi K F for her remarkable help and company. I extend my gratitude to Manoj Sir, Jolly Sir, Neena George, Treasa Sunitha George, Newly chechi, Leny teacher, Muralidharan M A, Shadhiya M A for her timely suggestions and strong support, July Chechi, for her friendship. I am also thankful to Sreedevi teacher, Midhun, Dhanya chechi for her friendship ,Rohit, Tinu and Sreehari for their assistance during mixing schedules.

Help rendered by Ajalesh during different stages of my work is appreciable and his timely suggestions have helped me manage schedule through a wiser route.

I gratefully acknowledge Mr.Abhilash Kuruveyil of Chemlok and Mr.Sarath and Santhosh sir, Apollo tyres in helping me procure materials of research without delay and for the valuable help during the analysis of samples. I would like to thank Ansu chechi, for her assistance in work through air.

I owe a lot to my parents, who encouraged and helped me at every stage of my personal and academic life, and longed to see this achievement come true .I would like to thank them for their love, prayers, care, patience and support, without which this thesis would not be a reality. I am grateful to devutti for her love, support and for being my best friend EVER and only with tears could I remember the hard times that I had sailed through with their assistance. Thanks to amma for she kept my lust lightened throughout my life and for all the pains she went through while she served as a strong pillar of support. I would have been a big zero without the support of my achan and amma. I thank Amma, jayachechi, manojetan, sruthy and swathy, for their support, love and prayers. Especially muthachan and ammuma for their prayers and are the real reason for me being at this juncture of my life.

To jayesh for being a supportive, caring husband whose support made me reach this point. I am also thankful to my little gowri for being a demandless daughter of mine and I just thank them with all my heart for all their inconveniences created during my research schedule and I am still not sure if I have done justice to them.

Finally, I would like to thank all those who inspired, guided and accompanied me during the course of my life.....

Nisha Nandakumar

Preface

The Human race of our century is in gluttonous search for novel engineering products which led to a skyrocketed progress in research and fabrication of filled polymers. Recently, a big window has been opened up for speciality polymers especially elastomers with promising properties. Among the many reasons why rubbers are widely used in the process industries, three are considered as important. Firstly, rubbers operate in a variety of environments and possess usable ranges of deformity and durability and can be exploited through suitable and more or less conventional equipment design principles. Secondly, rubber is an eminently suitable construction material for protection against corrosion in the chemical plant and equipment against various corrosive chemicals as, acids and alkalies and if property tailored, can shield ionising radiations as X-rays and gamma rays in medical industry, with minimum maintenance lower down time, negligible corrosion and a preferred choice for aggressive corroding and ionising environment. Thirdly, rubber can readily and hastily, and at a relatively lower cost, be converted into serviceable products, having intricate shapes and dimensions. In a century's gap, large employment of flexible polymer materials in the different segments of industry has stimulated the development of new materials with special properties, which paved its way to the synthesis of various nanoscale materials. At nano scale, one makes an entry into a world where multidisciplinary sciences meet and utilises the previously unapproached infinitesimal length scale, having dimension which measure upto one billionth of a meter, to create novel properties. The nano fillers augment the elastomers properties in an astonishing fashion due to their multifunctional nature and unprecedented properties have been exhibited by these polymer-nanocomposites just to beat the shortcomings of traditional micro composites. The current research aims to investigate the possibility of using synthesised nano barium sulphate for fabricating elastomer-based nanocomposites and thereby imparting several properties to the rubber. In this thesis, nano materials, their synthesis, structure, properties and applications are studied. The properties of barium sulphate like chemical resistance and radiopacity have been utilized in the present study and is imparted to the elastomers by preparing composites.

The thesis is divided into nine chapters.

Chapter 1 gives a comprehensive introduction and literature review pertaining to rubber composites, nanocomposites and nanofillers. It also includes the scope and objectives of the present work

Chapter 2 gives details of materials used in the present work and the experimental techniques employed for the preparation and characterization of the Rubber nanocomposites. The instruments used are also discussed.

Chapter 3 deals with the wet chemical preparation of nano barium sulphate with barium chloride and ammonium sulphate as precursors using polyvinyl alcohol as the dispersing medium. The modifications of the powders were carried out using stearic acid to impart surface activity to otherwise inert filler. Synthesized powders were characterized. The particle size of the powder obtained was in the range 23-25nm with spherical morphology. The powders had good radiopacity, opacity being higher for modified nano powders.

Chapter 4 is divided into two parts:

Part a: deals with performance of unmodified nano barium sulphate (BN) and modified nano barium sulphate (MBN) in natural rubber. The rubber nanocomposites were prepared by mixing on a two-roll mill. In this chapter cure characteristics, physico-mechanical properties, solvent sorption, thermal analysis and phase morphology of the rubber nanocomposites (RNC's) are included.

Part b: deals with performance of NR hybrid composites filled with modified nano barium sulphate and carbon black. The rubber nanocomposites were prepared by mill mixing. Synergistic effect of carbon and modified nano barium sulphate is investigated in NR. In this chapter cure characteristics, physico-mechanical properties, solvent sorption, thermal analysis and phase morphology of the hybrid rubber nanocomposites (RNC's) are included. The morphologies were investigated using scanning electron microscopy (SEM) and atomic force microscopy (AFM).

Chapter 5 is also divided into two parts:

Part a: deals with EPDM nanocomposites. The effect of modified and unmodified nano barium sulphate loading on cure characteristics, physico-mechanical properties, solvent sorption, thermal analysis and phase morphology are also

included. The effects of filler loading on mechanical properties and thermal stability were investigated.

Part b: deals with performance of EPDM hybrid composites filled with modified nano (MBN) barium sulphate and carbon black. The study aimed at fabricating hybrid composites with 40phr carbon black-MBN (varied) system with comparable properties to that of 50 phr carbon black, which enables replacement of 10 phr carbon black in EPDM with modified nano barium sulphate. The synergistic effect due to dual filler networks was researched.

Chapter 6 deals with the preparation of IIR based composites with modified and unmodified nano barium sulphate. The effects of loading on cure characteristics, physico-mechanical properties, solvent sorption, thermal analysis and phase morphology were studied. The effects of filler loading on mechanical properties and thermal stability were investigated. Carbon black filled composites were also prepared and studied and the properties showed only a marginal increase. The morphology was investigated using atomic force microscopy (AFM).

Chapter 7 deals with degradation and durability studies of elastomeric composites containing nano barium sulphate on exposure to aqueous sulphuric acid. This chapter is divided into three sections.

Section-a deals with study regarding the damage caused by acid to natural rubber gum vulcanizates, filled vulcanizates containing modified nano barium sulphate and hybrid system containing nano barium sulphate and carbon black. Measurements of tensile strength and tear strength and crosslink densities have been made in order to quantitatively estimate the extent of degradation at various stages of acid attack. The fracture surfaces of failed tensile and tear specimens have been investigated by means of SEM, both before and after acid ageing and attempts have been made to correlate the changes in the surface topography with the extent of fall in mechanical properties as a result of acid corrosion. The weight changes associated with acid sorption was studied with rubber lined metal inserts (prepared by adhering rubber to metal using chemlok 220 cover coat and 205 primer) and rubber samples by immersion method. From several concentration of acids 50 % H_2SO_4 was selected as medium and data pertaining to its behaviour over 150 hrs was noted and MBN filled RNC's exceed commercial barium sulphate filled and black filled composites in resisting acid corrosion as seen by retention in physical properties.

Section b: deals with the time dependent degradation of EPDM RNC's and impact of degradation was accounted in terms of retention of physical properties, weight change measurements with rubber samples and Mild steel metal inserts (prepared by adhering rubber to metal using chemlok 238 cover coat and 205 primer). The changes occurring in the composites were monitored over 15 weeks and 60 % H_2SO_4 was used and the chemical changes were traced via FTIR analysis of aged samples and the mechanism of attack proposed for clarifying the mode of hydrolytic attack. Morphology was investigated using SEM.

Section c: explains the acid degradation of IIR RNC's. Its inherent resistance to acids makes it suitable to be used in higher concentrations of acids and the study of resistance to 75 % H_2SO_4 was discussed in detail in the MBN filled RNC's to assess better acid resistance of IIR composites.

Chapter 8 is divided into three sections and these deals with the radiopacity studies on NR, EPDM and IIR composites and application of these elastomeric composites in the field of clinical X-ray analysis, where great attention is needed for facilities that shield operating personals and patients from unwanted radiation exposure. The X-ray generated by a general medical tube voltage is in the range starting from 40Kev, so importantly; this is the regular energy region of X-ray used for medical diagnosis. A series of nano barium sulphate-rubber composites have been produced on a laboratory scale, and their X-ray shielding power measured using a clinical X-ray. The X-ray radiographs were compared with that of composites filled with commercial precipitated barium sulphate and also the influence of nano modification on opacity analysed. The radiographic image was obtained with varying sample thicknesses. X-ray shielding ability of the prepared composites was also studied at different applied voltage (between 40-100 KeV) and exposure times of X-ray machine at 5mAs and conclusions are reached. The optical density measurements and hence the calculated attenuation coefficients supported the radiographic analyses

Part a: discusses the X-ray studies related to RCs of NR.

Part b: discusses the X-ray studies related to RCs of EPDM.

Part c: discusses the X-ray studies related to RCs of IIR.

Chapter 9 is the summary and conclusion and, future outlook of the study.

Contents

Chapter 1

INTRODUCTION	01 - 56
1.1	Introduction-----01
1.2	Elastomers -----05
1.3	Building blocks in elastomer composite fabrication -----10
1.3.1	Elastomers as matrix ----- 10
1.3.1.1	Natural Rubber ----- 10
1.3.1.2	Butyl Rubber (IIR) ----- 13
1.3.1.3	Ethylene Propylene Rubbers (EPM and EPDM)----- 14
1.3.2	Fillers ----- 15
1.3.2.1	Particle size and its role in reinforcement----- 19
1.3.2.2	The Particle structure ----- 20
1.3.2.3	Surface activity and filler performances----- 21
1.3.2.4	Surface area and reinforcement----- 22
1.4	Nanotechnology -----22
1.4.1	Synthesis of nano-scale materials----- 24
1.4.2	Diversity in Morphologies of nano materials ----- 27
1.4.3	Nanocomposites----- 28
1.5	State of the art research - elastomer nano composites -----30
1.6	Barium sulphate-----34
1.6.1	Uses of barium sulphate----- 36
1.6.2	Surface activity of barium sulphate:----- 38
1.7	Scope and objectives of the present work -----40
	References -----44

Chapter 2

MATERIALS AND EXPERIMENTAL METHODS	57 - 81
2.1	Materials-----57
2.1.1	Elastomers----- 57
2.1.2	Fillers used ----- 58
2.1.3	Accelerators used ----- 58
2.1.4	Plasticizers used ----- 59
2.1.5	Antioxidants ----- 60
2.1.6	Other compounding ingredients used ----- 60
2.1.7	Solvents used ----- 61
2.2	Experimental -----62
2.2.1	Mixing and homogenization of the compound----- 62
2.2.2	Cure characteristics ----- 62
2.2.3	Filler dispersion ----- 64
2.2.4	Strain-sweep studies ----- 65
2.2.5	Vulcanization ----- 66

2.3	Characterisation methods	66
2.3.1	Physical testing	66
2.3.2	Hot air aging studies	68
2.3.3	Solvent sorption experiments	68
2.3.4	X-ray diffraction analysis	70
2.3.5	Infrared Spectroscopy	71
2.3.6	Bulk density	71
2.3.7	BET adsorption	72
2.3.8	Thermogravimetric analysis	72
2.3.9	Differential scanning calorimetry(DSC)	72
2.3.10	Scanning electron microscopy (SEM)	73
2.3.11	Transmission electron microscopy	74
2.3.12	Atomic Force Microscopy	74
2.3.13	Acid immersion Tests	74
2.3.14	Radiopacity studies	77
	2.3.14.1 Optical density measurements	78
	2.3.14.2 Attenuation coefficient	78
	2.3.14.3 Half-value layer	79
	References	80

Chapter 3

PREPARATION, SURFACE MODIFICATION AND CHARACTERISATION OF NANO BARIUM

SULPHATE -----83 - 108

3.1	Introduction	84
3.2	Experimental	89
3.2.1	Chemicals	89
3.2.2	Preparation of nano barium sulphate in polyvinyl alcohol	90
3.2.3	Modification of nano barium sulphate	91
3.3	Characterisation	91
3.4	Results and Discussion	92
3.4.1	Bulk density	92
3.4.2	BET surface area	93
3.4.3	X-Ray Diffraction (XRD)	93
	3.4.3.1 Influence of calcination temperature on XRD	94
	3.4.3.2 Influence of dispersing medium (PVA w/v) on XRD	95
3.4.4	Fourier transform infrared resonance-(FTIR) spectroscopic studies	97
3.4.5	Studies using scanning electron microscopy (SEM)	98
3.4.6	Studies using transmission electron microscopy(TEM)	100
3.4.7	Radiopacity studies	100
3.4.8	UV-visible spectroscopy	101
3.4.9	Thermo gravimetric analysis (TGA)	102
3.4.10	DSC curves	104
3.5	Conclusions	104
	References	106

Chapter 4

NATURAL RUBBER -BARIUM SULPHATE

NANOCOMPOSITES ----- 109 - 156

Part-a

NATURAL RUBBER BASED NANOCOMPOSITES: NANO BARIUM SULPHATE/ MODIFIED NANO BARIUM SULPHATE FILLED RNCs

4a.1	Natural rubber barium sulphate nanocomposites-----	111
4a.1.1	Preparation of rubber nanocomposites-----	111
4a.1.2	Cure characteristics-----	112
4a.1.3	Cure kinetics-----	114
4a.1.4	Filler dispersion in the RNCs-----	116
4a.1.5	Dynamic properties measured in strain sweep for uncured compounds-----	118
4a.1.6	Mechanical properties of RNCs-----	119
4a.1.7	Morphology of fractured surface, SEM images-----	123
4a.1.8	Thermal stability of NR-MBN nanocomposites-----	124
4a.1.9	Crosslink density and swelling studies-----	127
	References-----	131

Part-b

SYNERGISTIC EFFECT OF CARBON BLACK FILLED NATURAL RUBBER-MODIFIED BARIUM SULPHATE HYBRID RNCs

4b.1	Natural rubber-carbonblack- modified nanobarium sulphate hybrid nano composites.-----	135
4b.1.1	Preparation of nanocomposites-----	135
4b.1.2	Cure characteristics-----	136
4b.1.3	Filler dispersion in the RNCs-----	138
4b.2	Dynamic properties measured in Strain sweep for uncured and cured compounds-----	140
4b.3	Mechanical properties-----	143
4b.4	Morphology of fracture surface: SEM and AFM studies-----	146
4b.5	Thermal studies: Thermal ageing and Thermogravimetric analysis-----	148
4b.5.1	Thermal Ageing-----	148
4b.5.2	Thermogravimetric analysis-----	150
4b.6	Crosslink density and swelling studies-----	152
	References-----	156

Chapter 5

ETHYLENE PROPYLENE DIENE RUBBER -

BARIUM SULPHATE NANOCOMPOSITES----- 157 - 206

Part-a

EPDM-BASED NANO COMPOSITES: BARIUM SULPHATE (BN)/MODIFIED NANO BARIUM SULPHATE (MBN) FILLED RNCs

5a.1	EPDM-Barium sulphate nanocomposites-----	158
------	--	-----

5a.1.1	Preparation of rubber nanocomposites	158
5a.1.2	Cure characteristics	160
5a.1.3	Cure kinetics	162
5a.1.4	Filler dispersion in the RNCs	164
5a.1.5	Mechanical properties of RNCs.	165
5a.1.6	Morphology of Fractured surface	169
5a.1.7	Thermal stability of EPDM-MBN nanocomposites.	170
5a.1.8	Dynamic properties measured in Strain sweep for EPDM-MBN composites: green and cured compounds	172
5a.1.9	Crosslinkdensity and swelling studies	173
	Reference	178

Part-b

SYNERGISTIC EFFECT OF CARBON BLACK FILLED EPDM-MODIFIED NANO BARIUM SULPHATE (MBN) HYBRID RNCs

5b.1	Ethylene propylene diene rubber-carbon black-modified nano barium sulphate hybrid nanocomposites.	182
5b.1.1	Preparation of nanocomposites	182
5b.1.2	Cure characteristics	183
5b.1.3	Filler dispersion in the RNCs	185
5b.2	Dynamic properties measured in strain sweep for uncured and cured compounds	187
5b.3	Mechanical properties	188
5b.4	Morphological studies, SEM and AFM images	192
5b.5	Thermal studies-Thermal ageing and TGA	194
5b.5.1	Thermal Ageing	194
5b.5.2	Thermogravimetric analysis	197
5b.6	Cross link density and swelling studies	199
	References	204

Chapter 6

ISOBUTYLENE ISOPRENE RUBBER - BARIUM SULPHATE NANOCOMPOSITES AND EFFECT OF NANOFILLER IN HAF-N330 FILLED IIR-HYBRID NANOCOMPOSITES ----- 207 - 228

6.1	IIR-Barium sulphate nanocomposites	209
6.1.1	Preparation of rubber nanocomposites	209
6.1.2	Cure characteristics	211
6.1.3	Mechanical properties of IIR-MBN RNCs and Hybrid RNCs.	212
6.1.3.1	Mechanical properties of IIR-BN/MBN RNCs.	212
6.1.3.2	Mechanical properties of IIR-CB-MBN hybrid RNCs.	215
6.1.4	Thermal studies on hybrid systems: Thermal aging and TGA-analysis	217
6.1.4.1	Thermal Aging	217
6.1.4.2	TGA-analysis of IIR-MBN-CB hybrid nanocomposites	220

6.1.5 Cross link density and swelling studies of IIR-CB-MBN hybrid composites -----	223
6.1.6 Morphology of IIR-MBN-RNCs and IIR-CB-MBN hybrid RNCs-----	225
References-----	228

Chapter 7

STUDIES ON SULPHURIC ACID CORROSION OF RUBBER - BARIUM SULPHATE

NANOCOMPOSITES ----- 229 - 287

Section-a

**CORROSION OF NATURAL RUBBER BASED RNCs:
NATURAL RUBBER BARIUM SULPHATE COMPOSITES AND
THEIR CORROSION IN SULPHURIC ACID**

7a.1 Natural rubber based composites -----	233
7a.1.1 Preparation of NR based composites-----	233
7a.1.2 Mechanical properties: Effect of acid concentration-----	233
7a.1.3 Swelling test -----	234
7a.1.4 Retention of tensile and tear strength after acid immersion -----	238
7a.1.5 Tests for acid resistance using rubber sheets adhered to Mild steel samples -----	242
7a.1.6 Interpretation of acid corrosion in terms of surface relief features of RNCs as observed in a SEM-----	244

Section-b

**CORROSION OF EPDM BASED RNCs:
ETHYLENE PROPYLENE DIENE RUBBER-BARIUM SULPHATE
COMPOSITES AND THEIR CORROSION IN SULPHURIC ACID.**

7b.1 EPDM based composites -----	251
7b.1.1 Preparation of EPDM based composites-----	251
7b.1.2 Mechanical properties: Effect of acid concentration: -----	251
7b.1.3 Swelling test -----	252
7b.1.4 Studies on the influence of acidic environment on physical properties of MBN RNCs.-----	257
7b.1.5 Effect of 60% sulphuric acid on crosslink density and mechanical properties of composites MBN ₀ and MBN ₁₅ -----	259
7b.1.6 FTIR analysis: Emergence of neo-functionalities on aging upto 15 weeks as evidenced from Infrared spectroscopy -----	265
7b.1.7 Proposal of a plausible mechanism for attack of acid on EPDM, supported by IR and mechanical studies -----	267
7b.1.8 Interpretation of acid corrosion in terms of surface relief features of MBN RNCs as observed in SEM-----	274

Section -c

CORROSION OF IIR BASED RNCs:

ISOBUTYLENE ISOPRENE RUBBER-BARIUM SULPHATE COMPOSITES AND THEIR CORROSION IN SULPHURIC ACID	
7c.1	Isobutylene Isoprene rubber based composites ----- 277
7c.1.1	Preparation of IIR based composites ----- 277
7c.1.2	Mechanical properties: Effect of acid concentration: ----- 277
7c.1.3	Immersion tests ----- 278
7c.1.4	Retention in mechanical properties on acid aging ----- 282
7c.1.5	Influence of acid degradation on composite morphology ----- 284
References	----- 286

Chapter 8

APPLICATION OF ELASTOMER - BARIUM SULPHATE COMPOSITES AS RADIOPAQUE POLYMERS

EVALUATION OF RADIOPACITY OF ELASTOMER-BARIUM SULPHATE COMPOSITES OF NR, EPDM AND IIR USING CLINICAL X-RAYS --- 289 - 334	
8.1	Introduction----- 290
8.2	Radiopaque polymers & radiopacity: The role of polymers in X-ray shielding ----- 292
8.3	Radiopacity and radiopacifiers----- 293
8.4	State-of-the art research----- 294

Part-a

STUDIES ON THE EFFECT OF MBN AND BN ON THE X-RAY OPACITY OF NATURAL RUBBER	
8a.1	Experimental Methods ----- 299
8a.1.1	Materials used. ----- 299
8a.1.2	Radiopacity Studies----- 299
8a.1.2.1	Determination of Optical density----- 299
8a.1.2.2	Determination of attenuation coefficient ----- 299
8a.1.2.3	Determination of Half-value-layer (HVL)----- 300
8a.1.3	Preparation of NR-opacifier composites. ----- 300
8a.2	Results and discussion ----- 302
8a.2.1	X-ray Analysis of Natural rubber based radiopaque compound. ---- 302
8a.2.1.1	X-ray radiographs of samples at constant potential. ----- 302
8a.2.1.2	Effect of thickness of rubber samples on visibility under X-rays. ----- 303
8a.2.1.3	Effect of changing applied voltage on visibility of the composites----- 304
8a.2.2	Optical density and linear attenuation coefficient with filler loading 305
8a.2.3	Physical properties ----- 307
References	----- 310

Part-b

**STUDIES ON THE EFFECT OF MBN AND BN ON THE X-RAY
OPACITY OF ETHYLENE PROPYLENE DIENE RUBBER.**

8.b.1	Experimental -----	314
8.b.1.1	Materials Used-----	314
8.b.1.2	Preparation of EPDM -opacifier composites. -----	314
8.b.2	Results and discussion -----	316
8b.2.1	X-ray Analysis of Ethylene Propylene Diene rubber based radiopaque compound. -----	316
8b.2.1.1	X-ray radiographs of samples at constant potential. -----	316
8b.2.1.2	The effect of sample thickness -----	317
8b.2.1.3	Effect of changing applied voltage on visibility of the EPDM composites.-----	317
8b.2.2	Optical density(OD) and linear attenuation coefficient (μ)of the composites -----	318
8b.2.3	Physical property: -----	320
References	-----	323

Part-c

**STUDIES ON THE EFFECT OF MBN AND BN ON THE X-RAY
OPACITY OF IIR COMPOSITES.**

8.c.1	Experimental -----	324
8.c.1.1	Materials Used-----	324
8.c.1.2	Preparation of IIR-opacifier composites.-----	325
8c.2	Results and discussion.-----	327
8c.2.1	X-ray Analysis of IIR based radiopaque compound. -----	327
8c.2.1.1	X-ray radiographs of samples at constant potential -----	327
8c.2.1.2	The effect of sample thickness -----	328
8c.2.1.3	Effect of changing applied voltage on visibility of the composites -----	328
8c.2.2	Optical density(OD) and linear attenuation coefficient (μ)of the composites -----	329
8c.2.3	Physical Properties-----	331
References	-----	334

Chapter 9

SUMMARY AND CONCLUSIONS ----- 335 - 342

LIST OF ABBREVIATIONS

LIST OF PUBLICATIONS

Chapter 1

INTRODUCTION

- 1.1 *Introduction*
- 1.2 *Elastomers*
- 1.3 *Building blocks in Elastomer composite fabrication.*
- 1.4 *Nanotechnology*
- 1.5 *State-of-the art research - Elastomer nano composites*
- 1.6 *Barium sulphate*
- 1.7 *Scope and Objectives of the present work*

1.1 Introduction

Discoveries and inventions have led to the progress of society towards the blue, i.e. a tremendous progress from river valley civilizations to the so called ‘nano world’ of the present century. Spinning of continuous yarns is most likely the important development of mankind, next to discovery of fire and invention of the wheel, which enabled him to continue to exist in and outside the tropical weather zones and extend his reign across the earth’s surface. Natural resources as cotton, flax and jute have been exceedingly used in designing fabrics, soon resulting in the first composites; i.e. the straw reinforced walls, and bows and chariots made of layers of wood, animal bones and horns. More tough materials as wood and metal were to soon replace these old-fashioned composites, which finally paved its way into natural and synthetic polymer based composites.

Advancements in the field of materials science and technology have given birth to fascinating and brilliant materials known as composites. With the initiation of the Composite era, things changed and inventory started to be concentrating in and around novel composites with enchanting properties. The demand of speckled species of composites in various facets of industry and society opened up a new door to the world of composites. A true renewal started with use of composite structures for many technical solutions during the second half of the 20th century. Apart from solely using these materials as insulators and

radar-domes, using composites to improve the structural performance of spacecraft and military aircraft became popular in the last two decades of the previous century. Nowadays the composite world has grown tremendously that, cost reduction during manufacturing and operation are the main technology drivers with the aim of popularising them into commoners of the society. Latest development is the use of composites to protect man against fire, radiations and their aftermaths and a tendency to a more eco-friendly design, leading to the return of natural fibers into the composite technology and utilisation of nanofilled composites for novel performances.

To be simple with explanation, a composite is any material made of more than a single component. Composite materials are solid multiphase materials, formed through the permutation of materials with different structural, physical and chemical properties. This makes composites different from the other multi component systems such as blends and alloys. Composites are widely used in such diverse applications as transportation, construction and consumer goods [1]. Composites offer dramatic combinations of component material properties such as weight, strength, stiffness, permeability, electrical and optical properties that is difficult to attain disjointedly by individual components. A composite material can be custom tailored to have specific properties that will meet unique desires. The optimum design of composite component materials and manufacturing process to meet the target properties for particular engineering applications is vital.

The need of composites takes its birth from the fact that polymers on its own are ineffective in providing all the superior properties like strength, low thermal coefficients, resistance to shock loads, resistance to thermal, chemical degradation and radiation etc. All these drawbacks can be remedied by incorporation of a new range of additives into it. Fillers have important roles in modifying properties of various polymers. Mineral fillers, metals and fibers have been compounded into rubbers, and the effect of fillers on properties of the polymers depends on their concentration, their particle size and shape as well on

their interaction with matrix. Such a combination is referred to as composite. A composite material can provide superior and unique mechanical and physical properties because it combines the most desirable properties of its constituents while suppressing their least desirable properties. The Composites are combination of two materials, in which one of the material, called the reinforcing phase, is in the form of fibers, sheets or particles and is embedded in the other material called the matrix phase. The matrix gives the composites their shape, surface appearance, environmental tolerance and overall durability while the reinforcement carries most of the structural loads thus giving macroscopic stiffness and strength and characteristic properties [2]. Typically the filler phase is embedded in the host matrix phase to make a composite which has properties a long way from either of the phases alone. Several matrices are available at present to suit as matrices to filled composites and polymers often have advantages over other materials such as metals and ceramics. They are widely used in various technical applications because of their unique advantages such as ease of production, light weight and ductility; however they have lower mechanical, modulus and strength properties compared to that of metals and ceramics. The commercial importance of polymers and their increasing use, results in the continuous demand for improvement in their properties to meet the necessary conditions. By means of the composite technology, polymer properties are enhanced, whilst maintaining their light weight and ductile nature [3].

The composites are classified into various classes based on the various desirous factors as: nature of matrix, their occurrences, size of fillers present and structural components as summarised in the flow diagram Fig.1.1

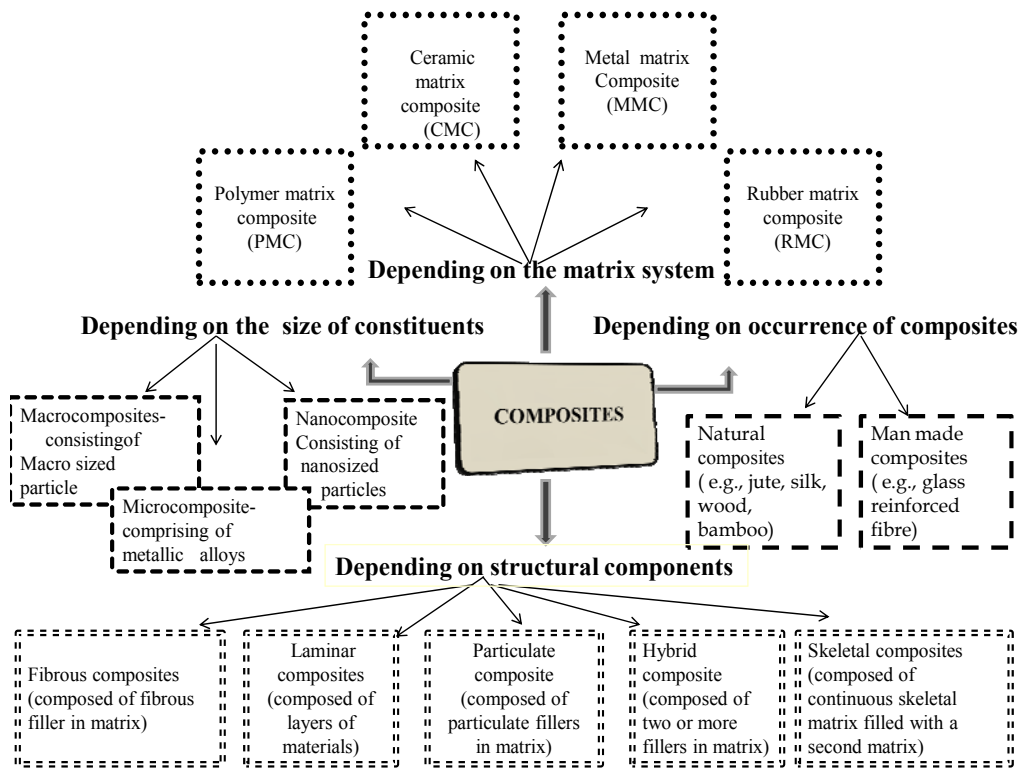


Figure1.1 Classification of composites

Nowadays, the application of polymer composites in industry has become state of the art. Polymer composites with enhanced mechanical, thermal, barrier and fire retardancy properties are widely used in very large quantities in diverse applications. However by the application of conventional fillers such as talc, calcium carbonate, fibers, etc, it often requires to use a large amount of filler in the polymer matrix to have significant improvements in the composite properties which may cause brittleness or loss of opacity [4]. The aspect ratio of the filler is very important and crucial for many properties in composite such as electrical, mechanical and thermal properties [5-8]. Polymer composites with the high aspect ratio of nano-fillers such as platelet clays, carbon nanotubes and nanofibers are receiving considerable attention due to their unique multifunctional and highly enhanced properties. Combination of filler nanoscale dimension and high aspect ratio with its nanoscale dispersion within polymer

matrix leads to the important improvements in the polymer properties at very low filler volume fractions. The final properties of reinforced polymers or the so called composites are influenced by the nature, properties and content of constituents, dimensions of components and micro structure of composite and interfacial interactions between continuous and dispersed phase. The efficiency of property improvements depends strongly on the properties of the filler, the adhesion between matrix and filler and especially as mentioned earlier on the aspect ratio of the filler. As a result of lower filler loading, the macroscopic homogeneity is well retained in the ultimate nanocomposites. Polymer nanocomposites are thus a new class of hybrid materials. [9].

1.2 Elastomers

Of the several polymer matrices, elastomer based systems offer multifarious properties meeting the demands of various industrial sectors. The history of elastomers dates back from 1600 BC. Ancient Americans in the region of Central Mexico extending south and east, including parts of Guatemala, Belize, Honduras and Nicaragua were processing rubber during this period. It is known that at least 3,000 years before the first Europeans (Christopher Columbus was probably the first European to see natural Rubber) saw natural rubber, these mesoamerican communities had developed ways of collecting it and forming it into a variety of objects such as toys, house hold products, and items related to ritual sacrifice to tribute payments [10]. The mention of rubber trees is to be found in the eighth decade of *De Orbe Novo* by Pietro Martire d Angliera published in Latin in 1516 [11]. Rubber was seldom utilised until 1823 when Charles Macintosh patented the use of coal tar to dissolve natural rubber and used it to fabricate waterproof apparels. However, rubber became an indispensable part of industry and of daily life following one of the effective discoveries and developments of mankind, namely the vulcanization technology in years 1839–1844 by Charles Goodyear and Thomas Hancock, i.e., the makeover of a material, which is sticky when hot and breakable when cold, to a high-deformable chemically cross-linked elastic

solid. Since that time the rubber industry was established and has shown a strikingly progressive development over the last period of more than a century. Goodyear's experiment of rubber with nitric acid aimed at discovering the stiffness of rubber which later was achieved by sulphur vulcanization. This can be considered as a predecessor to the study of chemical resistance of rubbers [12, 13]. By 1850, a wide range of rubber articles were developed. Many products such as sheets were useful in the mineral and chemical processing industries owing to rubber's elasticity and resilience. The wear and chemical resistances were the critical properties as far as the process plant and equipment were concerned.

Prior to the discovery of vulcanization technique, the elastomer industry had not flourished much. Once cured, rubber is a much more dimensionally stable and also a heat resistant material. At one extreme, a single sulphur atom connects the carbon atom of one chain to that of another and this single sulphur atom is the prime link, and the rubber chemist knows that this is a result of using an efficient vulcanization (EV) system. EV can be either achieved by adding to the rubber formulation, a sulphur donor accelerator or by using small amounts of elemental sulphur, about 0.3 to 0.8 phr, jointly with higher amounts of accelerator (2-5 phr). At the other extreme is a conventional cure system comprising 2-3 phr sulphur and smaller quantities of accelerator (~ 0.5-1.0 phr). This results predominantly in multiple sulphur atoms in the cross-link, known as polysulphidic cross-links. In between these two extremes lies the semi-EV system using about 1.5 phr elemental sulphur and a correspondingly adjusted accelerator level [14]. The first and by far the most important cross-linking agent is sulphur, which is relatively inexpensive and plentiful, and yet vital to the rubber industry. For a number of elastomers, the double bonds (unsaturation) are in plentiful supply on the polymer chain. Sulphur links one chain to another through these double bonds. Elastomers such as NR and SBR need only a low level of unsaturation to be utilized to produce a useful product; however this leaves the rest of unsaturation unused and therefore vulnerable to attack by

oxygen, ozone and heat. Reaction of the small percentage of double bonds actually used for vulcanization can be achieved with 2-3 phr of sulphur in a conventional cure system. If more sulphur (30 phr) is added to the compound, it becomes very stiff (without the aid of any filler) and the resulting material is called ebonite.

Although sulphur is the best known and most relevant vulcanizing agent, there is another class i.e. non-sulphur cross-linking agent. Peroxides belong to non-sulphur crosslinking agent. They do not need the reactivity of a double bond to cure, nor do they need accelerators, although chemicals known as coagents are often used to improve overall crosslinking. Peroxides typically react with the elastomer chains by removing hydrogen atoms from the carbon backbone of the polymer, thus creating highly active sites on the chain, called radicals, which attach to a similar site on another chain, creating a carbon to carbon (C-C) cross-link, which is stronger than a carbon sulphur (C-S)link and more thermally stable. Peroxide curing can crosslink certain elastomers which cannot be cured with sulphur, because of a total lack of double bonds, for example the copolymer of ethylene and propylene rubber (EPM). Elastomers which can be cured with peroxides are EPDM, EP, SBR, NR, BR, CR, certain FKMs and silicones. Butyl rubber cannot be cured in this way, as the peroxide causes degradation of the rubber. However bromobutyl rubber can be peroxide cured for use in certain applications [15].

Electron beam curing helps to achieve some crosslinks in rubber with a beam of electrons. Although not widely used throughout the industry such a process has found a place in partially cross-linking components of tyres, as an aid to tyre production, using a radiation dosage of about four mega rads [16]. Much higher doses would be needed to fully crosslink even thin rubber sections. Work has been carried out on the post curing of an SBR compound with electron beams, with claims of a significant improvement in resistance to ozone and crack initiation [17]. Though Sulphur is the classical cross-linking agent for unsaturated elastomers, such as NR, SBR, NBR, BR, and EPDM, in certain

cases, such as halogen containing elastomers, the preferred agent is a metal oxide. For example, CR is typically cured with a blend of the oxides of magnesium and zinc, which crosslink by removing some chlorine from the polymer chain. CIIR can also be cured with zinc oxide. For both elastomers organic chemicals are typically added to increase the rate of cure. Fluoroelastomers and polyacrylates may be cured with certain amines, and alternatively with bisphenols.

Advances in rubber technology have been continuous since the early discoveries because of the curiosity it evoked. Most discoveries of wear and abrasion were made with the tyre industry in mind, as it was the largest consumer of rubbers in the civil and military transport systems during the first and second world wars. Since many of these advances involved basic properties such as abrasion, tear and flex resistance, these could be readily adopted by rubber chemists who were designing products for the chemical, fertilizer, mineral and ore processing industries. The high strength of natural rubber can be attributed to its ability to undergo strain induced crystallization.

During 1927, Reimer and Tiemann [18-22] published their work on amino acids and in a short period this opened an entirely new vista for process industries. Polymer technology became a new study and research work in these avenues yielded a wide range of new materials. Research on the chemistry of natural rubber revealed an isoprene link; a monomer of the terpene group very much like the aminoacid links in large molecules of protein. Consequently, polymerisation of isoprene yielded polyisoprene; which was found to have similar properties to natural rubber. This started an avalanche of other polymers using styrene, butadiene, chlorobutadiene, etc. Thus, the beginning of synthetic rubber was announced. The scientific community felt the incongruity of the old term 'rubber' and coined a new term to cover the entire range, called 'elastomers' which is a contraction of 'elastic polymers'. Developments in the field of synthetic elastomers have progressed so rapidly that the whole concept

of rubber technology has changed several times and became adapted to changing demands from society. As a part of innovative technologies, the elastomer alone failed to supply the demands of industry. This problem opened up a new window to the world of composites. Thus, rubber started to be applied as a matrix with a dispersed phase incorporated within to enhance existing properties or to impart novel properties. At present, most elastomers used in chemical and mineral processing are used as composites due to their wide array of strength and properties. Elastomers can be bonded to textile fibers such as nylon, polyesters, polyaramides and others to increase strength and stiffness, with a loss in elongation. They can be bonded to metals to combine the rigidity and the strength of the steel equipment with the elasticity, corrosion and wear resistance of the rubbers. An elastomer compound development is usually a compromise of three P's which can be shown as an equilateral triangle, as shown in Fig.1.2. The rubber compounder tries to achieve the best compromise by choosing the elastomer or blends of elastomers and then adding various fillers and chemicals of which there are an almost infinite number of combinations. The mineral and chemical processing engineers see only the performance and price part of the triangle, but the rubber chemist has to deal with the processing through compounding, mixing and forming such as extrusion, molding, hand lay-up methods of forming and the vulcanizing steps [23-25].

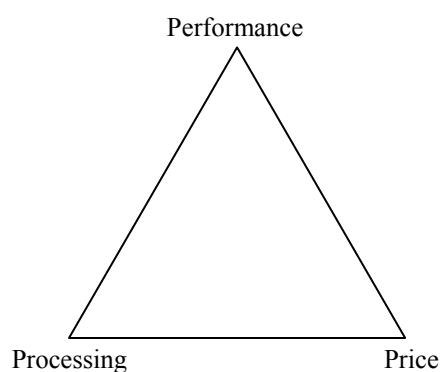


Figure 1.2 The 3 P's in Industry

1.3 Building blocks in elastomer composite fabrication

The primary blocks of composite construction include a dispersion medium, i.e. the matrix and the dispersed phase, i.e. the fillers:

1.3.1 Elastomers as matrix

Various elastomers have been used as matrices for filler reinforcement. Typically, the matrix has considerably lower density, stiffness and strength than those of the reinforcing filler material, but the combination of matrix and filler produces high strength and stiffness, while still possessing a relatively low density.

In a composite the matrix is required to fulfil the following functions:

- 1) To bind together the fillers by virtue of its cohesive and adhesive characteristics.
- 2) To provide environmental resistances and enable ease of handling.
- 3) To disperse the fillers and maintain the desired orientation and spacing.
- 4) To transfer stresses to the fillers by adhesion and / or friction across the filler-matrix interface when the composite is under load, and thus to avoid any catastrophic propagation of cracks and subsequent failure of the composites.
- 5) To be chemically and thermally compatible with the reinforcing fillers.
- 6) To be compatible with the manufacturing methods which are available to fabricate the desired composite components.

1.3.1.1 Natural Rubber

Natural rubber is a high molecular weight polymer of isoprene (2-methyl 1,3-butadiene) with a molecular weight of 10^5 to 10^6 . Polyisoprene has several isomeric forms and, in natural rubber 98-100 percent of the isoprene monomers in its macromolecule are joined in the cis 1, 4 configuration the structure of which is as shown in Fig. 1.3.

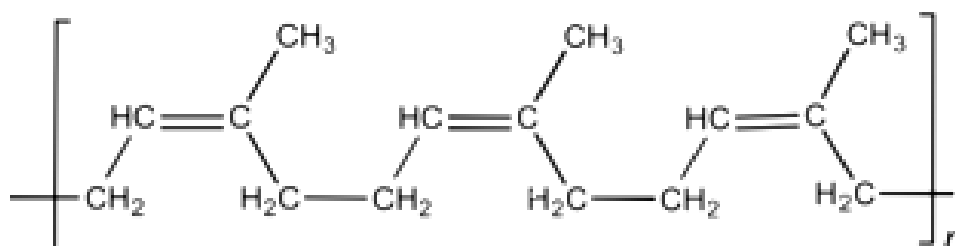


Figure 1.3 Structure of natural rubber (molecular weight of repeat unit: 68.12 g/mol)

It is an elastic hydrocarbon polymer that is found in nature as a milky colloidal suspension, or *latex*, in the sap of some plants and is the oldest known rubber and the most versatile one for fabrication into rubber goods [26]. The major commercial source of natural rubber latex is the Para rubber tree, this tree was called by the explorers as a “wonder tree” which received its botanical name as *Hevea Brasiliensis*. This tree is found in abundance in areas with tropical climate, such as Brazil, Venezuela, Malaysia and India and East coast African countries. The traditional method of slitting the bark and letting the milk drip to form solid mass called latex continues to be the sole method of obtaining natural rubber. The principal component of natural rubber is the rubber hydrocarbon (91-96 percent), a polyisoprene with the general formula $(C_5H_8)_n$. Natural rubber also contains 2.2-3.8 percent proteins and amino acids; 1.5-4.0 percent acetone-soluble substances (acetone extracts: oleic acid, stearic acid, linoleic acid, carotene); compounds of metals of variable valence, such as copper, manganese, iron (to 0.01 percent), sand and certain impurities.

Currently, a large number of activities are directed to improve fuel economy, having in mind that world population is growing and the demand for transportation vehicles is increasing rapidly, especially in developing countries. During the era of exploration in the botanical sciences, many people were seeking unknown plant species that could be useful to humanity, of which rubber tree is of prime impact. Natural rubber was the only high polymeric material serving humanity until the advent of polymer technology. The vulcanized

products made from NR retain high mechanical strength and can be compounded to own excellent elasticity. NR has very good abrasion resistance which, along with its low relative cost, makes it a major choice for slurry pump liners and impellers as well as for tank linings. It has very good dynamic mechanical properties and is therefore used in tyres, rubber springs and vibration mounts. Inherent weather resistance provided by the raw gum elastomer is poor. Significant components of weather, from the rubber technologist's point of view, are UV light and ozone. Addition of carbon black to a compound gives resistance to UV, and antiozonants, waxes; helps with ozone resistance. Ozone attack is of most concern for thin products and those that are subjected to stretching in service. Electrical insulation is very good and, like all elastomers, is dependant on compounding. Resistance to dilute mineral acid (although not oxidizing acids such as nitric) and dilute bases are good. The resistance to petroleum oils is poor, while resistance to alcohols (such as ethanol and methanol) and ketones (such as methyl ethyl ketone and acetone) is much better. Synthetic polyisoprene (IR) has basically similar properties to those of its natural counterpart and has a more consistent rate of curing and processing characteristics, at a current slightly higher price. Among various rubbers, natural rubber is very important since it possess the general features of other rubbers in addition to the following specific characteristics. Since it is of biological origin, it is renewable, inexpensive and creates no health hazard problems. It possesses high tensile strength due to strain induced crystallization. It also possesses superior building tack and good crack propagation resistance. Apart from the conventional rubber products, NR finds a few specialized applications. NR is a versatile and adaptable material which has been successfully used for transport and engineering applications such as automobile tyres, aero tyres, off-the-road and aerospace industries, civil engineering, railways, vibration engineering etc. Reinforcement of NR using particulate fillers and short fibers has been studied [26-28]. Cure characteristic and mechanical properties of natural rubber short nylon fiber composites were studied by Sreeja *et al.*,[29] Atsushi *et al.*,[30] studied

about the nanostructure in traditional composites of natural rubber . Yoshitaka and co workers [31] investigated the friction of short fiber-reinforced rubber on wet surfaces. Short fibers of natural occurrence have been selectively used for reinforcement of NR [32-36].

1.3.1.2 Butyl Rubber (IIR)

IIR is a copolymer of mainly isobutylene (~98%) and a small portion of isoprene (~2%) (Fig.1.4.) This Isobutylene- isoprene chain is responsible for butyl's major properties such as good resistance to oxidative and ozone degradation, to corrosive chemicals and low gas permeability.

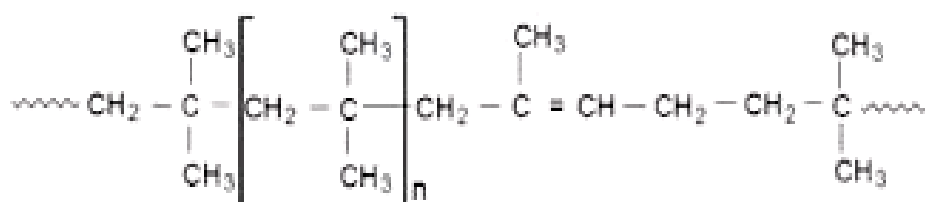


Figure 1.4 Structure of Isobutylene-Isoprene Rubber

It is non-polar and therefore resistant to polar chemicals, especially acids and bases at higher temperatures, and concentrations when compared with NR compounds. Mechanical properties are good enough and resilience at room temperature is very low and this leads to low resistance to impinging abrasion. Its main use in mineral and chemical processing industries is in the lining of tanks and pipes and pumps. IIR is incompatible with diene rubbers such as NR, SBR and BR. Small amounts of an IIR compound can contaminate other compounds and can be easily contaminated by other compounds. So the manufacturing facilities demands high degree of care to avoid such contamination. Chlorobutyl (CIIR) and Bromobutyl (BIIR) are prepared by halogenation of the butyl rubber. Halogenation gives increased reactivity. As a result, improvement occurs in vulcanization rates resulting in improved properties, superior to that of butyl rubber. The state of cure and reversion resistance and covulcanization with other

diene rubbers can also be suitably monitored. CIIR and BIIR vulcanizates have lower gas permeability, better weather and ozone resistance, higher hysteresis, better resistance to chemicals, better heat resistance and better adhesion to other rubbers than those of IIR. CIIR and BIIR vulcanizates are used in almost all applications met by IIR and have even replaced IIR in many applications such as belts, hoses and tank lining of digesters in rare earth and sand complex units.

1.3.1.3 Ethylene Propylene Rubbers (EPM and EPDM)

The Ethylene propylene polymers commercialized were merely the random copolymers of ethylene and propylene (EPM). As a result of the absence of unsaturation, the compound could only be crosslinked with peroxides. The peroxide cures did not satisfy the needs of the rubber industry owing to their limitations. To increase the reactivity for crosslinking, a third monomer, a diene is introduced during polymerization and the resulting rubber, the EPDM terpolymer combines a saturated polymer backbone with residual unsaturation in side groups and can be vulcanized with sulphur giving more flexibility in curing. A large series of dienes has been studied, but 5-ethylidene-2-norbornene (upto 10wt%ENB), dicyclopentadiene (upto 5 wt% DCPD), and 5-vinylidene-2-norbornene(less than 1wt %) are currently the dienes used in commercial EPDM's. One of the most popular grades of EPDM is that with ENB as diene (Fig. 1.5).

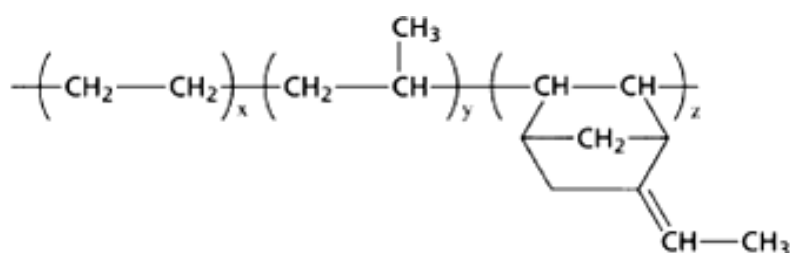


Figure 1.5 Structure of EPDM containing ENB as diene

EPDM rubber is much more commonly and frequently used in the process industries. Since EPDM's have fully saturated backbones (the unsaturation of the

diene is in the side chain), the resistance to ozone and oxygen is excellent. As non-polar hydrocarbon elastomers with an amorphous nature, EPDM rubbers have good electrical properties. The non-polar nature gives resistance to polar materials such as phosphate esters, many ketones and alcohols, many acids and bases, water and steam. Resistance to chlorinated solvents is fair enough. Resistance to non-polar oils, gasoline etc., is very poor although compounds with high loadings of carbon black and oil have lower volume swell, compared to other hydrocarbon elastomers. Resilience of EPDM is not appreciable and so resistance to impinging abrasion is much less when compared with NR vulcanizates, but much better than butyl vulcanizates and as such butyl rubber has been replaced in many applications requiring such abrasion resistance. Resistance to sliding abrasion where shearing forces come into play is good. EPDM rubber is called as crackless rubber in chemical and mining industry circles because of its excellent resistance to tear. Compression set property particularly at high temperatures is good, if properly compounded. Heat resistance of up to 200°C is achievable for special applications with proper compounding. Processing of this rubber is generally good except for the lack of building tack. This severely limits the use of EPDM in hand lay-up applications such as liners. However, with the use of proper solvents and adhesives this can be alleviated. Since EPDM rubber is costly and the price fluctuates widely, high filler and oil loadings are resorted to, to achieve relatively low cost compounds. But these compounds tend to have poor strength and abrasion resistance. High quality stocks, especially those with peroxide cures, are considerably more expensive than NR, BR or SBR stocks. EPDM is used in belts and hoses meant for conveying hot materials because of its excellent heat resistance. Its excellent chemical resistance makes it a preferred rubber for specialty belts, chemical hoses and pump liners [37-38].

1.3.2 Fillers

Elastomers are filled with small and hard particles to form composites, aiming at improving the mechanical properties like elastic modulus or resistance to

abrasion. The term filler is very broad and encompasses a very wide range of materials as, a variety of solid particulate materials (inorganic, organic) that may be irregular, circular, fibrous, or plate-like and are used in reasonably large volumes. There is a significant diversity in chemical structures, forms, shapes, sizes, and inherent properties of these compounds used as fillers. They are usually rigid materials, immiscible with the matrix in both molten and solid states, and, as such, form distinct dispersed morphologies. Their common characteristic is that they are used at relatively high concentrations (>5% by volume), although some surface modifiers and processing aids are used at lower concentrations. Fillers used in rubber industries may be classified on the basis of sources, properties and colour. Those grouped on the basis of sources could be organic or inorganic fillers and can further be subdivided according to chemical family (Table 1.1) or according to their shape and size or aspect ratio. Wypych [39] reported more than 70 types of particulates or flakes and more than 15 types of fibers of natural or synthetic origin that have been used or evaluated as fillers in thermoplastics and thermosets.

Table 1.1 Chemical families to which various fillers belongs to

Chemical family	Examples
Inorganics	
Oxides	Glass (fibers, spheres, hollow spheres, and flakes), MgO, SiO ₂ , Sb ₂ O ₃ , Al ₂ O ₃ , and ZnO
Hydroxides	Al(OH) ₃ and Mg(OH) ₂
Salts	CaCO ₃ , BaSO ₄ , CaSO ₄ , phosphates, and hydrotalcite
Silicates	Talc, mica, kaolin, wollastonite, montmorillonite, feldspar, and asbestos
Metals	Boron and steel
Organics	
Carbon, graphite	Carbon fibers, graphite fibers and flakes, carbon nanotubes, and carbon black
Natural polymers	Cellulose fibers, wood flour and fibers, flax, cotton, sisal, and starch
Synthetic polymers	Polyamide, polyester, aramid, and polyvinyl alcohol fibers

Traditionally, most fillers were considered as additives, which, because of their unfavourable geometrical features, surface area, or surface chemical composition, could only moderately increase the modulus of the polymer, whereas strength (tensile, flexural) remained unchanged or even decreased. Their major contribution was in lowering the cost of materials by replacing the most expensive polymer; other possible economic advantages were faster molding cycles as a result of increased thermal conductivity and fewer rejected parts. Depending on the type of filler, other polymer properties could be affected. The most commonly used particulate fillers are industrial minerals, such as talc, calcium carbonate, mica, kaolin, wollastonite, feldspar, and aluminum hydroxide. The most commonly used fibrous fillers are glass fibers and, recently, a variety of natural fibers. Carbon black and mineral fillers such as silica has been widely used in rubber industry for the past decades to develop enhanced properties. However, due to the high structure of carbon black strong shear fields or filler modifications are needed to ensure fine dispersion. Apart from carbon black, modified carbonized forms of natural materials are also well studied [40]. More recent additions, rapidly moving to commercial markets, are nanoclays such as montmorillonite and hydrotalcite, a variety of oxides, and nanofibers such as single- or multiple-wall carbon nanotubes. Graphene sheets and halloysite nanotubes are potential additives in advanced nanocomposites; the first are single layers of carbon atoms tightly packed in a honeycomb structure [41], whereas the second are naturally occurring nanotubes produced by surface weathering of aluminosilicate minerals [42].

A fine dispersion of filler resulting in good adhesion at the polymer/ filler interface is the basic requirement for attaining optimum reinforcement and low hysteresis in elastomers. The particle ‘size’, ‘structure’ and ‘surface’ characteristics of reinforcing materials are the three S-factors that influence and hence decide the reinforcing ability of a filler and, the filler particle size has the most noteworthy influence among the three S’s [43-46].

During the past decades, where reinforcement of the polymer was not a mainstream of concern to the rubber technologist, different types of clay minerals, barites, whittings etc. have been used as fillers to reduce the cost of the host matrix and impart certain properties to the so called rubber composites. Particulate fillers used in rubber industry in general can be classified as "Black" and "Non-black", depending on their origin, the former being mostly produced from petroleum feed stock and the latter from mineral sources. A wide range of black and non-black fillers have been incorporated into various rubber matrices with the aim of strengthening the matrix. Generally non-black particulate fillers are added to rubber compounds to improve the cured physical properties, reduce cost, and impart colour to the rubber products and along side opacity to corrosive acids and radiations were enabled. The most important particulate fillers being used in rubber industry are carbon black and silica. Silicates, barium sulphate, clays, whiting (calcium carbonate) and other mineral fillers are used extensively where a high degree of reinforcement is not essential. Most of these fillers have polar surfaces. Conversely, many polymers are hydrophobic; these will not readily wet hydrophilic fillers. It is therefore necessary to treat the filler surface to facilitate intimate polymer-mineral contact. Surface modification using coupling agents as silanes and surface treatments using fatty acids can improve the dispersion of the filler in the matrix and there by modify the characteristics of the filled polymer. Many of these additives work by reducing the polarity of the filler surface and thus improve wetting and dispersion in non-polar polymers [47].

The chemical composition and its effect on physical properties of the rubber compound typically result in classifying particulate fillers into three broad categories.

- 1) Non-reinforcing fillers or diluents
- 2) Semi-reinforcing fillers or extenders
- 3) Reinforcing fillers

Of the three classifications non-reinforcing filler is unable to provide any increase on these properties and it functions only as diluent [48]. Semi-reinforcing filler is a particulate material that is able to moderately improve the tensile strength and the tear strength, but does not improve the abrasion resistance. Reinforcing filler is a particulate material that is able to increase the tensile strength, the tear strength and abrasion resistance of natural/synthetic rubber. The term reinforcing filler has been coined to describe discontinuous additives, the form, shape, and/or surface activity of which have been suitably modified with the intention of improving the mechanical properties of the polymer, particularly strength. Inorganic reinforcing fillers are stiffer than the matrix and deform less, causing an overall reduction in the matrix strain, especially in the vicinity of the particle as a result of the particle–matrix interface. "Reinforcement" here refers to an improvement in end-use performance of the rubber compound associated with an increase in modulus and in the so-called ultimate properties including tensile strength, tear resistance and abrasion resistance [49].

1.3.2.1 Particle size and its role in reinforcement

The particle size of the filler may be considered as a physical contribution to reinforcement. Depending on the size of the filler particles, the composites are classified into macro, micro and nano composites. Improvement in the physical properties of the rubber vulcanizate is directly related to the particle size of the filler. The increase of tensile modulus and tensile strength is to an immense extent influenced by the particle size of the filler; smaller the particle size of the incorporated fillers greater the extent of reinforcement to the rubber compound than the coarse ones. The particle size on other hand is related directly to the reciprocal of surface area of the filler, an increase in surface area that is in contact with the rubber phase probably leads to the increase in reinforcing nature. Particulate fillers with a broadened particle-size distribution have better compact packing in the rubber matrix, which results in a reduced viscosity than that provided by the same volume of filler with a narrow particle size distribution. This phenomenon is an indication of

the fact that, reduction in particle size results in an increased polymer-filler interaction and average particle size; and the particle-size distribution also have a significant influence on reinforcement of the matrices. Another cause of concern is the presence of large particles or agglomerates in the rubber. The agglomerates reduces the surface area of contact between filler and rubber matrix and at the same time functions as failure initiation sites which would lead to premature failure of materials.

1.3.2.2 The Particle structure

The smallest individual building block is called as a particle and clusters of these particles fuse together to form aggregates. These primary aggregates flocculate together to form larger secondary agglomerates. These agglomerates are held together by vanderwaals forces of attraction. The detailed morphology of filler, especially carbon black is defined as the structure of the filler aggregate. Particle structure and anisometry of filler aggregate in addition to the surface area; the filler particle shape is an important factor that affects the performance of a rubber compound. Inorganic and mineral fillers possess considerable difference in geometry, depending on the crystal form in which it exists. Anisometry is at its minimum with materials that form crystals with nearly equal dimension in all the three directions. More anisometric are particles in which one dimension is much smaller than the two others, i.e. platelets. Anisometry is at its maximum in particles which have two dimensions much smaller than the third, so that they are rod-shaped. In compounds containing fillers having identical surface area and chemical nature but differing in shape, modulus increases with increasing anisometry [50]. Particles with a high aspect ratio, such as platelets or fibrous particles have a higher surface-to volume ratio, which results in higher reinforcement of the rubber compound. The greatest hardness is also provided by rod-shaped or plate-like particles, which can line up parallel to one another during processing, compared to spherical particles of similar diameter. Particle shape has a more pronounced effect on processing behaviour than on reinforcement

potential and provides important benefits in processing. It can also significantly increase modulus due to occlusion or shielding of some of the rubber phase in highly structured fillers such as structural aggregates of carbon black or silica [45]. An oil furnace black like N110, is highly reinforcing due to its fairly high structure. A thermal black like N990 has a large particle size, and low structure resulting in a much lower level of reinforcement but higher resilience.

1.3.2.3 Surface activity and filler performances

Filler surface activity provides the chemical contribution to the performance of the filler, while particle size provides physical contribution. When the filler effectively interacts with the matrix, chemical bonds will be formed, which results in better strength properties of polymer composites. When the polymer is physically absorbed on the surface of the filler, the mobility of the rubber molecules near the surface of the filler will be reduced in the absence of strong coupling bonds. Polymer-filler bonding develops through active sites on the filler surface resulting in 'bound rubber' attached to the filler surface. Bound rubber is the result of rubber to filler interactions which can be considered as a measure of the surface activity of the filler. The surface activity of the filler is reflected in the mechanical properties of the rubber composites such as tensile strength, modulus, abrasion and tear resistance [51]. Adhesion between polymer and filler may also be induced by using a coupling agent, which involves in the vulcanisation reaction to form polymer-filler networks and this mechanism of increasing strength is well established with both mineral fillers and carbon blacks [48]. Both mechanisms, lead to the formation of high modulus compounds, which clearly indicate that polymer filler bonding has taken place. Silane coupling agents have been successfully utilized to further increase the physical properties of a number of non-black fillers including calcium silicate, clay, mica, silica and talc [52].

1.3.2.4 Surface area and reinforcement

The most important factor, determining the degree of reinforcement, is the development of a large polymer - filler interface. It can be provided only by colloidal particle. Spherical particles 1 μ m size having a specific surface area of 6m²/cm³ constitutes approximately the lower limit for significant reinforcement and the upper limit of useful surface area is of the order of 300-400m²/cm³ and it is decided on the basis of considerations of dispensability and processability of the uncured compound and serious loss of rubbery characteristics of the composite [53]. The surface area of particulate solid is related to its particle size. If all the particles are considered as spheres of the same size, the surface area S per gram of filler can be calculated from the equation, $S = 6/dp$, where d is the diameter and p the density of the filler particle. In reality, particles have a distribution of size and are usually far from symmetrically distributed spheres. Different fillers of the same particle size may not impart the same reinforcement, e.g., carbon black and silica. The shape of particle also may be different for different fillers, viz., spheroidal, cubic/ prismatic, tubular, flaky or elongated. Non - spherical particles can also impart superior reinforcement [54].

1.4 Nanotechnology

Nanotechnology is one of the most vital technologies for interdisciplinary sciences and innovative industries. In the realm of material science and engineering, nanotechnology products can be synthesised from unit materials such as atoms and molecules to build ceramics, catalysts, and semiconductors. Therefore nanotechnology is one of the most attractive research areas. Nanoscale materials are commonly characterized by at least one dimension in the nanometer range (1 nm = 10⁻⁹ m) [55] (Fig. 1.6). By simple calculations, it can be estimated that the volume of one Bacillus cereus bacterium which is in the micrometer range could hold one million of 5 nm nanoparticles [56]. In the nano-scale range, the material structures and properties differ significantly from those of single atoms or

molecules but also from bulk materials. These unique properties bring nano-scale materials into an emerging wide area of applications.

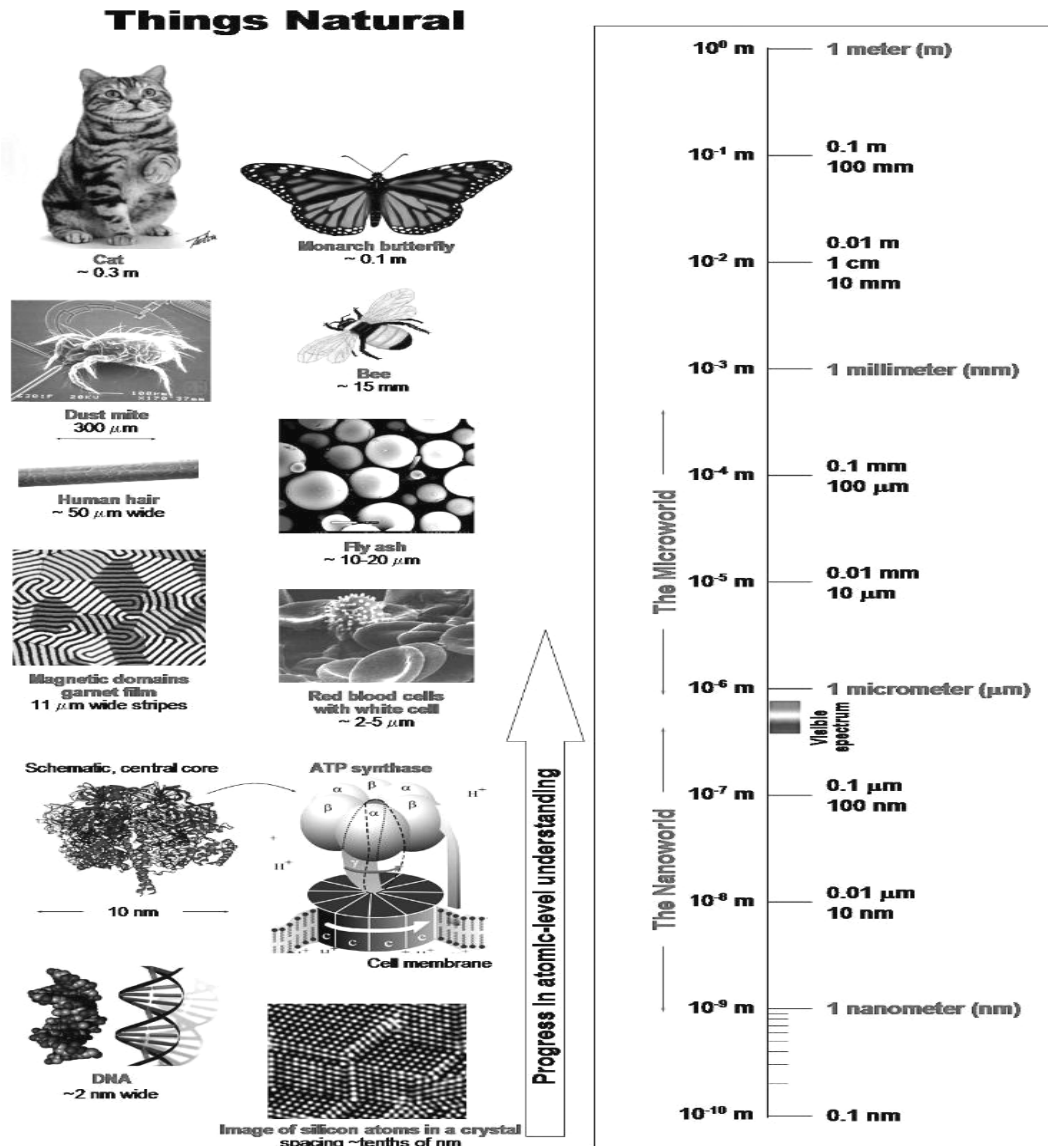


Figure 1.6 Nano scale materials existing in nature

(Adopted from: Office of basic energy Sciences, office of sciences U.S. DOE, version OS-26-06 pmd)

One of the interesting properties of nano-scale materials is the decreasing melting temperatures with decreasing size as an effect of the increasing number of surface atoms. Since the number of surface atoms increases with smaller particles, these atoms can be more easily rearranged than those in the centre of the particles, and thus the melting process can start earlier [56]. The outcome of the ever-increasing number of surface atoms with decreasing particle size also makes small metal nanoparticles becoming a highly reactive catalyst.

The nano-scale materials are categorized generally on the basis of number of dimensions which exist in the nanometer range. By reason of this dependence on the dimensions, nano-scale materials can be classified as: zero-dimensional (e.g. nanopores), one-dimensional (e.g. laminate structure), two-dimensional (e.g. nanowires/nanotubes), and three-dimensional structure (e.g. super lattices) (Fig. 1.7.) This classification system is useful one describing the type of structure of the nano-scale materials one would like to produce.

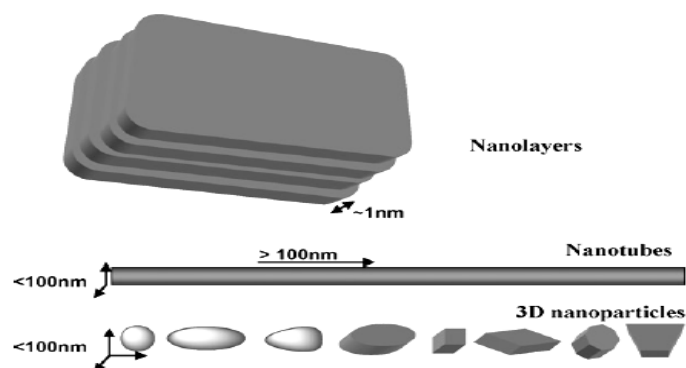


Figure 1.7 Dimensional classification of nanomaterials

1.4.1 Synthesis of nano-scale materials

Plentiful ways are available for nano-scale material synthesis. A broad classification divides these methods in general into two processes. The first is one which build materials from 'bottom up', i.e. atom by atom, in which the material is synthesised from atomic or molecular species via chemical reactions, allowing

for the precursor particles to grow in size. Second is one in which the nanomaterial is constructed ‘top down’ using processes that involves the reformation or the restructuring of atoms to generate the looked-for structures i.e. in this process we start with a bulk material and then break it into smaller pieces using mechanical, chemical or other form of energy [57]. The two approaches are schematically represented in block diagrams as in Fig. 1.8.

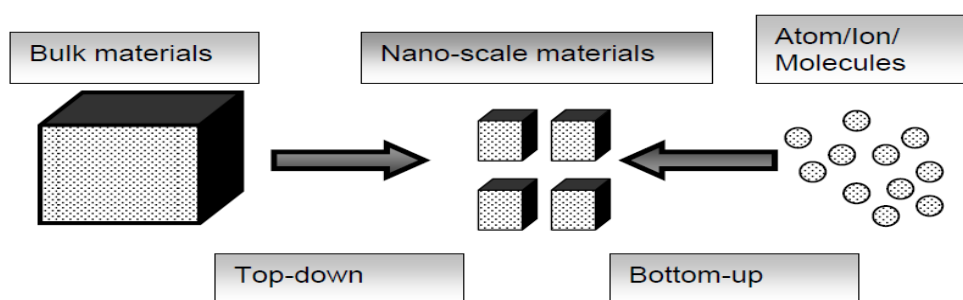


Figure 1.8 Schematic representation of Nano scale filler synthesis

The top-down routes are included in the typical solid-state processing of the materials. These routes are based on the reduction of micro sized materials into the nanosized ones.

High energy ball milling or microfluidizers are used to break down dispersed solids down to 100nm. Materials like metals, ceramic, and polymers in the form of powders having coarse-grained particles are crushed mechanically in ball milling applying hard materials such as steel or tungsten carbide [58]. This continual deformation due to applied forces results in large reduction of grain size since energy is being incessantly pumped into crystalline structures to generate lattice defects. This route is not apt for preparing uniformly shaped materials, and it is very tricky to realize very small particles even with high energy consumption.

Bottom-up routes are frequently used for preparing majority of the nano-scale materials, with their unique ability to yield a uniform size, shape, and

distribution of particles. Bottom-up routes effectively cover chemical synthesis, the precisely controlled deposition and well structured growth of materials. Within that bottom-up route, physical/aerosol and wet/chemical synthesis are widely used for particle creation. Physical vapour synthesis is most often used for the preparation of carbon black, colour pigments and fumed silica, using thermal plasma and lasers as heat sources [59]. This method involves the conversion of solid materials into gaseous components by physical processes. The gaseous material is cooled and thereafter re-deposited on a substrate with achievable modifications; such as reaction with another gas. Among the several nano material synthesis methods employed, wet precipitation is the simplest and cost effective method of material synthesis. Wet synthesis includes classical crystallization, bulk precipitation or emulsion precipitation. These routes involve the reaction of chemical reactants with other reactants in either an aqueous solution or non-aqueous solution. These chemical reactants react and self-assemble to produce a supersaturated solution with the product. This supersaturated solution at certain conditions results in particle nucleation. These initial nuclei then grow into nanometer size particles.

In the case of precipitation in bulk phase, solid particles can be generated from precipitation and crystallization processes based on the wet/chemical route. For that reason the theoretical basics of precipitation processes is to be discussed. The phase transformation of dissolved liquid molecules into a solid phase proceeds by a crystallization process and is relatively slow as the necessary super saturation is created by a reduction of temperature or by evaporation of solvent. On the other hand in case of classical precipitation, two chemical reactants are mixed. Then, a fast chemical reaction initiates the formation of a supersaturated solution which leads to the formation of solid particles as the result of the low solubility of the formed product. Precipitation is one of the oldest unit operations widely used in the chemical industry to produce defined solid particles. The Solvay process, which precipitates sodium bicarbonate,

is an interesting old example for precipitation, which is still widely used in large-scale production. [60]. Sol-gel methods are widely used for fine chemical preparation [61, 62]. These routes involve the reaction of chemical reactants with other reactants in either an aqueous or non-aqueous solution. These chemical reactants react and self-assemble [63] to produce a supersaturated solution with the product. This supersaturated solution at certain conditions results in particle nucleation. These initial nuclei then grow into nanometer size particles., Apart from this ,spray pyrolysis and drying [64], RF plasma synthesis [65], supercritical-water processing [66], vapour transport process [67], sonochemical or microwave-assisted synthesis [68] are also available for synthesis of nano materials.

1.4.2 Diversity in Morphologies of nano materials

Depending on the preparation method and selection of synthetic medium, wide variety of morphologies of the same material can be materialised which includes prismatic forms , bipyramidal dumbbell-like , ellipsoidal, spheres, nanorods, nanowires, whiskers [69-75], nanotubes [76] and columnar hexagonal-shaped nanomaterials [77]. Few among them are shown in Fig. 1.9 [78-79].

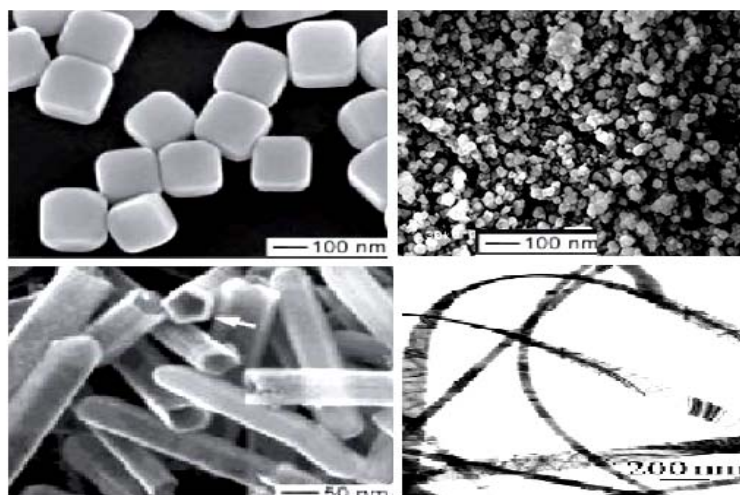


Figure 1.9 Diverse morphologies of nanoparticles

1.4.3 Nanocomposites

Nanocomposites are a new class of composites that are filled polymers which contains in it, at least one dimension of the dispersed particles in the nanometer regime; in order to improve performance properties [80-82].

In the case of nanocomposites, the properties of the material are more tied to the interface, so the control and manipulation of micro structural evolution is essential for the growth of a strong polymer–filler interface in such nanocomposites. And all one have to deal with while working on nano composites is in the atomic dimensions and hence, the properties of nanoclusters or particles are reflective of atoms rather than those in the bulk. The outstanding reinforcement of nanocomposite is primarily attributed to the large interfacial area per unit volume or weight of the distributed phase. The nanolayers has much superior aspect ratio than typical microscopic aggregates [83-84]. The aspect ratio ($=H/R$) is based on approximating particles as cylinders (area/volume = $1/H+1/R$) and is represented in logarithmic scale. Aspect ratios larger than one correlate to nanorods (length/diameter) and less than one to nanoplates (height/diameter) [11]. It is worth to mention, for example, that fully exfoliated and dispersed high-aspect ratio plates or rods, such as montmorillonite or SWNTs, breed internal interfacial area comparable to that of macromolecular structures, such as dendrimers or proteins, and two to three orders of magnitude more than traditional mineral fillers. Furthermore, another advantage of nanofillers is not only to reinforce the rubber matrix but also to impart a number of other properties such as barrier properties, flammability resistance, electrical / electronic and membrane properties, and polymer blend compatibility. In spite of tremendous research activities in the field of polymer nanocomposites for the duration of the last two decades, elastomeric nanocomposites are still in a stage of babyhood as far as their application is concerned. The major challenge in this regard is the replacement of vast portion of carbon black and silica which are mostly used in bulk amount in rubber compositions by a small amount of nanofillers to achieve desirable combination

of properties. Insightful research has combined the advances in diverse disciplines to elucidate the structure–property relationship in polymer nanocomposites. Developments in synthesis and processing have enabled formation and monitoring of engineered nano assemblies, while giant steps in analytical techniques such as microscopy and diffraction studies have enabled the precise determination of structural evolution across various length scales in the rubber material.

In general, three types of nanocomposites can be classified depending upon the number of dimensions of the dispersed phase in the nanometer range [82] as follows: 1) Nanocomposites that can be reinforced by isodimensional nanofillers which have three dimensions in the nanometer range. eg:-Spherical nanoparticles obtained by *in-situ* sol-gel methods [85,86] or by polymerization promoted directly from their surface [87]. 2) Nanocomposites which can be reinforced by fillers which have only two dimensions in the nanometer scale. eg:-carbon nanotube [88, 89] or cellulose [90, 91], 3) The reinforcing phase, in the shape of platelets, has only one dimension on a nano level. eg:- nano clays and layered silicates.

In the nanoparticles filled system, the distance between particles is comparable to the size of the interfacial region because of the increased number density of particles, and as a result, the relative volume fraction of interfacial material to bulk is drastically increased as the size becomes smaller.

Major advantages of nanocomposites:

- Lighter weight owing to low filler loading
- Reduced cost due to fewer amount of filler use
- Improved mechanical, thermal, optical, electrical, barrier properties, compared with conventional composites at very low levels of filler loading.

Methods for preparation and processing of various nanocomposites:

The incorporation of nanoscale particles into polymer can generally be done in five ways as follows:

- a) Solution method: involves dissolution of polymers in sufficient solvent with nanoscale particles and evaporation of solvent or precipitation.
- b) Melt mixing: In this, the polymer is directly melt-mixed with nanoparticle.
- c) In-situ polymerization: here, the nanoparticles are first dispersed in liquid monomer or monomer solution. Polymerization is carried out in presence of nanoscale particles.
- d) Template synthesis: This method is completely different from other methods. It uses polymers as template, and the nanoscale particles are synthesised from precursor solution.
- e) Mechanical mixing on a two roll mill: This is the classical method of compounding rubber matrices followed by incorporation of nano fillers on an open two roll mill [92].

1.5 State of the art research - elastomer nano composites

In the last two decades, the incorporation of nanomaterials in polymeric systems has opened up a new vista of nanostructured polymeric materials. The commendable interfacial interaction between the matrix and the nanofiller particles, recognized by the smaller size and enhanced surface area of these smart nano's imparts amazing properties to the matrices in which they are incorporated. These organic–inorganic hybrid materials play an important role as structural composites and, the developments in the field of synthetic elastomers have progressed so rapidly that the whole concept of rubber technology has changed several times. Polymer based organic and inorganic nanocomposites

have gained increasing attention in the field of interdisciplinary sciences [93-96]. Even if the consumption of synthetic rubber is increasing, it is a genuine fact that natural rubber is the most fascinating and industrially relevant rubbery material. The foremost reasons behind it include its high green strength owing to the non rubber constituents as, phospholipids and proteins, strain-induced crystallization behavior, amenability to vulcanization and stereoregularity. In order to attain good mechanical properties in accordance with the end use, the elastomers have to be reinforced with particulate fillers as carbon black and silica. Usually high percentages, around 40 wt% conventional fillers are needed to get ample reinforcement depending on application. These traditionally filled rubbers have high filler content and hence reduce the processability and increase the weight of the final product. In these state of affairs, the nano concept is highly important for rubber compounds since their application lies in its ability to provide reinforcement [97-103]. Apart from solely constructing a nanocomposite, works have been carried out in fabricating so called hybrid nano composites, by incorporating more than one filler which may be either in the nano or macro region, in order to derive the benefit of both nano and conventional fillers. Okada et al. [104] found that 10 phr of organoclay is enough to achieve a tensile strength in NBR equivalent to 40 phr carbon black loaded NBR and Arroyo et al. [101] have compared the reinforcement imparted in NR by organoclay and carbon black dual systems by constructing hybrid composites. A number of methods have been employed by scientists and industrialists for nanocomposites fabrication, such as melt mixing [105–108], two-roll mill mixing [109–114], solution mixing [115–121], latex stage mixing followed by coagulation method [122–129] and polymerization around fillers [128, 129].

Rubber/layered silicate nanocomposites exhibited excellent properties due to the high aspect ratio of layered silicates arising from their lamellar structure. In the presence of these fillers, rubber nanocomposites can form either intercalated or exfoliated structure or partly intercalated and exfoliated

structure [130, 131]. The maximum properties of these composites, due to the incompatibility between the organic (rubber) and inorganic (silicates) components, can only be attained by the organic modification of the silicates. Thus the interaction between hydrophobic rubber and hydrophilic filler has been improved to get unique physical and chemical properties. Commonly rubber industry concentrates on montmorillonite (MMT), hectorite, saponite and organically modified MMT. The literature reveals that unprecedented improvement in properties has been observed in elastomers with these nanofillers [101-103, 105–110, 115,122, 132–134]. Jeon et al. [135] have synthesised a modified Na-MMT using polyethylene glycol monooleate and polyethylene glycol diacrylate as modifiers to enhance the fine dispersion in rubber matrix. It has been revealed that the organic modification enhanced the fine dispersion of MMT effectively in the hydrophobic rubber matrix. Jia et al. [136] have observed a significant improvement in properties of SBR-clay nanocomposites. For the past few years, researchers have employed both natural and synthetic rubbers for the preparation of nanocomposites, viz, natural rubber [101,108,118–121, 137–144], SBR and XSBR [111, 145–151], HNBR and NBR [124,152–157], IR and ENR [105, 108], EPDM [100, 158, 159], EVA [160-163] and so on.

Carbon nanotubes have been used as reinforcing filler in elastomers instead of conventional fillers such as carbon black and silica. Liliane et al. [164–169] have studied the reinforcing effect of multiwalled carbon nanotubes in SBR, they have also compared the reinforcement of SBR by single fillers of carbon black and multiwalled carbon nanotubes and by mixture of carbon black and MWNTs. Jacob and coworkers [170] synthesised the nanocomposite of crosslinked natural rubber and single walled nanotubes. Studies have also been carried out with SiC nanoparticles and single-walled carbon nanotubes in natural rubber [171] and found that the tensile strength of the nanocomposite was enhanced even at lower concentration (1.5 wt%). Researchers have paid much interest in

nanocomposites of various rubbers and carbon nanotubes (SWNTs and MWNTs) such as NR [172–176], SBR [177, 178], HNBR [179], EPDM [180], PUR [181–188] and silicone rubbers [189–191]. Bhattacharyya et al.[192] have reinforced natural rubber using carboxylated multiwalled carbon nanotubes (c-MWCNT) dispersed with sodium dodecyl sulfate.

Nano silica have been employed by number of researchers to fabricate elastomers based composites both nanocomposites and hybrid nanocomposites. Nano inorganic spherical filler silica has been extensively used in the rubber industry. The introduction of ‘Green Tyres’ has enhanced the demand for silica particles and focus is now on in situ generation of silica particles to synthesise nanocomposites of polymer and silica particles [193]. Liu et al. [194] have used modified silica using basic cyclohexylamine. The physical property of the copolymer of LDPE-EVA was improved by the incorporation of pristine nanosilica. The interaction of hydrophilic silica filler with the copolymer has been improved in the presence of silane coupling agents [195]. A number of hybrid composites of nano silica and carbon black revealing synergy as earlier studied with nano clay- black systems have been reported [196-202].

Polyhedral oligomeric silsesquioxane (POSS) is a class of nanofillers with functional groups that are widely used in thermoplastics and thermosets as reinforcing agents. Sahoo et al. [203] have synthesised POSS with hydroxyl functional groups with an average diameter of 50 nm. They have used POSS nanoparticles as curing agent in certain functionalized rubbers such as fluorocarbon rubber (FKM) and carboxylated nitrile rubber (XNBR) and analyzed the physical properties. The results revealed that the POSS nanoparticles cross linked effectively in FKM and XNBR. Composites of silicone rubber and POSS were prepared by melt blending with special interest in the thermal stability of POSS macromers and the effects of mixing temperature and the subsequent vulcanization of polysiloxane [204]. The results showed that the condensation reaction could be possible at higher temperature,

leading to a partially amorphous structure of crystalline POSS; however, it was recrystallized upon cooling.

Nowadays efficient and environmentally friendly nanofillers are being developed from natural fibers and starch. NR filled with waxy maize starch nanocrystals showed that upto a loading of 20 wt% the physical properties were found to be higher. At 20 wt% the relaxed modulus at room temperature was 75-fold higher than that of unfilled matrix [205]. Apart from these reinforcing fillers the emergences of non-reinforcing fillers as effective reinforcement when their size is reduced to nano size realms have been widely applied. Mishra et al. [206] have compared the effect of commercial and nano CaSO_4 filler particles on the mechanical, physical and thermal properties of SBR. The matrix SBR has been reinforced with nano filler via in situ deposition technique. They have observed an enhancement in properties of SBR with nano CaSO_4 up to a filler loading of 10 wt%. According to them at higher loading all properties of SBR decreased due to the agglomeration of filler particles. Reports on the use of barium sulphate nanomaterials by Wang et al. [207,208] in PBD systems and by Zhao et al. in NR are seen in literature. Reinforcing effect of nano CaCO_3 in different compounds—NR and NR/NBR blend used in sports goods (laminated sheet for inflated balls), NR based cycle tube, bromobutyl based pharmaceutical closures and CPE/CSM blend used for coated fabric have been reported earlier [209-211].

1.6 Barium sulphate

Barium was first isolated by Sir Humphry Davy, an English chemist, in 1808 through the electrolysis of molten baryta (BaO). Barium is never found free in nature since it reacts with oxygen in the air, forming barium oxide (BaO), and with water, forming barium hydroxide [$\text{Ba}(\text{OH})_2$] and hydrogen gas (H_2). Barium is most commonly found as the mineral barite (BaSO_4) and witherite (BaCO_3) and is primarily produced through the electrolysis of barium chloride (BaCl_2). Barium sulphate, a common barium compound, is used as a filler for rubber, plastics and resins. It can be combined with zinc oxide to make a white pigment

known as lithophone or with sodium sulphate (Na_2SO_4) to make another white pigment known as blanc fixe. Industrial barium sulphate is usually colourless or milky white, but its colour can vary depending on the impurities trapped in the crystals during their formation. Barite is a mineral composed of barium sulfate, BaSO_4 . It is relatively soft, measuring 3 to 3.5 on Moh's scale of hardness. It is unusually heavy for a non-metallic mineral. The high density is responsible for its significance in various realms of applications. Commercially barite is chemically inert and insoluble. BaSO_4 is the most common mineral of barium. Barite is used in the production of wallpaper and in the manufacture of white paints. Barite, a name derived from the Greek word "barus"(heavy), is the mineralogical name for barium sulfate. Although barite contains a "heavy" metal (barium), it is a non-toxic chemical under Section 313 of the Emergency Planning and Community Right-to-Know Act of 1986, because it is very insoluble.

The commercial significance of barite is related almost entirely to its high specific gravity. As far as the modern industry is considered barium sulfate is widely used as a shading material for the X-ray photography being a good absorber of X-rays, a gamma-ray absorber, a white pigment, coupled with its characteristics harmlessness to humans and its strong shielding capability. Although all barium compounds are poisonous, barium sulfate can be safely ingested since it does not dissolve in water. It continues to be the most important radio-opaque component in radiographic contrast materials used for visualizing the intestinal tract. Numerous new barium sulfate preparations and corresponding patents confirm the unsurpassed basic suitability of this radio-opaque compound. Barium sulfate ceramic is a superlative optical reflector, and may soon become a viable component of optical circuits. Barium sulfate powder is also used in polymer system as fillers. For using as a filler, nanosized and superfine barium sulfate powder is expected to enhance the materials properties. And these fine barium sulfate powders are relatively highly sinterable which is very important

for preparation of BaSO₄ ceramic. Barium sulphate particles can lead to a significant improvement of optical characteristics and flow behaviour, and have been used widely in pigments, printing inks, and medicine. BaSO₄ has an orthorhombic crystal structure, the unit cell are $a = 8.88 \text{ \AA}$, $b = 5.46 \text{ \AA}$, and $c = 7.16 \text{ \AA}$. Fig. 1.10, below shows the BaSO₄ morphology as predicted using Cerius2® software [Van-Leeuwen, 1998][212-213].

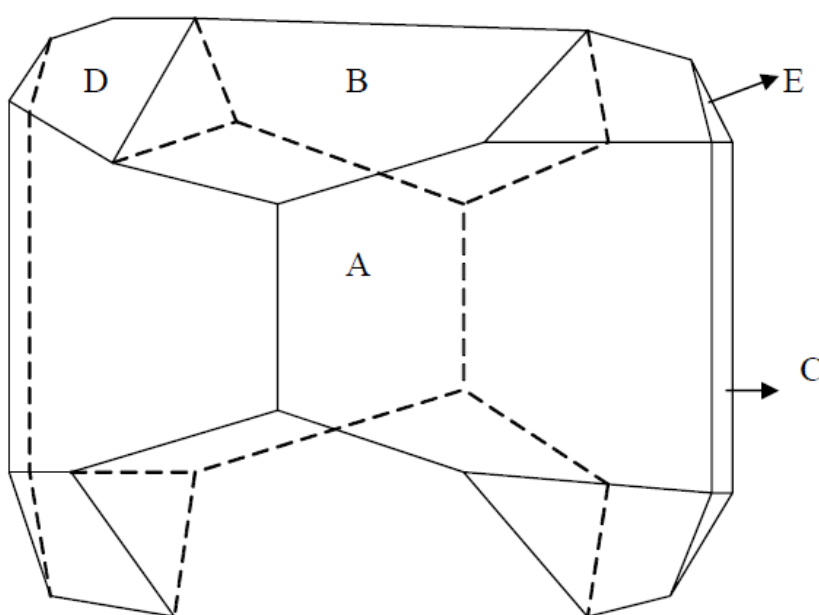


Figure 1.10 The predicted morphology of orthorhombic crystal structure of barium sulphate from the unit cell dimensions $a = 8.88 \text{ \AA}$, $b = 5.46 \text{ \AA}$, and $c = 7.16 \text{ \AA}$. The indicated faces are $A = \{101\}$, $B = \{011\}$, $C = \{200\}$, $D = \{111\}$, and $E = \{210\}$ [redrawn from Van-Leeuwen, 1998].

1.6.1 Uses of barium sulphate

Annual production of barium sulphate worldwide is approximately 5.4 million metric tons, dominated by China(33%), India(11%), and Morocco (8%). Ground barite for well drilling fluids accounts for 90% of all production. The balance is used in the manufacture of barium chemicals and glass and in filler applications.

Therapeutic Medicines and clinical X-rays: Because barium sulphate is insoluble and opaque to X-rays, blanc fixe meeting pharmacopeia specifications is used as an indicator in medical X-ray photography. Natural barite is used in concrete for the construction of facilities handling nuclear materials because it absorbs gamma radiation.

Coatings: Paints and primers represent the largest use for filler-grade barite. High-brightness micronized barite is used as an extender to provide the weight that customers equate with quality and because of its low binder demand, which allows high loadings. They function instead as extenders and spacers, keeping the pigment particles separated and uniformly disseminated to optimize light scattering.

Well drilling fluids: Drilling fluids are designed to cool the drill bit, lubricate the drill stem, seal the walls of the well hole, remove cuttings, and confine high oil and gas pressures by the hydrostatic head of the fluid column. In most drilling fluids barite is the major ingredient by weight percent.

Glass: In glassmaking barite saves fuel by reducing the heat-insulating froth on the melt surface, it reduces seeds and annealing time and improves glass toughness, brilliance, and clarity.

Polymers: Finely ground barite is used in rubber, where its weight, inertness, isometric particle shape, and low binder demand are advantageous. It has little effect on cure, hardness, stiffness, or aging. It is used in acid-resistant compounds, in white sidewalls for tyres, and in floor mats. Blanc fixe of semi-reinforcing nature is used to provide the same compound softness and resilience as barite but better tensile strength and tear resistance. Barite is used in PVC and polyurethane foam backings for carpeting and sheet flooring because of its ability to form dense coatings due to its high specific gravity and its ability to be used at high loadings.

Other uses: Micronized white barite and blanc fixe are used as fillers and extenders, primarily to add weight, in bristolboard, playing cards, and heavy printing papers. Blanc fixe is used in the base coat of photographic papers to supply an inert substrate for the silver halide emulsion coat. Finely ground (~325 mesh) barite is used as an inert filler in brake linings and clutch plates [214-217].

1.6.2 Surface activity of barium sulphate:

Precipitated barium sulphate is a known pigment, which can be used as a filler in the rubber industry, as an opacifier in art printing and photographic papers and in the polymer industry, and as a brightening agent and a fiber – dulling agent in the textile industry. Barium sulphate is produced in known manner from water soluble barium salts and water soluble sulphates by a wet chemical precipitating process. These conventional precipitating processes involve more or less time consuming crystallization from isothermally supersaturated solutions. Owing to the very low solubility of the precipitates the crystals are very small and the conversion almost amounts to about 100%. The optimum properties of pigments and extenders from the aspect of application technology will be achieved with certain particle size distributions. For this reasons, it is by no means enough to form the desired barium sulphate precipitate in a prescribed chemical composition but, the wet chemical process must be inhibited to result in the desired primary particle size. Precipitated barium sulphate is used as an inert pigment in numerous fields. Known fields of application includes the use of the precipitated barium sulphate as filler in the dyestuff and paint industry, in the plastic and rubber industry, or the use as a dulling agent in the fiber industry.

In these fields the barium sulphate is substantially used as inert white filler based upon the fact that it is substantially inert chemically and physically. In other applications, the filler is required to have functional properties in order to impart certain property profile to the system in which the filler is used. This is generally accomplished with so called active fillers, such as silicates, oxides,

carbonblack, sulphur, which may be of natural origin mineral or may be synthetically produced. All so called active fillers are characterised by having a surface reactivity owing to the presence of esterifiable hydroxyl groups, reducible carbonyl or carboxyl groups or radical splittable molecules (e.g. polysulphides)

Barium sulphate lacks such a surface activity. In the SO_4^{2-} tetrahedron, the central atom has its highest oxidation number. This high charge density of the Ba^{2+} ions ensures a saturation of the bond sites on the crystal surface by the Ba^{2+} ions. A known as well as a widespread measure of providing surface reactivity consisting of an after treatment with inorganic and/or organic adjuvants, such as a silanization, will not produce the desired results with barium sulphates because, by contrast with other oxide pigments, such as TiO_2 , ZnO and SiO_2 , and by contrast also with carbon, a particle of BaSO_4 has no surface centres which can be esterified and/or complexed and this deficiency inhibits the after treating agent and thus they cannot be fixed with formation of covalent bond. A strictly physical-mechanical application, such as the application of additional components by a simple admixing, will not produce the desired result. When coated barium sulphate is incorporated in a polymer system, the alternating agent bonded by physical sorption will be detached from the surface. In order to prevent a subsequent detaching, the after treating agent must be chemically fixed to the barium sulphate surface by a covalent bond or must be electro statically fixed to a surface.

Surface treatment, on the other hand, is the association of a processing aid with the mineral's surface only. One part of the treating agent molecule has an affinity for the mineral surface and the other for the organic medium. Surface treatments to hydrophobize the filler surfaces can be attained by using organic or inorganic surface treating agents. The commonly used inorganic and organic agents fall into the group of alkali silicates and organic ones may be alkyl/aryl sulphonates, sulphites or phosphoric acid esters and a mixture of any two or simply fatty acid. Properties of inorganic fillers can be further enhanced by treatment with organic stearates to make the particles hydrophobic. The suitable

method of modifying the surface of barium sulphate is to form a modifier coating on these precipitates by using certain inorganic or organic reagents. In a patent reporting the use of surface modifiers for barium sulphate, inorganic compounds selected from aluminium, barium, antimony, calcium, cerium, chlorine, cobalt, iron, phosphorous, carbon, manganese, oxygen, sulphur compounds or salts were used whereas organic modification used organic compounds from the group of alkyl sulphonic acid salt, sodium polyvinyl sulfonate, sodium dodecyl benzene sulfonate, or higher fatty acids [218-220].

1.7 Scope and objectives of the present work:

Elastomeric composites with special properties are highly important in that they can suit situations demanding strength and flexibility and they can be formed into any shape of choice; simple or complex. In recent decades researchers have been seeking new reinforcing fillers for elastomers that are environment friendly, inexpensive and readily available to act as reinforcement and also as partial replacement for carbon black. Manufacture of carbon black is dependent on non-sustainable supplies of petroleum and whose preparation and processing are hazardous and consume lot of energy. On the one hand replacement aims at cost reduction and on the other hand a synergistic effect of different fillers may be obtained due to cooperative interactions. Barium sulphate is widely used as filler in polymer industry and is eco-friendly and as a filler, it possess two inherent characteristics that could be transferred to an elastomer matrix once filled within. Of its strengths, one is its inherent resistance to chemicals especially acids and other one is its ability to be rendered opaque to radiations. The former property depends basically on the polymer characteristics initially and can be enhanced by incorporation of barium sulphate, where as the latter property is solely imparted by the filler and varies depending on filler's particle size and modifications. The general fields of application of filled acid resistant elastomers [221-224] are mainly in the fertiliser industry and fuel cell assemblies and as and when the sustenance of polymer property is necessary, these diluents fail to meet the purpose.

The vulnerability to ionising degradation depends on nature of polymer and almost all polymers are radiolucent and opacity to radiation depends mainly on nature of filler used, or exactly on nature of opacifier material incorporated. The traditional materials used to impart acid resistance and radiopacity in industrial applications are in majority based on lead materials. Lead brick linings were provided to act as corrosion resistant acid shields and lead based garments and screens, used as protection against X-rays for operating personals in clinical analysis. Though lead based materials excelled in their task, they have disadvantages such as heavy weight, easy crack formation and corrosion and poor processability and finally the menace of disposal once damaged. Irradiated lead becomes a mixed hazardous waste, the disposal of which is a cause of environmental concern. As far as aprons, garments and shields are concerned high weight factor is too risky [225]. Barium sulphate can act as a replacement for Pb based materials in clinical X-ray field, since its K-edge is such that it screens radiations from 37kVp to 60kVp which is the normal energy range used for whole body X-ray imaging. In such a situation, radiopaque elastomer composite based on barium sulphate filled composites assume significance. A literature survey conducted on barium sulphate filled composites reveals that, studies on barium sulphate filled composites are scarce or seldom published. In the reported works of composites filled with barium sulphate, it could be seen that even though the processability and technological properties of filled composites are attained, the property of the host polymer was not even retained and state even worsened at high loadings. Introduction of a non-reinforcing filler that too at higher loadings as a rule will deteriorate its property due to inert surface. But if its size is reduced and surface area increased, improvement in mechanical properties is expected. This material has been stamped under the category of non-reinforcing filler and its potential in imparting reinforcement has not yet been revealed under smaller length scales which is mainly attributed to its draw back i.e., lack of surface activity. Generally barium sulphate is chemically inert but introduction of surface activity into it by surface treatment

can impart improved wettability by polymer which can improve material properties amazingly and add essence to the inherent properties attributed to by barium sulphate as, radiopacity and acid resistance, owing to the reduced size and activated surface. Once surface activity has been imparted things will change and the filler can impart better strength properties in addition to opacities and resistance to acid. Apart from all these applications the nano barium sulphate filler synthesis aims at achieving amazing properties at these shorter length scales and a scope of using it as reinforcement in selected elastomers. Under these circumstances, when functional properties are to be introduced into polymers along with material strength use of nano fillers can help a lot. Nano fillers due to size reduction can act as reinforcement and at the same time can impart superior properties too. It can also assist in at least partially replacing the carbon black from numerable composite structures if properly tailored.

In the present work the possibility of using barium sulphate having nanoparticulate dimension as a reinforcement in elastomers and the synergistic effect in the presence of barium sulphate in carbon black filled composites have also been explored, it is expected that the presence of dual filler network will enhance filler dispersability in elastomers. Since barium sulphate is inert it will not be able to enhance strength properties drastically. In order to improve its interaction with elastomers, a surface treatment has been made using stearate modifiers. The use of modified barium sulphate nano filler is to improve the mechanical strength of elastomers and synergistic effect of dual fillers in carbon black filled system is expected. Improvements in radiopacity and acid resistance are also expected.

The specific objectives of the present work are:

- Synthesis and characterization of nano barium sulphate and its modification via surface treatment using fatty acid to convert its surface from hydrophilic to hydrophobic.

- Fabrication of nano composites of unmodified and modified barium sulphate by incorporating them in elastomers like natural rubber, ethylene propylene diene rubber and isobutylene isoprene rubber and exploring the influence of these fillers in reinforcing the matrices and imparting strength properties, solvent resistance and thermal stabilities.
- Hybrid composite fabrication is another objective: Adding carbon black(HAF) to the elastomers at higher loadings and attempting to partially replace this filler with low loadings of nano barium sulphate, in such a way that, the resultant polymer composites offer better or comparable properties with that of black filled systems.
- Evaluation of resistance of these nanocomposites as well as hybrid composites on immersion in sulphuric acid and exploration of the various mechanisms involved, if any in acid degradation of rubbers through various parameters like weight change, property change and emergence of neo-functionalities using Infrared spectroscopy.
- Determination of radiopacities of the composites with modified, unmodified barium sulphate of smaller particle size and commercially available forms of filler at higher loadings and determination of optical densities and corresponding attenuation coefficient to assess their shielding effectiveness to X-rays generated from a medical source.

References

- [1]. E.P.Giannelis; *Adv. Mater.* **1996**, 8, 29.
- [2]. H.F. Mark ;Encyclopedia of Polymer Science Engineering ,JohnWiley and Sons. New York .**1985**
- [3]. J. Jordan, K. I. Jacob, R.Tannenbaum, M. A Sharaf & Jasiuk ; *Mater. Sci. Eng. A.*,**2005**, 393, 1.
- [4]. Z.Zhang, & K.Friedrich;*Compos. Sci. Technol.*,**2003**, 63, 2029.
- [5]. M.H.Al-Saleh, & U.Sundararaj; *Polymer.*, **2010**, 51, 2740.
- [6]. N.Groosiord, , J.Loos, L. Laake, M.Maugey, C.Zakri, C.E. Koning & A.J. Hart; *Adv. Func. Mater.***2008** ,18, 3226
- [7]. R.Zhang, Q.Q.Ni, T. Natsuki, M.Iwamoto; *Composite Structures*, **2007**, 79, 90.
- [8]. P. Meneghetti, S.Qutubuddin; *Thermochimica Acta.*,**2006**, 442, 74.
- [9]. V. Mittal; *Materials*, **2009**, 2, 992.
- [10]. J.Loadman; Tears of the tree. The story of rubber – a modern marvel. Oxford University Press, Oxford. **2005**.
- [11]. P.Schnarr, L.E.Schaeffer, H.J. Wein; Elastomers in Mineral Processing industry-“Processing Plant Design, Practice and Control” October **2002**, Mineral Processing Plant Design, Control and Practice Conference in Vancouver, British Columbia ProceedingsVol. 2 Edited by By Andrew L. Mular, Doug N. Halbe, Derek J. Barratt
- [12]. W. P. Fletcher , A. N. Gent; *Trans.Inst.Rubber Ind.*, **1953**, 29, 266.
- [13]. J. Lebras; Rubber-fundamentals of its science and technology, Chemical Publishing Co, INC; NY USA.**1957**, 95.
- [14]. C.M.Blow; Editor, Rubber Technology and Manufacture, The Chemical Rubber Co., Ohio.**1971**, 509.
- [15]. A.Ciesielski ;An Introduction to Rubber Technology , Rapra Technology, **1999**, 33.

- [16]. B. Slade, *Elastomerics*, **1985**, 117, 11, 34.
- [17]. Basfar, W. J. Chappas, J. Silverman, *Rubber & Plastics News*. **1994**, 24, 9, 33.
- [18]. R.T. Morrison and R.N. Boyd, *Organic Chemistry*, 6th Edition, Prentice Hall, Englewood Cliffs, NJ, USA, **1992**, p.908.
- [19]. I.L. Finar, *Organic Chemistry*, Longmans, Green & Co., London, UK, **1951**, 1, 743.
- [20]. J.D. Hebworth, D.R. Waring and M.J. Waring, *Aromatic Chemistry*, Royal Society of Chemistry, Cambridge, UK, **2002**.
- [21]. J. Andraos, *Graphical Anecdotes by the Department of Chemistry*, York University, Toronto, Ontario, Canada. <http://www.chem.yorku.ca/NAMED/PDFFILES/graphical-anecdotes.pdf>
- [22]. P. Downey in *The Cutting Edge: An Encyclopedia of Advanced Technologies*, Ed., W. Allstetter, J.A. Angelo, Jr., and T. Day, Oxford University Press, Oxford, UK, **2000**, 210.
- [23]. website: en.wiktionary.org/wiki/k-value; **2012**
- [24]. website: www.deai.ie/glossary-of-BER-terms.html; **2012**.
- [25]. <http://en.wikipedia.org/wiki/Ablation>; **2012**.
- [26]. S.Kohjiya, Y.Ikeda; *J. Sol-Gel Sci. Technol.*, **2003**, 26, 495.
- [27]. M.Abdelmouleh, M.N Belgacem., A.Dufresne; *Compos. Sci. Technol.*, **2007**, 67, 1627.
- [28]. Debasish De, Debapriya De, A.Basudam; *J. Appl. Polym. Sci.*, **2006**, 101, 3151.
- [29]. T.D Sreeja, S.K.N Kutty, *J. Elastomers Plast.*, **2001**, 33, 225.
- [30]. K.Atsumi, K.Shinzo, I.Yuko, *Rubber Chem. Technol.*, **2007**, 80, 690.
- [31]. U.Yoshitaka, W.Noriaki, I.Tomoaki, U.Seichi, S.Shinji; *J. Appl. Polym. Sci.*, **2005**, 95, 82.
- [32]. J.George, K.Joseph, S.S Bhagavan., S.Thomas; *Mater.Lett.*, **1993**, 18, 163.

- [33]. S.Varghese, B.Kuriakose, S.Thomas; *Plast. Rubb.Comp. Proc.Appl.*, **1993**, 20, 930.
- [34]. S.Varghese, B.Kuriakose, S.Thomas, A.T.Koshy, *Ind. J. Nat. rubber*, **1991**, 4,55.
- [35]. S.Varghese, B.Kuriakose, S.Thomas, A.T Koshy; *J.Adhes.Sci.Technol.*, **1994**,8, 235.
- [36]. S.Varghese, B.Kuriakose, S.Thomas;*Rubber Chem. Technol.*,**1997**, 68,75.
- [37]. W. Hofmann, *Rubber Technology Handbook*, Carl Hanser Verlag, Munich, Germany, **1989**, 124.
- [38]. M. Morton, Ed., *Rubber Technology*; Van Nostrand Reinhold, New York, **1987**,3.
- [39]. G.Wypych; *Handbook of Fillers*,Chem. Tec. Publishing, Toronto, Canada, **2000**.
- [40]. P.Egwaikhide, F. E. kieimen,U.Lawal; *Sci. J. Chem.*, **2013**,1(5),50.
- [41]. Jacoby, *Graphene: carbon as thin as can be*. *C&EN*, **2009**,87 (9), 14.
- [42]. Y.Lvov,R.Price,HalloysiteNanotubes.Accessed May **2009** at [http:// www.Sigmaaldrich .com /materialsscience/nanomaterials/nanoclaybuilding/halloysite-nanotubes.html](http://www.Sigmaaldrich.com/materialsscience/nanomaterials/nanoclaybuilding/halloysite-nanotubes.html). **2009**.
- [43]. S.Thomas, R.Stephen ,*Rubber nanocomposites: preparation, properties, and applications* , John Wiley & Sons,Asia, **2010**,5.
- [44]. J.S.Dick; *Rubber Technology: Compounding and Testing for Performance*, Hanser Publishers, **2001**,523.
- [45]. F. R.Eirich ;*Science and Technology of Rubber*, Academic Press, New York,**1978** ,633.
- [46]. I.Franta; *Elastomers and Rubber Compounding Materials*, Elsevier, New York, ,**1989**, 588.
- [47]. I.Medalia, G.Kraus, In: *Science and Technology of Rubber*, Eds., J. E.Mark, B.Erman, and R. F Eirich., Academic Press, New York, **1994**,387.

- [48]. R.Rothon, Editor, Particulate-Filled Polymer Composites, Longman Scientific & Technical, New York, **1995**, 371.
- [49]. M.Xanthos, Functional Fillers for Plastics,, Wiley-VCH Verlag GmbH, Weinheim , **2010**, 2,9.
- [50]. M. J.Wang., Rubber Chem.Technol, **1998**, 71, 520,.
- [51]. S.Wolff, Rubber Chem. Technol.,**1996**,69,325.
- [52]. Morton, Editor;Rubber Technology, Van Nostrand Reinhold Co., New York, **1987**, 3rd ed., 631.
- [53]. I. Medalia, G.Kraus;In Science and Technology of Rubber, Eds., J. E.Mark , B.Erman, and R. F.Eirich, Academic Press, New York, **1994**, 387.
- [54]. S.Blow, In Handbook of Rubber Technology, Editor, S.Blow, Galgotia Publication Ltd, New Delhi, **1998**, 483.
- [55]. C.N.R. Rao, A.Müller, A.K.Cheetham; Nanomaterials – An Introduction,*The Chemistry of Nanomaterials: Synthesis, Properties and Applications*,Wiley-VCH, Weinheim,**2004**.
- [56]. K.J.Klabunde; Ed. *Nanoscale Materials in Chemistry*, Wiley and Sons, New York., **2001**.
- [57]. R.Kelsall, I.Hamley, M.Geoghegan; *Nanoscale Science and Technology*, Wiley and Sons, Weinheim,**2005**.
- [58]. K,Okuyama, I. W. Lenggoro;Chem Eng Sci,**2003**, 58, 537.
- [59]. K.Wagner, S.Pratsinis; *Powd. Technol.* **2005**, 150, 117.
- [60]. M .Singhal, V .Chhabra, P. Kang, D. O. Shah; Mater. Res. Bull,**1997**, 32, 239.
- [61]. T. Tsuzuki, P. G. McCormick; Scripta Mater,**2001**, 44, 1731.
- [62]. H.Yang, Z.Rongrong Shi, X.Li, X.Dong, Y.Yu; *J. of Alloys. Comp.*, **2005**,413(1-2), 302.
- [63]. J. M. Wang, L .Gao ;Inorg. Chem. Commun., **2003**,6,877.
- [64]. Y.W. Koh, M.Lin, C. K. Tan, Y. L. Foo, K. P. Loh; J. Phys. Chem B,**2004**,108,11419.

- [65]. W. D. Yu, X. M. Li, X. D. Gao; *Cryst. Growth Des.*, **2005**, *5*, 151.
- [66]. Hu, Y. J. Zhu, S. W. Wang ; *Mater. Chem. Phys*, **2004**, 421.
- [67]. J .H. Kim, W. C. Choi, H. Y. Kim, Y. Kang, Y.K. Park ; *Powder Technol.*, **2005**, 153,166.
- [68]. L. N. Wang, M .Muhammed, *J. Mater. Chem.*, **1999**, *9*, 2871.
- [69]. S. C. Lyu et al.; *Chem. Phys. Letters*, **2002**, 363,134.
- [70]. W. J. Li, E. W. Shi, W. Z. Zhong , Z .Yin ; *J. Cryst. Growth*, **1999**, 203,186.
- [71]. B. G. Wang, E.W. Shi , W. Z. Zhong ; *Cryst. Res. Technol.*, **1998** ,33, 937.
- [72]. C. H. Lu, C. H. Yeh; *Ceram. Int.*, **2000**, 26, 351.
- [73]. M. C. Neves, T .Trindade, A. M. B. Timmons, J. D. Pedrosa; *Mater. Res. Bull.*, **2001**, 36, 1099.
- [74]. U. Pal , P .Santiago ; *J. Phys. Chem. B*, **2005**, 109, 15317.
- [75]. Vayssieres.L; *Adv. Mater.*, **2003**, 15, 464.
- [76]. J. Q. Hu, Q .Li, N. B. Wong, C. S. Lee and S. T. Lee ; *Chem. Mater.*, **2002**, 14, 1216.
- [77]. Y. Sun, G. M. Fuge, N. A. Fox, D .J .Riley and M. N. Ashfold ; *R. Adv. Mater.* **2005** ,17, 2477.
- [78]. Y. H. Ni, X. W. Wei, X .Ma , J. M .Hong; *J. Cryst. Growth*, **2005**, 283, 48.
- [79]. 203.199.213.48/1041/1/Physical_and_chemical_methods.pdf
- [80]. M. Alexandre, P. Dubois; *Mater. Sci. Eng.*, **2000**, 28,1.
- [81]. S. Yariv, H. Cross; Eds., *Organo-Clay Complexes and Interactions*, Marcel Dekker, New York, **2002**.
- [82]. H .Van Olphen; *An introduction to Clay Colloid Chemistry*, Wiley, New York, **1973** , 2nd ed.
- [83]. J.E. Mark; *Polym. Eng. Sci.* **1996**, 36, 2905.
- [84]. J. Wen, G.L. Wilkes; *Chem. Mater.*, **1996**, 8, 1667.
- [85]. T. Von Werne, T.E. Patten; *J. Am. Chem. Soc.*, **1999**, 121, 7409.

- [86]. P.Calvert; Carbon Nanotubes, Editor, T.W. Ebbesen, CRC Press, Boca Raton, **1992**.
- [87]. M.S.Dresselhaus , P.Dresselhaus Avouris ;Carbon Nanotubes : Synthesis, Structure, Properties and Applications, Topics of Applied Physics, Eds., Springer-Verlag, Heidelberg, **2001**,80.
- [88]. V.Favier, G.R. Canova, S.C.Shrivastava, J.Y. Cavaille.; Polym. Eng. Sci., **1997**, 37, 1732.
- [89]. L.Chazeau, G.R.Canova, J.Y. Cavaille, R .Dendievel, B.Boutherin; J. Appl. Polym. Sci., **1999**, 71, 1797.
- [90]. F.Nastase, IoanStamatin, D. Claudia Nastase, D.Mihaiescu, A.Moldovan; Prog. Solid State Chem., **2006**, 34, 191.
- [91]. D.Qi, Y.Bao, Z.Weng , Z.Huang;Polymer,**2006**, 47, 4622.
- [92]. Pratheep Kumara, D. Depana, N. Singh Tomerb, R. Singha; Prog. Polym. Sci.,**2009** ,34, 479
- [93]. X.Yang, T.Dai, Y. Lu;Polymer, **2006**, 47, 441.
- [94]. Z. Wang, E. Han , W. Ke;Polym. Degrad. Stab. **2006**, 91, 1937.
- [95]. S.Patel, A.Bandyopadhyay, V. Vijayabaskar., A.K. Bhowmick; Polymer, **2005**, 46, 8079.
- [96]. Bandyopadhyay, M. D. Sarkar, A.K. Bhowmick, J. Appl.Polym. Sci.,**2005**, 95,1418.
- [97]. G.Heinrich & T.A. Vilgis; Polym. Net.. Macromolecules., **1993**,26, 1109.
- [98]. S.Westermann, M.Krutschmann, W.P. Hintzen, et al.; Macromolecules, **1999**,32, 5793.
- [99]. Al.Nakatani, W.Cen, R.C.Schmidt et al.; Polymer,**2001**, 42, 3713.
- [100]. A.Usuki, , A.Tukigase, M.Kato;Polymer, **2002**, 43,2185.
- [101]. M.Arroyo, M.A. Lopez-Manchado, and B. Herrero; Polymer, **2003**,44, 2447.
- [102]. M.D. Frogley, D.Ravich, H.D. Wagner; Compo. Sci.Technol.,**2003**, 63,1647.

- [103]. H.Zheng, Y.X.Zhang. et al.; Polym.Test., **2004**,23, 217.
- [104]. A.Okada, A.Usuki, T.Kurachi, O.Kamigaito;Hybrid organic-inorganic composites (eds J.E.Mark, C.Y.C. Lee, and P.A. Bianconi), ACS Symposium Series 585, ACS, Washington, D.C, Nanocomposites: State of the Art, New Challenges and Opportunities ,**1995**.
- [105]. Y.T.Vu, J.E.Mark, L.H.Pham, M.Engelhardt, J. Appl.Polym. Sci., **2001**,82, 1391.
- [106]. C.Nah, H.J Ryu, S.H. Han;Polym. Int.,**2001**,50, 1265.
- [107]. Z.Chen, and K.Gong; J. App.Polym.Sci.,**2002**,84, 1499.
- [108]. S.Varghese, J.Karger-Kocsis, K.G Gatos; Polymer, **2003**,44, 3977.
- [109]. M.A.Lopez-Manchado, J.Biagiotti, L.Valentini, J.M. Kenny; J.Appl. Polym.Sci., **2004**, 92, 3394.
- [110]. J.C.Gonzalez, H. Retsos,Verdejo et al;Macromolecules, **2008**,41, 6763.
- [111]. Y.Liang, W.Cao, Z.Li, et al.; Polym. Test.,**2008**,27, 270.
- [112]. Q.Liu, Y.Zhang, and H.Xu; Appl. Clay Sci., **2008**, 42, 232.
- [113]. H.Ismail, and R.Ramli; J. Reinf. Plastic Comp.,**2008**,27, 1909.
- [114]. X.Wang, A.Huang, D.Jia, and Y.Li;Euro. Polym. J., **2008**,44, 2784.
- [115]. M.Ganter, W.Gronski, P.Reichert and R.Mulhaupt ;Rubber Chem.Technol. ,**2000**,74, 221.
- [116]. M.Pramanik,, S.K.Srivastava, B.K.Samantaray, and A.K. Bhowmick; J.Appl.Polym.Sci,**2003**,87, 2216.
- [117]. H.S.Jeon, J.K.Rameshwaram, G.Kim, and D.H Weinkauff; Polymer,**2003**, 44, 5749.
- [118]. R.Stephen, S.Thomas, K.V.S.N.Raju et al.;RubberChem.Technol., **2007**,80, 672.
- [119]. R.Stephen, S.Varghese, K.Joseph and Z.Oommen; J. Membrane Sci., **2006**,286, 162.

- [120]. R. Stephen, C.Ranganathaiah, S.Varghese et al.; *Polymer*,**2006**,47, 858.
- [121]. R.Stephen, R. Alex, T.Chерian et al.; *J.Appl.Polym.Sci*,**2006**,101, 2355.
- [122]. L.Zhang, Y.Wang, Y.Wang et al.; *J.Appl.Polym.Sci*, **2000**,78,1873.
- [123]. Y.Wang, H.Zhang, Y.Wu et al.; *J. Appl.Polym. Sci.*, **2005**,96, 324.
- [124]. Y.P.Wu, L.Q. Zhang, Wang, et al.; *J. Appl.Polym. Sci.*,**2001**,82, 2842.
- [125]. Y.Wang, L.Zhang, C.Tang, and D.Yu;*J.Appl.Polym.Sci.*,**2000**,78, 1879.
- [126]. Q.X. Jia, Y.P.Wu, Y.Q.Wang, et al.;*Comp. Sci.Technol.*,**2008**,68, 1050.
- [127]. M.Du, B.Guo, Y.Lei, et al.;*Polymer*, **2008**,49, 4871.
- [128]. M.Xiong, L.Wu, S.Zhou, and B.You; *Polym. Int.*,**2002**,51, 693.
- [129]. Z.Pu, J.E.Mark, J.M.Jethmalani, and W.T. Ford; *Chem. Materials*, **1997**,9, 2442.
- [130]. Y.P.Wu, Y.Q.Wang, H.F.Zhang et al.; *Comp. Sci.Technol.*, **2005**,65, 1195.
- [131]. H.M.Jeong, M.Y.Choi and Y.T.Ahn; *Macromol. Res.*, **2006**,14, 312.
- [132]. M.Zanetti, G.Camino, R.Thomann, and R.Mulhaupt; *Polymer*, **2001**,42, 4501.
- [133]. V.Arrighi, I.J.McEwen, H.Qian, and M.B.S.Prieto; *Polymer*,**2003**,44, 6259.
- [134]. Y.Chen, S.Zhou, H.Yang, L.Wu; *J.Appl.Polym.Sci.*; **2005**,95, 1032.
- [135]. H.U.Jeon, D.H.Lee, D.J.Choi et al.; *J.Macromol. Sci.Part B, Phys.*,**2007**,46, 1151.
- [136]. Q.X.Jia, Y.P.Wu, M.Lu et al.; *Comp. Interfaces*,**2008**,15, 193.
- [137]. S.Joly, G.Garnaud, R.Ollitrault, and L.Bokobza; *Chem.Mater.*, **2002**,14, 4202.
- [138]. R.Magaraphan, W.Thaijaroen, and R.Lim-Ochakun, *Rub. Chem.Technol.*, **2003**,76, 406.
- [139]. M.A. Lopez-Manchado, M.Arroyo, B. Herrero, J. Biagiotti; *Polym.Int.*, **2004**,53, 1766.

- [140]. Y.Wang,H.Zhang,Y.Wu,etal.;J.Appl.Polym.Sci.,**2005**,96, 318.
- [141]. S.Varghese, K.G. Gatos, A.A.Apostolov, and J.Karger-Kocsis;J. Appl. Polym. Sci.; **2004**,92, 543.
- [142]. M.A. Lopez-Manchado, M.Arroyo, B.Herrero, J.Biagiotti; J.Appl. Polym.Sci, **2003**,89, 1.
- [143]. S.Varghese, and J.Karger-Kocsis; J.Appl.Polym.Sci., **2004**,**91**, 813.
- [144]. P.L.Teh, Z.A.Mohd Isak, A.S.Hashim,etal.; J.Appl.Polym.Sci.; **2006**,100, 1083.
- [145]. M.Ganter, W.Gronski, H.Semke et al.;Kautschuk Gummi Kunststoffe, **2001**,54, 166.
- [146]. S.Sadhu, and A.K.Bhowmick; Rub.Chem.Techn.; **2003**,76, 860.
- [147]. S.Sadhu, and A.K.Bhowmick; J.Appl.Polym.Sci,**2004**,92,698.
- [148]. Y.Wang,H.Zhang,Y.Wu,etal.;J.Appl.Polym.Sci.,**2005**, 97, 844.
- [149]. Q.X.Jia, Y.P.Wu, Y.L.Xu et al.;Macromol.Mater.Eng.,**2006**.291, 218.
- [150]. A.Mousa and J.Karger-Kocsis, Macromol.Mater.Eng.,**2001**,286, 260.
- [151]. F.Schon,W.Gronski; Kautschuk Gummi Kunststoffe,**2003**,56, 166.
- [152]. Y.Kojima,K.Fukumori, A.Usuki et al.; J.Mater.Sci.Lett.,**1993**,12, 889.
- [153]. Y.P.Wu, Q.X. Jia, D.S.Yu,and L.Q. Zhang;J.Appl.Polym.Sci,**2003**,89, 3855.
- [154]. J.T.Kim, D.Y.Lee, T.S.Oh, D.H. Lee; J.Appl.Polym.Sci.,**2003**,89, 2633.
- [155]. J.T.Kim,T.S.Oh,D.H.Lee;Polym.Int.,**2003**,52,1058.
- [156]. J.T.Kim,T.S.Oh,D.H.Lee;Polym.Int.,**2003**,52,1203.
- [157]. C.Nah,H.J.Ryu,W.D.Kim,Y.W.Chang;Polym.Int.;**2003**,52,1359.
- [158]. H.Zheng, Y.Zhang, Z.Peng, Y.Zhang;J.Appl. Polym. Sci.,**2004**,92, 638.
- [159]. K.G.Gatos, R.Thomann, J.Karger-kocsis;Polym.Int.,**2004**,53, 1191.
- [160]. M.Pramanik, , S.K.Srivastava, B.K.Samantaray, and A.K. Bhowmick; J. Polym. Sci.Part B Polym.Phy., **2002**, 40, 2065.

- [161]. S.K.Lim, J.W.Kim,I.J.Chin, H.J.Choi;J.Appl.Polym.Sci.,**2002**,86, 3735.
- [162]. J.Karger-Kocsis, C.M. Wu; Polym. Eng.Sci.,**2004**,44, 1083.
- [163]. R.Sengupta, S.Chakraborty, S.Bandyopadhyay, et al.;Polym. Eng.Sci., **2007**, 47, 1956.
- [164]. L.Bokobza;Polymer, **2007**,48, 4907.
- [165]. L.Bokobza,N.E. El Bounia;Compos.Interface, **2008**,15, 1.
- [166]. L.Bokobza, and C.Belin, J.Appl.Polym.Sci, **2007**,105, 2054.
- [167]. M. Kolodziej, L.Bokobza, J.L.Bruneel;Compos.Interface, **2007**, 14, 215.
- [168]. L.Bokobza, M.Kolodziej; Polym. Int.,**2006**,55, 1090.
- [169]. L.Bokobza, M.Rahmani, C.Belin et al.;J.Polymer Science Part B Polymer Physics, **2008**,46, 1939.
- [170]. [Q.Zhao, R.Tannenbaum,and K.I.Jacob; Carbon, **2006**,44,1740.
- [171]. K.Kuesseng and K.I.Jacob ;Euro. Polym.J.,**2006**,42, 220.
- [172]. G.Sui,W.H. Zhong,X.P.Yang,and Y.H.Yu; Mater. Sci.Eng.,**2008**, 485, 524.
- [173]. A.Fakhru'l-Razi, M.A.Atieh,N.Girun et al.;Compos. Str.,**2006**,75, 496.
- [174]. G.Suil, W.H. Zhong, X.P.Yang et al.; Polym. Adv. Technol., **2008**,1163.
- [175]. G.Sui,W.H.Zhong,X.P.Yang,Y.H.Yu,S.Zhao;Macromol.Mater. Eng.,**2007**,292, 1020.
- [176]. J.D.Wang,Y.F. Zhu,X.W.Zhou et al.;J.Appl.Polym.Sci,**2006**,100, 4697.
- [177]. X.Zhou,Y.Zhu,Q.Gong,and J.Liang;Mater. Lett.,**2006**, 60, 3769.
- [178]. X.Zhou,Y.Zhu and J.Liang;J.Appl.Polym.Sci,**2007**,106, 1836.
- [179]. D.Felheos, J.Karger-Kocsis,D.Xu;J. Appl. Polym.Sci.,**2008**,108, 2840.
- [180]. L.Valentini, J.Biagiotti, J.M.Kenny and M.A. Lo'pez Manchado;J. Appl. Polym.Sci., **2003**,89, 2657.
- [181]. Y.C.Jung, N.G.Sahoo and J.W.Cho;Macromol.Rapid Commun.,**2006**,23, 126.

- [182]. T.L.Wang, C.G.Tseng;J.Appl.Polym.Sci.,**2007**,105, 1642.
- [183]. X.Wang,Z.Du,C.Zhang et al.;J. Polym. Sci.Part A Polym.Chem.,**2008**,46, 4857.
- [184]. R.N.Jana, J.W.Cho;J.Appl.Polym.Sci.,**2008**,108, 2857.
- [185]. F.Buffa,G.A.Abraham,B.P.Grady and D.Resasco;J. Polym. Sci. Part B Pol. Phys.,**2007**, 45, 490.
- [186]. J.Xiong,Z.Zheng,W.Songet al.; Compos. Part A Appl. Sci. Manufacturing, **2008**,39, 904.
- [187]. N.G.Sahoo, Y.C.Jung, H.J.Yoo, J.W.Cho;Compos. Sci. Technol., **2007**, 67, 1920.
- [188]. J.Xiong,Z.Zheng, X.Qinet al.;Carbon, **2006**,44, 2701.
- [189]. M.J.Jiang, Z.M.Dang, S.H.Yao,and J.Bai; Chem.Phys.Lett., **2008**,457, 352.
- [190]. M.J.Jiang, Z.M.Dang,and H.P.Xu, Euro. Polym. J.,**2007**,43, 4924.
- [191]. G.T.Kim, E.S.Park;J. Appl. Polym. Sci.,**2008**,109, 1381.
- [192]. S.Bhattacharyya,C.Sinturel, O.Bahloulet al.;Carbon,**2008**,46, 1037.
- [193]. Y.Ikeda,S.Poompradub,Y.Morita, and Kohjiya, J. Sol-Gel Sci.Technol., **2008**, 45, 299.
- [194]. J.Liu,C.Wu, P.Zhang, and S. Zhao;J. Macromol. Sci., Part B Phys., **2008**,47, 689.
- [195]. S.Hui,T.K.Chaki and S.Chattopadhyay,J. Appl. Polym. Sci.,**2008**,110, 825.
- [196]. W.Bai, K.Li;Composites Part A;**2009**,40,1597.
- [197]. M.Arroyo, M.A. Lopez-Manchado, and B. Herrero; Polymer, **2003**,44,2453.
- [198]. A.K.Ghosh,S.Maiti, B.Adhikari,G.S.Ray, S.K.Mustafi;J.Appl.Polym. Sci.,**1997**;66:683
- [199]. X.Liu, S.Zhao, Y.Yang, X.Zhang, Y.Wu;Polym. Adv. Technol., **2009**, 20,818.
- [200]. L.Qu, G. Huang, P.Zhang, Y.Nie, G.Weng, J.Wu;Polym. Int., **2010**, 59, 1397.

- [201]. Y.Liu, L.Li, Q.Wang;J. Appl.Polym.Sci.,**2010**,118,1111.
- [202]. N.Rattanasom, T.Saowapark, C.Deeprasertkul;Polym. Test., **2007**, 26,369.
- [203]. S.Sahoo and A.K.Bhowmick;Rubber Chem.Technol.,**2007**,80, 826.
- [204]. L.Liu,M.Tian,W.Zhang et al.;Polymer,**2007**,48, 3201.
- [205]. H.Angellier, S.Molina-Boisseau, L.Lebrun, and A.Dufresne; Macromolecules, **2005**,38, 3783.
- [206]. S.Mishra and N.G.Shimpi,;J.Appl.Polym.Sci,**2007**,104, 2018.
- [207]. J.Wang,X.Zheng,E.Y.Chen,Z.Lu,Z.Zhu;J. Elast.Plast. **2009**,41,263.
- [208]. G.Zhao , L.Shi , D.Zhang, X.Feng , S.Yuan , J.Zhuo;J.mad., **2012**, 35, 847.
- [209]. RapraHandbook, Particulate filled polymer composites, 2nd Ed. J. F.Chen ;Inorganic nanoparticle filled nano composites ,Research Centre of the Ministry of Education for High Gravity Engineering & Technology, Dec. **2002**.
- [210]. S.Tsutsui;Ultrafine Precipitated Calcium Carbonate & its Function as Rubber Additive,Shirashi Central Laboratories Co.Ltd.,Nippon Gomu Kyokaishi, **2005**,78, 218
- [211]. G.Chen, G. Luo, Xu, J.Wang; Pow.Technol.,**2005**,153,90.
- [212]. M.L.J.Van-Leuween, Precipitation and Mixing, Dissertation, Delft Technical University;**1998**.
- [213]. R.S. Bottrill,C.C.J.Burton; Rosebery Zinc-Lead-Copper Orebody. Economic Geology of Australia and Papua New Guinea, 1. Metals, **1975**, 619.
- [214]. D.I.Groves;Madam Howard Plains Barytes Deposit. Technical Reports No. 8.Tasmania Department of Mines, **1964**.
- [215]. Anon; The Catalogue of the Minerals of Tasmania. Geological Survey Record No. 9,Tasmania Department of Mines. **1970**
- [216]. W.D.Birch;(Ed) Zeolites of Victoria. The Mineralogical Society of Victoria, **1989**, 2.
- [217]. C.Adherold,Krefeld,H.J.Rohrborn;US patent, 4894093,Jan.16,**1990**.

- [218]. S.Grothe,P.Fritzen,J.Winkler,B.Rohe;US Patent,0326114,Dec.31,**2009**.
- [219]. A.Poppe,D.Mlkolajetz,F.Hardinghaus,J.Park,K.Kohler,R.Stahl,D.C.Glende;
US Patent,0167535 Jul.19,**2007**
- [220]. Protective lining by the Protective Lining Applicators- a subdivision of the
Rubber Manufacturers Association, Rubber Manufacturers Association, **1975**
Washington DC.
- [221]. M. L. Berins, Plastics Engineering Hand book of the Society of Plastics
Industry Inc,Chapman&Hall, NY, **1991**.
- [222]. Hishfeld and Pison, Transactions of the American Society of Mechanical
Engineers, **1937**,59,471.
- [223]. Kenneth, N.Solenjohn,Harb, Chemical Process-Fundamental and Design,
Fourth Edition, McGraw Hill Companies Inc. US, **2005**.
- [224]. Blair rubber company's catalogues ,www.blairrubber.com
- [225]. Andrew Holmes, Siedle and Len Adams, HandBook of Radiation Effects.
Second Edition,Oxford university Press IncNY, USA, **2002**.

.....*✍*.....

MATERIALS AND EXPERIMENTAL METHODS

- 2.1 *Materials*
- 2.2 *Experimental*
- 2.3 *Characterization methods*

2.1 Materials

2.1.1 Elastomers

a) Natural rubber (NR)

The natural rubber used in the study was solid block rubber ISNR-5 of Mooney viscosity ML (1+4) at 100°C = 85, obtained from the Rubber Research Institute of India, Kottayam. The Bureau of Indian Standards specifications for the grade of rubber are given below

Parameter	Value
Dirt content, % by mass (max.)	0.05
Volatile matter, % by mass (max.)	0.80
Nitrogen, % by mass (max.)	0.60
Ash content, % by mass (max.)	0.60
Initial plasticity, Po (min.)	30.00
Plasticity retention Index (PRI) (min.)	60.00

b) **Isobutylene-isoprene rubber (IIR):** The detailed properties obtained from the technical brochure of Polysar butyl Exon: 301 are as follows:

Parameter	Value
Isobutene content	98wt%
Isoprene	2wt%
Molecular weight distribution	Narrow
Mooney viscosity, ML(1+8) 125°C	51MU
Ash content at 550 °C	>0.4%
Volatile matter	0.3%

c) Ethylene-propylene-diene monomer rubber (EPDM)

Nordel IP - 4640 hydrocarbon rubber, a product of Dupont dow elastomers was supplied by Vajra rubber products, Thrissur. The other properties of EPDM are as given below.

Parameter	Value
Mooney Viscosity, ML (1 + 4)at 125° C	40
Ethylene ,mass%	55
Propylene, mass%	40
ENB,mass%	5
Molecular weight distribution	Medium
Product Density, g/cc	0.86
Product Form	bale

2.1.2 Fillers used

a) Commercial Barium sulphate(precipitated)

Barium sulphate used for the study was obtained from Merck India, cochin Ltd.

b) High abrasion furnace black (HAF, N330)

High abrasion furnace black (N330) used in the study was supplied by M/s Philips carbon black India Ltd., Kochi, India. It had the following specifications.

Parameter	Value
Appearance	Black granules
DBP absorption	102 cc/100g
Pour density	376 Kg/m ³
Iodine number	82

2.1.3 Accelerators used

a) N-Cyclohexyl-2-benzothiazolesulfenamide (CBS)

CBS was obtained from Merchem Ltd., Cochin, India. The specification of CBS is given below,

Parameter	Value
Appearance, Colour	Pellets, Off white
Melting point	103°C
Flash point	177°C
Density(25°C)	1200Kg/m ³
Bulk density	540-580 Kg/m ³

b) Tetramethylthiuram disulfide (TMTD)

TMTD was obtained from Merchem Ltd., Cochin, India. The specification of TMTD is given below,

Parameter	Value
Parameter	Value
Appearance, Colour	White powder, Light cream
Melting point	136°C
Specific gravity	1.4

c) Zinc diethyldithiocarbamate (ZDEC)

ZDEC was obtained from Merchem Ltd., Cochin, India. The specification of ZDEC is as follows

Parameter	Value
Appearance	White powder
Melting point	172°C

2.1.4 Plasticizers used

a) Paraffinic oil

M/s. Hindustan Petroleum Ltd., India, supplied paraffinic oil. It had the following specifications

Parameter	Value
Viscosity gravity constant (VGC)	0.85
Aniline point	96°C

b) Aromatic oil

Aromatic oil was supplied by M/S.Hindustan Organic Chemicals (with specific gravity 0.95-0.98), Cochin. It had the following specifications.

Parameter	Value
Aniline point	38°C
Viscosity gravity constant	0.91

c) Naphthenic oil

Obtained from M/S.Hindustan Organic Chemicals, Cochin. It had the following specifications.

Parameter	Value
Aniline point	38°C
Viscosity gravity constant	0.85-0.9

2.1.5 Antioxidants**a) Vulkanox HS**

Commercial antioxidant vulkanox HS (1, 2-dihydro-2, 2, 4-trimethyl quinoline, polymerized) was obtained from Bayer India Ltd. Mumbai, It is having a specific gravity of 1.1

b) Para-phenylenediamine derivative

6PPD [N- (1, 3-dimethyl butyl)-N'-phenyl-p-phenylenediamine], was obtained from NOCIL Ltd., Thane, India and had a melting point of 141°C.

2.1.6 Other compounding ingredients used**a) Zinc oxide (ZnO)**

Zinc oxide (activator) was supplied by M/s Meta Zinc Ltd., Mumbai and had the following specifications.

Parameter	Value
Specific gravity	5.5
Zinc oxide content (%)	98
Heat loss, max (2h at 100°C)	0.5%

b. Stearic acid

Stearic acid (co-activator) was supplied by Godrej soaps Pvt. Ltd., Mumbai and had the following specifications.

Parameter	Value
Specific gravity	0.85
Melting point	50-69°C
Acid number	185-210
Iodine number	9.5
Ash content	0.1%

c) Sulphur

Sulphur (crosslinking agent), was supplied by Standard chemicals Co. Pvt. Ltd., Chennai and had the following specifications.

Parameter	Value
Specific gravity	2.05
Acidity, max	0.01%
Ash, max	0.015%
Solubility in CS ₂	98%

2.1.7 Solvents used

a) Toluene

Toluene was supplied by SD Fine chemicals Ltd., Mumbai and had the following specifications.

Parameter	Value
Boiling point	95°C
Acidity	0.012
Alkalinity	0.012
Non-volatile matter	0.002%

b) Sulphuric acid

AR grade sulphuric acid used for the preparations was supplied by Qualigens Fine Chemicals. It had the following specifications.

Parameter	Value
Molecular Weight	98.08
Assay (acidimetric),%	97-99
Wt. per ml at 20°C, (g)	1.835

2.2 Experimental

2.2.1 Mixing and homogenization of the compound

Mixes were prepared on a laboratory size two roll mixing mill (Santosh, SMX lab 613) (6 x 12 inch) as per ASTM D 3182–89(2011) [1] at a friction ratio of 1:1.25. The mill opening was set at 0.2 mm and the elastomer was passed through the rolls twice without banding. This was then banded on the slow roll with mill opening at 1.4 mm and was increased to 1.9 mm as the band became smooth. The temperature of the rolls was maintained at 70 ± 5 °C. The compounding ingredients were added as per procedure given in ASTM D 3184–89 and ASTM D 3182–89 in the following order: activator, filler, accelerator and curing agents. Before the addition of accelerator and sulphur, the batch was thoroughly cooled. After mixing all the ingredients, homogenization of the compound was carried out by passing the rolled stock end wise six times at a mill opening of 0.8 mm. The mill was opened to give a minimum stock thickness of 6 mm and the stock was passed through the rolls four times folding it back on itself each time and kept for 24 hours for maturation.

2.2.2 Cure characteristics

The cure characteristics of the mixes were determined using Rubber Processing Analyser, RPA 2000 supplied by Alpha Technologies, USA, as per ASTM D 2084-01 [2]. It is a computer controlled torsional dynamic rheometer with a unique test gap design, an advanced temperature control system and fully automated operation modes. A biconical die with a die gap of 0.487 mm was used to achieve a constant shear gradient over the entire sample chamber. The sample of approximately 5 g was placed in the lower die that is oscillated through a small deformation angle $\pm 0.2^\circ$ at a frequency of 50 oscillations per minute. The torque transducer on the upper die senses the forces being transmitted through the rubber.

Subsequently, the rubber compounds were vulcanized up to the optimum cure time at a pressure of 200 Kg/cm². The mouldings were cooled quickly in water at the end of the curing cycle and stored for maturation in a cool dark place for 24 h prior to physical testing.

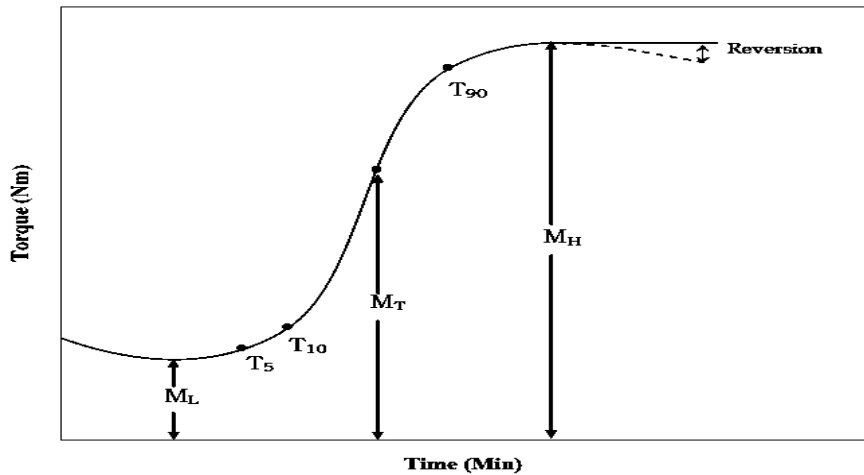


Figure 2.1 Typical cure curve obtained from RPA 2000

The following data can be taken from the time-torque curves. (Fig. 2.1)

- Minimum torque (D_{\min}): Measure of the stiffness of unvulcanized test specimen. It is the torque shown by the mix at the test temperature before the onset of cure.
- Maximum torque (D_{\max}): Measure of the stiffness or shear modulus of the fully vulcanized test specimen at the vulcanization temperature. It is the torque recorded once curing of the mix is completed.
- Scorch time (T_{10}): It is the time taken for attaining 10% of the maximum torque.
- Optimum cure time (T_{90}): Time taken for attaining 90% of the maximum torque. It is the time corresponding to a torque = $0.9(D_{\max} - D_{\min}) + D_{\min}$.
- Cure rate index (CRI): It is a measure of the rate of cure and was calculated using the formula, $CRI = 100 / (T_{90} - T_{10})$

2.2.3 Filler dispersion

a) Lee's approach :

The dispersion of filler within the matrix and formation of filler agglomerates were studied in detail by B.L.Lee[3]. This method is applicable for carbon black composites. In Lee's approach a new parameter 'L' is introduced which is defined as

$$L = \eta_r - M_r \quad (2.1)$$

Where $\eta_r = D_{\min}^f / D_{\min}^0$ and $M_r = D_{\max}^f / D_{\min}^0$, where D denotes the torque and the superscripts f and 0 are related to the loaded and unloaded polymer, respectively.

For ideal dispersions of fillers, $\eta_r = M_r$. This happens when the individual particles are well dispersed in the matrix. In the case of non-ideal dispersions, the value of L changes slowly at low filler loadings, but above a certain limit, it increases sharply. The rapid rise of the index L at high filler loadings may be ascribed to the predominance of agglomerates remaining relatively undispersed in the rubber matrix. In such a situation, it is assumed that the filler concentration has now reached the point where there is not enough rubber to fill the available voids in the filler.

b) Westlinning-Wolff's equation:

A mathematical expression has been proposed by Wolf in terms of rheometric data to characterize the filler structure present in rubber vulcanizates [4,5]. When a filler is incorporated into a compound, the maximum torque variation, observed during vulcanization increases.

$$\Delta D^f = D_{\max}^f - D_{\min}^f \quad (2.2)$$

The ratio between ΔD^f and ΔD^0 i.e., the torque variations for the loaded and unloaded compounds, respectively, is directly proportional to filler loading

by plotting the relative torque as a function of filler loading, a straight line is obtained whose slope was defined by Wolf as α_f , according to Westlinning-Wolff's equation given below .

$$(D_{\max}^f - D_{\min}^f) / (D_{\max}^0 - D_{\min}^0) - 1 = \alpha_f (mf/mp) \quad (2.3)$$

where mp is the mass of polymer in the compound and mf is the mass of filler in the compound and α_f is a specific constant for the filler, which is independent of the cure system and closely related to the morphology of the filler. The parameter α_f represents the final structure of the filler as it exists in the vulcanizates after all possible structure breakdowns that occurred during mixing and vulcanization. The reinforcement build-up and crosslinking reaction both take place during curing without affecting each other. The application of equation allows the definition of a filler specific constant, related to the filler structure, and also predicts whether or not crosslink density is unaffected by the presence of the filler, in which case, a straight line is obtained. The equation also shows that based on a single test, α_f can be calculated from the changes in the torque which occur during vulcanization of two compounds, the unloaded and loaded composition [6-9].

2.2.4 Strain-sweep studies

The strain sweep measurements on green compound were conducted to study the rubber-filler interaction. Rubber Process Analyzer (RPA 2000-Alpha Technologies) is a purposely modified commercial dynamic rheometer [10]. Such instrument was modified for capturing strain and torque signals, with the assistance of appropriate software. Filled rubber compounds exhibit strong non-linear viscoelastic behaviour, the well-known Payne effect, i.e., the reduction of elastic modulus with increasing strain amplitude [11]. RPA can do strain sweep tests in which the variation of storage modulus (G'), loss modulus (G'') and complex modulus (G^*) with change in strain amplitude are measured. With respect to its measuring principle, the RPA cavity must be loaded with a volume excess of test

material. According to ASTM D 5289, the manufacturer recommends to load samples of about 5.0 g (4.4 cm³) for a standard filled rubber compound with a specific gravity of 1.14 g/cm³. Samples for RPA testing were consequently prepared by die cutting 46 mm diameter disks out of around 2 mm thick sheets of materials. The testing temperature was selected as 100⁰C; a temperature below the curing temperature and the shear strain was varied from 0.5 to 100% keeping the frequency measurements at 0.5 Hz.

For strain sweep studies of the cured samples, uncured samples were taken and immediately after a cure cycle at their optimum cure times within the RPA cavity strain sweep at 60⁰C was carried out.

2.2.5 Vulcanization

Vulcanization of various test samples marked with mill grain direction were carried out on an electrically heated hydraulic press(Santosh, SMP-50) having 45cm x 45cm platen at corresponding curing temperatures at a pressure of 200 kg /cm² on the mould(15cm x15cm x 2cm) up to optimum cure times as obtained from RPA. After curing, pressure was released and stripped off sheets were cooled immediately by plunging into cold water, removed and stored in a dark place for 24 h, prior to testing.

2.3 Characterization methods

The following characterization methods were adopted for the vulcanizates.

2.3.1 Physical testing

a) Stress-strain properties

The measurements were carried out on a Shimadzu Universal testing machine (10 KN) with a grip separation of 40 mm, using a crosshead speed of 500 mm / min in agreement with ASTM D 412 [12].The tensile strength, elongation at break and modulus at different elongations were determined using dumb-bell shaped specimens punched out from the vulcanized sheets.

b) Tear resistance

Tear resistance of the samples were tested in agreement with ASTM D 624-1998, using un-nicked 90° angle test specimens that were punched out from the moulded sheets, along the mill grain direction. The measurements were carried out at a crosshead speed of 500mm per minute on a Shimadzu Model Universal testing machine according to ASTM D 412-68 and D 624-54 respectively. The tear strength was reported in N/mm.

c) Hardness

The hardness (Shore A) of the moulded samples was determined as per ASTM D 2240-03[13] using Shore A type Durometer. The tests were performed on unstressed samples of 30 mm diameter and 6 mm thickness. Readings were taken after 15 seconds of the indentation when firm contact has been established with the specimens.

d) Abrasion resistance

The abrasion resistance of the samples was determined using a DIN Abrader (DIN 53,516). Samples having a diameter of 6 ± 0.2 mm and a thickness of 6 mm were kept on a rotating sample holder and a 10N load was applied. Initially a pre run was given for the sample and its weight taken. The weight after final run was also noted. The abrasion loss in cc^3/h was calculated using the formula, (2.4),

$$\text{Abrasion loss} = (\text{weight loss}/\text{specific gravity}) \times (27.27) \quad (2.4)$$

e) Compression set

The samples (1.25cm thick and 2.8cm diameter) in duplicate compressed to a constant deflection (25%) were kept in an air oven at 70 °C for 22h. (ASTM D 395-1998 Method B) [14]. The samples were taken out, cooled to room temperature for half an hour and the final thickness measured. The compression set was calculated using the equation (2.5),

$$\text{Compression set (\%)} = [(T_i - T_f)/(T_i - T_s)] \times 100 \quad (2.5)$$

Where, T_i & T_f are the initial and final thickness of the specimen and T_s is the thickness of the spacer bar used.

2.3.2 Hot air aging studies

Measuring the tensile properties after ageing at 70, 100 °C for 24, 48, 96 hours in a hot air oven to assess resistance of the sample to ageing.

2.3.3 Solvent sorption experiments

Circular specimen of 20 mm diameter and 1 mm thickness were die cut using a sharp edged disc shaped die from the vulcanized rubber sheet. The samples were immersed in airtight diffusion bottles containing about 20 ml of toluene maintained at constant temperature (25°C). Samples were removed periodically and the surface absorbed solvent drops were wiped off carefully by placing them between filter wraps. The weighing was done within 30-40 seconds to minimize the error due to evaporation of other than surface adsorbed liquid. The mass of the sorbed sample was determined immediately on a digital balance with an accuracy of ± 0.01 mg. The weighing was continued till the point of equilibrium swelling is attained. The desorbed weights of the samples were also taken after complete removal of the solvent. The mole percent uptake of the sample is calculated from the diffusion data. The Q_t values were determined as equation (2.6).

$$Q_t = \frac{(\text{Wt. of the solvent sorbed at a given time}) / (\text{Mol. wt. of the solvent})}{(\text{Initial wt. of the rubber specimen} \times 100)} \quad (2.6)$$

At equilibrium swelling Q_t becomes Q_α . The mechanism of diffusion was investigated using the equation (2.7),

$$\log Q_t / Q_\alpha = \log k + n \log t \quad (2.7)$$

The value of k depends on the structural features of polymer, whereas the value of n determines diffusion mechanism. In the Fickian mode, case 1, the value of n is 0.5 and it occurs when the rate of diffusion of penetrant molecules is much less than the relaxation rate of the polymer chains. In case 2 or non-Fickian transport, where the n value is 1, the diffusion is rapid when compared with the simultaneous relaxation. However in the case of anomalous transport where the n value is in between 0.5 and 1, both solvent diffusion and polymer relaxation rate are comparable. The effective diffusivity, D of the rubber solvent system was calculated from the initial portion of the sorption curves using the equation (2.8) [15,16],

$$D = \pi [h\theta/4 Q_{\alpha}]^2 \quad (2.8)$$

Where h is the initial thickness of rubber sample, θ the slope of the linear portion of the sorption curve Q_t versus $t^{1/2}$, The permeation of a solvent into a polymer membrane will also depend on the sorptivity of the penetrant in the membrane. Hence sorption coefficient S has been calculated using the relation (2.9) [17],

$$S = W_s/W \quad (2.9)$$

Where W_s is the weight of the solvent at equilibrium swelling and W the initial weight of the polymer sample. Since the permeability depends on both diffusivity and sorptivity, the permeation coefficient has been determined using the relation(2.10) [18],

$$P = D \times S \quad (2.10)$$

As diffusion is influenced by polymer morphology, the molar mass between cross links M_c from the sorption data is also determined. The rubber solvent interaction parameter χ , which is needed for the estimation, has been calculated using the equation(2.11) [19],

$$\chi = \beta + V_s/RT(\delta_s - \delta_p)^2 \quad (2.11)$$

Where V_s is the molar volume of the solvent δ_s and δ_p are solubility parameters of solvent and polymer taken from the polymer handbook. R is the universal gas constant and T the absolute temperature, β is the lattice constant and is 0.38 in the calculation. Using χ values the molar mass between crosslinks (M_c) of the polymer was estimated from the Flory Rehner equation (2.12) [20,21],

$$M_c = \frac{-\rho_p V_s (V_r)^{1/3} X}{[(\ln(1 - V_r) + (V_r) + X(V_r)^2)]} \quad (2.12)$$

The volume fraction of rubber in the deswollen network was then calculated using the equation (2.13)[22],

$$V_r = \frac{(d - fw)\rho_p^{-1}}{(d - fw)\rho_p^{-1} + A_0\rho_s^{-1}} \quad (2.13)$$

2.3.4 X-ray diffraction analysis

X-ray diffraction finds application in finger print characterization of crystalline materials and their structure determination. It is one of the most magnificent tools for characterization in solid state and realms of material sciences. Powder X-ray diffraction is a standard method for the characterization and has been used to determine the crystalline phases, solid solutions, that are present and to measure the particle size and shape. The XRD patterns of the prepared nano powders i.e., modified and un modified barium sulphate were recorded on a diffractometer Rigaku Geiger flex with nickel filtered Cu $K\alpha$ ($\lambda=1.54 \text{ \AA}$) as a radiation source and at a 2θ scan speed of $1^\circ/\text{min}$ at 30 kV and 20 mA. Monochromatic X-rays, incident on a crystalline solid are diffracted owing to the crystal structure of the solid. For a maximum to occur in the diffraction pattern at a particular angle of incidence θ with respect to lattice planes (hkl), the Bragg equation (2.14),

must be satisfied: $n\lambda=2d\sin\theta$ (2.14)

where, d -interplanar distance between (hkl) planes, n -order of diffraction and λ -wave length of incident X-rays. Crystallite size D was calculated using the Scherrer equation (2.15), where λ -wave length of incident X-rays, 0.9 is shape factor (K), line broadening at half the maximum intensity is the (FWHM) in radians, θ is the Bragg angle.

$$D=0.9\lambda180/\pi\text{FWHM}\cos\theta \quad , \quad (2.15)$$

2.3.5 Infrared Spectroscopy

Infrared spectra are generated by the absorption of electromagnetic radiation in the frequency range 400 to 4000 cm^{-1} by a sample placed in the path of IR beam. Different functional groups and structural features in the molecules absorb energy at characteristic frequencies. It is based on the principle that molecules have specific frequencies at which they vibrate or rotate corresponding to discrete energy levels. The frequency and intensity of absorption are the indication of the bond strength and structural geometry in the molecule. The surface characteristics; i.e., existence of functional groups on the specimens were recorded with Bruker FT-5DX (Nicolet) spectrophotometer (infrared spectra) at wave numbers of $4000\text{--}400\text{ cm}^{-1}$.

2.3.6 Bulk density

Bulk density is defined as the weight per unit volume of a material. It is primarily used for powders or pellets. The test can provide a gross measure of size and dispersion of particles, which can affect material flow consistency and reflect packaging. The measurement requires (ASTM D 1895) a measuring cup, a cylindrical cup of 100 ± 0.5 ml capacity having a diameter equal to half of the height. Typically 39.9 mm inside diameter by 79.8 mm inside height. Funnel, having a 9.5 mm diameter opening at the bottom and mounted at a height 38 mm above the measuring cup. Close the small end of the funnel with hand or a suitable flat strip and pour ($115 \pm 5\text{ cm}^3$) samples into the funnel. Open the bottom of the funnel quickly and allow the material to flow freely into the cup. Weigh the material cup to the nearest 0.1g . Calculate the weight in grams of 1 cm^3 of the material.

2.3.7 BET adsorption

Surface area of the fillers can be determined by the BET method using nitrogen isotherm on a Micromeritics Tristar 3000, surface area and porosity analyzer, at SUD-Chemie Ltd. Edayar, EKM. Surface area was determined using the equation

$$S_{\text{BET}} = 4.353 V_m \quad (2.16)$$

where S_{BET} is the surface area in m^2/g and V_m is the molar volume of adsorbate gas (N_2) at STP.

2.3.8 Thermogravimetric analysis

Thermogravimetric analysis of the samples were carried out in TGA Q-50 thermo gravimetric analyzer (TA Instruments) under nitrogen atmosphere. It is performed to analyse the weight change of samples relative to change in temperature and such an analysis relies upon high precision in measurement of weight, temperature and temperature change. The thermal analyser usually comprises of a high precision balance with a pan loaded with the sample. The sample is in a small electrically heated oven with thermocouple for accurate measurement of temperature. Temperature was gradually increased and a plot of temperature and weight change was made for analytical purpose.

The sample weight varied from 5-10mg. The samples were heated from room temperature to 800°C at a heating rate of $20^\circ\text{C}/\text{min}$ and a nitrogen gas flow rate of 40–60 ml/min, to remove all corrosive gases formed during degradation and to avoid further thermo-oxidative degradation. The onset of degradation temperature, T_i , the temperature at which weight loss is maximum (T_{max}), and residual weight in percentage were evaluated.

2.3.9 Differential scanning calorimetry(DSC)

It is a technique for measuring the energy necessary to establish a nearly zero temperature difference between a substance and an inert reference material, as the

two specimens are subjected to identical temperature regimes in an environment heated or cooled at a controlled rate. Both the sample and the reference are maintained at nearly the same temperature throughout the experiment. The basic principle underlying this technique is that, when the sample undergoes a physical transformation such as phase transition, more (or less) heat will need to flow to it than the reference material to maintain both at the same temperature. Whether more or less heat must flow to the sample depends upon whether the sample is exothermic or endothermic. By observing the difference in heat flow between the sample and the reference, differential scanning calorimeters are able to measure the amount of heat absorbed or released during such transitions.

The sample was sealed in an aluminium pan with a perforated lid. The sample pan was placed in a differential scanning calorimetry cell Q-100, TA instruments calorimeter, under a dry nitrogen purge. The samples (~6mg) nano powders were used in our present study to confirm absence of phase transitions.

2.3.10 Scanning electron microscopy (SEM)

Scanning electron microscope is a very useful tool in polymer research for morphology studies and the procedure helps in detailing the topography, composition and microstructural informations of materials. Scanning electron microscopic studies of the tensile fractured surfaces of the vulcanizates was done on a Scanning electron microscope (JEOL JSM-6390L). In a typical SEM technique, thermionically emitted electrons from tungsten or lanthanum hexaboride cathode are accelerated towards anode. The electron beam moves in a raster fashion scanning the specimen resulting in back scattering of electrons of high energy, secondary electrons of low energy and X-rays. These signals are monitored by detectors (photomultiplier tube) and then magnified. An image of the investigated microscopic region of the specimen is thus observed in a cathode ray tube and photographed.

The SEM photographs reported in this work were made on the fractured surface of the tensile specimens of rubber samples and barium sulphate powders were placed in minute volumes on stub. The specimens were prepared and mounted on a metallic stub with the help of a conductive carbon tape in the upright position. The samples were rendered conductive by ultra thin gold coating before being subjected to SEM.

2.3.11 Transmission electron microscopy

The Transmission electron microscopy (TEM) imaging for the nano powders was carried out using a Transmission Electron Microscope CM-200 of Philips Technology. TEM was used in order to visualize the morphology and particle dimension of the synthesised nanopowders.

2.3.12 Atomic Force Microscopy

The samples were imaged using Nanosurf easy scan 2 operating in contact mode using NSC14/Cr-Au cantilever. The representative scans of the composite surface (each at $70 \times 70 \mu\text{m}^2$) at three different locations were obtained for each sample. Images were recorded in the constant force mode, under ambient conditions in air. In this mode, an electronic feedback circuit maintains a constant cantilever deflection while the tip is scanned over the surface by adjusting the height of the sample. In this way, a three dimensional image is produced by recording the z direction while scanning the sample in the x and y direction. It can also be used for studying filled systems for the shape of filler particles [22], filler distribution and also filler aggregation.

2.3.13 Acid immersion Tests

In order to assess the various parameters influencing the rubber composites in acidic environment, the samples were exposed to acid solutions; two kinds of immersion tests were carried out according to standards available:

- 1). Rubber samples were dipped in different concentrations of acids to assess the weight changes according to the international standard for immersion testing of rubber, dealing with change in weight of rubber samples when they are immersed in corrosive liquids. The testing was carried out at 25⁰C and duration of the test according to specification BS ISO 1817(British Rubber, vulcanized-Determination of effect of liquids, vary as follows: 24hrs, 48hrs, 96hrs, 168hrs and 30 days. The immersion test was carried out in the absence of direct sunlight in order to avoid atmospheric oxidation and the volume of immersion solution was adequate to immerse the sample of rubber. The test pieces were buffed smooth after die cut from rubber lining. The change in volume as well as weight of the test piece specimen after immersion with respect to time is recorded. The test chemicals and reagents used in immersion test are the combinations of following solvents , and the nature of attack are given in Table 1.1. From the results, i.e., the weight percentage obtained after immersion for chosen period of time, the compounds were graded according to the criterion presented in the Table 2.2 below.

Table 2.1 Immersion liquids and nature of attack

Name of chemicals present in medium	Nature	Density	Main type of attack on rubber
Water	Neutral	1.0	Diffusion
Sulphuric acid	Acidic	1.84	Diffusion

Table 2.2 Percentage weight variation of rubber samples over 28 days immersion in liquid media

No:	Variation of weight(%)	Grade	Remarks
1	<1	A	This compound is eminently suitable
2	>1 to <3	B	This compound is also suitable and serves the purpose reasonably.
3	>3 to <4	C	This compound is suitable only when the lining is protected over with brick lining.
4	>4	D	Cannot be recommended for rubber lining at all even with brick lining

- 2). The main field of application of acid resistance of elastomer based compounds is, the realm of acid resistant linings, in which the rubber composites covers the metal surface and provides sacrificial protection to the steel vessels beneath it. For assessing the fate of rubber covered mild steel in acid, cured rubber sheets were adhered on a (5x5)mild steel specimen. Natural rubber sheets were adhered to MS plates coated with chemlok 205 primer, using chemlok 220 as cover coat system. EPDM and butyl rubber were adhered using chemlok 238NW as cover coat system. The method followed in immersion testing of these samples followed one chemical consulting company, Andritz-Ruthner in Vienna, stipulated a method in which the percentage weight is not considered alone but it is combined with the area of the sample as well as the number of days of immersion. According to this procedure, vulcanised rubber sheets completely covered over mild steel(MS) plate samples of (5 x 5)are kept dipped in the chemical media and the weight of the sample in grams during the periods of immersion (of 12 days, 40 days or 80 days) are recorded and referred as 'g'. The days are recorded as 'D'. The surface areas of the samples are noted before commencing the test and this is referred as m^2 .

From the data obtained a graph is plotted as g/m^2 against D or g/m^2 square root of D, against D. For a good quality rubber lining compound, the curve should be as near to the X axis as possible, i.e., it should have a low slope. Similarly, for the same quality of rubber lining the curve drawn with latter X,Y axes will exhibit a rise in the beginning but later on, it should fall off rapidly. Swelling of elastomers by liquid is known to be a diffusion controlled process and up to the equilibrium swelling ratio, the volume of liquid absorbed is proportional to the square root of the time during which the elastomer has been immersed in the liquid. SEM photographs and IR analysis as mentioned in previous sections also assists in accounting degradation[23-24].

2.3.14 Radiopacity studies

In diagnostic radiography, X-rays are produced when high-energy electrons collide with a target in an X-ray tube (Fig. 2.2). In the X-ray tube, by thermionic emission, electrons are generated at the filament end of the X-ray tube. Then a kinetic energy is given to them by applying a high voltage between the filament and the target and, if a voltage of 100,000 volts (100 kVp) is applied to the X-ray tube, the electrons will strike the target producing X-rays with energies ranging from 0 to 100 keV. Here, kVp is the voltage applied to the X-ray tube and keV is the energy of the X-ray. With increasing kVp, the intensity of the X-ray beam increases, i.e., more X-rays of all energies are generated. The energy of the X-rays is determined by the voltage applied to the tube, kVp, quantity of X-rays by the milliamperes (mA) of current flowing in the X-ray tube. The higher the mA, the higher the radiation dose and one of the factors that affect image quality is the number of X-rays reaching the film. The goal is to keep the mA as low as possible and the kVp as high as possible to achieve a compromise between the the number of photons reaching the film and optimum image i.e., the image contrast.

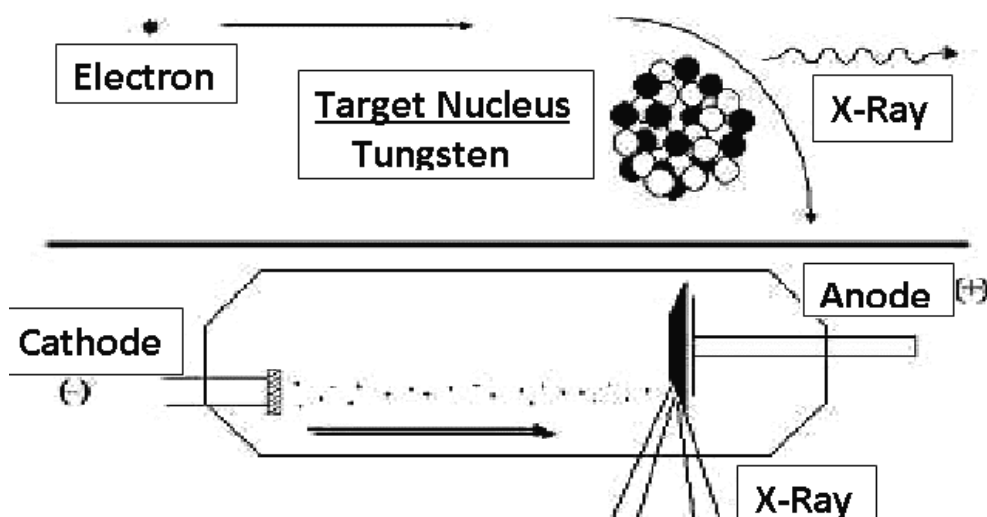


Figure 2.2. Generation of X-rays

Radiopacity of different systems were studied using X-rays from a general clinical X-ray instrument Collimex-II, GE medical systems DXD-300/DX 300 X-ray generator. In this technique, the radiation from X-ray tube is transmitted through the material and reaches the film(Film used : speed class 200, Kodak (BaSrSO₄:Eu, neutral dye in the blue spectral emission). After processing the film (the radiograph) the negative image is obtained. The filled radiopaque NR vulcanizates were compression moulded to 1 cm thick and 60 mm diameter for radiopacity studies.

2.3.14.1 Optical density measurements

The optical density was measured using densitometer. It is a device for determining the degree of darkening of X-ray film or photographic film and hence the amount of radiation received. This instrument consists of a light source, a tiny aperture through which the light is directed and a light detector (photocell) to measure the light intensity transmitted through the film. The term optical density refers to the degree of blackening of the film. The degree of blackness is directly related to the intensity of radiation. In other words the measurement of blackness is called photographic density or optical density (OD).

$$\text{Optical density} = \log_{10}(I_0/I_t) \quad (2.17)$$

Where I_0 is the intensity of light incident on the film .It is the intensity of the light transmitted through the film. The optical density of X-ray films were measured using a CDIT densitometer. The optical density is directly proportional to radiation exposure [25].

2.3.14.2 Attenuation coefficient.

For the determination of attenuation coefficient, the X-ray photographs were taken using collimator in order to reduce scattering. The attenuation

coefficient was calculated using the equation. The attenuation coefficient of the sample was calculated using the equation given below,

$$I/I_0 = e^{-\mu x} \quad (2.18)$$

For the calculation of the value of μ , optical density of background of the film was taken as I_0 and optical density of the sample was taken as I . 'x' the thickness of the sample and μ the attenuation coefficient. Attenuation is the reduction in the intensity of an X-ray beam as it traverses matter by either the absorption or deflection of photons from the beam. Attenuation coefficient is a measure of the quantity of radiation attenuated by a given thickness of an absorber, specifically referred to as linear attenuation coefficient.

2.3.14.3 Half-value layer

Half value layer measures the intensity of a beam. The half-value layer is the absorber thickness required to reduce the intensity of the original beam by one half. The product of the linear attenuation coefficient and half value layer is equal to 0.693.

$$\text{HVL} = 0.693/\mu \quad (2.19)$$

The determination of half-value layer is a commonly used method in calculating barrier requirements for diagnostic installations. It is the thickness of a specific substance that, when introduced into the path of beam of radiation, reduces the exposure rate by one half.

References

- [1]. ASTM. Annual Book of ASTM Standards 1998. Vol. 09.01. Rubber, Natural and Synthetic-General Test Methods. Carbon Black, Designation D 3184-89, ASTM, Philadelphia, PA 1995, (Reapproved **1995**).
- [2]. The American Society for Testing and Materials, Annual book of ASTM standards **2001**, ASTM D 2084-01
- [3]. B.L.Lee; Rubber. Chem. Technol. **1979**,52,1019.
- [4]. H.M.Costa, L.L.Y.Visconte, R.C.R. Nunes, C.R.G. Furtado; Int. J. Polym. Mat.**2004**,53,475.
- [5]. S.Wolf; Rubber. Chem. Technol., **1996**,69,325.
- [6]. G.Kraus; Rubber. Chem. Technol. **1978**,51,297.
- [7]. M.S .Sobhy, D.E.El-Nashar, NA.Maziad ;Egypt J. Sol., **2003**,26,241.
- [8]. Westlinning H, Wolf S. Kautsch Gummi Kunststoffe, **1966**;19:470.
- [9]. S.Wolf, M.Wang. Rubber. Chem. Technol., **1992**,65,329.
- [10]. J. L. Leblanc. and M.Cartault; J. Appl. Polym. Sci.. **2001**, 80,2093.
- [11]. R. Payne, and W.E.Whittaker; Rubber Chem. Technol.,**1971**,44,440.
- [12]. ASTM. Standard test methods for vulcanized rubber and thermoplastic elastomers-tension.ASTM D412-98a (Reapproved 2002) C West Conshohocken: ASTM International, **2003**.
- [13]. ASTM. Standard test method for rubber property-durometer hardness. ASTM D2240-03 West Conshohocken: ASTM International, **2003**
- [14]. Compression set. ASTM D 395-98 (method B), **2008**.
- [15]. J.Crank; The mathematics of diffusion. Secod Ed. Oxford: Clarendon Press,**1975** 244.
- [16]. L. N.Britton, R .B.Ashman, T. M. Aminabhavi, and P. E Cassidy; J. Chem. Edn.,**1988**,65, 368.

- [17]. S.Aprem, K.Joseph A. P.Mathew, S.Thomas;J. Appl. Polym. Sci., **2000**, 78, 94.
- [18]. R. S. Khinnava, T. M.Aminabhavi, J.Appl.Polym. Sci.,**1991**,42, 2321.
- [19]. P.J.Flory,J . Rehner; J. Chem. Phys.,**1943**, 11,512.
- [20]. P.E.Cassidy, T.M.Aminabhavi, C.M.Thompson; Rubber Chem. Tech., **1983**,56, 594.
- [21]. Y.Kojima, A.Usuki, M.Kawasumi, A.Okada, Y.Fukushima, T.Kurauchi, O.Kamigaito,J. Mater.Res., **1993**,8,1174.
- [22]. D.T. Van Haeringen, H. Schonherr, G.J. Vansco, L. Van der Does, J.W.M. Noordermeer, P.J.P. Janssen;Rubber Chem. Technol.,**1999**,72, 862.
- [23]. www.andritz.com
- [24]. V.C. Chandrasekaran; Tank Linings for Chemical process Industries, Smithers Rapra U.K,**2009**,1.
- [25]. H. E. Johns and J. Cunningham; The physics of radiology Fourth edition, Charles C Thomas (publisher),USA S.Graham and Thomas; An introduction to physics for radiologic echnologist, W.B.Saunders Company.



PREPARATION, SURFACE MODIFICATION AND CHARACTERISATION OF NANO BARIUM SULPHATE*

- 3.1 *Introduction*
- 3.2 *Experimental*
- 3.3 *Characterisation*
- 3.4 *Results and discussion*
- 3.5 *Conclusions*

Monodispersed spheroid Barium Sulphate (BaSO₄) nano-powders with porous structures were prepared via, facile single step procedure. Liquid-liquid chemosynthesis involving direct precipitation of barium sulphate from barium chloride (BaCl₂) and ammonium sulphate (NH₄)₂SO₄ in aqueous polyvinyl alcohol (PVA) was employed. PVA, a polymeric surfactant acts like a template for particle growth and assists morphology control and can be easily removed after synthesis by calcination. The dried and calcined nano powders were characterised by X-ray diffraction (XRD), Infrared Spectroscopy (IR), UV- spectra, X-ray studies, Scanning Electron Microscopy (SEM), Transmission Electron Microscopy (TEM), and Thermo Gravimetric Analysis (TGA). The studies revealed that the porous nature and size of the particles were highly governed by PVA content and calcination temperatures. The powder synthesized in 3% w/v PVA showed an average particle size ranging from 20-23 nm. The Monodispersed porous powders were stable and showed spheroid like structures up to 600⁰C; after which the nanostructure is lost drastically and agglomeration leads to structure collapse forming lumpy flakes. The surface treatment of optimised nano powders were carried out using stearic acid as modifier and characterised.

* **NishaNandakumar**, PhilipKurian; Powder Technology 2012,224:51.
doi:10.1016/j.powtec.2012.02.022

A part of this work have been presented at:

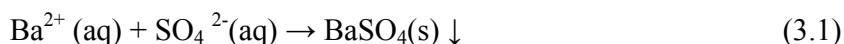
National Seminar on Quantum Chemistry and Nano Techniques - SNM college Malliankara, Kerala - Nov. 2009

3.1 Introduction

Nanotechnology can be considered as a wonderful realm of science which combines chemistry, physics, material science, electronics and biosciences. It is an enchanting technology of the twenty first century, ranging from novel building materials in aerospace technology to life saving medicines. Normally, the term nano encompasses the range 1–100 nm. With respect to diversity in the application, nanotechnology offers uniqueness and flexibility not observed in any other field of technological innovations.

Barium sulphate, which is commonly named as barite is used far and wide because of its high specific gravity (4.5), X-ray opacity, inertness and whiteness [1,2]. Its precipitated form is a known pigment, which can be used as filler in rubbers, as an opacifier in art printing and photographic papers and in the plastic industry, and as a brightening agent and a fiber-dulling agent in the textile field. Barium sulphate has been integrated into epoxy resins to form electrically insulating composites with X-ray attenuation properties. It is also applied in the bio-mineralization and molecular recognition realms of research[3-5]. It is a very good thermo luminescence material, which is used in the radiation dosimeter field. Owing to the very low solubility of the precipitates, the conversion almost always amounts to about 100% with small crystals.

At present, the development of a well-controlled large-scale production of nanoparticles is a very important facet in nanotechnology. The optimal properties of pigments and extenders from the side of application technology will be achieved with certain particle size distributions. For this reason it is by no means adequate to form the desired barium sulphate precipitate in a prescribed chemical composition, but the aqueous chemical process must be controlled to result in the desired particle size. Crystallization and precipitation processes are extensively used in the chemical industry. One of the most celebrated crystallization processes is the reaction of barium (Ba^{2+}) and sulphate (SO_4^{2-}) ions into barium sulphate (BaSO_4), as shown in Eq. 3.1 [6,7],



Liquid/liquid reaction is the focal method of the preparation of nano-BaSO₄. This technique has some divisions such as direct precipitation[8], micro emulsion, membrane separation, micro channel reaction and impinging streams[9]. Preparation of BaSO₄ particles has been extensively studied in order to weigh up the effect of mixing, precipitation models, agitator speed and feed position on particle size distribution, crystal growth and morphology. BaSO₄ as a model system is excellent since a considerable body of information exists as seen from process mentioned in literature on barite morphology control, possibly due to the importance of this mineral in cosmetics, paper making and offshore oil field applications [10-21]. Up to this date, many different approaches have been projected to produce BaSO₄ nanoparticles, as- precipitation [22], micro emulsion [23], filtration dispersion method [24], modifying different organic acids [25], membrane dispersion [26], presence of polymeric additives [27] addition of different additives,[28-31] induction by LB (Langmuir-Blodgett technique) monolayer otherwise known as LB films and micro emulsion [32]. These methods resulted in a noteworthy change in morphology, but the size was normally in the micron scale rather than nanometre scale. The size and analogous morphology obtained in water/oil micro emulsions or reverse micelle [33] approach could be guarded well by adjusting the molar ratio of water to surfactant. The product yield was low in such methods because of the poor solubility of salts in conventional emulsions. There were also some reports about preparation of organo-modified BaSO₄, [34] but the BaSO₄ obtained was in micron scale. Even if preparation of organo-capped BaSO₄ was previously described, the stipulation was not suited to the industry.

In recent times, a great deal of attention has been placed on the mass production of BaSO₄ nanoparticles. The fact that the physico-chemical properties of BaSO₄ nanoparticles were determined by size and shape, and the menace created by its tendency to aggregate, increased the need to find the most suitable method to prepare BaSO₄ nanoparticles with well defined size and morphology. In

general, barium sulphate is produced by the reaction of a barium salt such as sulphide, chloride or nitrate with sulphuric acid or its salt such as sodium sulphate in an aqueous solution.

Hari Bala et al. prepared nanoparticles of barium sulphate with average particle size of 24.3nm using water-alcohol solution as medium [1]. Qi et al. [35] synthesized spherical and cubic BaSO₄ nanoparticles with a barite structure in Triton X-100/*n*-hexanol/cyclohexane/water water-in-oil micro emulsions containing ammonium sulphate ((NH₄)₂SO₄) and barium acetate(Ba(Ac)₂), respectively. Owing to their cage-like nature, the micro emulsion droplets effect the size of the particles. On the other hand, in the process discussed above, many kinds of raw materials, organic solvents and surfactants are used up, which habitually result in heavy expenditure and environmental pollution.

Jia and Liu [36] synthesized nano sized BaSO₄ particles using a membrane reactor, in which the Na₂SO₄ solution permeated through the micro pores of an ultra filtration (UF) membrane and progressively flowed into the BaCl₂ solution to control the dispersion ratio, nucleation and growth rates. The drawback of the process was that, because of its high viscosity, a colloidal suspension of BaSO₄ is likely to block the narrow-diameter pores of the ultra filtration membrane.

Nanoparticles of barium sulphate (BaSO₄) have been synthesized by Mohamed El-Shahate et al. from barium nitrate by precipitation method in the presence of water soluble organic polycarboxylic polymer as modifying agent. The results indicate that spherical BaSO₄ nanoparticles are obtained with poor crystallites and diameters ranging from 30-35 nm [37], V. Ramaswamy et al. synthesized barium sulphate using barium chloride (BaCl₂) and ammonium sulphate as reagents by an ordinary precipitation process in the presence of ethanol/water mixed solvents. From the XRD results, the size of the particles ranged from 85nm to 54nm. The particle size decreased when the volume % of ethanol is increased [38]. The large scale production of nano fillers through these processes demands use of organic solvents, which reduces its cost effectiveness in industry.

Precipitated BaSO₄ is used in dosimetry [39]. It is used as an inert filler in dyes and paints, rubbers and blended cements [40]. In Industry, barium sulphate is used as inert white filler based upon the fact that it is substantially inert chemically and physically. Surface active silicates, oxides, black or sulphur are used, because these ‘fillers’ have functional properties in order to impart certain property enhancements. Barium sulphate lacks such a surface reactivity. In the SO₄²⁻ tetrahedron of barium sulphate, the central atom is in its highest oxidation state. The high charge density of the Ba²⁺ ion ensures a saturation of the bond sites on the crystal surface by the Ba²⁺ ion. In the case of barium sulphate there are no surface centres which can be complexed or esterified [41]. Establishing interactions between filler and polymer is one prospect of enhancing the properties of these nano/macro composites. It is hence advantageous to carry out surface modification of barium sulphate in a targeted manner, in order to set up interactions in an effective manner. An appropriate choice of functional group for selective surface modification is necessary since, it can influence the interaction between the particle and polymer matrix selected. From the literature it could be found that mainly two types of surface treatments have been widely accepted for barium salts the organic modification and the inorganic modification.

Barium sulphate particles of size ranging between 35-55nm were prepared in the presence of polycarboxylate modifier [42]. Shinozuka et al. patented a method of producing surface treated barium sulphate. The method comprises of an addition of aqueous solution of alkali silicate to an aqueous slurry of barium sulphate, which contains an excess of barium ions to deposit barium silicate on barium sulphate and then an addition of mineral acid to form hydrous silica [43]

Grothe et al. patented the inorganic surface modification using inorganic compound selected from Al, Ba, Ca, Ce, Cl, Co, Fe, N₂, Sr, Vd, Zn, Sn or Zr compound or salts. They carried out organic modification using compound selected from alkyl sulfonic acid salt, sodium polyvinyl sulfonate, Sodium-N-alkyl benzene sulfonate, sodium polystyrene sulfonate, sodium dodecyl benzene sulfonate, sodium

laurylsulphate, sodium cetylsulphate, oleyl-cetyl alcohol sulphate, isostearic acid, stearic acid and oleic acid. Surface modification of inorganic salts using N-alkyl and N-fluoro alkyl phosphonic acids have been reported earlier [44].

Similarly Aderhold et al. carried out surface modification of barium sulphate using inorganic and organic additives [45]. Shen et al. reports a simple method to prepare barium sulphate nanoparticles by use of tetradecanoic acid, hexadecanoic acid and stearic acid as modifiers [46]. In the present work stearic acid is chosen as modifier with the view of application of prepared nano fillers into rubber matrix in which the modifier has a peptiser action(Fig .3.1).

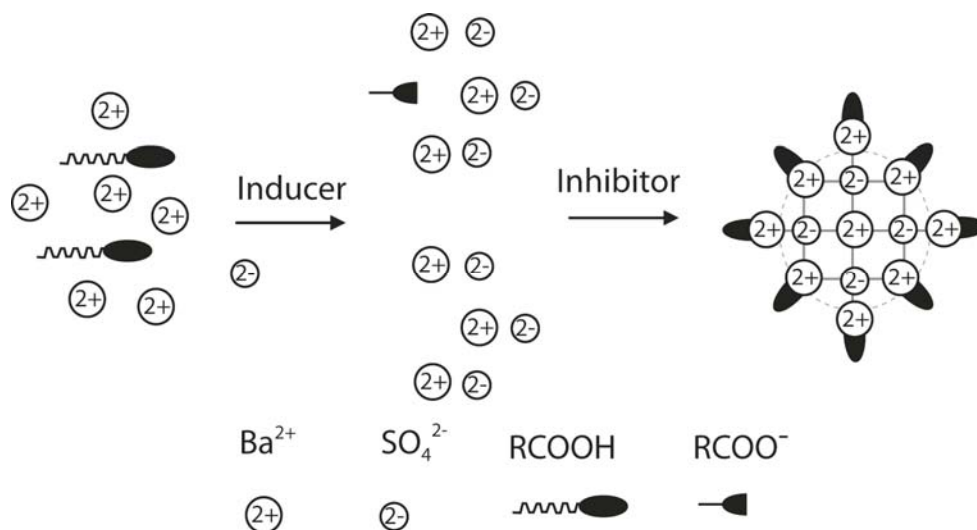


Figure 3.1 The possible mechanism of the BaSO_4 nanoparticles modified by organic acid [45]

This chapter deals with the synthesis of spheroid BaSO_4 nano-powder with porous structures via a facile single step procedure. The method highlights the preparation of porous nano bariumsulphate at room temperature in PVA as size reducing medium. We investigated the influence of PVA on morphology and size and its role in yielding porous nano materials. The modification of optimised nano barium sulphate was carried out using 2wt% stearic acid. We varied the experimental conditions such as concentration of PVA and calcination

temperatures; and compared the nature of barium sulphate formed during each condition at constant molar ratio of reactants.

The benefits of present synthesis are

- a). This method minimises the excessive use of raw materials, organic solvents and surfactants making it cost effective and eco-friendly.
- b). The precursors used in the present method are common sources of barium and sulphate.
- c). The method uses the PVA, a polymeric surfactant which assists particle growth and morphology control and can be easily removed subsequent to synthesis by calcination.

It is expected that the addition of PVA produce a matrix into which formed barium sulphate particles will be incorporated enabling them to be in nano scale. The interaction between the hydroxyl groups of dispersing medium and the hydroxyl groups adsorbed on surface of barium sulphate would result in co-condensation. The synthesized nano powder is calcined to remove the dispersing medium. The modification of optimised nanofiller were carried out using stearic acid as modifier and characterised.

3.2 Experimental

3.2.1 Chemicals

All chemicals used for investigations in this work are given in Table 3.1.

Table 3.1 Chemicals used

Chemical	source	purity
BaCl ₂	Merck	99.99%
(NH ₄) ₂ SO ₄	Merck	99.99%
Poly vinyl alcohol	Spectrochem Ltd.	Mwt.1,25000
Stearic acid	Godrej soaps Ltd	acid number 185-210
Ethanol	Alpha chemicals	AR grade
BaSO ₄	Merck	99.99%

3.2.2 Preparation of nano barium sulphate in polyvinyl alcohol

All the chemicals mentioned in section 3.2.1 were used without further purification. The preparations were carried out at ambient temperature (ca.25⁰c) in a glass beaker. 20 ml of 0.5 M BaCl₂ was initially thoroughly mixed with 20ml of water (slightly acidified) containing 0%w/v, 1%w/v, 3%w/v, 5%w/v and 7%w/v of PVA respectively and all solutions showed a turbid appearance soon after mixing, though no visible precipitation was observed. Then 10mL of 1.0M (NH₄)₂SO₄ was added drop wise from a micro burette at low rate to the mixture under vigorous magnetic stirring. The mixture was stirred at of 50-60 rpm for another one minute after complete addition of reagent and kept under static conditions for 5 hrs before the white precipitate was washed. The precipitate was washed thoroughly with distilled water to remove excess PVA, reactants and by-products. Vacuum filtration of sample was done and the cake obtained after filtration was dried at 80⁰C for 2hrs.

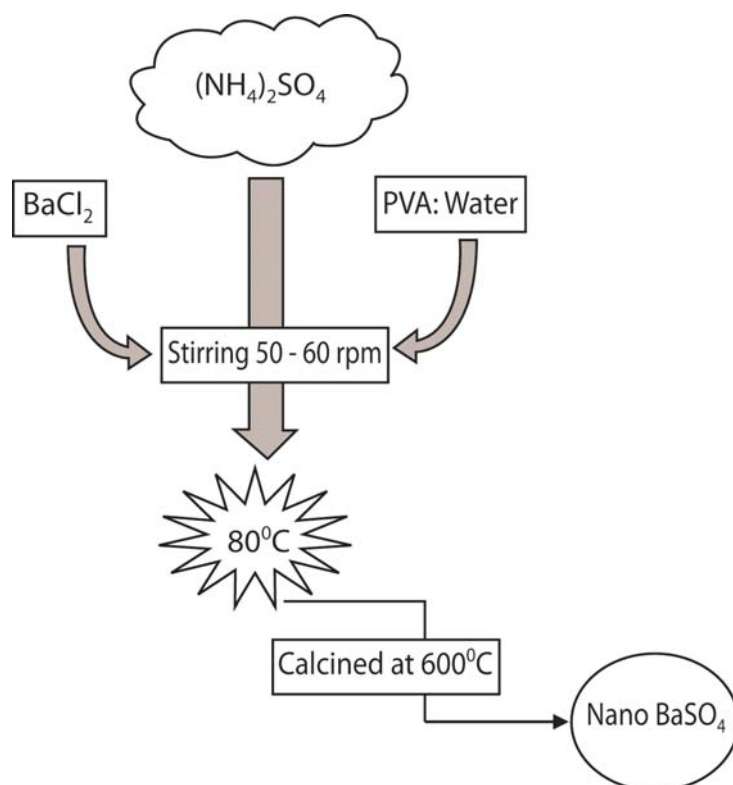


Figure 3.2 Schematic overview of the preparation of nano barium sulphate

The dried sample was then ground into fine powders and then kept in the muffle furnace at 400⁰C, 600⁰C and 800⁰C for 4 hrs. During this time the organic part was removed and fine powders were obtained. The same process was repeated by taking different percentages of dispersing mediums. The conditions were optimized and large scale preparation was done using 3000ml borosil beaker as reactor. The yield of this process is 95% and an overview of the entire reaction was given in Fig. 3.2. Different batches of barium sulphate are given in Table 3.2.

Table 3.2 Different batches of barium sulphate

(The code used, BN_x-yD, 'BN' represents nano barium sulphate; 'x' stands for w/v% of PVA solution; 'y' stands for temperature of calcination, 'D' for degree Celsius)

Sample Name	PVA %	Calcination temperature ⁰ C
BN0	0%	600 ⁰ C
BN1-400D	1%	400 ⁰ C
BN3-400D	3%	400 ⁰ C
BN5-400D	5%	400 ⁰ C
BN7-400D	7%	400 ⁰ C
BN1-600D	1%	600 ⁰ C
BN3-600D	3%	600 ⁰ C
BN5-600D	5%	600 ⁰ C
BN7-600D	7%	600 ⁰ C
BN1-800D	1%	800 ⁰ C
BN3-800D	3%	800 ⁰ C
BN5-800D	5%	800 ⁰ C
BN7-800D	7%	800 ⁰ C

3.2.3 Modification of nano barium sulphate

The nano particles (0.1g/ml) were sonicated for 1 hr to get a homogeneous aqueous dispersion of nano barium sulphate in 1:1 ethanol–water solution. 2wt % alcoholic stearic acid solution was added into it and sonicated for 3 minutes. The pH of the solution was adjusted to be between 8 to 9 using ammonia solution. After stirring, the solution was kept for 30 min to allow the precipitate to settle down. The precipitates were rinsed with doubly distilled water and pure

alcohol, dried at 100 °C and finally crushed to fine powders. The modified particles were then characterized.

3.3 Characterisation

The prepared powders were characterised by bulk density, BET surface analysis, X-ray diffraction, FT-IR, SEM, TEM, Radiopacity studies using Collimex general X-ray instrument, UV-visible spectrum, TGA and DSC(details in section 2.3.4-2.3.14).

3.4 Results and Discussion

3.4.1 Bulk density

The bulk density of the prepared samples is shown in Table 3.3.

Table 3.3 Bulk densities of the prepared barium sulphate samples

Sample Name	Bulk density g/cm ³
Commercial	0.1827
BN0	0.1876
BN1-400D	0.4742
BN3-400D	0.5738
BN5-400D	0.5278
BN7-400D	0.5123
BN1-600D	0.6126
BN3-600D	0.7012
BN5-600D	0.6712
BN7-600D	0.6725
BN1-800D	0.3156
BN3-800D	0.3476
BN5-800D	0.3059
BN7-800D	0.2932
MBN	0.6959

From the Table 3.3 it is clear that synthesized nano barium sulphate has higher bulk density than the commercial as well as in the absence of dispersing medium. It is also evidenced that 3% PVA is the best dispersing medium to prepare nano barium sulphate and 600⁰C is the optimum calcination temperature. It is evident from the highest bulk density of the sample BN3-600D. The bulk density as well as the data in the forthcoming sections confirm that optimum PVA concentration is 3g/100ml and optimum calcination temperature is 600 ⁰C. It is clear that as the calcination temperature increases bulk density decreases indicating a structural collapse resulting in lowering of surface area. Bulk density of nano barium sulphate sintered at 600 ⁰C shows a marginal decrease after modification (MBN). This indicates that the particle size slightly increases with modification. The presence of modifying group on the surface of the nanoparticles increases the particle size.

3.4.2 BET surface area

Representative samples were selected for surface area determination. Table 3.4 shows surface area for commercial barium sulphate, nano barium sulphate BN3-600D and MBN (organically modified nano barium sulphate) samples.

Table 3.4 Surface areas for different BaSO₄ samples

Sample name	BET surface area m²/g
Commercial	0.5 ± 0.04 m ² /g
Unmodified	22.42 ± 0.08 m ² /g
Modified	21.36 ± 0.13 m ² /g

3.4.3 X-Ray Diffraction (XRD)

The XRD patterns of the barium sulphate powders synthesized with 0, 1, 3, 5 and 7 weight by volume percentage aqueous solutions of PVA as medium and calcined at 400 ⁰C, 600 ⁰C, 800 ⁰C are shown in Fig. 3.3 and 3.4 respectively. The XRD patterns of modified nano fillers and optimised nano fillers

are shown in Fig. 3.3. All the samples have an intense peak at 42-43 ° which is a characteristic feature of BaSO₄. From the shortening and broadening of this intense peak, the particle size was calculated using Scherrer formula[21]. The samples display the typical orthorhombic structure of BaSO₄. The d-values of BaSO₄ nano material is 4.34_x, 2.12₅ and 3.90₄ (JCPDS No: 83-1718), 3.44_x, 3.10_x and 2.12₇ (JCPDS No: 83-2053) These d-values were calculated using the Bragg equation, the suffixes represent the intensity of the peak identified, x=100% intensity of the peak, 2=20% peak intensity, 7=70% intensity and so on. with *hkl* values of (101), (311), (111) and (210), (211), (401) respectively. The XRD pattern was indexed with reference to the unit cell of the barite structure (a~8.87, b~5.45, c~7.15Å); space group (Pnma) [46].

3.4.3.1 Influence of calcination temperature on XRD

The influence of calcination temperature on the particle size was analysed using XRD-spectra of nano BaSO₄ synthesized in 3%PVA solution at different calcination temperatures viz. 400°C, 600°C and 800°C for 4 hrs (Fig. 3.3) for the fact that at all calcination temperatures sample BN3 showed higher bulk density. All the samples were white in colour. Only BaSO₄ peaks were observed in the XRD spectra of all samples except for a calcination temperature of 400°C. This indicated that all other powders had high purity. The intensity and width of diffraction peaks differed between samples calcined at different temperatures. The spectra revealed that as the calcination temperature increased the crystallinity of the sample increased and grain size increased, where as at 600°C the grain size fall into 10nm range as calculated using the Scherrer formula from broadening of XRD for intense peak. At 400°C the grain size is small (9nm) as indicated by the broadening and shortening of peaks. A well defined crystalline peak of barium sulphate is missing at 400°C, and hence this temperature is not sufficient for post synthesis treatment. At 800°C pure nano barium sulphate was formed but agglomeration takes place as observed by narrow peak formation with large (45nm) size. Powder calcined at 600 °C yields small grain size with

high purity. It is the optimum temperature that ensures complete removal of PVA template from the nano BaSO₄ and the peaks in the spectra indicated the formation of controlled monodispersed powder at this temperature. More over all the calcined powders showed smaller grain size than the BaSO₄ prepared in aqueous medium without PVA support indicating that, presence of PVA had a dispersive and protective effect on the powders which assists in size control even after its removal through calcination. The calculated particle sizes are summarised in Table 3.5.

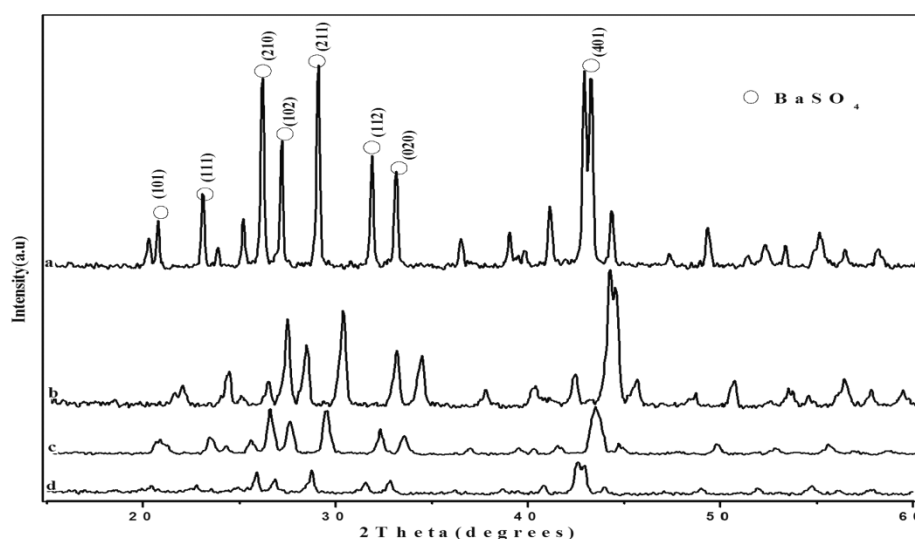


Figure 3.3 Influence of calcination temperature on XRD (a) without PVA (b) BN3-800D (c) BN3-600D, (d) BN3-400D

3.4.3.2 Influence of dispersing medium (PVA w/v) on XRD

The XRD patterns of the barium sulphate powders synthesized with 0, 1, 3, 5 and 7 weight by volume percentage aqueous solutions of PVA as mediums are shown in Fig. 3. 4. Only BaSO₄ peaks were observed in the XRD spectra. This indicated that all the powders had high purity. XRD reveals that as the PVA concentration increased the intensity of the peaks and crystallinity, decreased as indicated by the shortening and broadening of peaks. The barium sulphate BN3-600D, prepared with 3% PVA solution, had a minimum grain size of ~10 nm. As

the concentration of PVA increased further, the crystallinity of the powder is found to decrease as indicated from the broadening of the peaks. Moreover all the powders prepared in the presence of PVA showed smaller grain size than that prepared without PVA, emphasizing the dispersive and protective effect of PVA. Thus XRD assisted analysis revealed that 3% PVA aqueous solution is an optimum medium for nano powder synthesis. This effective polymer coating on each mole of the reactant and every single Ba^{2+} ion coated with PVA reacts with a single SO_4^{2-} leading to reduced agglomeration of powders formed.

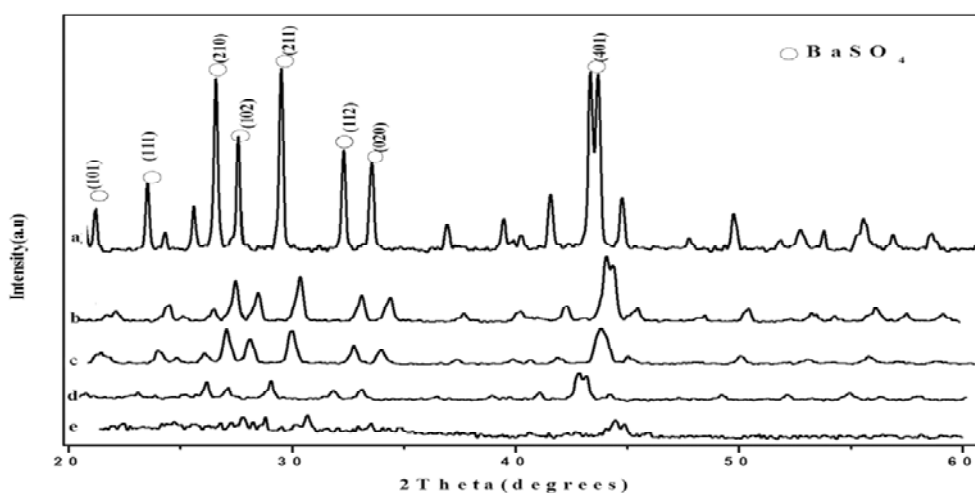


Figure 3.4 Influence of PVA w/v on XRD (a) without PVA (b) BN1-600D (c) BN3-600D (d) BN5-600D (e)BN7-600D

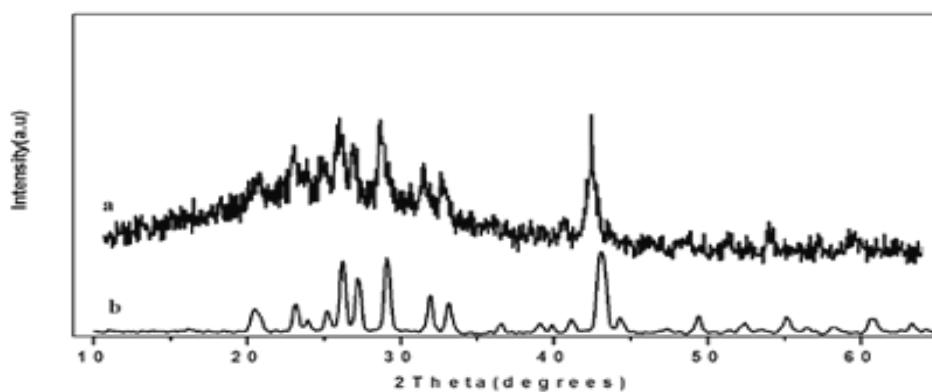


Figure 3.5 XRD patterns of a) MBN b) BN3-600D

Table 3.5 Average Particle size of the BaSO₄ samples

Sample name	Average Particle size (nm)
Commercial BaSO ₄	159.9
BN0	150
BN3-600D	10
MBN	12

3.4.4 Fourier transform infrared resonance-(FTIR) spectroscopic studies

The Infrared (IR) spectra of BaSO₄ prepared without PVA, nano BaSO₄ powder materials prepared in 3% PVA solution calcined for 4hrs at 600⁰C and stearic acid modified nano fillers are shown in Fig. 3.6. The IR spectrum of precipitated barium sulphate without PVA is shown in Fig. 3.6(c). The presence of broad absorption band at 3405cm⁻¹ here, corresponds to hydrogen bonding. This gets weakened for BaSO₄ prepared in 3% PVA calcined at 600⁰C Fig. 3.6(b). IR spectra of all samples had peaks centred at 1189, 1096 cm⁻¹ and shoulder at 982, 640 cm⁻¹ which corresponds to symmetrical vibrations of sulphate ions.

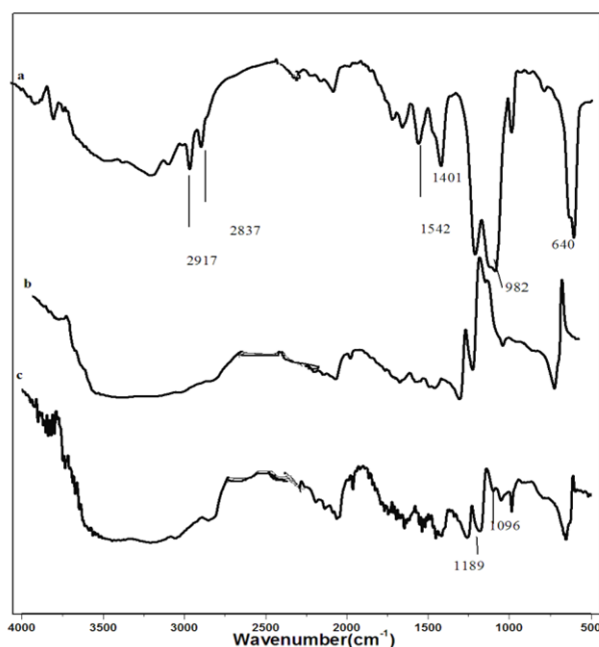


Figure 3.6 FTIR spectra of: (a) MBN, (b)BN3-600D, (c)Without dispersing medium

The interaction between carboxylate ions and BaSO_4 causes a shift from $1080\text{--}1130\text{ cm}^{-1}$ (peaks of pure BaSO_4) to $1073\text{--}1192\text{ cm}^{-1}$. The peaks at 2917 , 2837 cm^{-1} could be assigned to the symmetric and asymmetric vibrations of $-\text{CH}_2-$ and $-\text{CH}_3$ groups and the peak at 1401 cm^{-1} was ascribed to the scissoring of $-\text{CH}_2-$ or the symmetric deformation of the $-\text{CH}_3$ group. All the above bands were attributed to the non-polar part in organic acid. IR spectrum of MBN is devoid of the peak at 1704 cm^{-1} corresponding to free organic acid group. Instead a peak at 1542 cm^{-1} corresponding to carboxylate ion appeared, indicating a better interaction between barium sulphate and modifier. The FT-IR spectra showed that the particles contained organic acid and there were no corresponding peaks in XRD patterns. This may be because the organic acid was absorbed on the surface of BaSO_4 rather than entering the BaSO_4 crystal to form composite[45].

3.4.5 Studies using scanning electron microscopy (SEM)

The SEM images of nano powders prepared without PVA and in 3% PVA calcined at 400°C , 600°C , 800°C respectively are shown in Fig. 3.7a; Fig.3.7a-d. From the SEM images, the reduction in size of the BN3-600D as evidenced from XRD analysis was further confirmed.

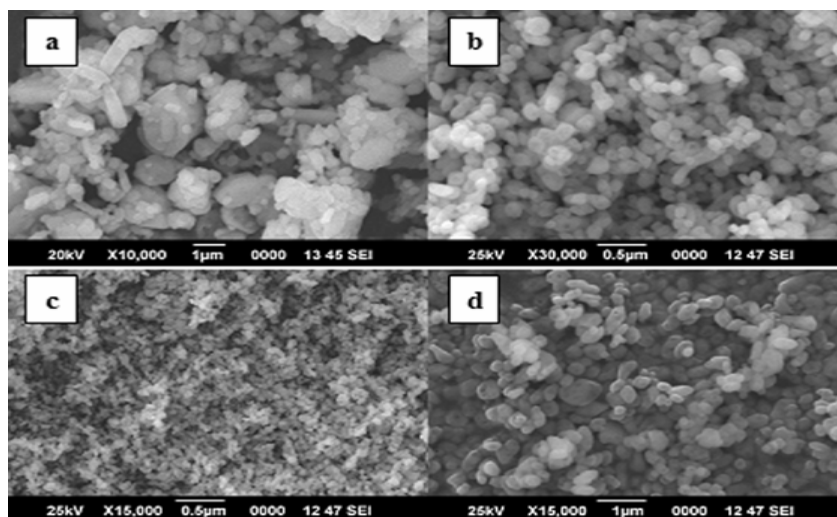


Figure 3.7a SEM photographs of BaSO_4 nano material (a)BN0 (b)BN3-400D, (c)BN3-600D (d)BN3-800D

The SEM images of modified (MBN) and unmodified nano(BN3-600D) fillers are as shown in Fig. 3.7b. The slight increase in particle size for the modified nano powders was observed in Fig.3.7b. The related EDAX analysis of samples prepared in 3% aqueous PVA solution calcined at 600⁰C and that of modified nano powders is shown in Fig3.7b (b). The EDAX Fig. 3.8a contains only peaks for barium (Ba), sulphur(S) and oxygen (O), which indicates the purity of the material.

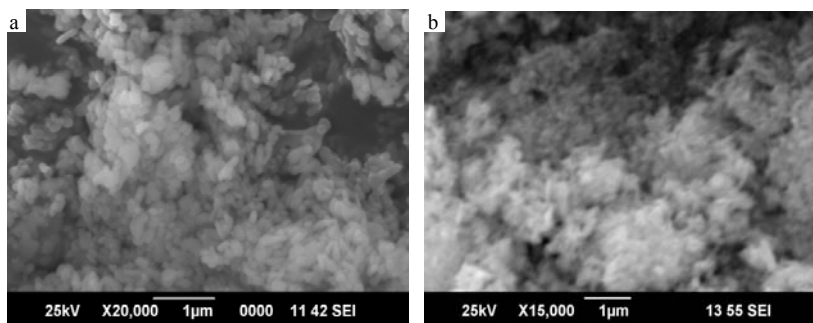


Figure 3.7b SEM micrograph of a) BN3-600D b) MBN

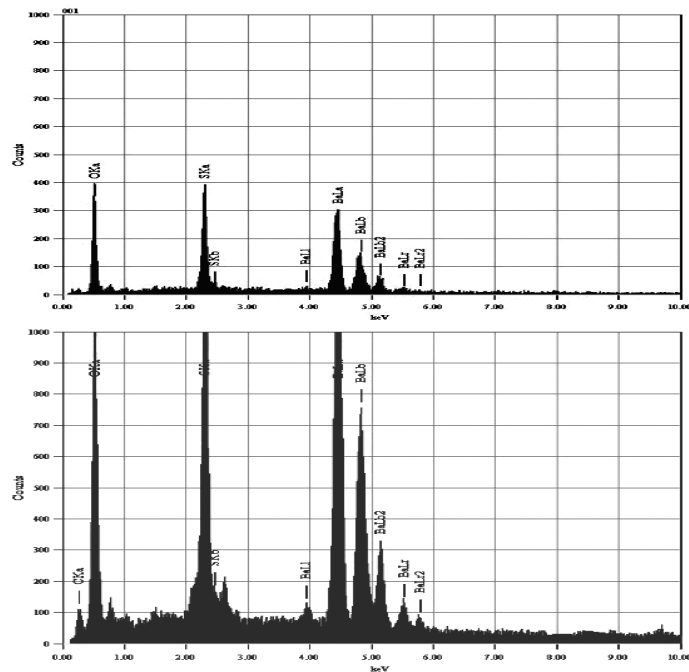


Figure 3.8 EDAX patterns of BaSO₄ nanoparticles a)BN3-600D b)MBN

The analysis of these results exhibits the presence of Ba, S and O in the ratio 1.0:0.9:4.0 close to the stoichiometry of BaSO_4 within experimental error. Fig. 3.8b evidences effective modification as can be seen from emergence of carbon peaks in MBN.

3.4.6 Studies using transmission electron microscopy(TEM)

The TEM images (Fig3.9a) of BaSO_4 synthesized in 3% PVA solution and calcined at 600°C confirms the formation of nano particles. The particle size obtained from TEM was 23nm. MBN had an average particle size of 25.3nm. The sample has regions that appear brighter than the surroundings because they have absorbed fewer electrons [47].

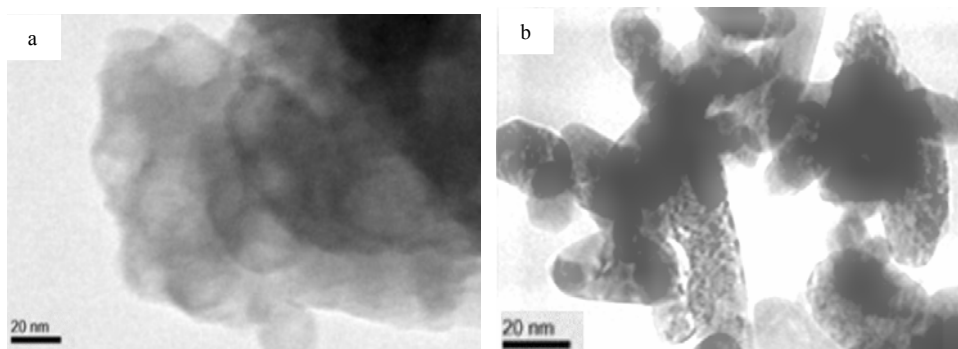


Figure 3.9 TEM image of a) MBN b) BN3-600D

3.4.7 Radiopacity studies

Scanned images of X-ray photographs of the barium sulphate samples are shown in Fig. 3.10. The MBN (Fig. 3.10.c) filled PET box show intense radiopacity which is due to the improved interaction between fillers leading to close packing of fillers in a given volume on modification. The BN3-600D (Fig. 3.10.b) species also show good radiopacity and it is clear that nano materials exhibit improved radiopacity than its macro counterparts. BC (Fig. 3.10.a) is the commercial barium sulphate used for the sake of comparing radiopacity[48].

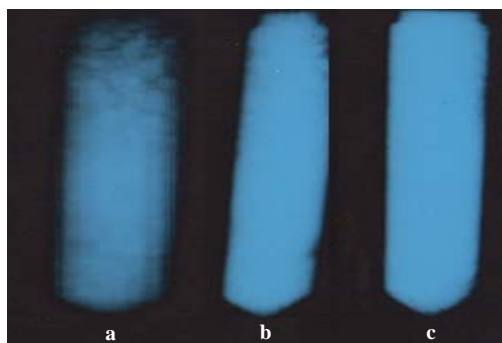


Figure 3.10 X-ray photographs of barium Sulphate samples (a)BC (b)BN3-600D (c)MBN

3.4.8 UV-visible spectroscopy

The UV-visible spectrum of nano BN and MBN is compared in Fig. 3.11 and the spectrum indicates that absorbance increases as size is reduced and is further influenced by modification. Light scattering depends on the particle size and the wavelength of corresponding light. Due to the reduction of particle size radiation absorption increases. The ability to scatter light increases the hiding power of the pigment and therefore the hiding power decreases as the particle size increases[49,50].

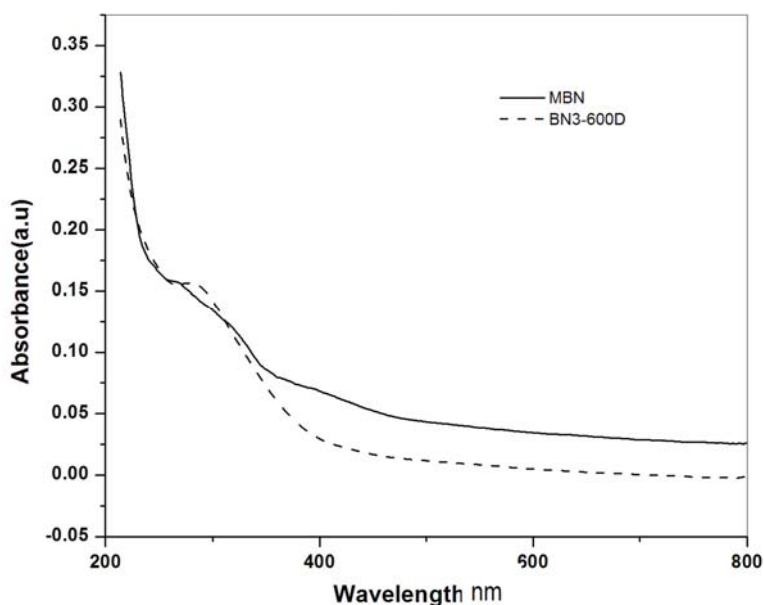


Figure 3.11 UV-visible spectrum of barium sulphate samples a) MBN b) BN3-600D

3.4.9 Thermo gravimetric analysis (TGA)

Thermal analysis of the prepared nano particles was carried out to know the possible changes occurring when the materials were subjected to heat treatment. Thermo gravimetric analysis of dried sample prepared in 3% PVA and that of dried MBN was carried out in the temperature range from 40 to 800⁰C. The thermal behaviour of these powders are shown in Fig. 3.12. The Fig. 3.12 (a) represent TGA patterns of BaSO₄ synthesized in 3% PVA solution. It is clear from the patterns that the thermograms showed weight loss up to a calcination temperature of 600⁰C. Increasing the calcination temperature from 400 to 600⁰C the weight loss of ~0.50% accounts for the removal of PVA coating. Moreover on increasing the temperature from 600⁰C, the weight loss is negligible, this confirms that a minimum calcination temperature of 600⁰C is required for the complete removal of PVA from the nano BaSO₄. The residue of 98.5% indicates that the pure powders can be synthesized by this method facilitating complete removal of dispersing agent. Fig. 3.12(b) shows the TGA traces for MBN ie., organically surface treated nano BaSO₄. The curve suggest a residue of 93%. Tg analysis of pure stearic acid [45] pointed that it decomposed between 200-450⁰C, however nano modified by stearic acid began to loose at 200⁰C and major decomposition is from 500 to 600⁰C. The decomposition temperature of stearic acid modified barium sulphate was higher than that of pure stearic acid ,resulting from the interaction between the modifier and bariumsulphate.

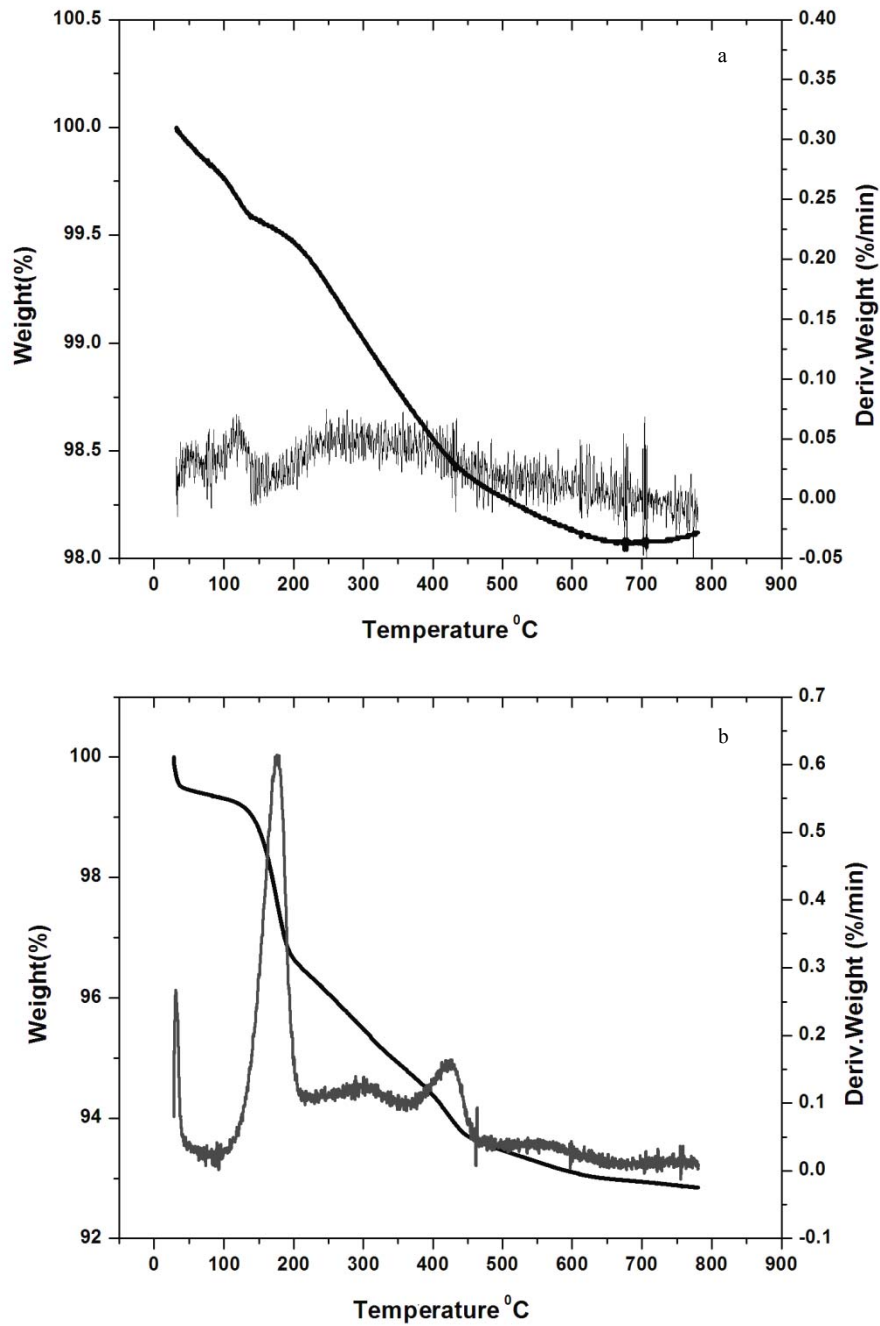


Figure 3.12: TG-DTG curves of a) BN3-600D, b) MBN

3.4.10 DSC curves

No noticeable peak was seen in DSC curve, as shown in Fig. 3.13, which indicate that the nano BaSO₄ is pure, orthorhombic phase, which is well associated with the XRD results. Similar behaviour is observed for MBN with an endothermic peak at 350^oC which is due to stearic acid and not due to phase transitions in the nano material [50] prepared.

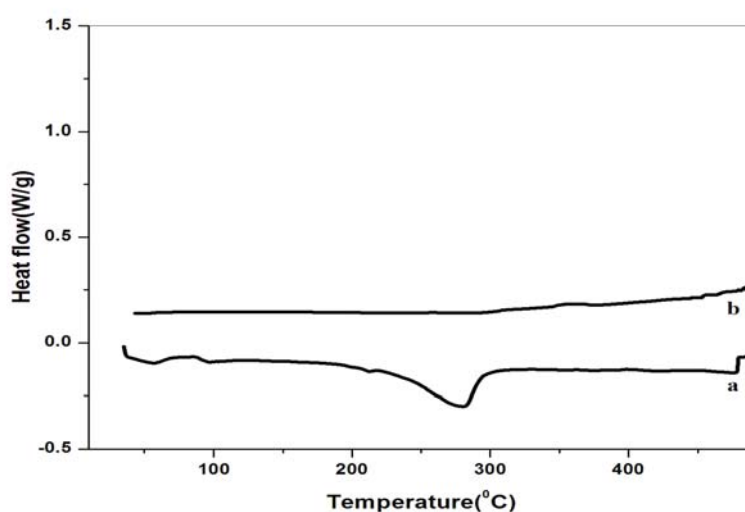


Figure 3.13: DSC curves of a) MBN b) BN3-600D

3.5 Conclusions

Under controlled conditions nanobarium sulphate was successfully prepared by a wet precipitation route in aqueous solution of polyvinyl alcohol. The particle size of the barium sulphate was controlled by optimising the precipitation medium and its concentration. Nanobarium sulphate prepared by this method has a particle size less than 25 nm which is lower than that of the commercially available forms. The particle size of barium sulphate was found to be 10 nm from the XRD results. The result also shows that, synthesized barium sulphate is predominantly crystalline in nature. SEM and TEM pictures revealed an average particle size of 23nm for synthesized nano powder. Nano

bariumsulphate surface was effectively modified by stearic acid and TEM images confirmed that the agglomeration tendency of the nanoparticles can be reduced by the modification without much increment in size. Nano barium sulphate is having high purity as revealed by FT-IR, EDAX, TGA and DSC studies. Radiopacity improved with size reduction as seen from X-ray images. This method has many advantages, such as simplicity, high purity, high yield and moreover offers an eco-friendly route to superfine compound synthesis.

References

- [1]. H.Bala., W.Fu, J.Zhao, X.Ding, Y.Jiang; Colloids Surfaces A:Physicochem. Eng. Aspects.,**2005**, 252,129.
- [2]. H.Bala., W.Fu, J.Zhao, X.Ding, Y.Jiang ; Colloids Surfaces A:Physicochem. Eng. Aspects, **2006**, 274,71.
- [3]. J.Unsworth, B.A.Lunn, P.C.Innis;J.Mater. Sci. Lett., **1993**, 12,132.
- [4]. S. Mann;Nature, **1993**, 365, 499.
- [5]. B.R. Heywood, S.Mann;Adv. Mater., **1994**, 6, 9.
- [6]. R. Kieffer, D.Mangin, F. Puel and C. Charcosset;Chem. Eng. Sci., **2009**, 64, 1885.
- [7]. A.A.Oncul, K. Sundmacher, A. Seidel-Morgenstern and D. Thevenin;Chem. Eng. Sci., **2006**, 61, 652.
- [8]. D.Adityawarman, , A.Voigt, P. Veit and K. Sundmacher; Chem.Eng. Sci., **2005**, 60, 3373.
- [9]. G.Wu, H. Zhou and S. Zhu; Mater. Lett., **2007**, 61, 168.
- [10]. B. R. Heywood and S. Mann; Langmuir, **1992**, 8, 1492.
- [11]. B. R. Heywood and S. Mann;J. Am. Chem. Soc., **1992**, 114, 4681.
- [12]. L. Litvin, S. Valiyaveetil, D. L. Kaplan and S. Mann; Adv. Mater., **1997**, 9, 124.
- [13]. P. J. J. A. Buijnsters, J. J. J.M. Donners, S. J. Hill, B. R. Heywood, R. J. M. Nolte, B. Zwanenburg and N. A. J. M. Sommerdijk; Langmuir, **2001**, 17, 3623.
- [14]. L. A. Bromley, D. Cottier, R. J. Davey, B. Dobbs, S. Smith and R. Heywood; Langmuir, **1993**, 9, 3594.
- [15]. F.Wang, G.Xu.,Z.Zhang, X.Xin; Colloids and Surfaces A: Physicochem. Eng. Aspects, **2005**, 259, 154.
- [16]. L. Qi, H. Coffen and M. Antonietti;Angew.Chem., Int. Ed., **2000**, 39, 604.
- [17]. M. Uchida, A. Sue, T. Yoshioka and A. Okuwaki; Cryst. Eng Comm., **2001**,5.

- [18]. J. D. Hopwood and S. Mann; Chem. Mater., **1997**, 9, 950.
- [19]. M. Li and S. Mann; Langmuir, **2000**, 16, 7088.
- [20]. J. D. Hopwood and S. Mann; Chem. Mater., **1997**, 9, 1819.
- [21]. D. C. Y. Wong, Z. Jaworski and A. W. Nienow; Chem. Eng. Sci., **2001**, 56, 727.
- [22]. Y. Yoshikawa, G.H. Nancollas; J. Cryst. Growth, **1984**, 69, 357.
- [23]. L. Qi, J. Ma, H. Cheng, Z. Zhao; Colloids Surfaces A: Physicochem. Eng. Aspect, **1996**, 108, 117.
- [24]. G. Chen, G. Luo, J. Xu, J. Wang, Pow. Technol., **2005**, 153, 90.
- [25]. Y. Shen, C. Li, X. Zhu, A. Xie, L. Qiu, J. Zhu; J. Chem. Sci., **2007**, 119, 19.
- [26]. S.W. Li, J.H. Xu, Y.J. Wang, G.S. Luo; Pow. Technol., **2009**, 195, 213.
- [27]. H. Colfen, L. Qi, Y. Mastai, L. Borger; Cryst. Growth Des., **2002**, 2, 191.
- [28]. F. Wang, G. Xu, Z. Zhang, X. Xin; Colloids and Surfaces A: Physicochem. Eng. Aspects, **2005**, 259, 151.
- [29]. Jones, F., A. Oliviera, G.M. Parkinson, A.L. Rohl and A. Stanley et al.; J. Cryst. Growth, **2004**, 262, 572.
- [30]. Q.A. Wang, J.X. Wang, M. Li, L. Shao and J.F. Chen et al.; Chem. Eng. J., **2009**, 149, 473.
- [31]. A. Gupta, P. Singh and C. Shivakumara; Solid State Commun., **2010**, 150, 386.
- [32]. B.M. Nagaraja, H. Abimanyu, K.D. Jung and K.S. Yoo; J. Colloid Interf. Sci., **2007**, 316, 645.
- [33]. X. Sui, Y. Chu, S. Xing and C. Liu; Mater. Lett., **2004**, 58, 1255.
- [34]. Y. Shen, C. Li, X. Zhu, A. Xie and L. Qiu et al.; J. Chem. Sci., **2011**, 119, 319.
- [35]. L. Qi, J. Ma, H. Cheng, Z. Zhao; Colloids Surf. A: Physicochem. Eng. Aspects, **1996**, 108, 117.
- [36]. Z. Jia, Z. Liu, J. Membr. Sci.; **2002**, 209, 153.

- [37]. M. El-Shahate, S. Ismaiel and I. Mostafa Bakr; *Am. J. Nanotech.* **2011**, 2, 106.
- [38]. V. Ramaswamy, R. M. Vimalathithan, V. Ponnusamy ; *J. Ceramic Processing Research.*, **2011**, 12, 173.
- [39]. N. Salah,, S.S. Habib, Z.H. Khan, S. Al-Hamedi and S.P. Lochab; *J. Luminescence*, **2009**, 129, 192.
- [40]. D. Andrea, S.C and A.Y. Fadeev; *Langmuir*, **2003**, 19, 7904.
- [41]. Y. Wu, K. Liu, D. Li, Y. Guo, S. Pan, *Appl. Surf. Sci.*, **2011**, 258, 1619.
- [42]. M.E.I Saraya, M.A. Tantawy, H. El-Didamony and A.M.E. Abd-El-Rahman; *American J. Nanotech.*, **2011**, 2(1), 106.
- [43]. K. Shinozuka, K. Ottu, H. Fukumoto; US patent, 4,505,755 19/1985 106/308B, **1985**.
- [44]. S. Grothe, P. Fritzen, J. Winkler, B. Rohe.; US patent US2009/0318594 A1 24/**2009**.
- [45]. Aderhold, Krefeld, Rohrborn, Vluyn ; US patent 4,894,093 16/1990 106/471, **1990**.
- [46]. Y. Shen, C. Li, X. Zhu, A. Xie and L. Qiu; *J. Chem. Sci.*, **2007**, 119, 319.
- [47]. Y. Sheng, B. Zhou, J. Zhao, N. Tao and K. Yu ., *J. Colloid Interf. Sci.*, **2004**, 272, 326.
- [48]. R.J. Hill; *The Canadian Mineralogist* **1977**, 15, 522.
- [49]. M.H. Qu, Y.Z. Wang, C. Wang, X.G. Ge, D.Y. Wang, Q. Zhou; *E. Polym. J.*, **2005**, 41, 2569.
- [50]. V.S Nisha Joseph. R; *Rubber Chem. Technol.*, **2006**, 79, 1.
- [51]. J. Ginestar; *J. Cosmetics & Toiletries*. **2003**, 118, 73.
- [52]. P. Stamatakis, B.R. Palmer, C.F. Bahren, G.C. Salzman, T.B. Alien; *J. Coat. Technol.*, **1990**, 62, 95.

..........

**NATURAL RUBBER - BARIUM SULPHATE
NANOCOMPOSITES**

Part-a Natural rubber based nanocomposites:

Nano bariumsulphate (BN)/modified nano barium sulphate (MBN) filled RNCs

Part-b Synergistic effect of carbon black filled natural rubber-modified barium sulphate hybrid RNCs

Part-a**NATURAL RUBBER BASED NANOCOMPOSITES: NANO BARIUM SULPHATE/
MODIFIED NANO BARIUM SULPHATE FILLED RNCs**

Natural rubber-nano barium sulphate elastomer composites (RNCs) using both unmodified and modified barium sulphate were prepared by mill mixing. Cure characteristics, filler dispersion, mechanical properties and thermal stability of the elastomeric composites were evaluated. The amount of filler was varied from amount 0 to 15 phr. Modified barium sulphate (MBN) increased the rate of cure reaction. Compared to NR-BN RNCs, NR-MBN RNCs showed higher tensile strength, tear strength and modulus values and lower elongation at break. Characterization of the RNCs using scanning electron microscopy showed that there were changes in the morphology of the fracture surface with filler loading. Thermal stability of the RNCs improved with MBN concentration. The kinetic parameters of thermal degradation of the composites were estimated by Freeman-Carroll, and Coat-Red fern methods. The swelling studies were conducted on MBN-RNCs to estimate their superior behaviour and mechanism indicated a deviation from fickian mode. Overall enhancement in properties was obtained from NR- MBN₂ system.

Introduction

The addition of numerous varieties of inorganic fillers has already been researched and applied extensively to strengthen the properties of the existing polymer materials, especially the elastomers. The size and dispersion of inorganic particles have a great effect on the physico-mechanical properties as well as the processability of polymer composites. The incorporation of nanofillers to elastomeric matrices is a promising means for property modification [1, 2]. Some nano fillers have improved the performance of the composites outstandingly owing to their high specific surface area compared to traditional fibers or particles [3, 4]. Rubber is widely used as an important matrix material for the preparation of composites due to its good mechanical properties and high elastic recovery. Natural rubber (NR) is an addition polymer, an elastomeric hydrocarbon obtained as a milky white fluid known as latex from *Hevea Brasiliensis*. Vulcanized products made from NR have high mechanical strength, very good dynamic-mechanical properties and is therefore used in tyres, rubber springs etc. Since the modulus and tensile strength of gum vulcanizates are low, an additional reinforcing phase is necessary for the practical applications of rubbers [5]. Rubber is generally reinforced with fillers such as carbon black (CB), silica, silicates and fibers. The full reinforcing effects from these fillers are diminished due to their large size and agglomeration. Therefore, application of the well-dispersed nanofillers into rubber matrix to obtain beneficial mechanical and physical properties is becoming crucial. The uniqueness of NR lies in its biological origin, renewable and hazard free nature. Synthetic polyisoprene (IR) has basically properties similar to those of its natural counterpart and has a more consistent rate of curing and processing characteristics, at a slightly higher relative price. However, still NR fits number of applications in which it cannot be replaced by synthetic alternatives.

Barite is a mineral consisting of barium sulphate, which is widely used in polymer industries [6, 7]. In chapter3, the nano barium sulphate (BN) had been

successfully synthesized using precursors reported by earlier technique [8], but a novel PVA medium, as the raw material. The reinforcing effect of this synthesized barium sulphate nano powders on natural rubber has been investigated. The mechanical properties of elastomeric composites depend upon aspect ratio of the filler as well as compatibility of filler with matrix [9, 10]. The inertness to chemicals and opacity to x-rays can be imparted effectively to polymer by improving the natural rubber-filler interaction in barium sulphate filled composites. Even though barium sulphate is hydrophobic in nature, the size reduction influences the reinforcement which is further enhanced on treatment with modifier. Present part of this chapter, deals with fabrication of NR composites using modified and unmodified nano barium sulphate (BN, MBN) and characterization thereof.

4a.1 Natural rubber barium sulphate nanocomposites

4a.1.1 Preparation of rubber nanocomposites

Nano powders were synthesised via chemosynthetic pathway in presence of PVA (section 3.2.2) and modified using stearic acid (section 3.2.3). The nano barium sulphate powders obtained is here after referred to as BN and the modified compound as MBN and the filler loadings are represented as subscripts to this notation. The formulation for the preparation of the NR-RNCs is given in Table 4.1. Two series of RNCs were prepared- first series with varying amounts of BN and the second with varying amounts of MBN. The RNCs were prepared in a laboratory size two-roll mill at a friction ratio of 1:1.25 as per ASTM standards (section 2.2.1). The mixes were kept for 24 h for maturation. The optimum cure time at 150°C was determined using a Rubber Process Analyzer. The compounds were compression moulded at 150°C in an electrically heated hydraulic press (section 2.2.5). The samples were cured to their respective optimum cure times. After curing, the pressure was released and the sheets were suddenly cooled in water. These sheets were used for subsequent tests. The samples for rest of the studies were prepared according to procedures mentioned in section (2.3.1-2.3.3).

Table 4.1 Compounding formulation of natural rubber used for the present study

Compounding ingredient	MBN0/ BN0 (phr)	MBN1/ BN1 (phr)	MBN2 /BN2 (phr)	MBN5/ BN5 (phr)	MBN10/B N10 (phr)	MBN15/B N15 (phr)	MBN25/B N25 (phr)
NR	100.0	100.0	100.0	100.0	100.0	100.0	100.0
ZnO	5	5	5	5	5	5	5
Stearic acid	2	2	2	2	2	2	2
MBN	0	1	2	5	10	15	25
BN	0	1	2	5	10	15	25
Sulphur	2.5	2.5	2.5	2.5	2.5	2.5	2.5
TMTD	0.1	0.1	0.1	0.1	0.1	0.1	0.1
CBS	0.6	0.6	0.6	0.6	0.6	0.6	0.6
HS	0.75	0.75	0.75	0.75	0.75	0.75	0.75

4a.1.2 Cure characteristics

The cure characteristics of the rubber compounds are essential as it predicts the performance of the compounds during processing, scorch safety, stability and hence the physico-mechanical properties of the final vulcanizates. The curing characteristics of all the vulcanizates are summarized in the Table 4.2. Rubber nanocomposites with surface treated nano barium sulphate register superior accelerating effect on the cure characteristics.

Cure time represents the time corresponding to the development of 90% of the maximum torque and scorch time is the time required for the torque value to reach 10 % of maximum torque. It is a measure of the processing safety, i.e., the time available for safe processing prior to the onset of vulcanization reaction. In the presence of organo treated nanofiller, both the cure time and scorch time of NR filled vulcanizates reduced, the effect being well registered at a filler loading of 2 phr in the MBN series. The decrease in cure time indicates that filler incorporation activates the cure reaction and also, the MBN series promotes cure acceleration compared to BN series. These results are again supported by the cure kinetic studies and cure rate index values, which will be discussed in the following sections.

The maximum torque is an index of the extent of crosslinking reactions and represents the elastic modulus of the fully vulcanized rubber. It is also a measure of the filler-rubber matrix interaction. The maximum torque value (D_{\max}) also showed an increase with MBN loading. The D_{\max} is increased by 21% for MBN₁₅ which directs to an increase in modulus of the composites. This effect is essentially attributed to the carboxylate groups in the barium sulphate nano particles, which came from the organic surface treatment using stearic acid. Fatty acids are regarded to be as indispensable activators in conjunction with zinc oxide. They solubilize the zinc oxide and the secondary effect is increased in the amount of zinc sulphide produced. The zinc salts of fatty acids, which are a type of surfactant, also solubilize insoluble accelerators to form the actual catalyst. One of the roles of the activators such as zinc carboxylates is to facilitate the opening of the elemental sulphur ring to form polysulfide ions, which increases the vulcanization rate but has little effect on the vulcanization efficiency [11]. Although the carboxylate itself accelerate the vulcanization process the organo treated barium sulphate give rise to a further noticeable increase in the vulcanization rate, which could be attributed to a synergistic effect between the filler and modifier. Unmodified nano hardly varies the cure characteristics of the rubber, probably due to a poor compatibility between the unmodified BN and hydrophobic polymer.

The minimum torque; D_{\min} , represents the effective viscosity of the mixtures before vulcanization. In the case of polymer composites filled with various particulate fillers [12], the minimum torque in cure curve is considered to be a direct measure of the filler content and can be considered as a measure of stiffness of the unvulcanized compound. The D_{\min} values do not vary much with nano loading suggesting that the processability of the composites is not affected.

Stearic acid, in conjunction with some metallic oxides, notably zinc oxide, form the activating system during sulphur vulcanization [13]. The essence of activating the vulcanization process is that sulphur acting on its own is a very

slow process. Activation increases the efficiency of crosslink formation. The use of stearic acid and zinc oxide as activating system is a standard practice in rubber compounding [14].

Table 4.2 Cure characteristics of natural rubber based RNCs

Filler loading (phr)	Minimum torque (dNm)		Maximum torque (dNm)		T ₁₀ (minutes)		T ₉₀ (minutes)	
	BN	MBN	BN	MBN	BN	MBN	BN	MBN
0	0.15	0.15	2.52	2.52	2.51	2.51	5.89	5.89
1	0.02	0.01	2.53	2.60	2.47	2.44	5.54	5.24
2	0.08	0.07	2.53	2.78	2.43	2.41	5.57	5.17
5	0.03	0.03	2.55	2.79	2.21	2.18	5.45	5.48
10	0.08	0.07	2.68	2.89	2.25	2.23	5.53	5.57
15	0.02	0.02	2.77	3.05	2.05	2.03	5.49	5.41
25	0.02	0.02	2.81	2.82	2.08	2.08	4.98	4.76
50	0.02	0.02	2.00	1.93	1.53	1.53	4.54	4.43

Table 4.2 shows the cure characteristics of Natural rubber based RNCs. The result obtained is an indication that stearic acid has varying degree of influence on the physical properties of natural rubber vulcanizates. As part of the activating system, stearic acid, in combination with zinc oxide during mill processing, helps in the dispersion of other compounding ingredients by exerting a plasticization action on the stock compound [15]. Also during vulcanization, it helps in activating the vulcanization system, by increasing the efficiency of the penetration and consolidation of the elemental sulphur at the anchoring point of the network [16] referred to as internal lubrication effect [17].

4a.1.3 Cure kinetics

The plots of $\ln (D_{max} - D_t)$ against time t of the MBN series and BN series RNCs are presented in Fig. 4.1 and 4.2. The plots are found to be linear which proves that the cure reactions proceed according to first order kinetics.

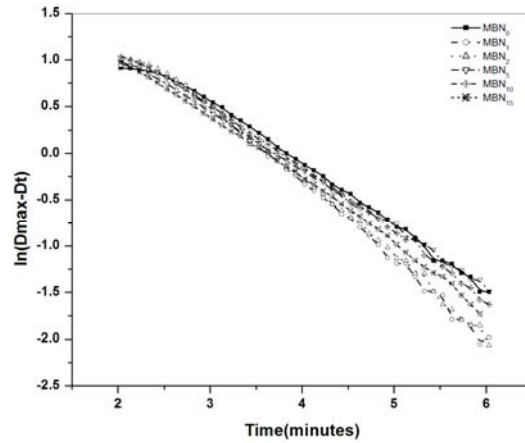


Figure 4.1 $\ln(D_{max}-Dt)$ against time t of the MBN series

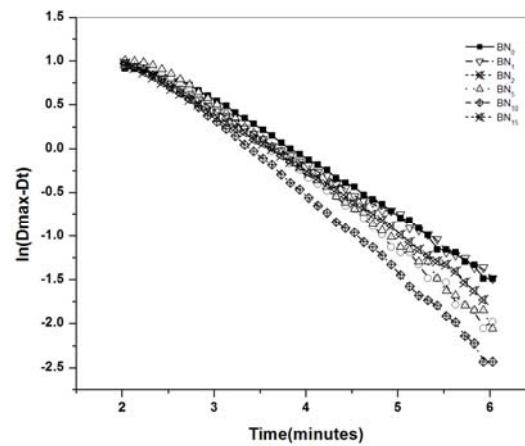


Figure 4.2 $\ln(D_{max}-Dt)$ against time t of the BN series

The cure rate constants (k) were calculated from their slope and the cure rate index (CRI) values were determined (section 2.2.2) for both series. The variation of these with filler loading for the MBN and BN series is presented in Fig. 4.3 (a) and (b), respectively. For the MBN series, both CRI and the kinetic rate constants increase with loading up to 2 phr, after which, both decreases but still cure activation is present as indicated by the higher CRI value than that of gum. CRI was higher for surface treated nanocomposites. In the case of BN series, both parameters increase with loading and remain constant on further filler incorporation. The increase in

CRI and cure reaction constant with loading indicates the activation of cure reaction. These results are in accordance with the results of rheometric data (section 2.2.2).

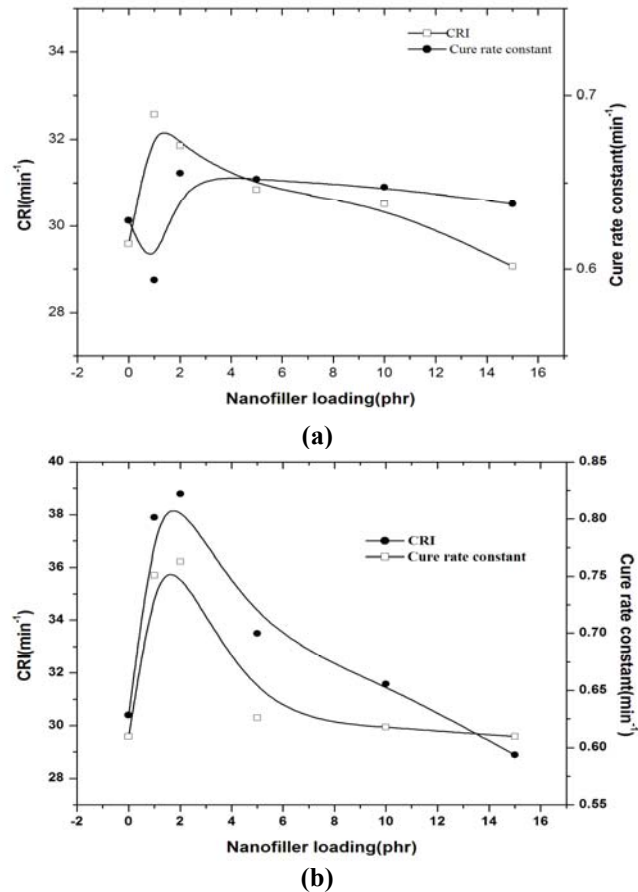


Figure 4.3 Plot of rate constant and CRI vs loading for the (a) BN series RNCs (b) MBN series RNCs

The cure rate indices of cure reactions of different composites were estimated and the graphical illustrations are given in Fig. 4.3(a) and (b).

4a.1.4 Filler dispersion in the RNCs

Maximum torque increases during vulcanization in the case of filled compounds. The increase in torque of the filled compound was found to be

proportional to filler loading. Fig. 4.4 represents the relation between $D_{\max}-D_{\min}$ against filler loading of BN and MBN. The increase in Δ torque indicates that the incorporation of nano barium sulphate affects cross linking between the polymer chain, which being more registered with MBN series.

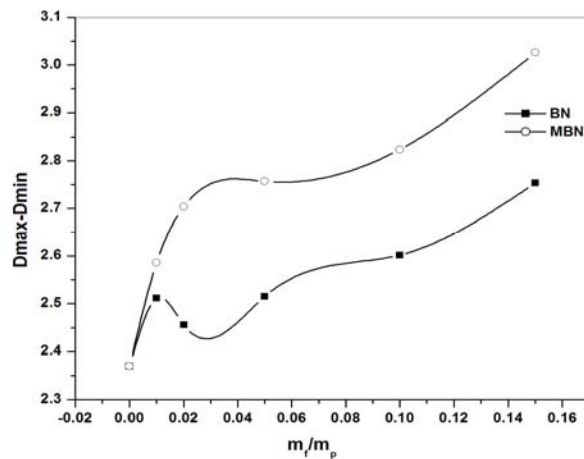


Figure 4.4 Plot of Δ torque with filler loading for RNCs

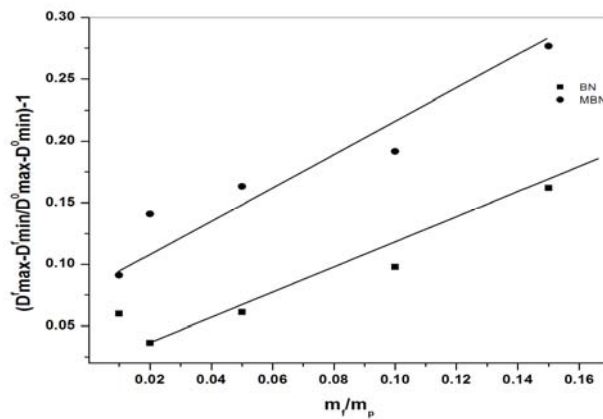


Figure 4.5 Plot of relative torque as a function of filler loading for RNCs

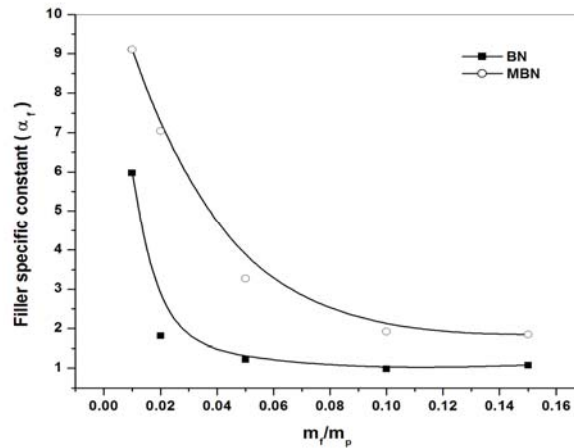


Figure 4.6 Variation of filler specific constant with filler loading for RNCs

The slope of the linear plot, showing the relative torque increase with filler loading, was defined by westlinning-wolfs equation (section 2.2.3.b). In the Fig. 4.5 and 4.6 the relative torque and filler specific constants are respectively plotted against the filler fraction and according to these plots α_f values for MBN filled composites is 9.1 and those for BN filled composite is 6.23. The higher α_f value of MBN-NR nano composites is due to the enhanced filler-rubber interactions.

4a.1.5 Dynamic properties measured in strain sweep for uncured compounds

The strain sweep measurements were conducted on uncured RNCs to investigate the rubber–filler interaction. The dependency of dynamic properties on the strain amplitude at smaller deformation throw light on the filler–filler networks in a rubber matrix.

The Fig. 4.7 (a) and (b) shows the strain dependence of complex modulus G^* for the BN and MBN filled RNCs respectively. The unfilled rubber shows no indication of non-linearity in the green compound. After the filler incorporation, the low strain modulus G_0 rises above the high strain modulus G_α , resulting in non-linear visco-elastic behaviour, and known as Payne effect G_0-G_α . In the case

of BN series there is an increase in Payne effect along with filler loading as indicated by the nonlinear strain dependence of complex modulus; where as in MBN series linearity is maintained at lower loadings. This increase in modulus or non-linear behavior is caused by the formation of filler-filler interactions formed by filler loading. It is to be noted that, the existence of a filler network is not necessarily corresponding to the existence of a filler network, which is percolated through the whole specimen. Filler-filler contacts in local sub networks are also denoted as filler networking and yield the Payne effect. The lowered Payne effect in MBN series shows higher filler-rubber interaction, due to uniform dispersion of modified nano barium sulphate in NR matrix.

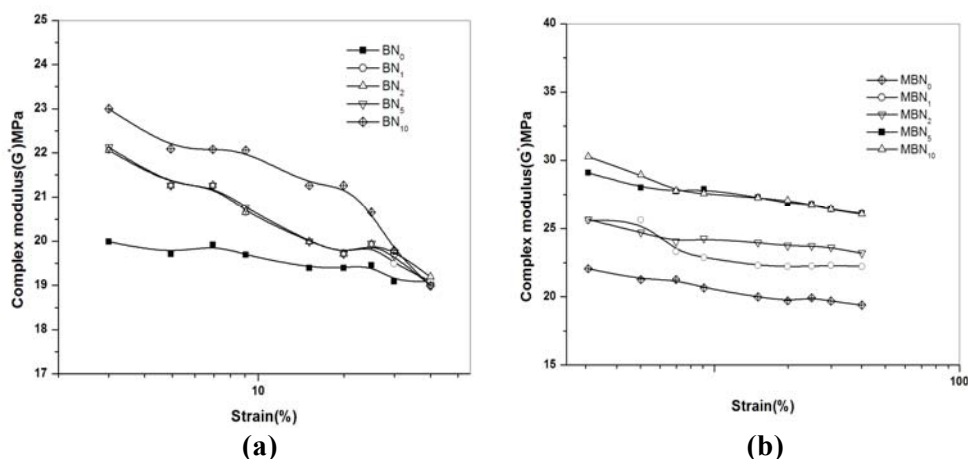


Figure 4.7 Dependence of Complex modulus (G^*) on strain amplitude of green compound at different loadings (a) BN series (b) MBN series

4a.1.6 Mechanical properties of RNCs

The increase in tensile strength (Fig. 4.8) of the MBN RNCs denotes the reinforcing nature of these fillers. As the filler loading is increased, more surface area is available for interaction between filler particles and the rubber matrix. Hence reinforcement increases with increase in filler loading for MBN series. For BN series, the tensile strength was maximum at 10 phr BN loading. But it was lower than that of gum. This is due to non treated surface of nano filler that has no modifiers within, to enable it to strongly bond with rubber. The filler BN is less

hydrophobic filler and hence it interacts least with NR and hence fails to impart strength properties to the rubber. With surface treated MBN better property is attained at a lower loading i.e., at 2 phr which is an indication of increased interaction between surface treated nano barium sulphate and rubber. An increase in tensile strength of about 31% is registered at this level of filler loading. The tear strength (Fig. 4.11) increases with filler loading upto 10 phr for BN as well as MBN series. The higher tear strength value of MBN RNCs is due to better interaction of nano particles with matrix. The smaller size of the nano particles along with modifier helps it to arrest or deviate the tear cracks, resulting in higher tear resistance. Elongation at break (Fig.4.10) decreases at low filler concentration indicative of the reinforcing effect of surface treated nano and beyond 10 phr it shows a marked increase. 300% modulus (Fig. 4.9) registered its maximum at 2 phr filler loading in both the series. Generally, wear resistance is thought to affect not only the performance, but also the life of rubber products. The nano-BaSO₄ has this unique property. Abrasion loss shows a continuous decrease with filler loading (Fig. 4.12). The MBN composites give significantly lower value for abrasion loss compared to the BN composites. The abrasion loss of the NR composites changed significantly with the addition of stearic acid modified nano-BaSO₄. Abrasion loss registered a decrease of 33% on addition of 2phr MBN. Compression set, as expected, is higher at higher filler loadings. The fillers that are reinforcing in nature will adversely affect the elastic properties, especially at elevated temperatures. This is reflected as higher compression set of the composites. However, in the case of MBN composites the set is relatively lower compared to the BN compounds, indicating that the extent of agglomeration in the case of MBN is lower. The compression set (Fig. 4.13) values increased on progressive addition of both the filler series; but a lowering of 14% is observed for 2phr MBN which may be due to uniform filler dispersion at this filler level. The hardness (Fig. 4.14) values also indicate superior reinforcement offered by MBN filled NR. The nature and trend of the graphs are similar, but the tensile strength values, abrasion loss and compression

set of MBN series composites are superior to that of BN series composites, showing that surface treatment has increased the interaction between rubber and filler.

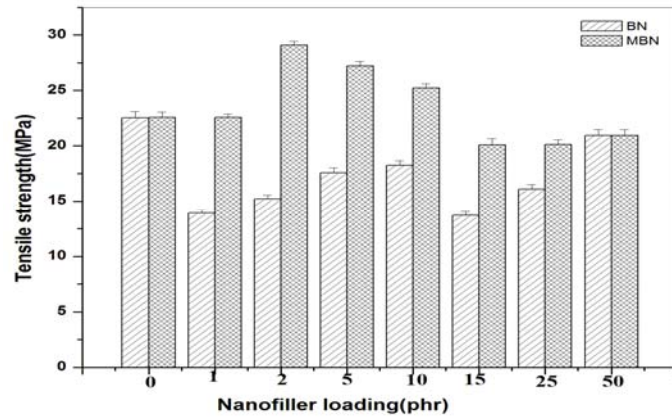


Figure 4.8 Variation of tensile strength with loading

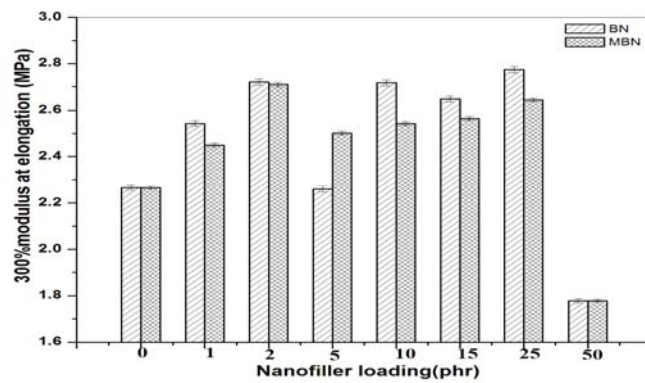


Figure 4.9 Effect of loading on the 300% modulus of the RNCs

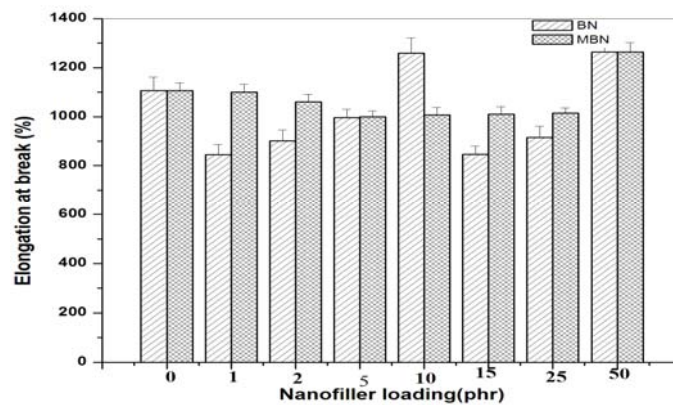


Figure 4.10 Effect of loading on elongation at break of the RNCs

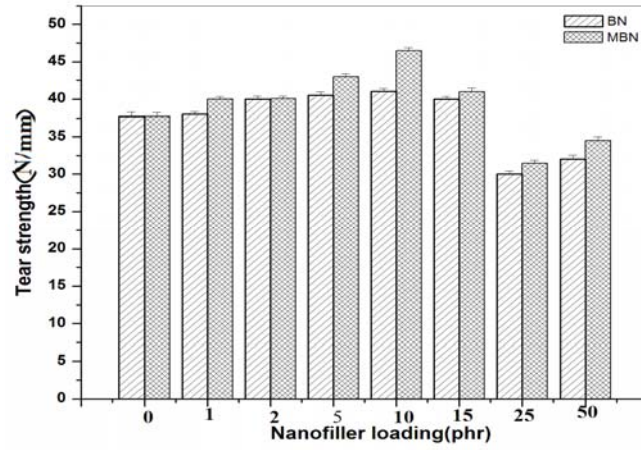


Figure 4.11 Variation of tear strength with loading

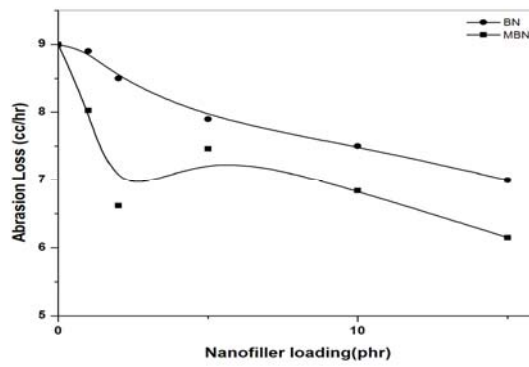


Figure 4.12 Variation of abrasion loss with loading

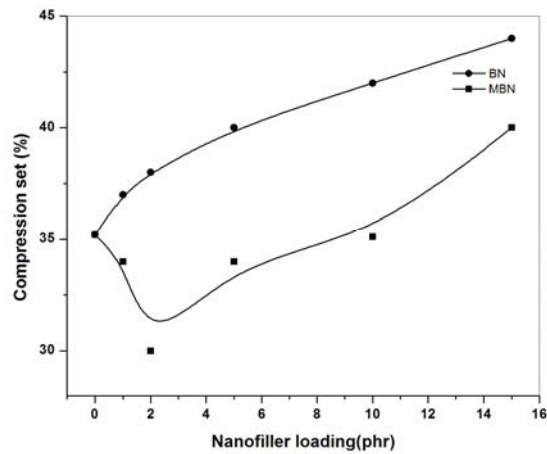


Figure 4.13 Variation of compression set with loading

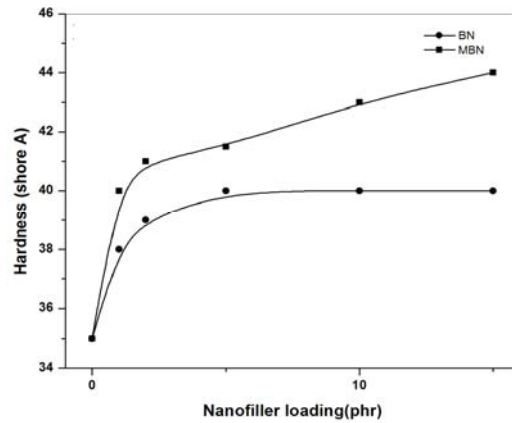


Figure 4.14 Variation of hardness with loading

4a.1.7 Morphology of fractured surface, SEM images

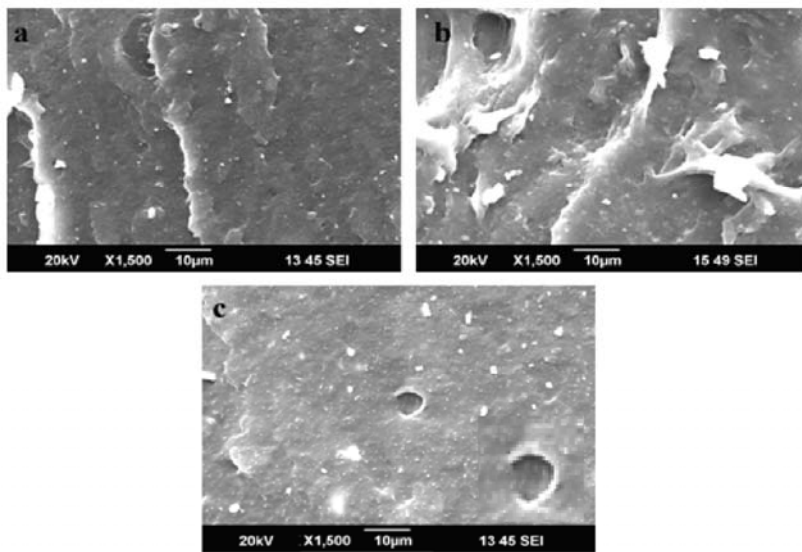


Figure 4.15 SEM photographs of tear fractured surfaces of (a) MBN_0 (b) MBN_2 (c) MBN_{10} natural rubber based RNCs

The SEM images of tear fractured surfaces of MBN filled systems are shown in Fig. 4.15. At higher filler loadings the surface roughness reduced and even craters resulting from filler pull outs are seen, which indicates poor filler dispersion. In the case of MBN_2 filled system, (Fig. 4.15b) the abundance of tear lines and irregular surface indicate an enhanced rubber-filler interaction. At higher loadings

agglomeration resulted in filler pullouts (resulting in 3-5 μ m craters) as seen in Fig. 4.15(c).

4a.1.8 Thermal stability of NR-MBN nanocomposites

The TG curves of the MBN series RNCs are shown in Fig. 4.16. The thermal characteristics as estimated by TGA are presented in Table 4.3. The degradation behaviour of the materials could be clearly read from the Differential thermogravimetry (DTG) curves shown in Fig.4.17. The temperature onset of degradation (T_i), the temperature at which the rate of decomposition is maximum (T_{max}), the peak degradation rate (R_{max}) and the decomposition temperature at 5% weight loss, $T_{-5}(\%)$ and 50% weight loss $T_{-50}(\%)$ are given in Table 4.3. The pure NR (MBN_0) gives a single degradation between 300 and 400 $^{\circ}C$ and peak maximum at 373.8 $^{\circ}C$. With increasing nano concentration, weight loss due to the NR degradation is still observed, but the relative intensity decreases. The onset of this degradation shows a slight shift to higher temperatures with increasing nano concentration, though the temperature of maximum degradation remains the same. MBN_{15} shows lower rate of degradation when compared to MBN_0 . To summarize, the rate of maximum degradation decreases from 1.457 to 1.123%/ $^{\circ}C$ with filler loading and modified nano filled systems are having superior thermal stability compared to unfilled counterparts. This may be attributed to the poor interfacial interaction between the filler and the matrix in the case of unmodified nano mixes. Nano barium sulphate when surface treated contributes to effective interaction between the filler and the matrix due to its small particle size and hence improves the interfacial adhesion. Strong interface renders the matrix stiff and makes the diffusion of heat and gases through the bulk more difficult. This makes the matrix thermally more stable in the presence of nano filler.

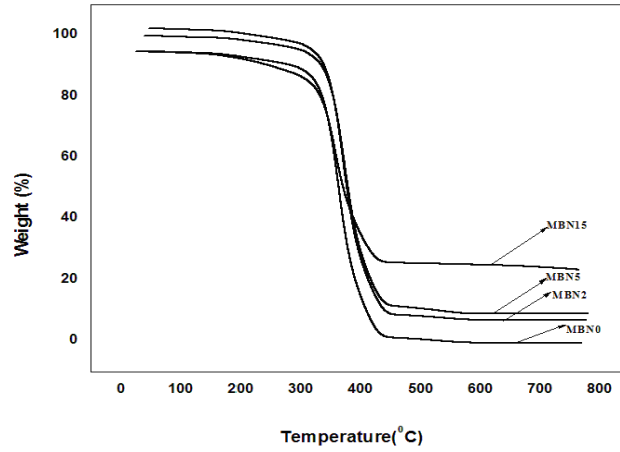


Figure 4.16 TGA traces of MBN series RNCs

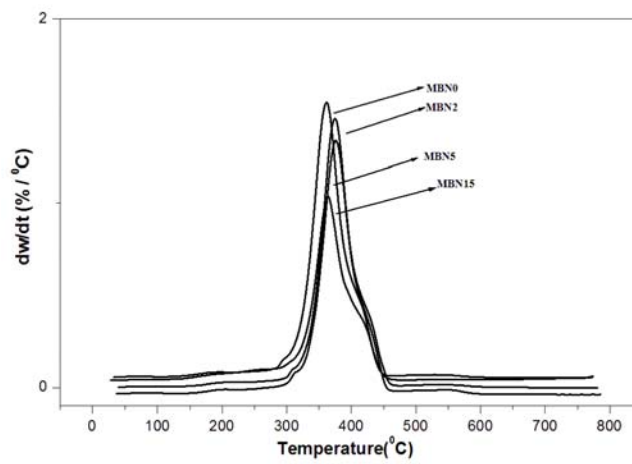


Figure 4.17 DTG curves of MBN series RNCs

Table 4.3 Thermal degradation data of MBN series RNCs

Sample code	T _i (°C)	T _{max} (°C)	R _{max} (%/ °C)	T ₋₅ (%)	T ₋₅₀ (%)
MBN ₀	315.3	373.8	1.457	301.67	377.53
MBN ₂	318.5	375.5	1.361	304.01	378.95
MBN ₅	320.1	375.6	1.358	304.21	379.31
MBN ₁₅	322.0	375.9	1.123	312.4	389.51

The kinetics of the thermal degradation reaction was followed using TGA. The Coats and Redfern (CR) (integral method)[18] and Freeman-Carroll (FC) equations (differential method)[19-20] were used to calculate the kinetic parameters. The representative plots of both methods are shown in Fig. 4.18 and 4.19 (for sake of brevity the plots of MBN₀, MBN₁₅ alone are included).

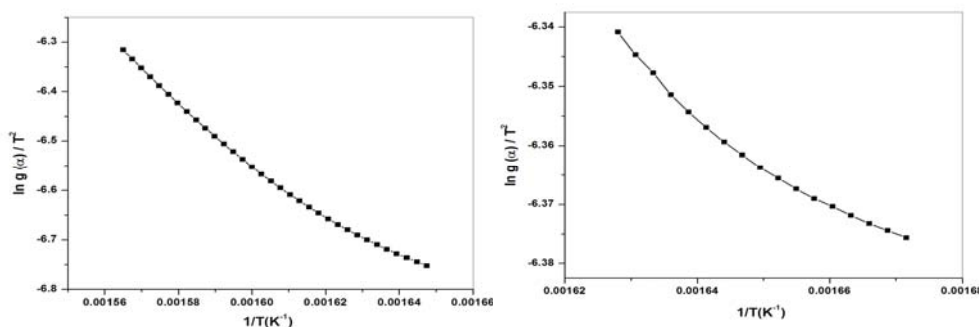


Figure 4.18 Coats Redfern representative plots of (a) MBN₀ (b) MBN₁₅

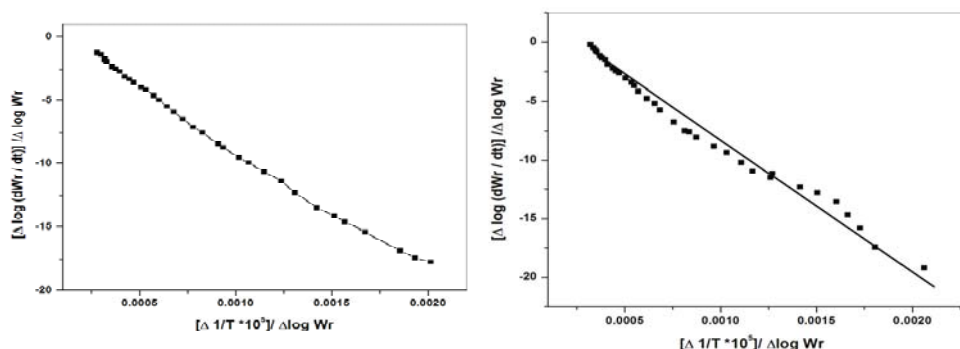


Figure 4.19 Freeman Carroll representative plots of (a) MBN₀ (b) MBN₁₅

The figures above show that the degradation of gum mix and the composites follow first-order kinetics. The role of nano filler seems to be very limited. This is because the degradation under nitrogen proceeds primarily by the thermal decomposition of the backbone chain. In the molecular level where the degradation is thermally initiated, the reactant is primarily the rubber hydrocarbon and hence the rate is dependant only on their concentration. Similar results have been reported earlier. Activation energy increases with filler content. Activation energy of the gum compound increases by the addition of nano filler according to FC methods. But a

generalization regarding the trend could not be derived from any of these methods. The activation energies obtained from the corresponding plots are presented in Table 4.4.

Table 4.4 Activation energies of NR-MBN RNCs

Sample code	Activation Energy, E_a kJ/mol	
	Coats-Red fern	Freeman Carroll
MBN ₀	101.25	152.15
MBN ₂	95.55	152.45
MBN ₅	95.02	153.93
MBN ₁₅	98.00	154.22

As shown in Table 4.4, estimates of activation energy vary widely amongst the two methods. There are several obvious sources of error that can be responsible for this variation. For the integral methods, i.e., CR equation, the different approximations to the integral of the Arrhenius equation lead to systematic errors in the values of the activation energy. The precision of the quantities plotted according to the Freeman and Carroll equation can be poor because of the error-propagation effects resulting when two experimentally determined values are ratioed. In summary, all the methods indicate the order of the degradation reaction to be one. A better trend for the change in activation energy can be derived from FC method as evidenced by plots and Table 4.4. The TGA-DTG curves still evidences improved thermal stability in filled nanocomposites compared to NR.

4a.1.9 Crosslink density and swelling studies

Swelling studies of NR-MBN composites.

Diffusion studies of the RNCs were carried out (as in section 2.3.3) using toluene as the penetrant and crosslink density was calculated followed by diffusion, sorption and permeation coefficients.

The sorption curves at room temperature were obtained by plotting $Q_t\%$ of penetrant vs square root of time. The sorption curves of MBN filled NR are shown in Fig. 4.20. The initial swelling rate is very high owing to the large concentration gradient. This places the polymer under heavy solvent stress. This concentration gradient decreases with advanced swelling, the rate of swelling decreases and the difference in concentration becomes negligible when it reaches the equilibrium swelling. In the MBN filled RNCs as filler loading increases $Q_t\%$ decreases which may be due to the decrease in volume fraction of rubber with filler loading.

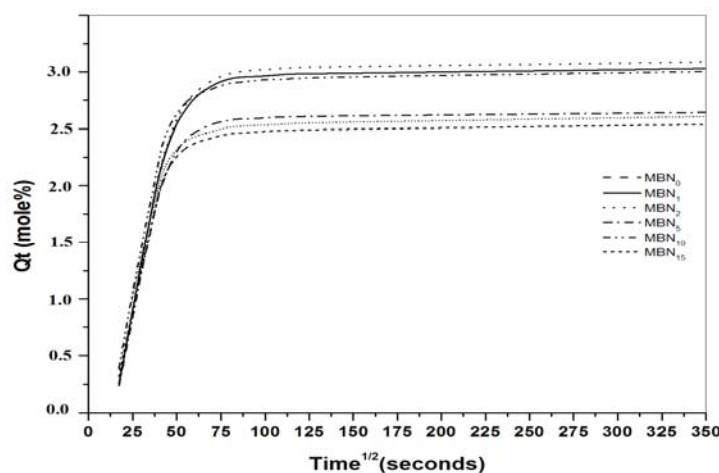


Figure 4.20 Sorption curves of natural rubber based RNCs with MBN

The value of k depends on the structural features of polymer, whereas the value of n determines diffusion mechanism. The n values for MBN filled RNCs are shown in column 2 of Table 4.5. For the fickian mode, the value of n is 0.5 and it occurs when the rate of diffusion of penetrant molecule is much less than the relaxation rate of the polymer chains. For non-fickian transport, where the n value is 1, the diffusion is rapid when compared with the simultaneous relaxation process. However in the case of anomalous transport where the n value is in between 0.5 and 1, both solvent diffusion and polymer relaxation rate are comparable. The effective diffusivity, D of the rubber solvent system was calculated from the initial portion of the sorption curves[21,22].

From the Table 4.5 it is seen that the value of n lies between 0.5 and 1.0. Thus the transport mechanism can be considered to be anomalous where rearrangement of polymer molecules occurs at a comparable rate to that of the change in concentration. As the loading increases, the value of n decreases which indicates that polymer relaxation increases compared to rate of diffusion of penetrant. This is again supported by decrease in diffusion coefficient with loading. The diffusion process depends on concentration gradient between solvent and rubber. As the loading increases this gradient decreases and hence a decrease is registered in the case of coefficient of diffusion. The sorption and permeation data, as shown in the Table 4.5, decrease with loading which is a reflection of decrease in volume fraction of absorbing phase with increased loading. Permeation decreases since it is a collective phenomenon consisting of both diffusion and sorption. Arriving at the crosslink density values it could be seen that as the filler loading increases, upto 2 phr, there is an increase in crosslink density beyond which the cross link density decreases, which may be due to the occlusion of filler particles between the rubber chains. This is supported by tensile strength values. The better mechanical properties exhibited by MBN₂ system may be due to the higher crosslink density compared to higher filler loaded RNCs [23-25].

Table 4.5 Sorption data of Natural rubber based RNCs with MBN

Sample code	n	Diffusion coefficient, $D \times 10^{-7}$ ($\text{cm}^2 \text{s}^{-1}$)	Sorption Coefficient S	Permeation coefficient, $P \times 10^{-6}$ ($\text{cm}^2 \text{s}^{-1}$)	Crosslink density, $\times 10^{-5}$ (g mol/cc)
MBN ₀	0.6748	9.92	3.83	3.79	4.81
MBN ₁	0.6503	7.89	3.56	2.81	4.82
MBN ₂	0.6451	6.82	3.03	2.06	6.06
MBN ₅	0.6235	6.24	2.99	1.87	5.76
MBN ₁₀	0.5832	6.12	2.94	1.51	5.65
MBN ₁₅	0.5067	5.98	2.52	1.50	5.43

Conclusions:

Natural rubber/barium sulphate composites (NR-BaSO₄ RNCs) with sufficient mechanical properties can be prepared by mechanical mixing. Two varieties of fillers BN and MBN were used for the preparation. Addition of MBN to NR improves its cure characteristics and the cure reaction follows first order kinetics. In the presence of MBN filler, both cure rate and the kinetic rate constants increased with loading up to 2 phr, beyond which, both these values decreased. Fine dispersion of BN particles in the NR matrix is not achieved by mill mixing, but on modification with stearic acid, the prepared MBN, helped to improve dispersion. The higher α_f value of MBN-NR evidenced the enhanced filler-rubber interactions. The tear and abrasion resistances were enhanced with MBN loading. The tensile strength decreases with increase in BN concentration showing its inability to get intimately mingled with matrix. Among the BN series, at 10 phr of filler loading (BN₁₀), better tensile strength is observed and with surface treated MBN better property (31% increment compared to gum) is attained at a lower loading indicating increased interaction between surface treated nano barium sulphate and rubber. The smaller particle size of the filler along with modifier helped in arresting the tear cracks, resulting in higher tear resistance. The MBN composites showed minimal abrasion loss compared to the BN composites. Compression set, in the case of MBN composites is relatively lower compared to the BN compounds, and agglomeration in the case of NR-MBN RNCs is lowered. Thermal stability increased with MBN concentration. Thermal degradation process followed first order kinetics as evidenced from FC and CR plots. The kinetic analysis, solvent resistance and diffusion phenomenon also evidenced stabilisation of NR-MBN RNCs. Permeation in NR RNCs decreased with filler loading. The mode of solvent sorption mechanism deviated from fickian mode. The properties presented their maximum at a filler level of 2phr MBN in natural rubber based RNCs.

References

- [1]. M.A.Osman, A.Atallah, M.Muller, U.W.Suter; *Polymer*, **2001**, 42, 6545.
- [2]. C.A.Cooper, D.Ravich, D.Lips, J.Mayer, H.D.Wagner; *Compos. Sci. Technol.*, **2002**, 62, 1105.
- [3]. M.D. Frogley, D.Ravich, H.D.Wagner; *Compos. Sci. Technol.*, **2003**, 63, 1647.
- [4]. F.Yatsuyanagi, N.Suzuki, M.Ito, H.Kaidou; *Polymer*, **2001**, 42, 9523.
- [5]. N.D.Alberola, K.Benzarti, C.Bas, Y.Bomal, *Polym. Compos.*, **2001**, 22,312.
- [6]. M.H. Qu, Y.Z. Wang, C.Wang, X.G. Ge, D.Y.Wang, Q.Zhou ;*Eur. Polym. J.*, **2005** ,41 ,2569.
- [7]. M.H. Qu, Y.Z.Wang, Y.Liu, X.G.Ge, D.Y.Wang, C.Wang; *J.Appl. Polym. Sci.*, **2006**,102,564.
- [8]. J.Z. Hang, Y.F.Zhang, L.Y.Shi, X.Feng; *J. Mater. Sci.*, **2007**,42,9611.
- [9]. C.Ge, P.Ding, L.Shi, J.Fu; *J.Polym. Sci. Part B.Polym.Phys*, **2009**,47,655.
- [10]. M .Akiba,A.S Hashim;*Prog.polym.sci.*,**1997**,22,475
- [11]. G .Mathew, B.Kuriakose, S.Thomas, *J.Elastomers.Plast.*, **1997**,29,163.
- [12]. W.Hofmann;*Rubber Technology Handbook*.Gardener/Hanser Publications Inc.Cincinnati, OH. **1996**.
- [13]. K.Nagdi;*Rubber as Engineering Material*, 1st edition. Hanser: Munich, Germany, **1992**.
- [14]. F.W. Barlow; *Rubber Compounding: Principles, Materials and Technique*, 2nd edition, Marcel Dekker: New York, NY,**1993**.
- [15]. P.J. Fairclough, P.M.Swift; *Rubber Developments*,**1993**, 4(46),21.
- [16]. P.J. Wang; *J. Rubber Development.*, **1994**,47(³/₄),17.
- [17]. A.W.Coats, J.P.Redfern ;*Nature* ,**1964**,68,201.
- [18]. J. P.Lin, C.Y. Chang , C.H.Wu, Shin-Mins, *Polym. Degradation Stab.*, **1996**, 53.

- [19]. E. S.Freeman, B.Carroll; J. Phys. Chem.,**1958**, 62, 394.
- [20]. J.Crank; The mathematics of diffusion., 2nd Ed. Oxford: Clarendon Press,
1975, 244.
- [21]. L. N.Britton, R .B. Ashman, T. M.Aminabhavi, P. E. Cassidy;J. Chem. Edn.,
1988, 65,368.
- [22]. S. Aprem, K.Joseph, A. P. Mathew,S.Thomas, J. Appl. Polym. Sci.,
2000,78,941.
- [23]. R. S. Khinnava, and T. M. Aminabhavi;J. Appl. Polym. Sci., **1991**, 42, 2321.
- [24]. P. J. Flory and Jr.Rener; J. Chem. Phys.,**1943**,11, 521.
- [25]. P.E.Cassidy, T.M.Aminabhavi, C.M.Thompson; Rubber Chem. Tech., **1983**,
56,594.

Part-b

**SYNERGISTIC EFFECT OF CARBON BLACK FILLED NATURAL RUBBER-MODIFIED
BARIUM SULPHATE HYBRID RNCs**

Novel hybrid rubber nanocomposites based on natural rubber, modified nano barium sulphate and carbon black-HAF-N330 were prepared by mechanical mixing with the aim of determining the synergistic effect of dual filler networks in the natural rubber matrix. The investigation aimed at replacing, at least by a smaller fraction, carbon black from its composites using an eco-friendly filler. In order to optimise the synergistic effect of carbon black and MBN in the natural rubber matrix, systematic analyses were performed on NR-CB-MBN hybrid RNCs containing various combinations of black and MBN, which revealed that the properties strongly depended on the extent of the dispersion of black and MBN fillers. The amount of MBN filler was varied from 0 to 15 phr and that of carbon black was fixed at 30phr. The results were compared with that of 40 phr black containing composites. Incorporating 5 phr MBN to the control NR composite containing 30 phr carbon black resulted in an obvious synergistic effect, including cure activation, improvement in the mechanical properties and enhancing the thermo oxidative resistance. This CB30+MBN₅ system excelled CB40 filled NR-RNCs in all properties. These hybrid RNCs showed higher tensile strength, tear strength and modulus values and lower elongation at break compared to black alone filled systems. Characterization of the RNCs using scanning electron microscopy showed that there were changes in the morphology of the fracture surface with filler loading. The thermal stability of the RNCs improved with MBN concentration. Transport mode showed anomalous behaviour. Overall enhancement was registered in hybrid RNCs filled with 5phr MBN.

Introduction:

Generally for formulation of the rubber compounds, carbon black (CB) is incorporated in rubber matrix as a reinforcement to modify the mechanical properties of finished goods and to control the viscoelastic behaviour of the compound during processing, prior to curing. The addition of CB into the elastomers is of commercial importance since it enhances the technical properties [1,2]. Carbon black generally consists of elemental carbon in the form of nearly spherical particles of colloidal size that coalesce into particle aggregates and agglomerates, and are obtained by the partial combustion or thermal decomposition of hydrocarbons. The primary particles tightly fuse together so that the particles or these carbon black aggregates cannot be separated by normal rubber processing techniques. About 90% of the worldwide production of carbon black is used in the rubber industry, especially in rubber tire applications. It is not only the most widely used but also the oldest reinforcing filler used to improve tensile and tear strength, modulus, hardness, abrasion and thermal resistance[3,4]. However, the production of carbon black is dependent on non-sustainable supplies of petroleum. The preparation and processing techniques are hazardous and are energy consuming. Moreover it causes pollution and imparts black colour to rubber[5].

In the past two decades, researchers have been in the hunt for new reinforcing fillers that are environment friendly, inexpensive and readily available to partially replace carbon black. The replacement aims primarily at cost reduction on one hand and on the other, a synergy of different fillers that might be obtained due to the complicated interactions through mixed network formation. These fillers like silica, kaolin, sepiolite etc. are inorganic in nature and hence incompatible with organic polymer matrices. Their reinforcing effect was much lower than with carbon black. However, with the development of nanocomposites, it is possible to tailor the surface of the silicate layers to become organophilic, which can enhance the properties of the polymer significantly. Indeed Liu,et al. had reported the synergistic reinforcement of

carbon black-modified clay in natural rubber. It was found that NR with the hybrid filler exhibited superior mechanical properties over that of black as single phase filler [6].

Investigations carried out by Rattanasom, et al. revealed that the use of hybrid silica/carbon black improved the mechano-dynamic properties of NR vulcanizates when the silica/carbon black ratio was 20/30 or 30/20 [7]. Certain rubber-clay nanocomposites reported in the literature have mechanical properties similar to or better than rubber filled with carbon black [8-10]. Magaraphan, et al. [11] prepared natural rubber nanocomposites with octadecylamine functionalized MMT, which presented higher tensile strength and elongation than NR containing 20 phr carbon black. Meneghetti, et al. [12] studied the effect of carbon black on SBR-clay nanocomposites. It is reported that the synergistic effect of carbon black and organoclay brought similar property enhancements with carbon black alone but at half filler loading. In all these carbon Black filled RNCs, reinforcement is generally attributed to the nanoscale particle size, large specific surface area, high structure degree of carbon black and the formation of extensive rubber-Black networks [13,14].

In this part of the chapter, carbonblack filled NR was prepared and compared with NR-CB-MBN hybrid nanocomposites. The synergistic effect of carbon black and MBN was investigated in NR samples, which contained both fillers at different concentration.

4b.1 Natural rubber-carbonblack- modified nanobarium sulphate hybrid nano composites.

4b.1.1 Preparation of nanocomposites

Nano powders were synthesised via chemosynthetic pathway in presence of PVA (section 3.2.2) and modified using stearic acid (section 3.2.3). The carbon black loadings are represented as CB and modified nano barium sulphate is named as MBN. The filler loadings are represented as subscripts to this notation. The

formulation for the preparation of the RNCs is given in Table 4.6. Two series of RNCs were prepared with varying amounts of MBN; first series with constant loading of carbon black at 30phr and second one with 40phr. The RNCs were prepared in a laboratory size two-roll mill at a friction ratio of 1:1.25 as per ASTM standards (section 2.2.1). During the final sheeting at low nip gap, the fillers were oriented along the mill direction. The mixes were kept for 24 h for maturation. The optimum cure time at 150°C was determined using a Rubber Process Analyzer. The compounds were compression moulded at 150°C in an electrically heated hydraulic press (section 2.2.5). The samples were cured to their respective optimum cure times. After curing, the pressure was released and the sheets were immediately cooled in water. These sheets were used for subsequent tests. The samples for rest of the studies were prepared according to procedures mentioned in section (2.3.1-2.3.3).

Table 4.6 Compounding formulation of natural rubber composites

Compounding ingredient	Phr						
NR	100.0	100.0	100.0	100.0	100.0	100.0	100.0
ZnO	5	5	5	5	5	5	5
Stearic acid	2	2	2	2	2	2	2
Aromatic oil	8.5	8.5	8.5	8.5	8.5	8.5	9.5
MBN	0	2	5	10	15	25	0
Sulphur	2.5	2.5	2.5	2.5	2.5	2.5	2.5
TMTD	0.1	0.1	0.1	0.1	0.1	0.1	0.1
CBS	0.6	0.6	0.6	0.6	0.6	0.6	0.6
HS	0.75	0.75	0.75	0.75	0.75	0.75	0.75
HAF	30	30	30	30	30	30	40

4b.1.2 Cure characteristics

The cure characteristics of the hybrid rubber nanocomposites are shown in Table 4.7. The maximum torque value of the black filled composites is a direct measure of shear modulus and it was found to increase with filler loading

indicating an enhancement of stiffness of the nanocomposites. The cure activation by stearate modifier is observed as cure time reduction.

Table 4.7 Cure characteristics of Natural rubber based hybrid RNCs

Sample code (phr)	Minimum torque (dNm)	Maximum torque (dNm)	T ₁₀ (minutes)	T ₉₀ (minutes)
CB40	0.09	4.86	1.43	5.56
CB30	0.06	3.95	1.74	5.28
CB30+MBN2	0.09	4.87	1.59	5.55
CB30+MBN5	0.09	5.31	1.50	4.83
CB30+MBN10	0.08	4.70	1.43	5.12
CB30+MBN15	0.05	4.96	1.47	5.41
CB30+MBN25	0.08	5.02	1.49	5.02
CB30+MBN50	0.01	4.00	2.03	5.33

The plot of $\ln (D_{max} - D_t)$ against time t of the carbon black filled NR-MBN hybrid RNCs at 150 °C is presented in Fig. 4.21. The plots are found to be linear which proves that the cure reactions proceed according to first order kinetics. The cure rate constants (k) were calculated from the slope and the cure rate index (CRI) values were determined according to equation given in section 2.2.2 . The variation of these with filler loading is presented in Fig. 4.22. For the NR-CB-MBN series, CRI increases with a combination of CB30+MBN₅, after which, it decreases but still cure activation is present as indicated by the higher CRI value than 30CB.

The increase in CRI with loading indicates the activation of cure reaction. These results are in accordance with the results of rheometric data (section 2.2.2)

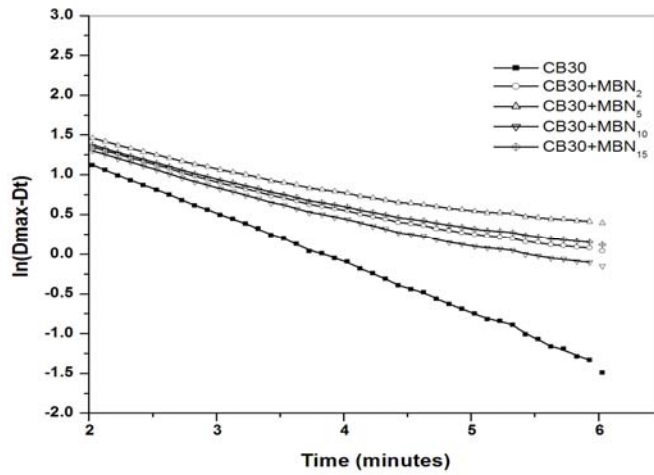


Figure 4.21 $\ln(D_{\max} - D_t)$ against time t of the NR-CB-MBN filled hybrid RNCs

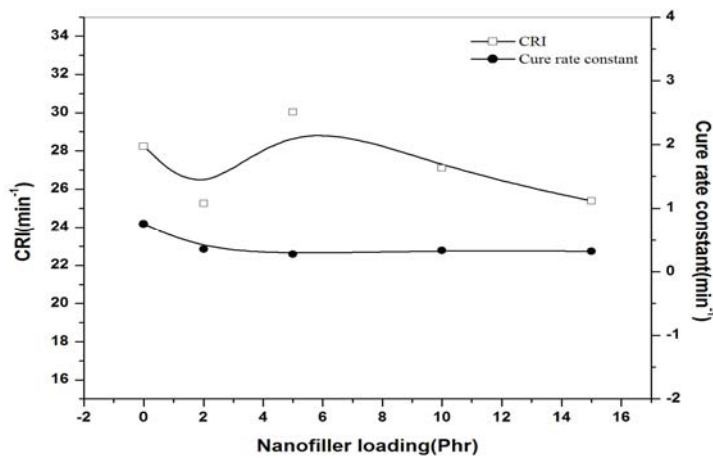


Figure 4.22 Plot of rate constant and CRI vs loading for the NR-CB-MBN series RNCs

4b.1.3 Filler dispersion in the RNCs

Maximum torque increases during vulcanization in the case of filled compounds. Fig. 4.23 represents the relation between $D_{\max}^f - D_{\min}^f$ against filler loading of hybrid composites. The increase in Δ torque indicates that the incorporation of nano barium sulphate affects cross linking between the polymer chains, which is more pronounced with 5 phr MBN filled hybrid composite series. In Fig. 4.23, Wolff equation is applied for the NR-CB-MBN hybrid

system. It is a measure of the structure of the fillers in the matrix. The higher α_f value found for the MBN-5, CB-30 compounds ($\alpha_f = 0.90$) would be an evidence for this filler combination to be more viable. The absolute value of α_f was calculated (section 2.2.3.b) and is plotted in Fig. 4.23. The value of α_f increases with loading. This means that this system form less agglomerates in the matrix. With further additions, there is a tendency for agglomeration. These observations are in agreement with those obtained from Lee's approach.

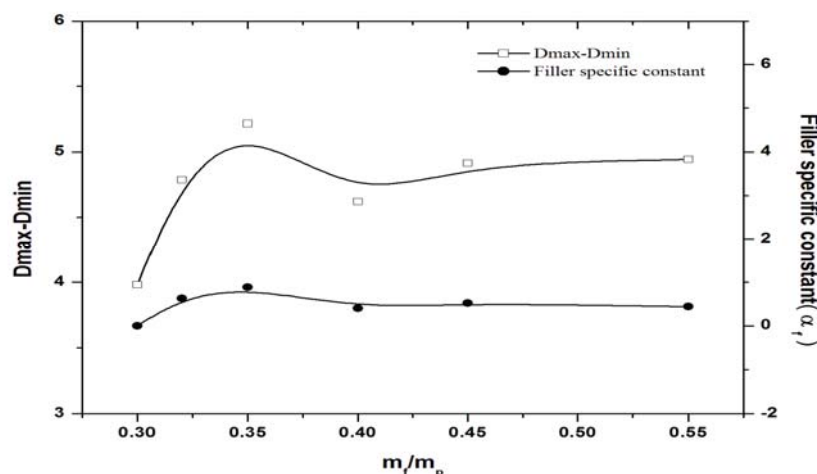


Figure 4.23 Variation of Δ Torque and Filler specific constant with filler loading for NR-CB-MBN hybrid RNCs

The dispersion of filler within the matrix and formation of filler agglomerates were studied in detail by B. L. Lee. This method is applicable for carbon black composites. Even in well dispersed filler rubber systems, differences in the degree of filler agglomeration in the cured and uncured state can be observed (Fig. 4.24). The index L decreases with filler loading pointing to the reduced agglomeration of the filler in the elastomers and later on increases slightly showing a tendency of agglomeration at higher MBN loading. The value of L is found to be higher for samples containing carbon black alone than the hybrid filler network. This indicates poor dispersion of carbon black particles compared to CB-MBN in the NR matrix. Thus the incorporation of carbon black

along with MBN shows better processability compared to carbon black alone filled composites.

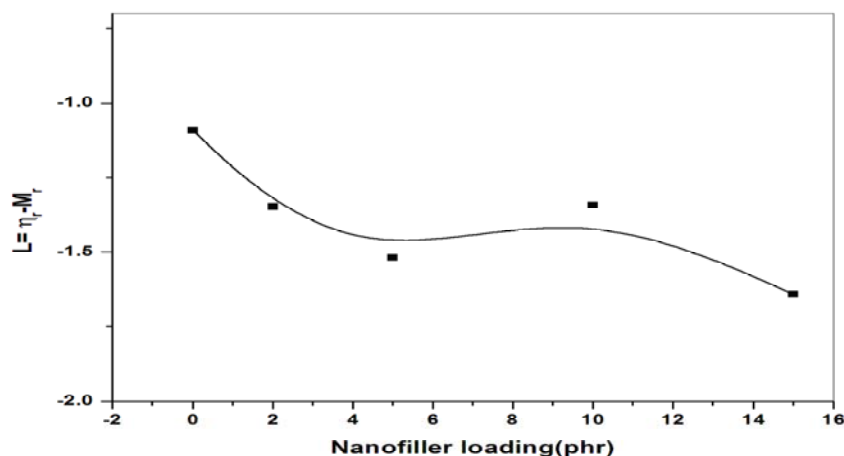


Figure 4.24 Variation of parameter L for NR-MBN-30CB hybrid RNCs with MBN loading.

4b.2 Dynamic properties measured in Strain sweep for uncured and cured compounds

The strain sweep measurements were conducted on uncured and cured hybrid RNCs to investigate the rubber-filler interaction. The dependency of the dynamic properties on the strain amplitude at small deformations can give a better understanding on the filler-filler networks in a rubber matrix [15].

The Fig. 4.25 a and b show the strain dependence of complex modulus G^* for the NR-CB-MBN filled RNCs, uncured and cured, respectively. Viscoelastic properties of uncured, filled compounds can provide useful information about the rubber–filler interaction, without the complication of crosslinking that is introduced during curing cycle. When the nano MBN is mixed with carbon black, the effect on the complex modulus is superior to that of carbon black alone. On increasing MBN incorporation in carbon black filled nanocomposites, steady increase in modulus is observed. This is owing to the formation of three different types of filler networks arising from the simultaneous use of two fillers.

The carbon black network, MBN/CB network and MBN/MBN network of which MBN/CB networks are stronger than any other network as observed from the graph. It is seen that in dual filler system the break down and reformation of dual network begins at a higher strain than MBN alone and CB alone systems. The strain sweep studies after curing showed the modulus values are strain independent and a drop in the modulus occurred at high strains. Since the compounds are cured the modulus values are high but the behaviour is the same as that of the uncured compounds. The higher values of modulus at low strains indicate the improved rubber filler interaction. The increased value at low strains reflects the higher values of hydrodynamic effect, which is dependent on the particle size and shape[16]. Fig. 4.26 a and b shows the comparative graphs to explain synergy that plays in a dual network system in uncured and cured state. The CB30+MBN₅ system showed much superior modulus among lower loaded samples than 30CB system and more or less, it slightly resembled 40CB system. It is observed that as the carbon black content increases, the aggregates tend to associate into agglomerates and these so called filler network is responsible for such an increase in modulus with increased black content. When aggregates are close together they agglomerate occluding the rubber shell and thus this rubber shell has high modulus than polymer matrix. These shell networks are less rigid and hence break down at lower strains but the break down proceeds less rapidly [17-18].

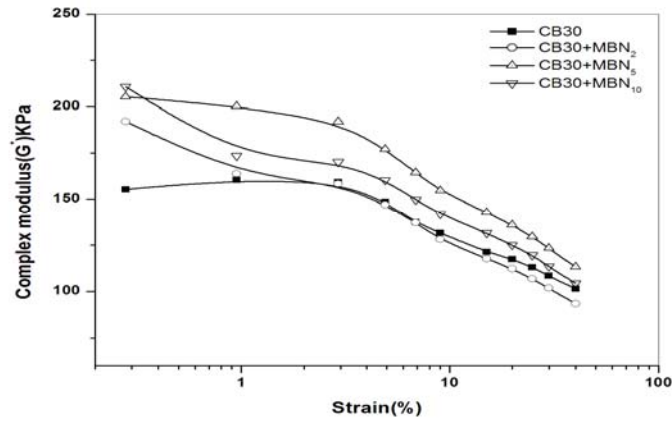


Figure 4.25.a Dependence of Complex modulus (G^*) on strain amplitude of uncured NR-CB-MBN hybrid compounds at different loadings

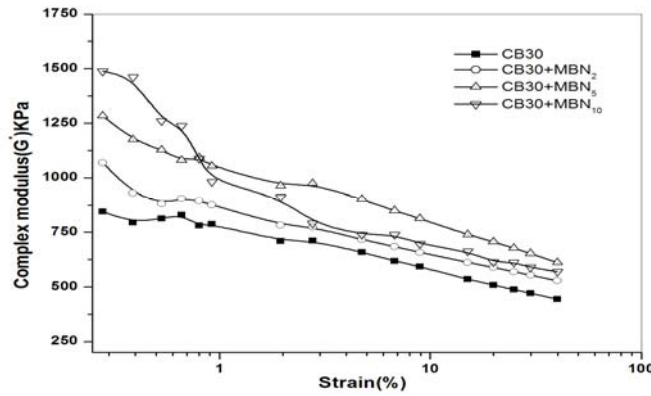


Figure 4.25.b Dependence of Complex modulus (G^*) on strain amplitude of cured NR-CB-MBN hybrid compounds at different loadings

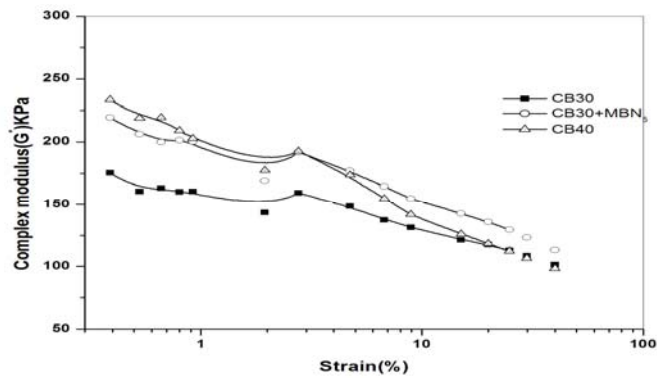


Figure 4.26.a Dependence of Complex modulus (G^*) on strain amplitude of uncured NR-CB compounds at different loadings

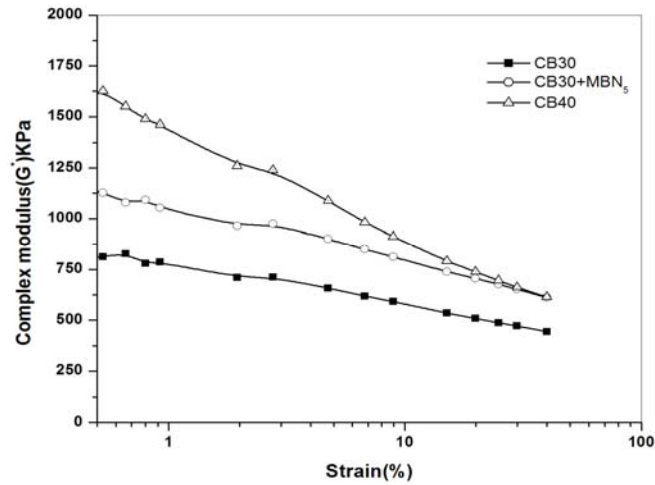


Figure 4.26.b Dependence of Complex modulus (G^*) on strain amplitude of cured NR-CB compounds at different loadings

4b.3 Mechanical properties

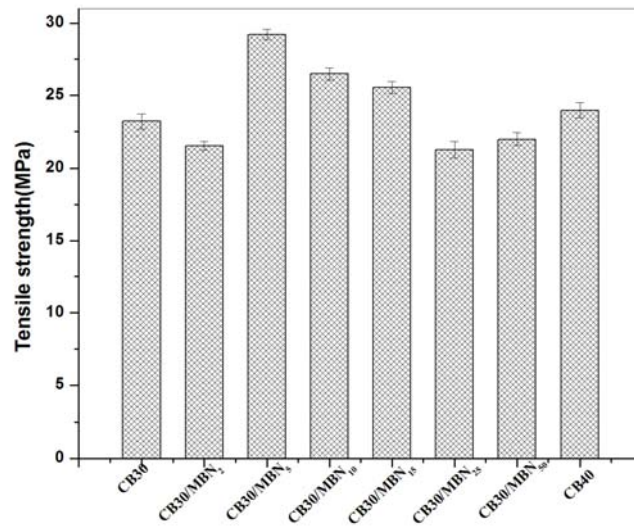


Figure 4.27 Variation of tensile strength with loading for NR-CB-MBN hybrid RNCs

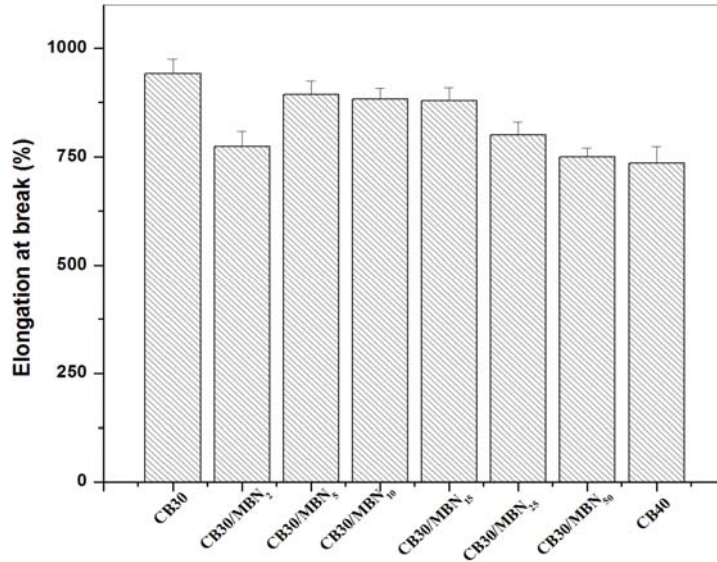


Figure 4.28 Variation of elongation at break with loading for NR-CB-MBN hybrid RNCs

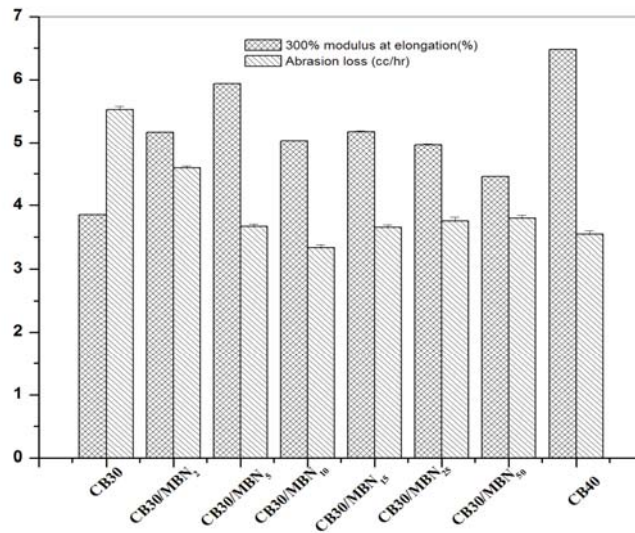


Figure 4.29 Variation of modulus at 300% and abrasion loss with loading for NR-CB-MBN hybrid RNCs

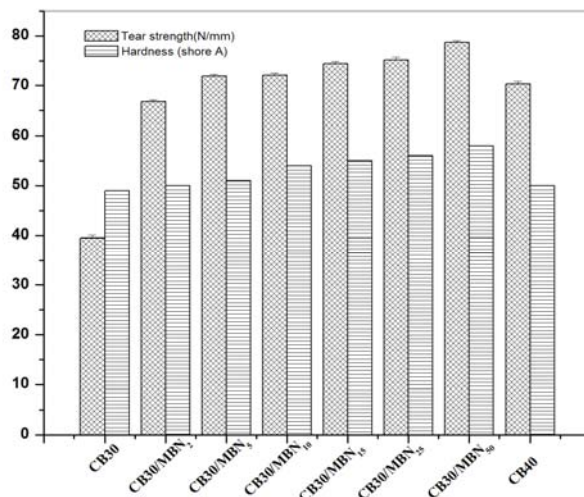


Figure 4.30 Variation of tear strength and hardness with loading for NR-CB-MBN hybrid RNCs

The mechanical properties of NR-CB composites containing 30 and 40 phr carbon black are compared with NR-CB30-MBN hybrid RNCs containing varied MBN loading, as shown in Fig. 4.27 to 4.30. As the carbon black content increased from 30 to 40 phr, tensile strength, tear strength and hardness increased owing to the resistance to crack propagation resulting from the reduced inter-aggregate distance within the carbon black. The graphs reveal an increase in tensile strength upto 5 phr nano filler and on further addition the property decreased and remained constant. It is noteworthy that even 5 phr of MBN in combination with 30CB is enough to impart tensile strength equivalent to 40phr of black in NR. The 300% modulus is also comparable. With the addition of 5phr of MBN into 30CB containing NR, tensile strength, tear strength, hardness and modulus increased, though elongation at break decreased. All other properties were better or even comparable with NR-40CB composite. With further filler incorporation (i.e., 50phr of MBN) tear strength and hardness improved but all other properties decreased and finally remained constant, which is due to agglomeration of fillers. When compared to NR-CB30, NR-MBN₅ hybrid RNCs registered a 26% increase in tensile strength. When compared with NR-CB40 a 22% increment in tensile strength and 9% decrease in

modulus were seen for MBN₅ hybrid RNCs. It could be concluded that optimum CB-MBN ratio was CB30:MBN5. This proportion indicated a balanceable state of saturation for the synergistic effect between carbon black and MBN on reinforcing NR. In comparison with NR/CB(100/40) the tensile strength, tear strength and abrasion resistance of hybrid RNCs increased. The abrasion loss of hybrid RNCs decreased on addition of MBN upto 10 phr. Further filler addition increased the abrasion loss as the filler aggregates formed were pulled out from the matrix leading to the formation of voids and holes. During abrasion of the rubber sample, uniformly distributed MBN and carbon black particles were introduced into the abrasion surface, and this contributed to lower the loss due to strong filler-polymer adhesion.

4b.4 Morphology of fracture surface: SEM and AFM studies

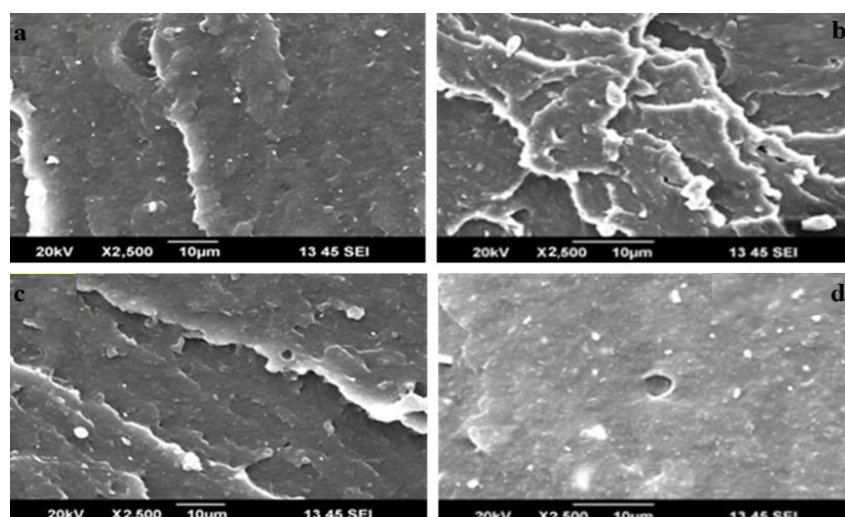


Figure 4.31 SEM photographs of tear fracture surfaces (a) CB30 (b) CB30+MBN5 (c) CB40 (d) CB30+MBN₁₅

Fig. 4.31 is the cross-section of a typical NR-CB-MBN hybrid RNC. As shown in Fig. 4.31.b, carbon black-MBN₅ dual network and rubber matrix have formed a macro-homogenous system. This indicates that, fine filler dispersion is made possible by the presence of 5phr of MBN along with 30 phr black and could effectively enhance the reinforcement effect of carbon black on rubber as

seen from strength studies. As a comparison, the SEM morphology of carbon black alone filled systems are shown in Fig. 4.31.a & 4.31.c, which is almost the same as that of hybrid RNCs. Comparing Fig. 4.31.b and 4.31.a it could be found that addition of MBN can improve the dispersibility of carbon black in hybrid RNCs and reduce the agglomeration of carbon black. The increased tear lines on fracture surface evidences that these RNCs certainly have enhanced strength properties compared to their black alone filled counterparts. Fig. 4.31.d showed that the carbon black and nano filler combination of 30/15 lead to loose agglomerate formation, as evidenced from crater formation of nearly 2µm diameter. These holes represent filler pullout during tear.

The proper dispersion of carbon black can not only reduce energy consumption during mixing, but also improve the mechanical properties of vulcanizates. These are evidenced from SEM images and the 3-D images of the superior system and the comparison diagrams are as shown in Fig. 4.32 (comparison made with that of carbon black alone filled systems).

The Fig. 4.32 shows 3-D AFM images of a) CB30 and b) CB30+MBN₅. The topography reveals that the dispersion is improved in the presence of nano filler along with 30CB, as can be seen from uniform surface as seen from 3D images shown below.

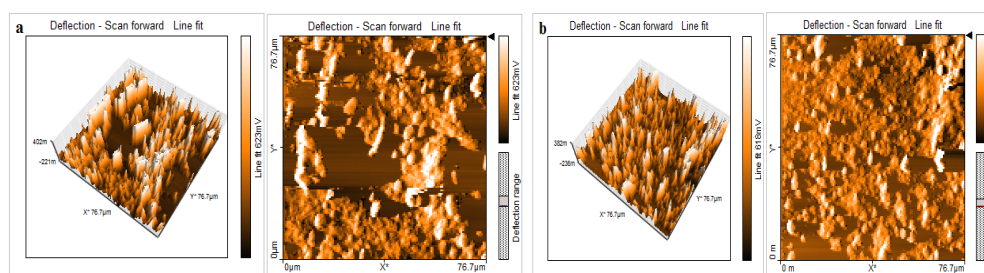


Figure 4.32 3D AFM images and 2D surface topography of (a) CB30 and (b) CB30+MBN₅ hybrid RNCs

Fig. 4.32 shows 3D AFM images and 2D surface topography of CB30 and CB30+MBN₅ hybrid RNCs. The ridges formed by filler can be clearly seen in

CB30 (a) and rubber surface devoid of any filler is seen visibly in their corresponding 3D-images. The valleys in between the hills formed by filler-polymer regions indicate poor rubber-filler interaction. In Fig. 4.32.b, uniform rough surface formation is evidenced from uniform rubber-filler structures of NR-CB-MBN system.

4b.5 Thermal studies: Thermal ageing and Thermogravimetric analysis

4b.5.1 Thermal Ageing

The retention of properties on thermal ageing is given in Table 4.8. The graphical representations of the variation in tensile strength and tear strength properties are given in the Fig. 4.33 a and b. During thermal ageing, cross-link formation or cross-link breakage can take place or an existing cross-link may break and a stable linkage can be formed. It is observed that there is an initial increase in the tensile modulus after 24 hrs of ageing and after that there is a decline. The increase in modulus is due to the agglomeration of filler particles at higher temperature or due to increased cross links.

Table 4.8 Retention of properties on thermal ageing for natural rubber based NR-CB-MBN hybrid RNCs

Filler loading (phr)	% retention in tensile strength			% retention in tear strength			% retention in 300% modulus		
	24 hrs	48hrs	96hrs	24 hrs	48hrs	96hrs	24 hrs	48 hrs	96hrs
CB40	97	91	87	99	95	88	101	94	86
CB30	97	90	85	96	86	75	100	86	83
CB30+MBN ₂	97	92	88	98	91	80	103	95	88
CB30+MBN ₅	97	98	95	100	94	88	101	94	89
CB30+MBN ₁₀	98	94	92	97	92	87	104	95	87
CB30+MBN ₁₅	98	96	92	100	97	91	103	96	88
CB30+MBN ₂₅	96	96	95	98	94	90	100	95	89

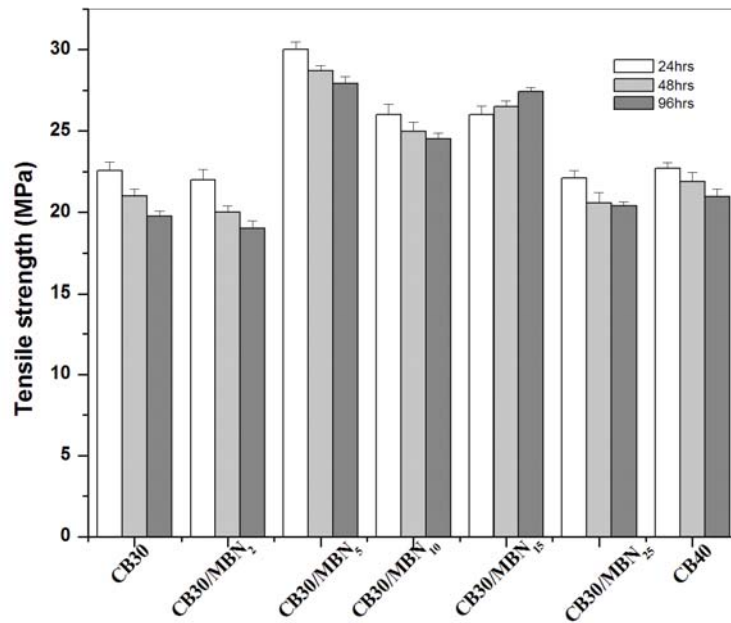


Figure 4.33.a Tensile strength of natural rubber based *NR-CB-MBN hybrid RNCs* on thermal ageing

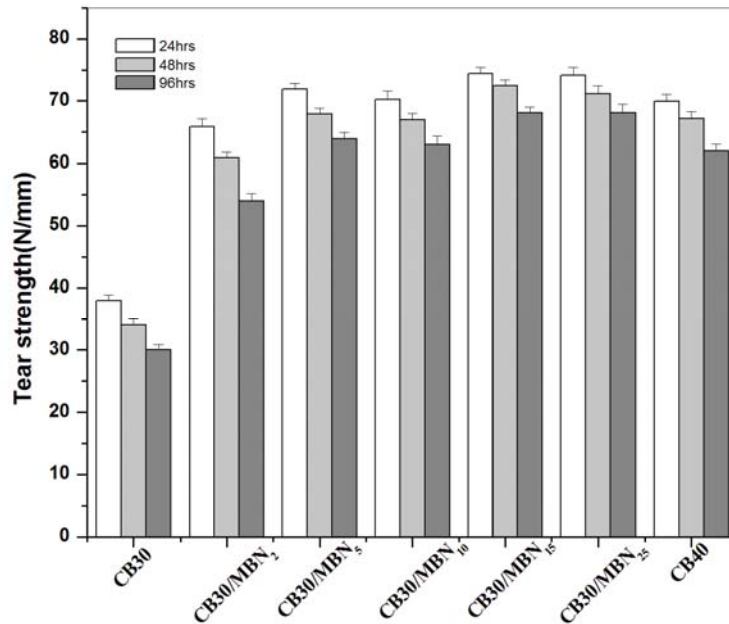


Figure 4.33.b Tear strength of natural rubber based *NR-CB-MBN hybrid RNCs* on thermal ageing

Tensile strength decreased, while tear strength showed no change after 24 hours of ageing for 5 and 15 MBN filled hybrid RNCs (Table 4.8). But a gradual decline after 24 hours was observed for both samples. Modulus enhancement on ageing may be due to additional cross linking during ageing. It can be seen from the figures that the composites with the MBN₅ showed a better resistance to thermal degradation. This may be due to the increased rubber filler interactions, which lead to an increased occlusion of rubber molecules in the voids of nano-carbon black network.

4b.5.2 Thermogravimetric analysis

The TG curves of the NR-CB-MBN hybrid rubber nanocomposites series are shown in Fig. 4.34. The thermal characteristics as estimated by TGA are presented in Table 4.9. The degradation behaviour of the materials could be clearly read from the Differential thermogravimetry (DTG) curves in Fig. 4.35. The temperature of onset of degradation (Ti), the temperature at which the rate of decomposition is maximum (Tmax), the peak degradation rate (Rmax) and the decomposition temperature at 5% weight loss (T_{-5%}) and 50% weight loss (T_{-50%}) are given in Table 4.9. The NR-CB30 composites give a single degradation between 300 and 400 °C and a peak maximum at 372.6 °C. With the incorporation of MBN, weight loss due to the NR degradation is still observed, but the relative intensity decreased. The incorporation of nano filler in combination with 30CB shifts the onset of degradation to higher temperature, though the temperature of maximum degradation remains the same. As the nano loading increased, a lowering in the rate of degradation is observed. On comparison with NR-CB40, in CB₃₀ composites the thermal behaviour has been slightly improved. MBN₁₅ shows lower rate of degradation than MBN₅ filled hybrid RNCs. The rate of maximum degradation decreased from 1.0490 to 0.9801%/°C with filler loading and modified nano filled systems in conjunction with CB are having superior thermal stability when compared with carbon black alone filled systems. Nano barium sulphate when surface treated contributes to effective interaction between the filler and the matrix

due to its small particle size and hence improves the interfacial adhesion. Strong interface renders the matrix stiff and makes the diffusion of heat and gases through the bulk more difficult. This makes the matrix thermally more stable in the presence of nanofiller-carbon black dual networks.

Table 4.9 Thermal degradation data of natural rubber based hybrid RNCs

Sample code	Ti(°C)	Tmax (°C)	Rmax (%/ °C)	T _{.5%}	T _{.50%}
CB30	319.5	372.6	1.05	260.26	388.86
CB30+MBN ₅	326.1	376.1	0.997	267.43	392.48
CB30+MBN ₁₅	323.78	373.05	0.98	269.8	394.37
CB40	320.08	373.05	1.02	247.65	386.69

The improvement of thermo oxidative resistance was attributed to three factors: (1) chemical activities of filler and polymer (2) strong polymer–filler interactions and (3) uniform dispersion of fillers[19]. CB and MBN are chemically inert and do not react with oxygen, under the current test conditions. The dense polymer–filler networks hinder the access of oxygen to the nanocomposites.

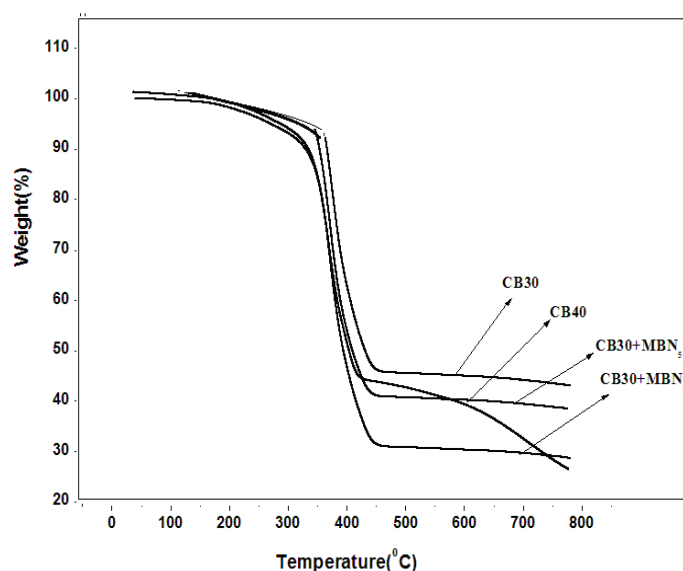


Figure 4.34 TGA traces of NR-CB-MBN hybrid RNCs

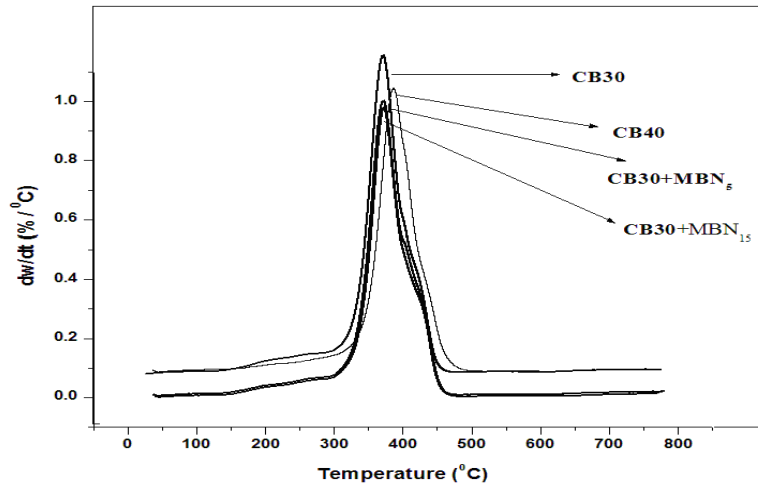


Figure 4.35 DTG curves of NR-CB-MBN hybrid RNCs

4b.6 Crosslink density and swelling studies

Swelling studies of NR-CB-MBN hybrid composite

The solvent sorption studies on the hybrid nanocomposites were done in toluene and the sorption curves are plotted in Fig. 4.36. It is clear from the plots that as the filler loading increased the maximum solvent uptake of gum vulcanizates decreased, the effect being much more pronounced with nano filled rubber samples.

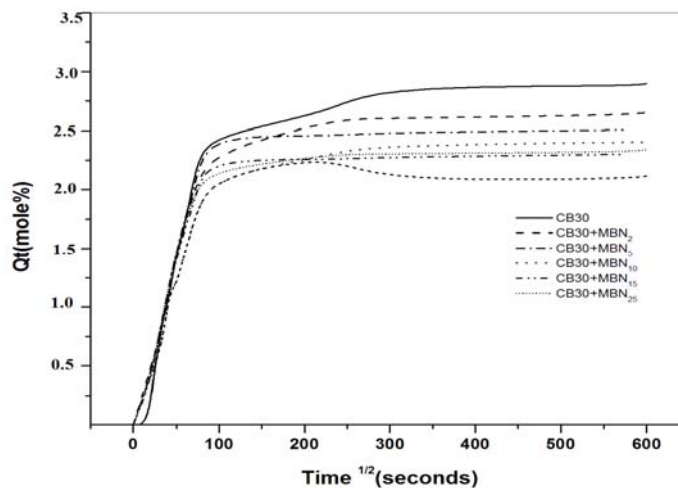


Figure 4.36 Sorption data of Natural rubber-CB-MBN based hybrid RNCs

Table 4.10 Sorption data of natural rubber-CB-MBN hybrid RNCs

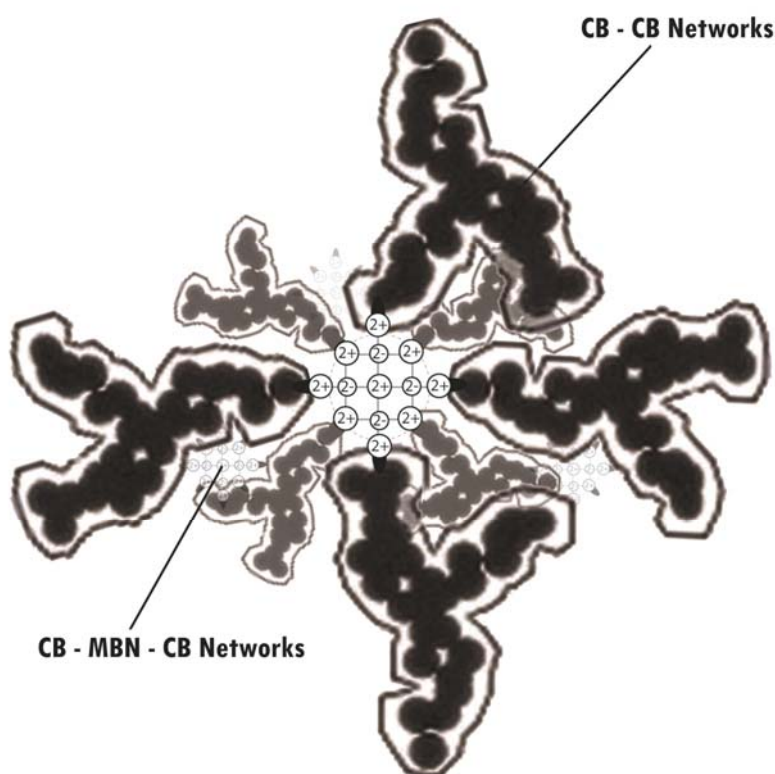
Sample code	n	Diffusion coefficient, $D \times 10^{-7}$ ($\text{cm}^2 \text{s}^{-1}$)	Sorption Coefficient S	Permeation coefficient, $P \times 10^{-6}$ ($\text{cm}^2 \text{s}^{-1}$)	Crosslink density, $\nu \times 10^{-5}$ (g mol/cc)
CB30	0.6191	6.14	2.66	1.63	13.63
CB30+MBN ₂	0.6031	5.93	2.44	1.45	14.27
CB30+MBN ₅	0.6252	5.85	2.21	1.29	14.84
CB30+MBN ₁₀	0.6808	5.69	1.95	1.11	14.09
CB30+MBN ₁₅	0.7041	5.58	2.12	1.18	14.38
CB30+MBN ₂₅	0.7166	6.53	2.09	1.36	13.24

The diffusion coefficient, D for the samples are tabulated in Table 4.10. The diffusion coefficient varies with solvent uptake and shows a maximum for gum vulcanizates. The changes in permeability and diffusivity of carbon black filled nano composites are conventionally explained as an outcome of strong filler-matrix interaction which restricts and limits the diffusion of toluene through entangled matrix-filler networks. The permeation of toluene into a polymer membrane will also depend on sorptivity of penetrant in the membrane, the calculated values of sorption coefficient is given Table 4.10. The net effect of both the phenomena accounts for the permeation coefficient and values obtained are as seen in the same table. It is clear from the data that the permeability of nanocomposites decreases with nano filler content and is dominated by sorption. Moreover the black filled composites exhibits improvement in strength and mechanical properties whereas, the permeability is not much influenced. This may be attributed to the build up of filler network which leads to increase in filler volume fraction. The incorporation of 30phr of carbon black in NR reduces the diffusion coefficient by about 38%. A hybrid combination of this composite with even 2 phr of MBN improves diffusion resistance to 40% which is the same as the diffusion resistance exhibited by 2phr of MBN alone. Even 5 phr of MBN composite alone is able to reduce diffusion coefficient by 37% i.e., the resistance to solvent permeation has been improved dramatically.

Conclusions:

Natural rubber-barium sulphate-carbon black filled composites (NR-CB-MBN hybrid RNCs) with sufficient mechanical properties can be prepared by mechanical mixing. The effect of nano filler-carbon black dual filler loading on cure characteristics, mechanical properties and transport properties of hybrid RNCs were investigated. Fine dispersion of carbon black particles in the NR matrix is not achieved by mill mixing, but the presence of MBN, helped to improve dispersion, as is evidenced from the higher α_f value of NR-CB-MBN RNCs. Presence of 5phr of MBN in NR-CB30 composites improved tensile strength, tear strength, hardness and modulus values and all the properties were comparable with NR-CB40 composite. At higher loadings deterioration in properties resulted due to agglomeration of fillers. Compared to NR-CB30, NR-CB30-MBN₅ hybrid RNCs registered a 26% increase in tensile strength, 22% increment in tear strength and 9% decrease in modulus were seen for the same hybrid RNCs when compared with NR-CB40 RNCs. NR-CB-MBN composites could be successfully fabricated with eminent properties at an optimum CB/MBN ratio of CB30:5MBN. This proportion indicates a balanceable state of saturation for the synergistic effect between carbon black and MBN on reinforcing NR. The abrasion loss of hybrid RNCs decreased with MBN loading, due to strong filler-polymer adhesion. Proper dispersion of carbon black reduced energy consumption during mixing, and improved the mechanical properties of vulcanizates. Comparison of SEM images and the 3-D AFM images confirmed the stability hybrid RNCs. The hybrid composites have better resistance to thermal ageing which was supported by TGA results. The incorporation of nano filler in combination with 30CB shifted the onset of degradation to higher temperature, though the temperature of maximum degradation remained the same. Rate of maximum degradation decreased with filler loading. Modified nano filled systems in conjunction with carbon black have superior thermal stability when compared to CB alone filled systems. The black filled composites exhibited improvement in strength and mechanical properties whereas, the

permeability is not much influenced. The incorporation of 30phr of carbon black in NR reduced the diffusion coefficient by about 38%. A hybrid combination of this composite with even 2 phr of MBN improved diffusion resistance by 40%. The transport mode exhibited anomalous behavior. Surface treated barium sulphate proved to be a better candidate in partial replacement of carbon black from natural rubber composites. It offered the benefit of minimizing hazardous carbon black, though at minimal levels, with ecofriendly filler. To conclude a possible mechanism may be proposed for the synergy between CB-MBN systems in elastomer network which is responsible for superior properties of hybrid RNCs



References

- [1]. C.Barres, A.Mongruel, M.Cartault, J.L.LebLANc; J. Appl. Polym. Sci., **2003**, 87, 31.
- [2]. T.Sajayanukul, P.Seaoui, C.Sirisinha; J.Appl.Polym. Sci., **2005**, 97, 2197.
- [3]. W.Bai, K.Li ;Compos Part A ,**2009**,40,1597.
- [4]. M.Arroyo, M.A López-Manchado, B.Herrero; Polymer, **2003**,44,2447.
- [5]. L.Qu,G.Huang,P.Zhang,Y.Nie, G.Weng, J.Wu ; Polym Int **2010**,59,1397.
- [6]. Y.Liu, L .Li, Q.Wang; J Appl. Polym. Sci., **2010**,118,1111.
- [7]. N.Rattanasom, T. Saowapark, C.Deeprasertkul ; Polym Test, **2007**, 26,369.
- [8]. M.Arroyo, L. M.A.Manchado, B.Herrero;Polymer, **2003**,44, 2447.
- [9]. A.K. Ghosh, S.Maiti, B .Adhikari, G.S.Ray, S.K.Mustafi; J Appl Polym Sci, **1997**, 66,683.
- [10]. Y.Wang, L.Zhang, C.Tang, D.Yu; J. Appl. Polym. Sci.,**2000**,78, 1879.
- [11]. R.Magaraphan, W.Thaijaroen, and R.Lim-Ochakun;Rubber Chem.Technol., **2003**, 76, 406.
- [12]. P.C.Meneghetti; Synthesis and properties of Rubber-clay nanocomposites, PhD Thesis, Case Western Reserve University, **2005**, 114.
- [13]. X.Liu, S .Zhao, Y.Yang, X.Zhang, Y.Wu; Polym Adv Technol **2009**,20,818.
- [14]. J.Sapkota, M.Poikelispaa, A.Das, W.Dierkes, J.Vuorinen; *The Free Library* 01 Mar.**2013** (accessed November 05 2013)
- [15]. J.B. Donnet;Rubber Chem. Technol., **1998**,71,323.
- [16]. S.Wolff, M. J.Wang; Kautsch. Gummi Kunstst., **1994**,47, 17.
- [17]. M.J.Wang; Rubber Chem. Technol., **1998**,71,520.
- [18]. J.D.Wang, Y.F.Zhu, X.W.Zhou, G.Sui, J.Liang;J.Appl. Polym.Sci., **2006**,100,4697.
- [19]. J.L. Leblanc; Prog. Polym .Sci.; **2002**,27,627.

.....✂.....

**ETHYLENE PROPYLENE DIENE RUBBER -
BARIUM SULPHATE NANOCOMPOSITES***

Part a: EPDM-based nanocomposites: barium sulphate (BN)/ modified nano barium sulphate (MBN) filled RNCs

Part b: Synergistic effect of carbon black filled EPDM-MBN hybrid RNCs (EPDM-CB-MBN)

Part-a**EPDM-BASED NANO COMPOSITES: BARIUM SULPHATE (BN)/MODIFIED NANO BARIUM SULPHATE (MBN) FILLED RNCs**

Nano barium sulphate (BN) and modified nano barium sulphate (MBN) filled ethylene propylene diene monomer (EPDM) composites were prepared by proper compounding on a two roll mill and moulded into desired shapes for testing. The cure characteristics, filler dispersion, mechanical properties, and thermal stability of the elastomeric composites were evaluated. The amount of filler was limited upto 15phr. Compared to EPDM-BN RNCs, EPDM-MBN RNCs registered better mechanical properties and cure characteristics. An increase of 35% in tensile strength was registered with 2phr MBN filled EPDM which indicates a reinforcing effect of otherwise diluent, barium sulphate. RNCs prepared were characterised using scanning electron microscopy. Modified nano filled elastomeric composites were having superior thermal stability compared to unmodified counter parts, thermal endurance of these elastomeric composites improved with MBN concentration. The onset of degradation showed a slight shift to higher temperatures with increasing nano concentration, though the temperature of maximum degradation remained the same. Swelling studies were conducted on MBN-RNCs to estimate their superior behaviour and mechanism indicated a minor deviation from fickian mode. Overall enhancement was evidenced in the case of EPDM-MBN₂ system.

* A part of this work have been presented at:
Nisha Nandakumar, Philip Kurian; Advancements in Polymeric Materials, CIPET Bhubaneswar-Feb.2010.

Introduction

Natural rubber crystallizes on stretching imparting higher tensile strength to the gum vulcanizates, whereas synthetic rubbers are generally weak and requires incorporation of reinforcing fillers to produce high strength. Synthetic polymers like EPDM, shows no self reinforcing effect, as it is unable to undergo stress induced crystallization on stretching. Nowadays, elastomer based nanocomposite technology has been extended to synthetic rubbers besides NR. Nano fillers like clays, silica and CNT's have been incorporated into ethylene propylene diene terpolymer (EPDM) to impart tailored properties to composites and act as reinforcement to the host matrix [1.1]. In the present research work EPDM, which is a typical non-polar rubber with good ageing properties, high filler loading capacity and widely used in automobile sectors, was used as a base rubber matrix for the preparation of EPDM-Barium sulphate nanocomposites. Barytes as well as elastomer-baryte composites are important radiopaque materials finding application as X-ray opaque elastomers. Acid resistance offered by these materials is also important. Presently, two types of barium sulphate fillers , unmodified nanofiller BN and modified BN referred to as MBN were used for the study. The fillers were mixed with the bulk EPDM matrix with sulphur as curing agent. The variation in the cure characteristics, morphology, mechanical properties, and thermal stability of the different nanocomposites had been analyzed and compared with each other and also with their respective controls. The sorption studies were carried out using toluene as solvent in order to assess the mode of solvent transport through these elastomeric composites. These studies were conducted to assess the reinforcing properties of the composites. Acid resistance and radiopacities of the composites have been dealt with in Chapters 7 and 8 respectively.

5a.1 EPDM-Barium sulphate nanocomposites

5a.1.1 Preparation of rubber nanocomposites

Nano powders were synthesised via chemosynthetic pathway in presence of PVA (section 3.2.2) and modified using stearic acid (section 3.2.3). The nano barium sulphate powders obtained is hereafter referred to as BN and the

modified compound as MBN and the filler loadings are represented as subscripts to this notation. The formulation for the preparation of the RNC's is given in Table 5.1. Two series of RNC's were prepared-first series with varying amounts of BN and the second with varying amounts of MBN. The RNC's were prepared in a laboratory size two-roll mill at a friction ratio of 1:1.25 as per ASTM standards(section 2.2.1). During the final sheeting at low nip gap, the fillers were oriented along the mill direction. The mixes were kept for 24 h for maturation. The optimum cure time at 160°C was determined using a Rubber Process Analyzer. The compounds were compression moulded at 160°C in an electrically heated hydraulic press (section 2.2.5). The samples were cured to their respective optimum cure times. After curing, the pressure was released and the sheets were suddenly cooled in water. These sheets were used for subsequent tests. The samples for rest of the studies were prepared according to procedures mentioned in section (2.3.1-2.3.3).

Table 5.1 Compounding formulation for EPDM based RNCs

Compounding ingredient	MBN ₀ /BN ₀ (phr)	MBN _{0.5} /BN _{0.5} (phr)	MBN _{1.5} /BN _{1.5} (phr)	MBN _{2.0} /BN _{2.0} (phr)	MBN _{2.5} /BN _{2.5} (phr)	MBN ₃ /BN ₃ (phr)	MBN ₅ /BN ₅ (phr)	MBN ₁₀ /BN ₁₀ (phr)	MBN ₁₅ /BN ₁₅ (phr)
EPDM	100.0	100.0	100.0	100.0	100.0	100.0	100.0	100.0	100.0
ZnO	5	5	5	5	5	5	5	5	5
Stearic acid	2	2	2	2	2	2	2	2	2
MBN / BN	0	0.5	1.5	2.0	2.5	3	5	10	15
	0	0.5	1.5	2.0	2.5	3	5	10	15
Sulphur	1.5	1.5	1.5	1.5	1.5	1.5	1.5	1.5	1.5
TMTD	0.5	0.5	0.5	0.5	0.5	0.5	0.5	0.5	0.5
CBS	1.0	1.0	1.0	1.0	1.0	1.0	1.0	1.0	1.0
ZDC	0.5	0.5	0.5	0.5	0.5	0.5	0.5	0.5	0.5

5a.1.2 Cure characteristics

The curing characteristics of all the vulcanizates are summarized in the Table 5.2. In the presence of organo-treated nanofiller both the cure time and scorch time reduced, the effect being well registered at a filler loading of 2 phr in the MBN series. The decrease in cure time indicates that filler incorporation activates the cure reaction and also, the MBN series promotes cure acceleration compared to BN series. The cure time is reduced by more than 2 minutes for compounds containing 2phr MBN filler. These results are again supported by the cure kinetic studies and cure rate index values, which will be discussed in the following sections. The maximum torque value (D_{\max}) also showed an increase with MBN loading. The D_{\max} increased by 7% for MBN₁₅ which directs to an increase in modulus of the composites. This effect is essentially attributed to the carboxylate groups in the barium sulphate nano particles, which came from the organic surface treatment using stearic acid. Fatty acids are normally regarded as vital activators in conjunction with zinc oxide. The zinc salts of fatty acids, which are a type of surfactant, also solubilize insoluble accelerators to form the actual catalyst. They facilitate the opening of the elemental sulphur ring to form polysulfide ions, which increases the vulcanization rate but has little effect on the vulcanization efficiency [1.2].

Although the carboxylate itself accelerate the vulcanization process the organo treated barium sulphate gives rise to a further evident increase in the vulcanization rate, which could be due to the synergy of the filler and modifier. This enhancement is found only at lower loadings and on increased addition it diminishes owing to agglomeration and /or adsorption of basic accelerators on modifier surface leading to increase in cure time. Unmodified nanofiller hardly varies the cure characteristics of the rubber, probably due to a poor compatibility between the unmodified BN and hydrophobic polymer. Another reason for the lower cure time at higher loading is the increase of thermal transition of EPDM in presence of MBN which promotes the vulcanization process. Modified nano have increased specific surface by acid treatment, which results in improved

thermal transition, filler–filler and filler–matrix interactions. Within the composite system, there could be two paths of thermal transition. In one path, heat can pass from MBN flakes-polymer-MBN flakes and in the other path through direct contact between the MBN flakes. The second path of thermal conduction will be more effective for higher filler concentration which increases the interaction between the fillers, which in turn increases the process of vulcanization [1]. The D_{\min} values do not vary much with nano loading suggesting that the processability of the composites is not affected.

Table 5.2 Cure characteristics of EPDM based RNCs

Filler loading (phr)	Minimum torque (dNm)		Maximum torque (dNm)		T ₁₀ (minutes)		T ₉₀ (minutes)	
	BN	MBN	BN	MBN	BN	MBN	BN	MBN
0	0.31	0.31	6.16	6.16	1.97	1.97	9.35	9.35
0.5	0.31	0.34	6.17	6.43	1.96	1.91	9.13	8.41
1.5	0.31	0.36	6.18	6.37	2.02	1.75	9.50	7.89
2.0	0.32	0.36	6.35	6.55	1.90	1.73	9.35	7.09
2.5	0.32	0.36	6.42	6.56	1.79	1.70	9.05	7.13
3.0	0.34	0.37	6.47	6.57	1.75	1.71	8.93	7.21
5.0	0.40	0.39	6.52	6.63	1.95	1.72	9.30	7.46
10.0	0.30	0.41	6.12	6.53	2.00	1.62	9.00	8.05
15.0	0.30	0.42	6.01	6.60	2.40	1.53	9.15	8.23

Stearic acid, in combination with some metallic oxides, notably zinc oxide, form the activating assembly during sulphur vulcanization [2]. The essence of activating the vulcanization process as mentioned in Chapter4 is that sulphur acting on its own is a very slow process; hence the essence of activating the vulcanization process is to increase the efficiency of crosslink formation. The use of stearic acid and zinc oxide as activating system is a standard practice in rubber compounding [3].

The result obtained above as in Table 5.2. is an indication that stearic acid has varying degree of influence on the physical properties of EPDM

vulcanizates. As part of the activating system stearic acid in combination with zinc oxide, during mill processing helps in the dispersion of other ingredients by exerting a plasticization action on the stock [4] Also during vulcanization, it helps in activating the vulcanization system, by increasing the efficiency of the penetration and consolidation of the elemental sulfur at the anchoring point of the network [5] referred to as internal lubrication effect [6].

5a.1.3 Cure kinetics

The plot of $\ln(D_{max} - D_t)$ against time t of the MBN series and BN series RNC's at 160 °C is presented in Fig. 5.1 and 5.2. The plots are found to be linear which proves that the cure reactions proceed according to first order kinetics

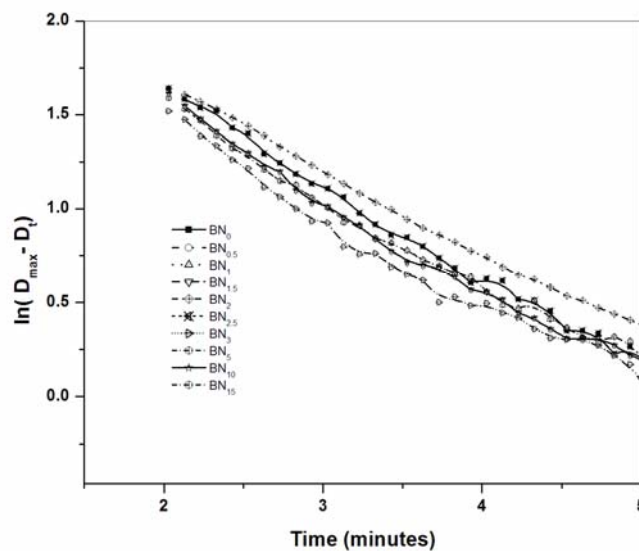


Figure 5.1 $\ln(D_{max} - D_t)$ against time t of the BN series

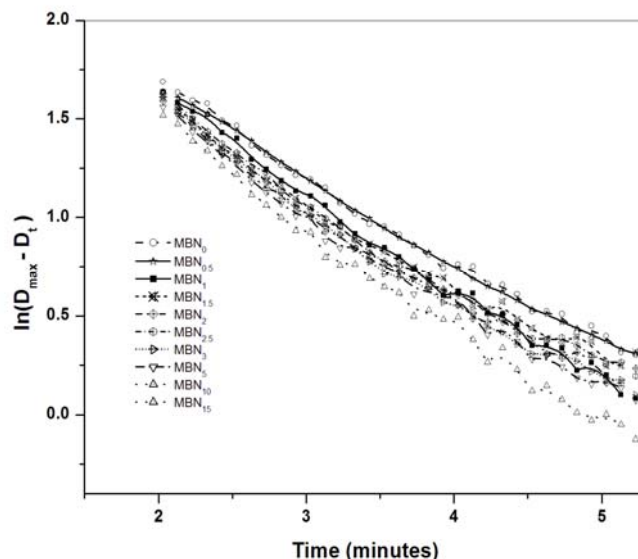


Figure 5.2 $\ln(D_{\max} - D_t)$ against time t of the MBN series

The cure rate constants (k) were calculated from their slope and the cure rate index (CRI) values were determined according to equation described in section 2.2.2 for both series. The variation of rate constant and cure rate index with filler loading for the MBN and BN series is presented in Fig. 5.3 (a) and (b) respectively. For the MBN series, both CRI and the kinetic rate constants increase with loading up to 2 phr, after which, both decreases. But still cure activation is present as indicated by the higher CRI value than gum, and the CRI was higher for surface treated nanocomposites. In the case of BN series, both parameters increase with loading and remain constant on further filler incorporation. The increase in CRI and cure reaction constant with loading indicates the activation of cure reaction [7-9]. These results are in accordance with the results of rheometric data (section 5.3).

The cure rate index of cure reactions of different composites were estimated and the graphical illustrations are given in Fig. 5.3(a) and 5.3(b).

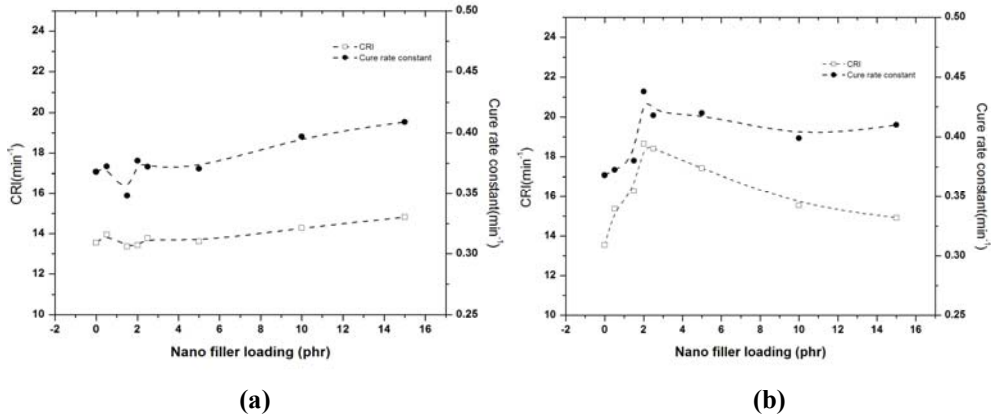


Figure 5.3 Plot of rate constant and CRI vs loading for the(a)BN series RNCs (b) MBN series RNCs

5a.1.4 Filler dispersion in the RNCs

Maximum torque increases during vulcanization and the ratio between the increase in torque of the filled compound was found directly proportional to filler loading. Fig. 5.4 represents the relation between $D_{max}^f - D_{min}^f$ against filler loading of BN and MBN. The increase in Δ torque indicates that the incorporation of nano barium sulphate affects cross linking between the polymer chain, which is significantly more registered with MBN series.

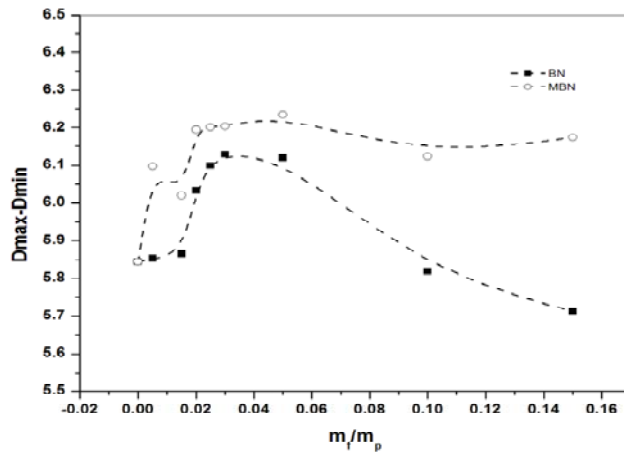


Figure 5.4 Variation of Δ Torque with filler loading for EPDM- RNCs

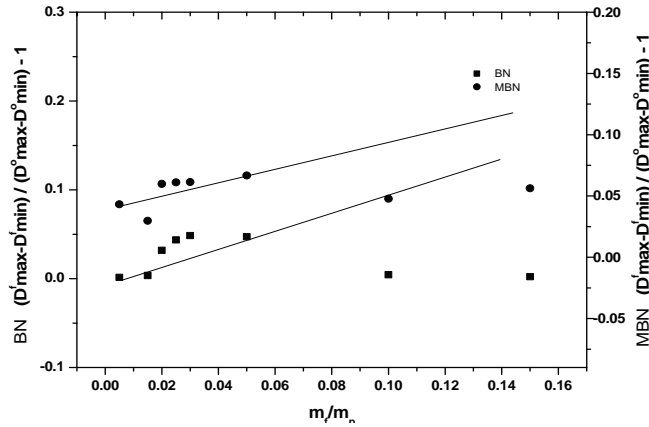


Figure 5.5 Plot of relative torque as a function of filler loading for EPDM-RNCs

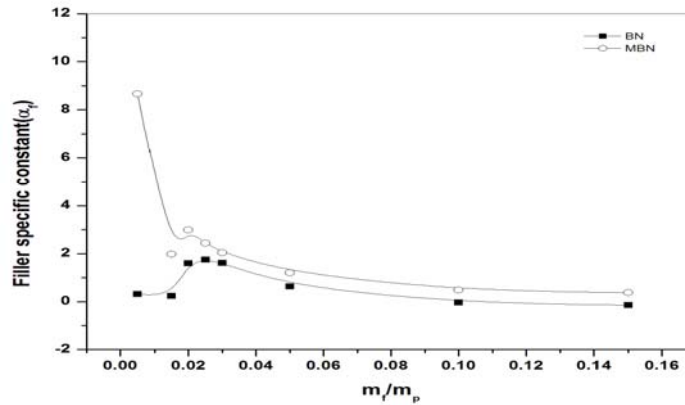


Figure 5.6 Variation of filler specific constant with filler loading for EPDM-RNCs

The slope of the linear plot showing the relative torque increase with filler loading was defined by westlinning-wolfs equation (section 2.2). In the Fig. 5.5 and 5.6 the relative torque and filler specific constants are respectively plotted against the filler fraction and according to these plots α_f values for MBN filled composites are higher than those for BN filled composites. The higher α_f value of MBN-EPDM nano composites are due to the enhanced filler-rubber interactions.

5a.1.5 Mechanical properties of RNCs.

The increase in tensile strength (Fig. 5.7) of the RNCs denotes the reinforcing nature of the fillers. As the filler loading is increased, more surface area is available

for interaction between filler particles and the rubber matrix; hence reinforcement increases with increase in filler loading. Tensile strength was nearly same as gum for BN-RNCs, which is due to non treated surface of nano that has no modifiers within, to enable it to bond with rubber. Among the BN series, upto 10 phr of filler loading, tensile strength remained unchanged but on increased filler loading a slight decrease could be observed indicating the dilution effect of inert barium sulphate. With surface treated MBN better property is attained at a lower loading i.e., at 2 phr which indicates increased interaction between surface treated nano barium sulphate and rubber. An increase in tensile strength of about 35% is registered at this level of filler loading. Tear strength (Fig. 5.8) increases with filler loading upto 10 phr with BN as well as MBN series. The higher tear strength value of MBN- RNCs is due to better interaction of nano with the matrix. The smaller particle size of the nano filler along with modifier helps to arrest or deviate tear cracks, resulting in higher tear resistance. Elongation at break (Fig. 5.9) remains un varied initially and during further filler loading and beyond 5 phr it shows a marked increase which indicates the reinforcing effect of surface treated nanofiller. The 100% modulus (Fig. 5.10) registers an increase of 6% at 2 phr filler loading and at higher loading of 15 phr it even increases upto 15% for MBN-RNCs. The fillers that are reinforcing in nature will adversely affect the elastic properties, especially at elevated temperatures. This is reflected in the higher compression set of the composites. However, in the case of MBN composites the set is relatively lower compared to the BN compounds, indicating that the extent of agglomeration in the case of MBN is lower. The compression set (Fig. 5.11) increases on progressive addition of both the filler series; but a lowering is observed for MBN at high loading which is due to agglomerate formation. The hardness (Fig. 5.12) values also indicate superior reinforcement offered by MBN filled EPDM. The nature and trend of the graphs are similar, but the tensile strength of MBN series composites is superior to that of BN series composites. This is due to the surface treatment which enhances the interaction between rubber and filler.

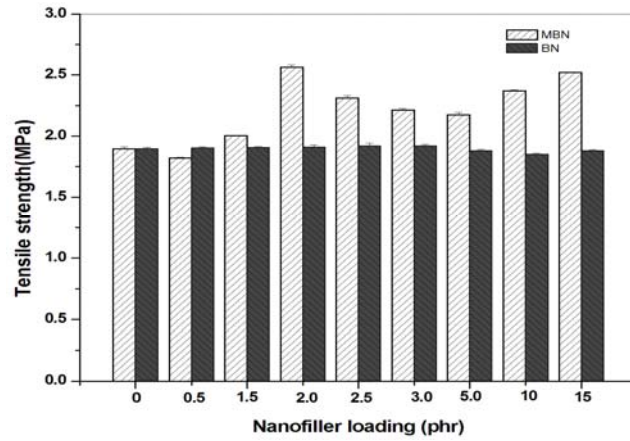


Figure 5.7 Variation of tensile strength with loading for EPDM-RNCs

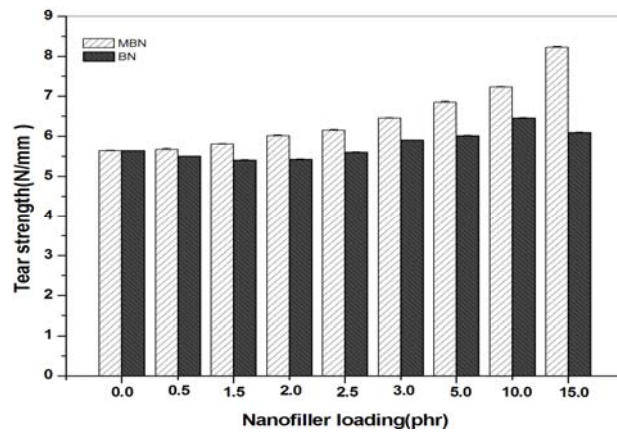


Figure 5.8 Variation of tear strength with loading for EPDM-RNCs

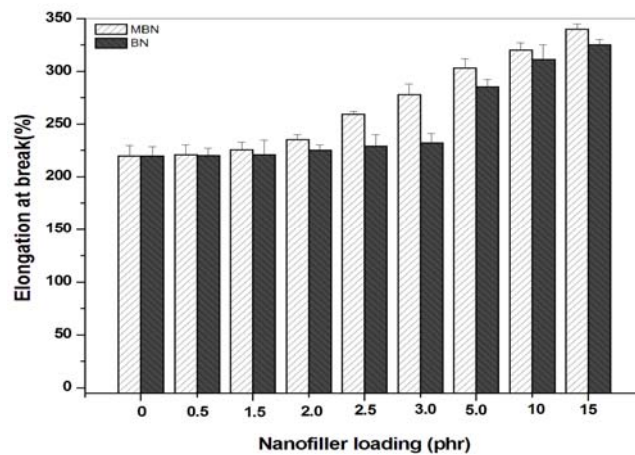


Figure 5.9 Effect of loading on elongation at break of the EPDM-RNCs

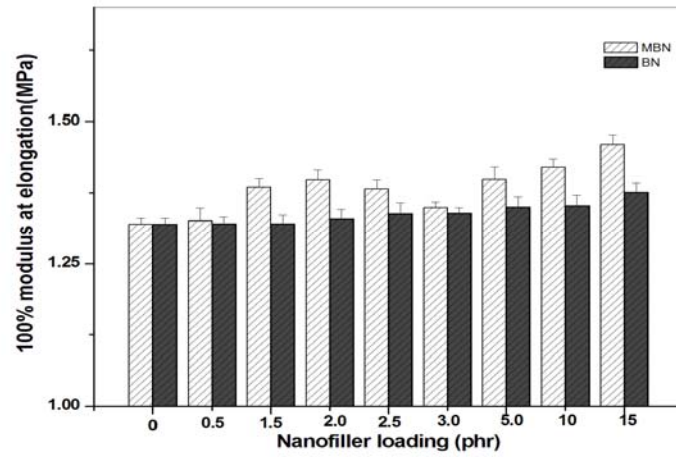


Figure 5.10 Effect of loading on the modulus of the EPDM-RNCs

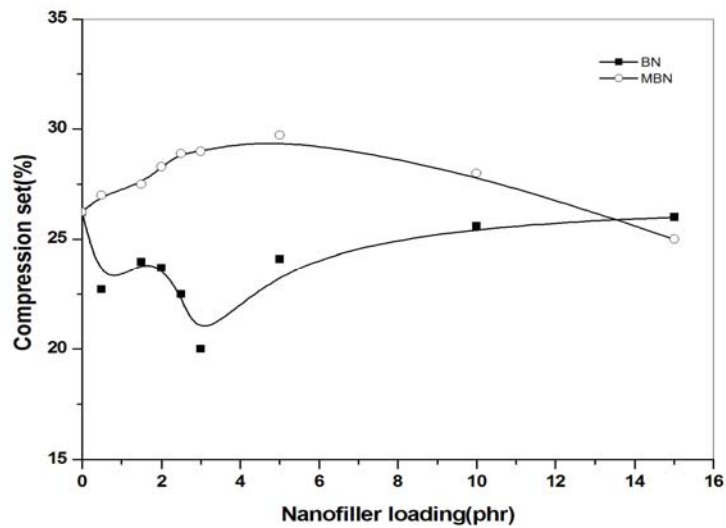


Figure 5.11 Variation of Compression set with loading for EPDM-RNCs

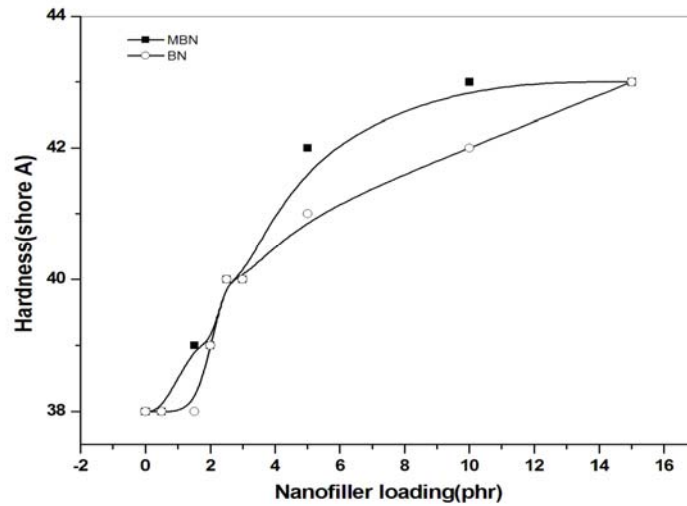


Figure 5.12 Variation of Hardness with loading for EPDM-RNCs

5a.1.6 Morphology of Fractured surface

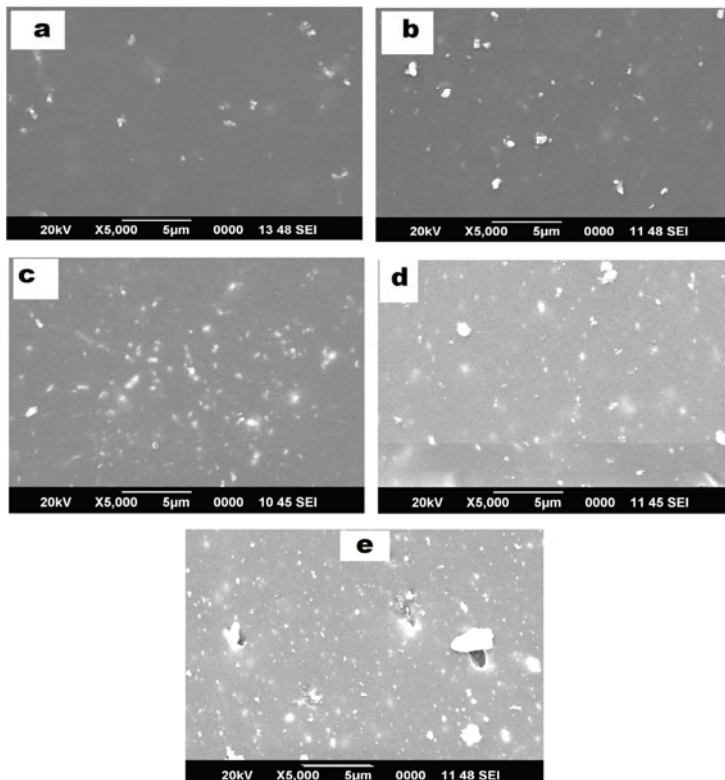


Figure 5.13 The morphologies of fracture surface as seen from SEM for a) MBN₀ b)MBN₂ c)MBN₅ d) MBN₁₀ e) MBN₁₅ EPDM based RNCs.

SEM morphologies of fracture surfaces indicate that the dispersion of filler is not homogeneous at higher loadings and several bulk clusters can be seen clearly. In Fig. 5.13(e) large clusters of approximately 1-2 μm size could be seen, whereas at lower loadings cluster formation is not at all taking place, evidencing uniform dispersion. Fig. 5.13(b) displays that agglomeration is absent in the SEM micrograph of lower loading samples. The dispersion state of MBN (stearic acid pre-treated nano-BaSO₄) filled system is improved as expected, and filler agglomerates are absent in the visual field.

5a.1.7 Thermal stability of EPDM-MBN nanocomposites.

From the previous studies of composites we could conclude that MBN-RNCs can exhibit better properties due to filler rubber interaction than BN-RNC. So detailed properties of MBN is discussed in forthcoming sections. The TG curves of the MBN series RNCs are shown in Fig. 5.14. The thermal characteristics as estimated by TGA are presented in Table 5.3. The degradation behaviour of the materials could be clearly read from the Differential thermogravimetry (DTG) curves in Fig. 5.15. The temperature of onset of degradation (T_i), the temperature at which the rate of decomposition is maximum (T_{max}), the decomposition temperature at 5% weight loss ($T_{-5\%}$) and 50% weight loss ($T_{-50\%}$) are given in Table 5.3. The pure EPDM (MBN₀) gives a single degradation between 400 and 500 °C and peak maximum at 483.87°C. With increasing nano filler concentration, weight loss due to the EPDM degradation is still observed, but the relative intensity decreases. The onset of this degradation shows a slight shift to higher temperatures with increasing nano concentration, though the temperature of maximum degradation remains the same. MBN₁₅ shows lower rate of degradation when compared to MBN₀, or to summarize the rate of maximum degradation decreases with filler loading and modified nano filled systems are having superior thermal stability compared to unfilled counterparts or unmodified counter parts. This may be attributed to the poor interfacial interaction between the matrix in the case of the unmodified nano mixes. Nano barium sulphate when surface treated contributes to

effective interaction between the filler and the matrix due to its small particle size and hence improves the interfacial adhesion. Strong interface renders the matrix stiff and makes the diffusion of heat and gases through the bulk more difficult. This makes the matrix thermally more stable in the presence of nanofiller. The thermal studies reveal slight degrees of stabilisation only, which is due to inherent stability of EPDM.

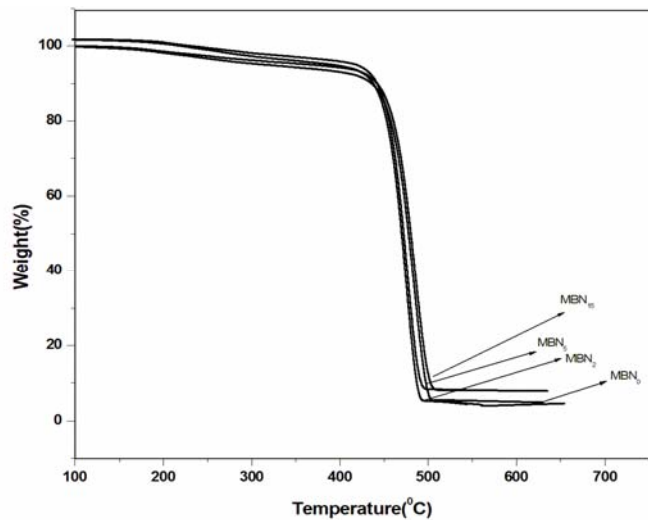


Figure 5.14 TGA traces of MBN series EPDM-RNCs

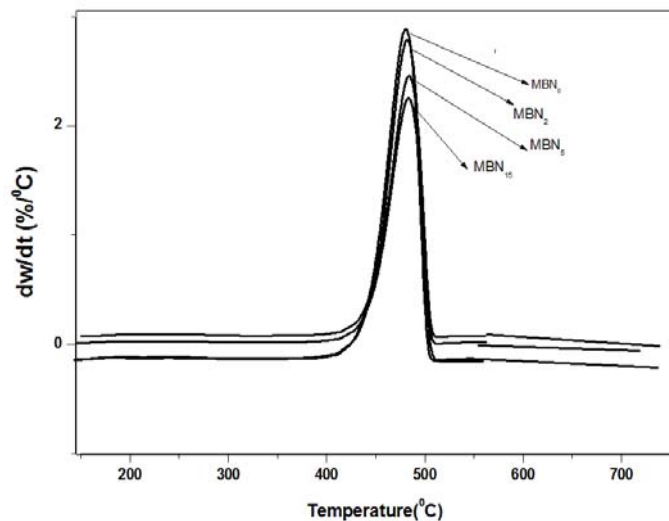


Figure 5.15 DTG curves of MBN series EPDM-RNCs

Table 5.3. Thermal degradation characteristics of MBN series EPDM-RNCs

Sample code	Ti(°C)	Tmax (°C)	T _{-5%}	T _{-50%}
MBN ₀	429.0	483.8	313.8	477.8
MBN ₂	429.2	484.2	313.9	478.1
MBN ₅	429.5	484.8	316.5	479.6
MBN ₁₅	430.0	485.0	322.0	480.9

5a.1.8 Dynamic properties measured in Strain sweep for EPDM-MBN composites: green and cured compounds

The strain sweep measurements were conducted on uncured and cured RNCs to investigate the rubber-filler interaction. The dependence of the dynamic properties on the strain amplitude at low deformation can give a better understanding on the filler-filler networks in a rubber matrix.

Fig. 5.16 (a) and (b) shows the strain dependence of complex modulus G^* for the MBN, filled RNC's uncured and cured respectively. The unfilled rubber shows no indication of non-linearity in the green compound. After the filler incorporation, the low strain modulus G_0 rises above the high strain modulus G_α , resulting in non-linear visco-elastic behaviour, known as Payne effect G_0-G_α . In the case of MBN series linearity is maintained at lower loadings. This increase in modulus or non-linear behaviour is caused by the formation of filler-filler interactions formed by filler loading. This is due to the fact, that the inter aggregate distances become smaller with rising filler content, and therefore the probability of formation of network increases. It should be noted that, the existence of a filler network is not necessarily corresponding to the existence of a filler network, which is percolated through the whole specimen. Filler-filler contacts in local sub networks are also denoted as filler networking and yield the Payne effect. The low Payne effect in MBN series indicates higher filler-rubber interaction due to uniform dispersion of modified nano barium sulphate in the matrix. The figures show that the complex moduli at low strains are comparatively low for the composites with MBN. In the

case of uncured compound the values do not show a regular increase indicating a non uniform distribution. The strain sweep studies after curing showed similar trend as that of the uncured compounds. The figures show that the modulus values are strain independent and a drop in the modulus occurred at high strains. The modulus values are high, since the compounds are cured, but the behaviour is the same as that of the uncured compounds. Values at low strains increased gradually with the increase in concentration of MBN. The higher values of modulus at low strains indicate the improved rubber filler interaction. The increased value at low strains reflects the higher values of hydrodynamic effect, which is dependent on the particle size and shape [10].

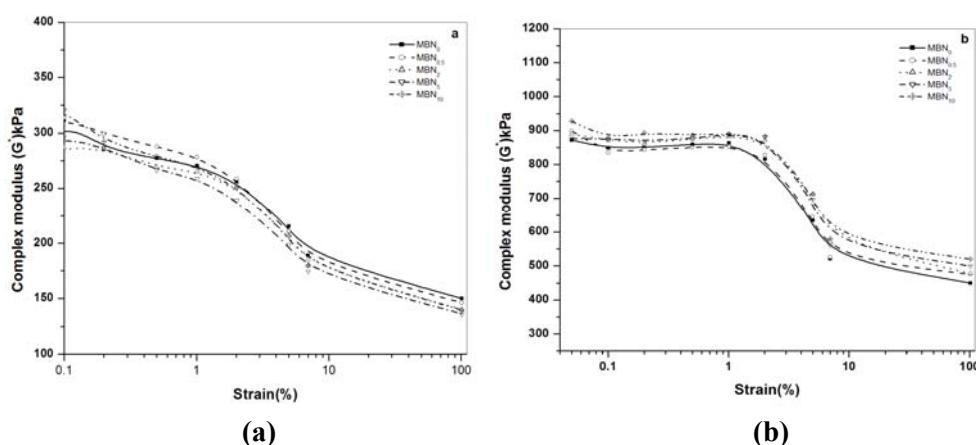


Figure 5.16 Dependence of Complex modulus (G^*) on strain amplitude of compound at different loadings of MBN series (a) green compound (b) Cured compound

5a.1.9 Crosslinkdensity and swelling studies

Swelling studies of EPDM-MBN composites.

Diffusion studies of the MBN-RNC's alone were carried out as explained in section 2.3.3, using toluene as the penetrant and crosslink density was calculated followed by diffusion, sorption and permeation coefficients. The sorption curves at room temperature were obtained by plotting $Qt\%$ of penetrant vs. square root of time of selected compositions to get a general idea regarding nature of swelling with filler loading in EPDM-RNCs. The sorption curves of

MBN filled EPDM are shown in Fig. 5.17. The initial swelling rate is very high owing to the large concentration gradient. This places the polymer under heavy solvent stress. This concentration gradient decreases with advanced swelling, the rate of swelling decreases and the difference in concentration becomes negligible when it reaches the equilibrium swelling. In the MBN filled RNCs, as filler loading increases $Q_t\%$ decreases which may be due to the decrease in volume fraction of rubber with filler loading.

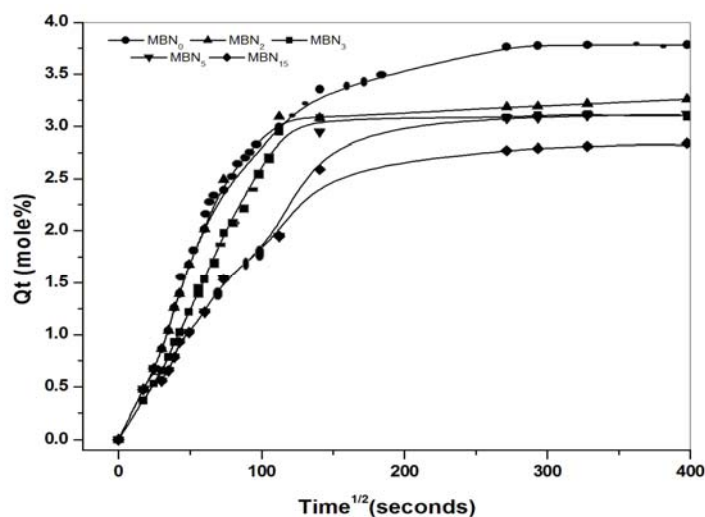


Figure 5.17 Sorption curves of EPDM-MBN based RNCs

The value of k depends on the structural features of polymer, whereas the value of n determines diffusion mechanism. The n values for MBN filled RNC's are shown in column 2 of Table 5.4. For the fickian mode, case 1, the value of n is 0.5 and it occurs when the rate of diffusion of penetrant molecule is much less than the relaxation rate of the polymer chains. For case 2 or non-fickian transport, where the n value is 1, the diffusion is rapid when compared with the simultaneous relaxation process. However in the case of anomalous transport where the n value is in between 0.5 and 1, both solvent diffusion and polymer relaxation rate are comparable. The effective diffusivity, D of the rubber solvent system was calculated from the initial portion of the sorption curves [11, 12].

From the Table 5.4 it is seen that the value of n lies between 0.5-1.0. The transport mechanism can be considered to be anomalous when rearrangement of polymer molecules occurs at a comparable rate to that of the change in concentration. As the loading increases the value of n decreases, which indicates that polymer relaxation is higher compared to rate of diffusion of penetrant, which is due to the intervention effect of fillers between polymer chains. Polymer chain mobility is restricted at higher concentration due to the increased population of filler particles in between the chains.

During diffusion, the polymer swells and mass flow takes place in addition to the molecular diffusion. Table 5.4 shows the variation of intrinsic diffusion coefficient of MBN filled EPDM- RNCs. As the loading increases the diffusion coefficient also increases though gradual at lower concentrations [13-15].

Transport of penetrant molecules through polymer proceeds via a two stage sorption and diffusion process. At first, the penetrant molecules are sorbed by the polymer followed by diffusion. Diffusivity is a kinetic parameter which depends on the polymer segmental mobility. The increase in diffusion coefficient with filler content is thus quite unexpected. Incorporation of fillers separates the polymer chains allowing the diffusion of penetrant molecules through the rubber phase. This can increase the diffusion coefficient. The larger diffusion coefficient at higher filler loadings is due to the formation of some channels, which promote diffusion through the filler aggregates. Moreover, the non polar nature of both the penetrant and rubber support the diffusion of the solvent through the medium [16].

Sorption and permeation decrease with loading, which is a reflection of decrease in volume fraction of absorbing phase with increased loading. Permeation decreases since it is a collective phenomenon consisting of both diffusion and sorption. Hence it could be concluded as; sorption controls the permeability in EPDM-RNCs.

Arriving at the crosslink density values it is seen that as the filler loading increases upto 2 phr there is an increase in crosslink density beyond which the cross link density decreases which may be due to the occlusion of filler particles between the rubber chains This is supported by tensile strength values. The better mechanical properties exhibited by MBN₂ system may be due to the higher crosslink density compared to higher filler loaded RNCs. The overall mechanism deviated slightly from fickian mode.

Table 5.4 Sorption curves of MBN series EPDM-RNCs

Sample code	n	Diffusion coefficient, $D \times 10^{-7} (\text{cm}^2 \text{s}^{-1})$	Sorption Coefficient S	Permeation coefficient, $P \times 10^{-6} (\text{cm}^2 \text{s}^{-1})$	Crosslink density, $\nu \times 10^{-5} (\text{moles gm}^{-1})$
MBN ₀	0.5484	5.23	3.48	1.82	2.68
MBN ₂	0.5432	5.32	3.26	1.73	3.50
MBN ₃	0.5398	5.52	2.89	1.60	3.58
MBN ₅	0.5291	6.13	2.57	1.58	3.35
MBN ₁₅	0.5268	6.21	2.34	1.45	3.30

Conclusions

EPDM/barium sulphate composites (EPDM/BaSO₄ RNCs) with sufficient mechanical properties can be prepared by mechanical mixing. Two nanofillers BN and MBN were used for the preparation of elastomeric nanocomposites. Effect of nano filler loading on cure characteristics, mechanical properties and transport properties of EPDM-RNCs were investigated. Addition of MBN to EPDM improved its cure characteristics and the cure reaction followed first order kinetics. In the presence of MBN filler, both cure rate and the kinetic rate constants increased, with loading up to 3 phr and at higher loadings both values decreased. Fine dispersion of BN particles in the EPDM matrix was only partially achieved by mill mixing. Modification with stearic acid helped to

improve the dispersion of MBN. Reinforcement increased with increased filler loading. The tensile strength for BN-RNCs were similar to that of gum upto 10 phr and then decreased with filler loading indicating the dilution effect of inert barium sulphate. With surface treated MBN better property was attained at a lower loading of 2 phr indicating increased interaction between surface treated nano barium sulphate and EPDM matrix. A 35% increase in tensile strength was registered at this level of filler loading. Tear strength increased with filler loading upto 10 phr for both the filler series. Elongation at break remained unvaried initially and beyond 5 phr it markedly increased indicating reinforcing effect of surface treated nano filler. The fillers that are reinforcing in nature will adversely effect the elastic properties, especially at elevated temperature and is manifested here as higher compression set of the composites. For MBN composites the set is relatively lowered compared to the BN compounds, indicating the lower extent of agglomeration. The nature and trend of the graphs are similar but the tensile strength values for MBN series composites are superior to that of BN series composites which is due to the enhanced interaction between rubber and surface treated filler. SEM morphology of fractured surfaces at lower loading indicated a uniform dispersion without any cluster formation, while at higher loadings a non homogeneous dispersion with several agglomerates were visible. TGA, DTG traces of RNC's revealed weight loss with decreased relative intensity. The temperature of maximum degradation remained the same. The rate of maximum degradation decreased with filler loading and modified nano filled systems had superior thermal stability compared to unfilled counterparts or unmodified counter parts. Thermal studies revealed slight degrees of stabilisation only, which is due to inherent stability of EPDM. Permeation in EPDM-RNCs, decreased with filler loading. The mode of solvent sorption mechanism showed minor deviation from fickian mode.

Reference

- [1]. 1. Haisheng Tan, A. I. Isayev ;Rubber Chem.Technol.,**2008**,81,138.
2. Z.H.Wang,Y.L. Lu,J.Liu, Z.M.Dang,L.Q.Zhang and W.Wang; Polym. Adv. Technol.,**2010**.
- [2]. W.Hofmann;RubberTechnologyHandbook.Gardener/Hanser Publications Inc.Cincinnati, OH. **1996**.
- [3]. K.Nagdi;Rubber as Engineering Material, 1st edition. Hanser: Munich, Germany, **1992**.
- [4]. F.W.Barlow;Rubber Compounding: Principles, Materials and Technique, 2nd edition, Marcel Dekker: New York, NY,**1993**.
- [5]. P.J. Fairclough, P.M.Swift;Rubber Developments,**1993**, 4,21.
- [6]. P.J.Wang ; J. Rubber Development., **1994**,47(³/₄),17.
- [7]. A.L.N da Silva, M.C.G. Rocha, M.A.R.Moraes, C.A.R.Valente, F.M.B.Coutinho Polym. Test., **2002**,21,57.
- [8]. B.T.Poh,H.Ismail, E.H.Quah, P.L .Chin;J. Appl. Polym .Sci., **2001**,81,47.
- [9]. F.S.Deghaidy; Egypt J. Sol., **2000**,23,167.
- [10]. S.Kohjiya,Y.Ikeda ; Rub. Chem. Technol., **2000**, 73,534.
- [11]. J.Crank; The mathematics of diffusion.,2nd Ed. Oxford: Clarendon Press, **1975**, 244.
- [12]. L. N.Britton, R .B. Ashman, T. M.Aminabhavi, P. E. Cassidy;J. Chem. Edn., **1988**, 65,368.
- [13]. S. Aprem, K.Joseph, A. P. Mathew,S.Thomas; J. Appl. Polym. Sci., **2000**, 78,941.
- [14]. R. S. Khinna, and T. M. Aminabhavi;J. Appl. Polym. Sci., **1991**, 42, 2321.
- [15]. P. J. Flory and Jr.Rener; J. Chem. Phys.,**1943**,11, 521.
- [16]. P.E.Cassidy, T.M.Aminabhavi, C.M.Thompson; Rubber Chem. Tech., **1983**, 56, 594.

Part-b**SYNERGISTIC EFFECT OF CARBON BLACK FILLED EPDM-MODIFIED NANO BARIUM SULPHATE (MBN) HYBRID RNCs**

Novel hybrid rubber nanocomposites based on EPDM, modified nano barium sulphate (MBN) and carbon black were prepared by proper compounding on a two-roll mill with the aim of determining the synergistic effect of dual filler networks. The investigation aimed at replacing, at least by a smaller fraction, carbon black from its composites using eco-friendly filler. To optimise the synergistic effect of carbon black and MBN in the EPDM matrix, systematic analyses were performed on EPDM-CB-MBN hybrid RNCs containing various combinations of black and MBN, which revealed that the properties strongly depended on the extent of the dispersion of black and MBN fillers. The amount of MBN filler was varied from 0 to 15 phr and that of carbon black was fixed at 40phr. The results were compared with that of 50 phr carbon black containing composites. Incorporating 2.5 phr MBN to the control EPDM containing 40 phr carbon black resulted in an obvious synergistic effect, including cure activation, improvement in the mechanical properties and enhancing the thermo oxidative resistance. This CB40+MBN_{2.5} system excelled CB50 filled EPDM-RNCs by all means. These hybrid RNCs showed higher tensile strength, tear strength and modulus values and lower elongation at break compared to black alone filled systems. Characterization of the RNCs using scanning electron microscopy showed that there were relevant changes in the morphology of the fracture surface with dual filler loading. The thermal stability of the RNCs improved marginally with MBN concentration, and transport mode showed anomalous behaviour. Better results were exhibited by hybrid RNC's filled with 2.5phr MBN.

Introduction

Carbon black (CB) acts as strong reinforcing filler and is hence used most popularly in the automobile industry [1]. Almost 90% of the produced carbon black, all over the world, is used in the tyre trade and at present, carbon black is the principal reinforcement for rubber compounds [2, 3]. There is a continuous demand for new, low cost, low-weight, and environment- friendly reinforcing filler in the rubber industry [4, 5]. These fillers must be capable of at least partially replacing the supply of carbon black industry and, in the past 20 years many reinforcing fillers were developed as alternatives to carbon black such as kaolin, silica and sepiolite [6]. Extensive studies have been done on rubber/clay nanocomposites, showing that the stiff anisotropic nanoclay exhibits strong reinforcing effect in many rubber matrices, even at remarkably low filler content. [7-12]. Several investigations have shown that clay layers in hybrid composites with black can bend around carbon black particles to form structure called “nanounits”[13-15] to yield improved properties. It is well known that CB particles in rubber matrix tend to agglomerate to form filler network at practical filling level. The filler network contributes a lot to the reinforcement [16] and it is the main parameter governing the dynamic response of filled rubber [17]. The strength and architecture of the filler network are controlled by the amount, particle size, geometry, as well as surface chemistry of the filler. As all these fillers are inorganic in nature, these are not compatible with polymer matrices that are organic in nature. Due to this incompatibility concern, the reinforcing effect of these fillers in the polymer matrices is very much lower than the CB. Polymer-layered silicate nanocomposites have shown drastic improvements in thermal, mechanical and barrier properties at very low loading of these types of inorganic layered silicate [18-20]. To make the layered silicate compatible with the polymer matrices, the silicate layer surfaces have been organically modified by exchanging the alkali cations with alkyl ammonium ions [21-23] This enhances the physical, mechanical and thermal properties of the polymer-layered silicate

nanocomposites than their respective controls [7,24,25]. The improvement in the properties imparted by the organically modified nanoclay to the elastomeric composites have developed a new type of composite, known as rubber-CB-clay hybrid nanocomposites [26]. This type of hybrid nanocomposites facilitates the partial replacement of CB by organically modified nanoclay in elastomeric composites with out hindering its unique properties. According to Arroyo, et al. [7], synergistic reinforcement of CB and nanoclay in natural rubber composites have been studied by Qu et al. [27]. Engelhardt and coworkers have reported the effects of intercalation and exfoliation of clay platelets on the mechanical properties of the cis-1,4-polyisoprene and epoxidized natural rubber[28]. Li, et al. have reported the effects of exfoliation of organoclay on the mechanical properties and thermal stability of EPDM rubber by melt extrusion method[29]. Schon and co-workers have investigated the effect of nanosilica on the mechanical properties like surface elastic moduli of silica-reinforced styrene butadiene rubber (SBR), ethylene propylenediene rubber (EPDM) and SBR/EPDM rubber blends by atomic force microscopy (AFM) based mapping [30].

In the past two decades, researchers have been seeking new reinforcing fillers that are environment-friendly, inexpensive and readily available to partially replace CB. The replacement aims at cost reduction, on one hand and on the other synergy of different fillers might be obtained due to the complicated interactions through mixed network formation. These fillers like silica, kaolin, sepiolite etc. are inorganic in nature and hence incompatible with organic polymer matrices. Their reinforcing effect was much lower than with carbon black. Ethylene propylene diene terpolymer(EPDM), which is a typical non polar rubber with good ageing properties and high filler loading capacity and widely used in automobile sectors, was used as a base rubber matrix for the preparation of EPDM-CB-nano barium sulphate hybrid nanocomposites[31,32]. Synthesised nano barium sulphate that was organically

modified using stearates, were used for this study based on their ability to impart property enhancement in EPDM as seen in chapter 5 part I. The nano filler was incorporated in the bulk EPDM matrix in presence of CB with sulphur as curing agent. The variation in the curing characteristics, morphology, mechanical properties, solvent properties and thermal stability of the different MBN–CB hybrid nanocomposites had been analyzed and compared with each other and also with their respective controls. The synergistic effect of carbon black and MBN was investigated in EPDM samples, which contained both fillers at different concentration.

5b.1 Ethylene propylene diene rubber-carbonblack-modified nano barium sulphate hybrid nanocomposites.

5b.1.1 Preparation of nanocomposites

Nano powders were synthesised via chemosynthetic pathway in presence of PVA (section 3.2.2) and modified using stearic acid (section 3.2.3). The carbon black loadings are represented as CB and modified barium sulphate is named as MBN and the filler loadings are represented as subscripts to this notation. The formulation for the preparation of the RNCs is given in Table 5.5. Two series of RNCs were prepared, first series with varying amounts of MBN with constant loading of carbon black (HAF-N330) at 40phr and second one with 50phr of carbon black alone. The RNCs were prepared in a laboratory size two-roll mill at a friction ratio of 1:1.25 as per ASTM standards (section 2.2.1). The mixes were kept for 24 h for maturation. The optimum cure time at 160°C was determined using a Rubber Process Analyzer. The compounds were compression moulded at 160°C in an electrically heated hydraulic press (section 2.2.5). The samples were cured to their respective optimum cure times. After curing, the sheets were suddenly cooled in water. These sheets were used for subsequent tests. The samples for rest of the studies were prepared according to procedures mentioned in section (2.3.1-2.3.3).

Table 5.5 Compounding formulation of EPDM used for the present study

Compounding ingredient	phr								
EPDM	100.0	100.0	100.0	100.0	100.0	100.0	100.0	100.0	100.0
ZnO	4	4	4	4	4	4	4	4	4
Stearic acid	1.5	1.5	1.5	1.5	1.5	1.5	1.5	1.5	1.5
Naphthenic oil	8.5	8.5	8.5	8.5	8.5	8.5	8.5	8.5	8.5
MBN	0	0.5	1.5	2	2.5	3	5	10	15
Sulphur	1.5	1.5	1.5	1.5	1.5	1.5	1.5	1.5	1.5
TMTD	0.5	0.5	0.5	0.5	0.5	0.5	0.5	0.5	0.5
CBS	1	1	1	1	1	1	1	1	1
ZDC	0.5	0.5	0.5	0.5	0.5	0.5	0.5	0.5	0.5
HAF	40	40	40	40	40	40	40	40	40

5b.1.2 Cure characteristics

The cure characteristics of the hybrid rubber nanocomposites are shown in Table 5.6. The maximum torque value of the black filled composites is a direct measure of shear modulus and is found to increase with nano filler loading which indicates that with increasing filler content there is an enhancement in the stiffness of the nanocomposites. The cure activation by stearate modifier is observed as cure time reduction.

Table 5.6 Cure characteristics of EPDM based hybrid RNCs

Sample code	Minimum torque (dNm)	Maximum torque (dNm)	T ₁₀ (minutes)	T ₉₀ (minutes)
CB50	0.53	12.52	1.50	11.33
CB40	0.35	10.62	1.75	13.50
CB40+MBN _{0.5}	0.37	11.53	1.57	12.80
CB40+MBN _{1.5}	0.39	11.75	1.55	12.32
CB40+MBN ₂	0.40	11.77	1.48	11.23
CB40+MBN _{2.5}	0.41	12.86	1.42	10.09
CB40+MBN ₃	0.41	12.92	1.39	11.29
CB40+MBN ₅	0.43	13.05	1.40	12.20
CB40+MBN ₁₀	0.49	12.89	1.31	11.86
CB40+MBN ₁₅	0.43	12.71	1.35	11.90

The plot of $\ln(D_{max} - D_t)$ against time t of the carbon black filled EPDM-MBN hybrid RNC's at 160 °C is presented in Fig. 5.18. The plots are found to be linear which proves that the cure reactions proceed according to first order kinetics. The cure rate constants (k) were calculated from the slope and the cure rate index (CRI) values were determined (section 2.2.1). The variation of these parameters with filler loading is presented in Fig. 5.19. For the EPDM- CB-MBN series, both CRI and the kinetic rate constants increase with a combination of CB40+MBN_{2.5}, after which, both decreases but still cure activation is present as indicated by the higher CRI value than CB40.

The initial increase registered in CRI and cure reaction constant with loading indicates the activation of cure reaction [33-35] which levels off beyond 3 phr of filler loading. Similar trend is also seen in the variation of cure time (Table 5.6).

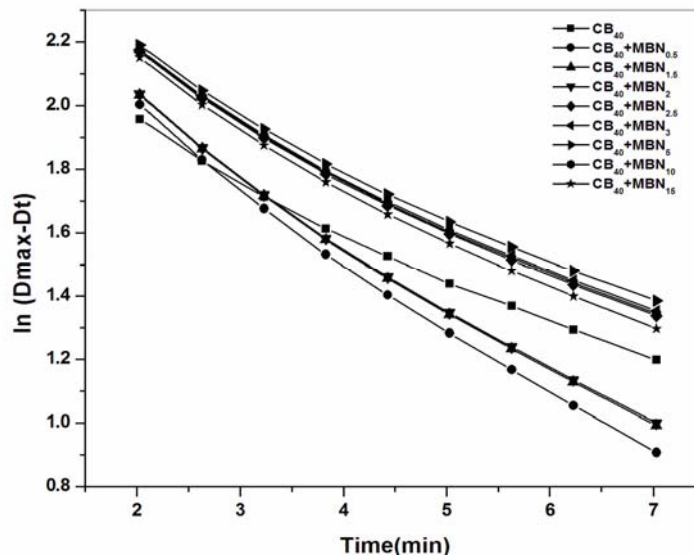


Figure 5.18 $\ln(D_{max} - D_t)$ against time t of the EPDM-CB-MBN filled hybrid RNCs

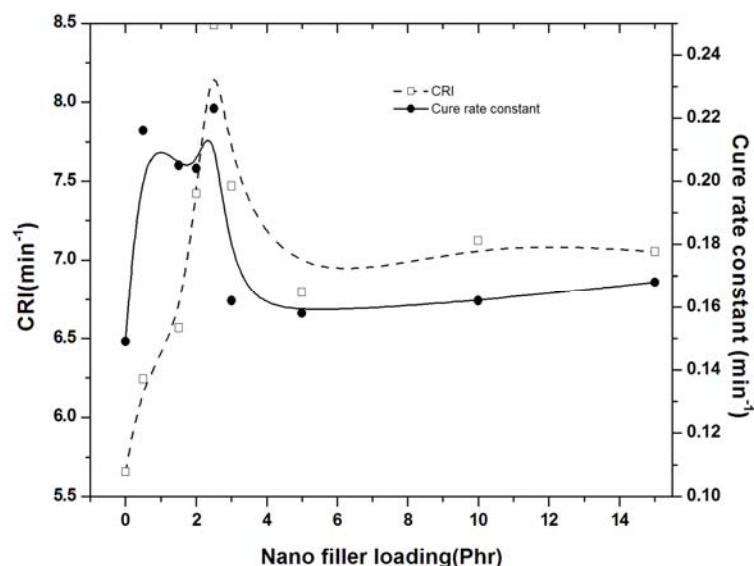


Figure 5.19 Plot of rate constant and CRI vs loading for the EPDM-CB-MBN series RNCs

5b.1.3 Filler dispersion in the RNCs

Maximum torque increases during vulcanization in the case of filled compounds. The increase in torque of the filled compound was found to be directly proportional to filler loading. Fig. 5.20 represents the relation between $D_{\max}^f - D_{\min}^f$ against filler loading of hybrid composites. The increase in Δ torque indicates that the incorporation of nano barium sulphate affects cross linking between the polymer chains, which is being more registered with 2.5 MBN filled hybrid composite. In Fig. 5.20, Wolf equation is applied for the EPDM-CB-MBN hybrid system. It is a measure of the structure of the fillers in the matrix, the higher α_f value found for the CB40+MBN_{2.5} compounds evidences for this filler combination to be more viable. The absolute value of α_f for each composite was calculated (section 2.2.3.b) and is plotted in Fig. 5.20 The value of α_f increases with loading. This means that this system form less agglomerates in the matrix. With further additions, there is a tendency for agglomeration. These observations are in agreement with those obtained from Lee's approach.

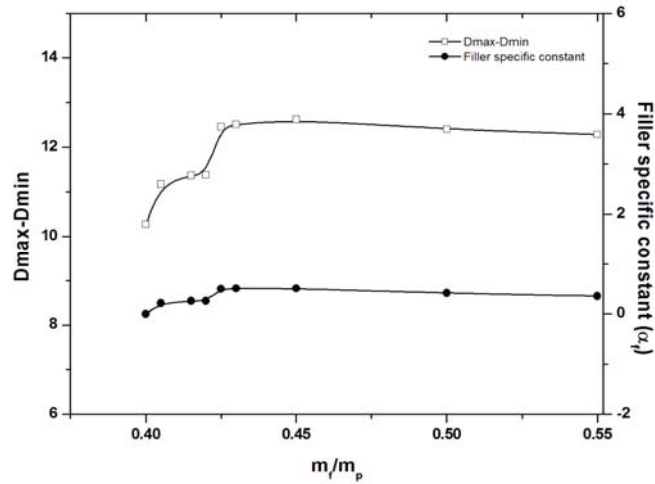


Figure 5.20 Variation of Δ Torque and filler specific constant with filler loading for EPDM-CB-MBN hybrid RNCs

The dispersion of filler within the matrix and formation of filler agglomerates were studied in detail by B.L.Lee, as shown in Fig. 5.21.

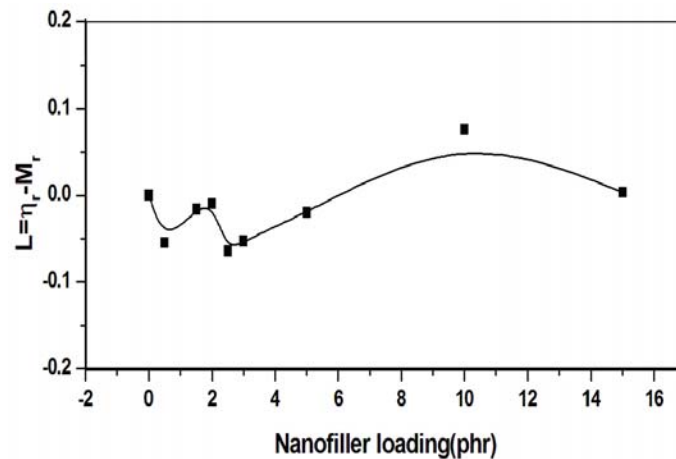


Figure 5.21 Variation of parameter L for EPDM-40CB-MBN hybrid RNCs with MBN loading

This method is applicable for carbon black composites. Even in well dispersed filler rubber systems, differences in the degree of filler agglomeration in the cured and uncured state can be observed. The index L decreases with filler

loading pointing to the reduced agglomeration of the filler in the elastomers and later on increases slightly which shows a tendency of agglomeration at higher MBN loading. The value of L is found to be higher for samples containing carbon black alone than the hybrid filler network. This indicates poor dispersion of CB particles compared to CB-MBN dual networks in the EPDM matrix. Thus the incorporation of carbon black along with MBN shows better processability compared to CB filled composites. At higher loadings L increases, indicating the presence of filler agglomeration.

5b.2 Dynamic properties measured in strain sweep for uncured and cured compounds

The strain sweep measurements were conducted on cured hybrid RNCs to investigate the rubber–filler interaction. The dependence of the dynamic properties on the strain amplitude at low deformation can give a better understanding on the filler–filler networks in a rubber matrix. Fig. 5.22 shows the strain dependence of complex modulus G^* for the EPDM-MBN-CB filled RNCs. When the nano MBN is mixed with carbon black, the effect on the complex modulus is superior to that of carbon black alone. On increasing MBN incorporation in carbon black filled nanocomposites, a steady increase in modulus is observed. This is due to the formation of three different types of filler networks arising from the simultaneous use of two fillers. The CB network, MBN-CB network and MBN-MBN network of which MBN-CB networks are stronger than any other network as observed from the graph. It is seen that in dual filler system the break down and reformation of dual network begins at a higher strain than MBN, CB systems when present alone. The strain sweep studies after curing showed similar trend as that of the uncured compounds. The figures show that the modulus values are strain independent and a drop in the modulus occurred at low strains. Since the compounds are cured the modulus values are high. The higher values of modulus at low strains indicate the improved rubber filler interaction. The increased value at high strains reflects the

higher values of hydrodynamic effect, which is dependent on the particle size and shape[36].

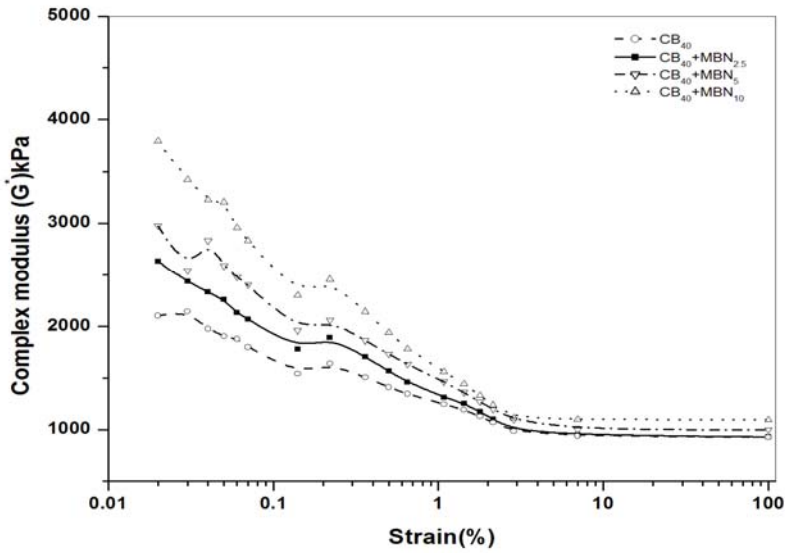


Figure 5.22 Dependence of Complex modulus (G^*) on strain amplitude of cured EPDM-CB-MBN hybrid compounds at different loadings

5b.3 Mechanical properties

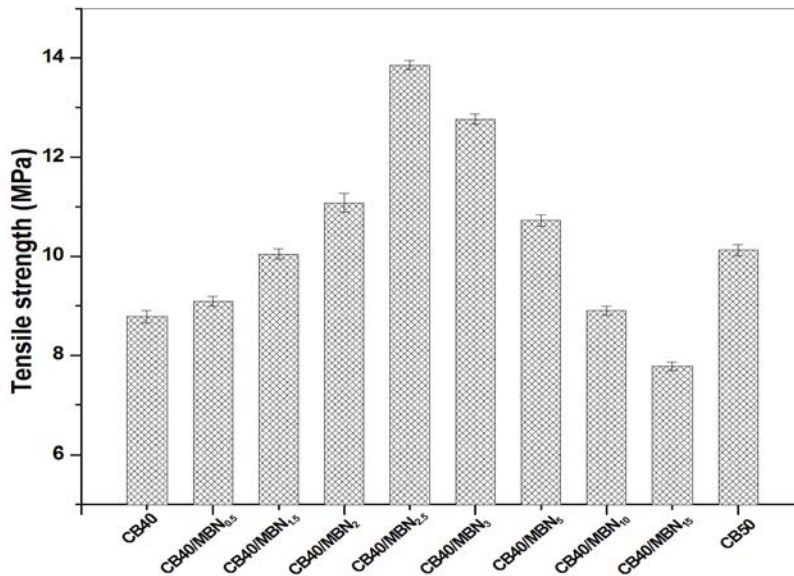


Figure 5.23 Variation of tensile strength with loading

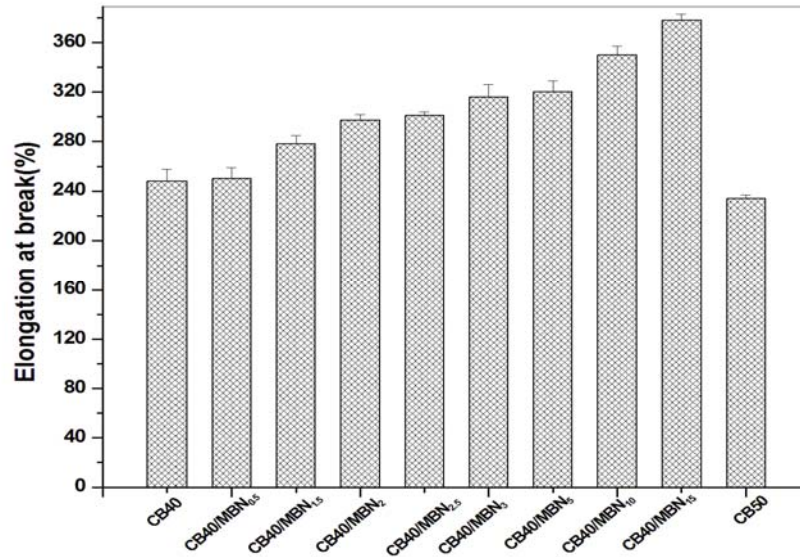


Figure 5.24 Variation of elongation at break with loading

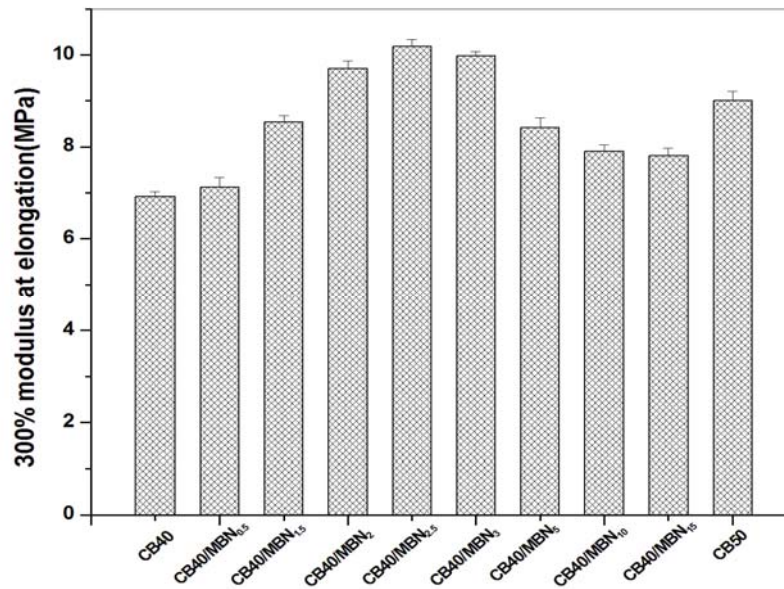


Figure 5.25 Variation of modulus at 300% with loading

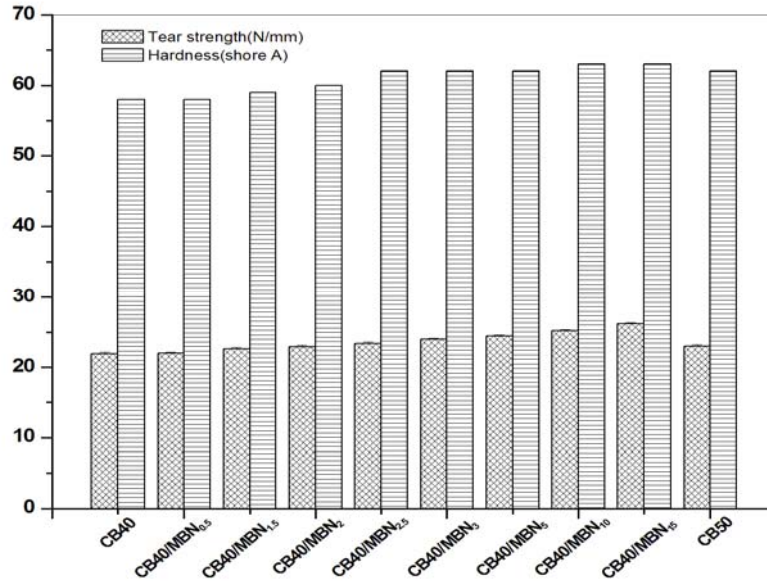


Figure 5.26 Variation of tear strength and hardness with loading

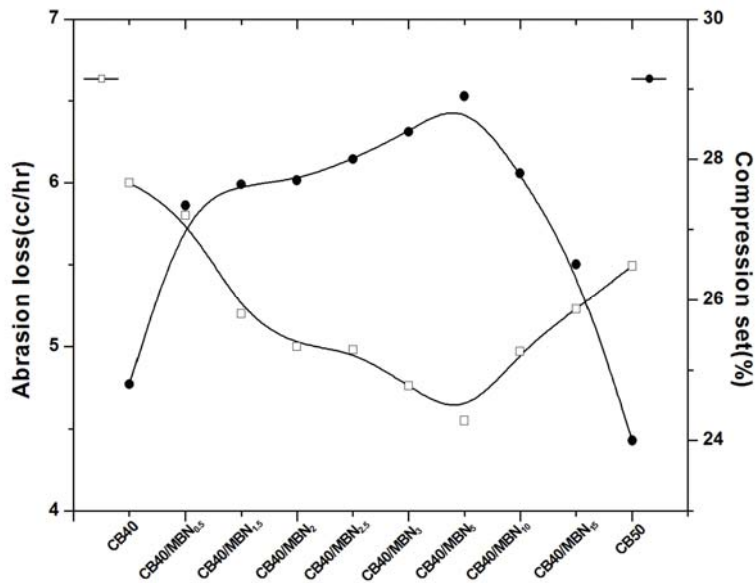


Figure 5.27 Variation of compression set and abrasion loss with MBN loading in EPDM-CB40 hybrid RNCs

The mechanical properties of EPDM-CB composites containing 40 and 50 phr CB are compared with EPDM-CB40-MBN hybrid RNCs containing

varied MBN loading, as shown in Fig. 5.23 to 5.27. As the CB content increased from 40 to 50 phr an increase is registered in tensile strength, tear strength and hardness. This is due to the resistance to crack propagation resulting from the reduced inter-aggregate distance within the CB. The graphs reveal the increasing tensile strength upto 5 phr nano and on further addition the property decreased and remained constant. It is noteworthy that even 2.5 phr of MBN in combination with 40CB is enough to impart tensile strength superior to that of 50phr of black in EPDM. For composite CB40+MBN_{2.5} the tensile strength marked an increment of 42.2% when compared to CB 40 systems; whereas on comparing the same composite with CB50 system it could be seen that, this hybrid filled EPDM composite registered an increment of 36% in tensile strength. This reports that dual filler network is far more superior in imparting reinforcement to CB alone filled systems. As the filler loading increased in CB40 system, the 300% modulus registered its maximum value at 2.5 phr filler system and was about 47% superior to black alone filled systems. The synergy in action resulted in 13% increment in hybrid system than 50 CB alone filled systems. With the addition of 2.5 phr of MBN into 40CB containing EPDM, tensile, tear, hardness and modulus increased. Elongation increased with filler loading, and was higher than CB40, CB50 systems; indicating the lubricant action of modified MBN, on EPDM networks which enable polymer chains in easy slippage. Additionally, the lubrication of coated stearic acid molecules results in the easier slippage of the EPDM rubber chains on the surface of nano-barium sulphate particles, which might be another important reason. All the properties were better or even comparable with EPDM/CB40 composite. With further filler incorporation (ie., upto 15phr of MBN) tear strength and hardness improved but all other properties decreased and finally remained constant, which is due to agglomeration of fillers. When compared to EPDM-CB40, MBN filled hybrid RNCs registered an overall increase of 19% in tear strength. It could be concluded that optimum CB-MBN ratio in EPDM to obtain equivalence with CB50 is; CB40+MBN_{2.5}. This combination indicates a balanceable state of

saturation for the synergistic effect between CB and MBN on reinforcing EPDM. In comparison with EPDM/CB(100/40) the tensile strength, tear strength and abrasion resistance of hybrid RNCs increased. Compression set (%) yielded poor values for EPDM hybrid RNCs. The abrasion loss of hybrid RNC's decreased upto 10 phr of MBN added. Further filler addition increased the abrasion loss, as the filler aggregates formed are pulled out from the matrix leading to the formation of voids and holes. During abrasion of the rubber sample, uniformly distributed MBN and CB particles were introduced into the abrasion surface. The strong filler- polymer adhesion contributed to the decrease in abrasion loss. The composites resisted loss due to abrasion far better than black alone filled composites.

5b.4 Morphological studies, SEM and AFM images

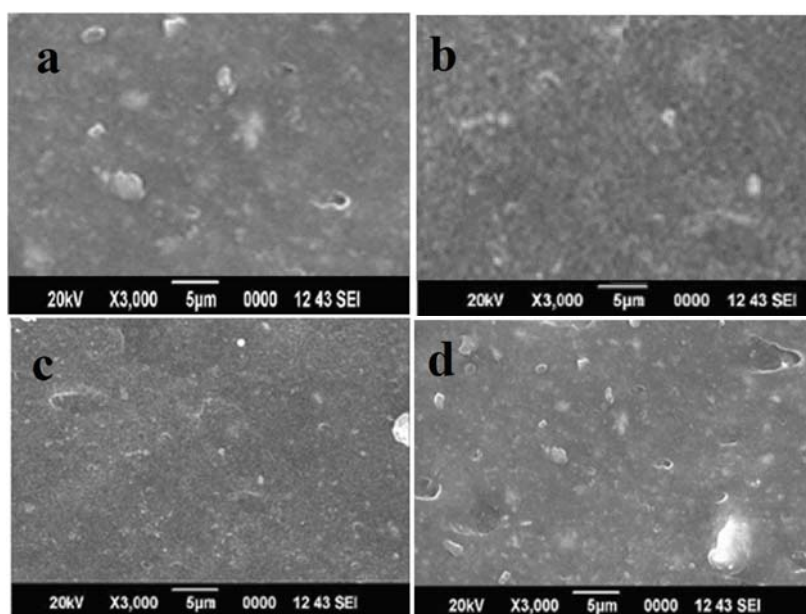


Figure 5.28 SEM photographs of fracture surfaces of EPDM based hybrid RNCs (a)CB40 (b)CB40+MBN_{2.5} (c) CB40+MBN₅ (d)CB40+MBN₁₅

Fig. 5.28 is the cross-section of fractured surfaces of typical EPDM-CB-MBN hybrid RNC. Fig. 5.28.a shows EPDM–CB40 composites, in which

clusters are visible. Fig. 5.28.b shows carbonblack-MBN_{2.5} dual network and rubber matrix have formed a macro-homogenous system, this indicates that, fine filler dispersion is made possible by the presence of 2.5 phr of MBN along with 40 phr black and could effectively assist the reinforcement effect of carbon black on rubber as seen from strength studies. As a comparison, the SEM morphology of carbon black alone filled systems are shown in Fig. 5.28a, which is almost the same as that of hybrid RNCs. Comparing Fig.5.28a and 5.28b it is found that addition of MBN can improve the dispersibility of carbon black in hybrid RNCs and reduce the agglomeration of carbon black. The increase in roughness on fracture surface evidences that these RNCs certainly have enhanced strength properties compared to their black alone filled counterparts. Fig. 5.28.d shows that the carbon black and nano filler combination of 40/15 lead to loose agglomerate formation, as evidenced from crater formation of nearly 0.9µm diameter. These holes represent filler pullout during strain endurences.

The proper dispersion of carbon black can not only reduce energy consumption during mixing, but also improve the mechanical properties of vulcanizates. Nano filler–carbon black combination can assist improved dispersion. These are evidenced from SEM images and the 3-D images of the superior system and the comparison diagrams are as shown in Fig. 5.29.

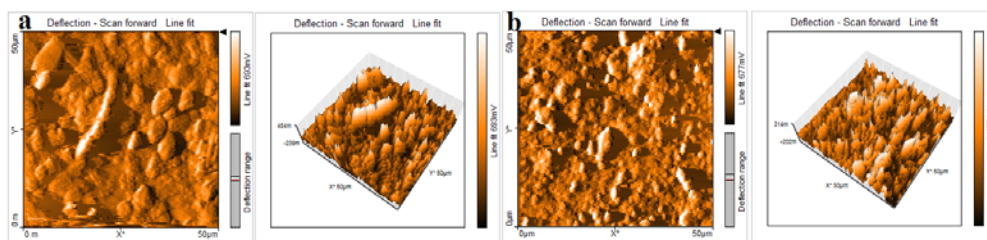


Figure 5.29 2-D (l.h.s) surface topography and 3-D (r.h.s) AFM images of (a)CB40 and (b)CB40+MBN_{2.5}

The figure shows AFM images of the superior composition CB40+MBN_{2.5} and control sample CB40. The topography reveals that the dispersion is improved in the presence of nano filler along with 40CB as can be seen from uniform 3D- images

in Fig.5.29 b. In Fig. 5.29a, ridges formed by filler can be clearly seen and rubber surface devoid of any filler is seen visibly in their corresponding 3D-images. The valleys in between the hills formed by filler-polymer regions indicate poor rubber-filler interaction. In Fig. 5.29 b uniform rough surface formation is evidenced from uniform rubber-filler structures of EPDM-CB-MBN system.

5b.5 Thermal studies-Thermal ageing and TGA

5b.5.1 Thermal Ageing

The retention of properties on thermal ageing is given in the Table 5.7. The graphical representations of the variation in tensile and tear properties are given in Fig. 5.30 and 5.31. During thermal ageing, cross-link formation or cross-link breakage can take place or an existing cross-link may break and a stable linkage can be formed. It is observed that there is an initial increase in the tensile modulus after 48 hrs of ageing at 100 °C and after that there is a decline. The increase in modulus is due to the agglomeration of filler particles at higher temperature and due to increased cross links. In the case of filled EPDM rubbers there is a probability of formation of newer crosslinks on heating owing to free double bond near methyl substituent of ENB, left unused on vulcanization, or due to making and breaking of S-S linkages. The rate of crosslink formation depends on the stability of composites and the additional crosslinks initially increase the modulus and strength properties; while accelerated ageing leads to degradation of rubber. Under the present state of study the composites offer better resistance upto 48hrs of ageing at 100°C, with hybrid systems exhibiting superior properties. The figure gives the exact variations in tensile strength and tear strengths on ageing, where as the table summarises data as retention in property compared to their unaged composites discussed previously.

Table 5.7 Retention of properties on thermal ageing for EPDM based EPDM-CB-MBN hybrid RNCs

Filler loading (phr)	% retention in tensile strength		% retention in tear strength		% retention in 300% modulus	
	24 hrs	48hrs	24 hrs	48hrs	24 hrs	48 hrs
CB50	96	100	97	87	108	110
CB40	93	103	95	85	110	112
CB40+MBN _{2.5}	97	99	97	96	103	99
CB40+MBN ₃	97	98	98	95	102	98
CB40+MBN ₅	98	98	96	94	104	100
CB40+MBN ₁₀	98	99	97	94	104	102
CB40+MBN ₁₅	95	102	97	93	100	101

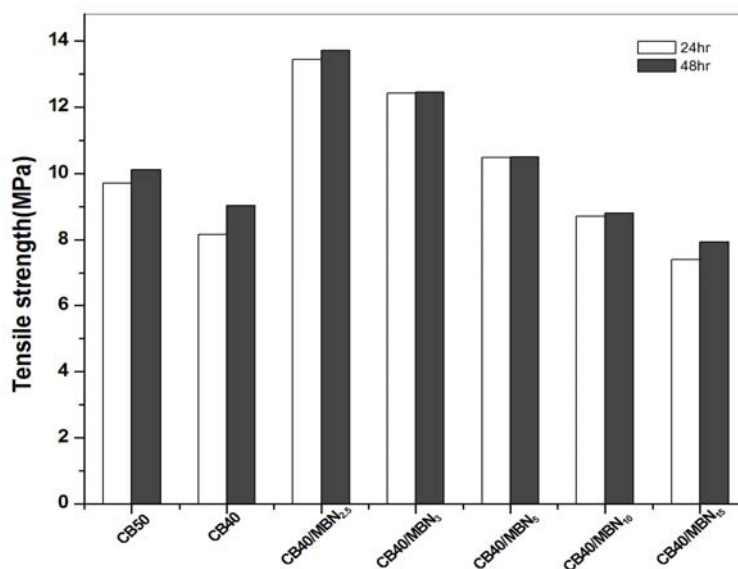


Figure 5.30 Tensile strength of EPDM-CB-MBN hybrid RNCs on thermal ageing

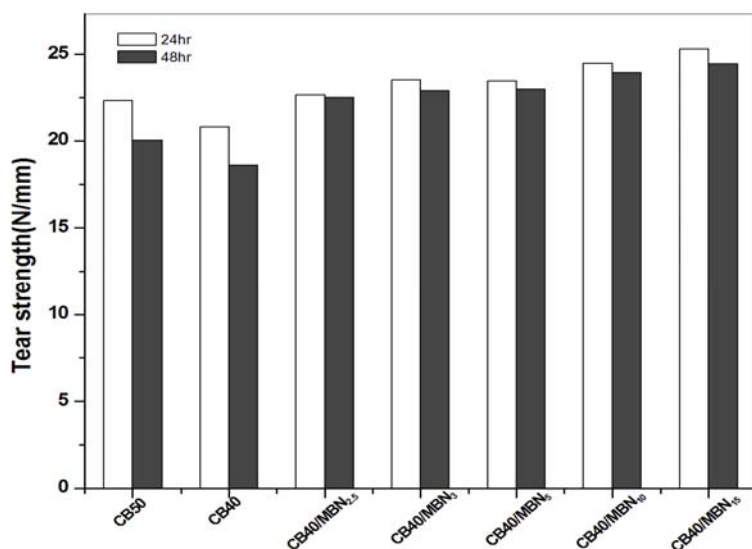


Figure 5.31 Tear strength of *EPDM-CB-MBN hybrid RNCs* on thermal ageing

Tensile strength showed a gradual increase with time of ageing which is due to the increase in crosslinking with temperature in the case of EPDM having unsaturated ENB, while crosslinking was reduced in the presence of nanofiller-CB dual networks as seen from retention in tensile strength. The tear strength exhibited nearly 97% retention for all the composites after 24hrs of ageing. On increasing the time of ageing, the tear strength decreased beyond 90% for CB filled composites, where as for dual filler networks, the deterioration was rather slow, indicating better thermal stability. Modulus enhancement on ageing may be due to additional cross linking leading to stiffening during ageing. It can be seen from the figures that the composites with 2.5 phr MBN showed a better resistance to thermal degradation in combination with CB40. Though retention seems to be better for black filled composites from tabulated data, the figures clarify that even after ageing, the properties are higher for MBN filled hybrid systems. This may be due to the increased rubber filler interactions, which lead to an increased occlusion of rubber molecules in the voids of nano-carbon black network.

5b.5.2 Thermogravimetric analysis

In the case of MBN filled EPDM RNCs, cure rate is accelerated beyond 2.5 phr loading. The reason for the lower cure time at higher loading is due to the increase in thermal transition of EPDM in presence of MBN, which promotes the vulcanization process. This modified barium sulphate has increased specific surface by surface treatment, which results in improved thermal transition, filler–filler and filler–matrix interactions. Within the composite system, there could be two paths of thermal transition. In one path, heat can pass from MBN-polymer-MBN flakes and in the other path through direct contact between the MBN spheroids. The second path of thermal conduction, will be more effective for higher filler concentration which increases the interaction between the fillers which in turn increases the process of vulcanization. The TG curves of the EPDM-CB-MBN hybrid rubber nanocomposites series are shown in Fig.5.32. The thermal characteristics as estimated by TGA are presented in Table 5.8 The degradation behaviour of the materials could be clearly read from the Differential thermogravimetry (DTG) curves in Fig. 5.33. The temperature of onset of degradation (T_i), the temperature at which the rate of decomposition is maximum (T_{max}), the peak degradation rate (R_{max}) and the decomposition temperature at 5% weight loss ($T_{-5\%}$) and 50% weight loss ($T_{-50\%}$) are given in Table 5.8. The EPDM/CB40 composites gives a single degradation between 400 and 500⁰C and peak maximum at 437.22 ⁰C. With the incorporation of MBN, weight loss due to the EPDM degradation is still observed, but the relative intensity decreased. The incorporation of nano filler in combination with 40CB shifts the onset of degradation to a marginally higher temperature, though the temperature of maximum degradation remains the same. As the nano loading increase a lowering in the rate of degradation is observed. On comparison with EPDM-CB40, thermal behaviour of EPDM-CB40-MBN composites has been slightly improved. MBN₁₅ shows lower rate of degradation than MBN₅ filled hybrid RNC's. To summarize the rate of maximum degradation decreases from 1.04 to 0.98%/⁰C with filler loading and modified nano filled systems in

conjunction with CB are having superior thermal stability when compared with CB alone filled systems. The degradation under inert atmosphere accounts for the fact that MBN fillers do not contribute much to thermal stability owing to the high thermal stability of host matrix EPDM itself. This fact is ascertained by similar maximum temperatures of degradation of nano bariumsulfate filled matrix.

Table 5.8 Thermal degradation data of EPDM based hybrid RNCs

Sample code	Ti(°C)	Tmax (°C)	Rmax (%/ °C)	T _{.5%}	T _{.50%}
CB40	437.2	492.6	1.04	286.1	492.2
CB40+MBN _{2.5}	438.0	493.1	1.00	287.4	492.4
CB40+MBN ₅	437.9	493.2	0.98	288.8	494.6
CB40+MBN ₁₅	439.2	494.1	0.99	289.6	496.9

The improvement of thermo oxidative resistance was attributed to three factors: (1) chemical activities of filler and polymer; (2) strong polymer–filler interactions; (3) uniform dispersion of fillers[37,38]. The dense polymer–filler networks hindered degradation of nanocomposites.

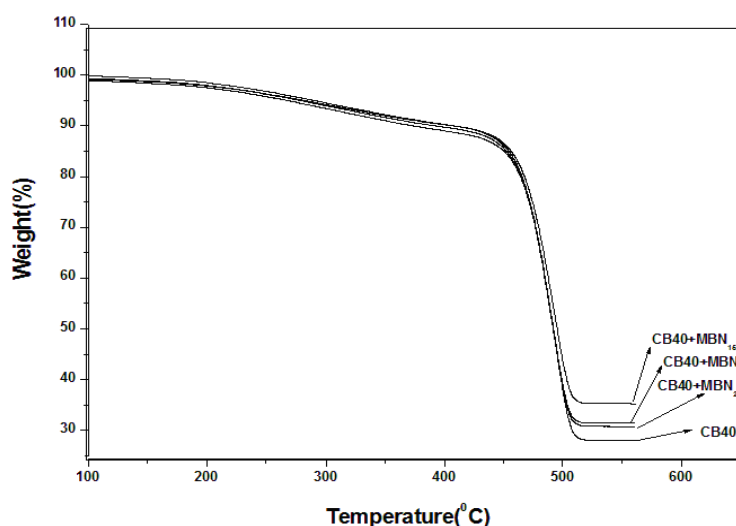


Figure 5.32 TGA traces of EPDM-CB-MBN hybrid RNCs

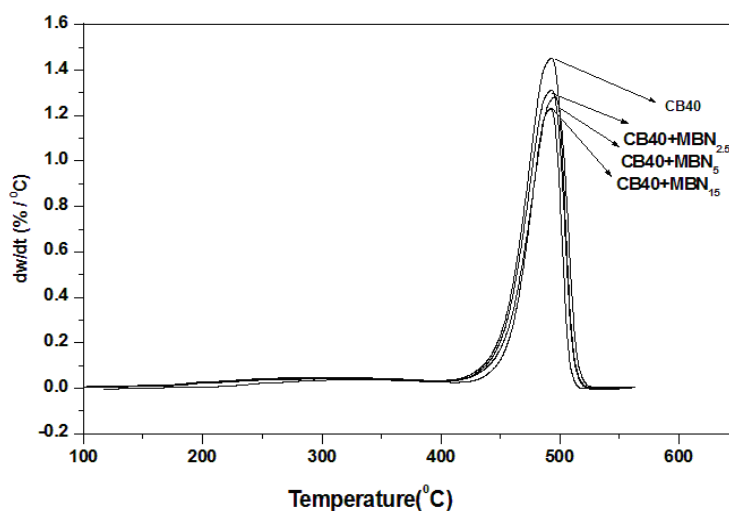


Figure 5.33 DTG traces of EPDM-CB-MBN hybrid RNCs

5b.6 Cross link density and swelling studies

Swelling studies of EPDM-CB-MBN hybrid composites

The solvent sorption studies on the hybrid nanocomposites were done in toluene and the sorption curves are plotted in Fig. 5.34. It is clear from the plots that as the filler loading increased the maximum solvent uptake of gum vulcanizates decreased, the effect being much more pronounced with nano filled rubber samples.

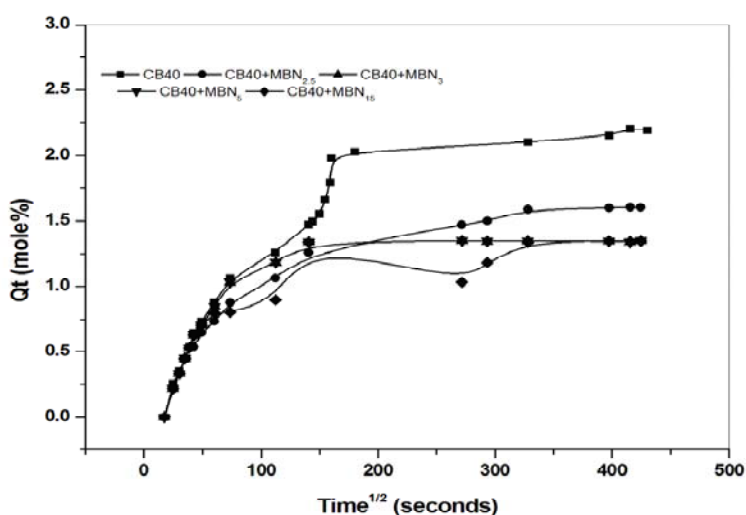


Figure 5.34 Sorption data of EPDM -CB-MBN based hybrid RNCs

The diffusion coefficient, D for the samples are tabulated in Table 5.9. The diffusion coefficient varies dependent on solvent uptake, which shows a maximum for gum vulcanizates as seen in part 1 of this chapter. The changes in permeability and diffusivity of nanocomposites are conventionally explained as an outcome of strong filler-matrix interaction which restricts and limits the diffusion of toluene through entangled matrix-filler networks. The permeation of toluene into a polymer membrane will also depend on sorptivity of penetrant in the membrane. Calculated values of sorption coefficient are given in Table 5.9. The net effect of both the phenomenon accounts for the permeation coefficient and values obtained are as seen in the same table. It is clear from the data that the permeability of nanocomposites decreases with nano content and is dominated by sorption. Moreover, the black filled composites exhibit improvement in strength and mechanical properties whereas, the permeability is not much influenced. This may be attributed to the build up of filler network which leads to increase in filler volume fraction. The incorporation of 40phr carbon black in EPDM reduces the diffusion coefficient by about 35%. A hybrid combination of this composite with even 2.5 phr of MBN improves diffusion resistance to 45%. i.e. the resistance to solvent permeation have been improved dramatically. Better properties are registered at CB40+MBN_{2.5} filler loading, and so did the solvent transport as seen from data below. This effect may be due to the presence of polar filler that enhances dispersion of black fillers through out the matrix forming a dual network; that restricts the flow of non-polar solvent through a non-polar matrix network. Though the solvent transport decreased upto 15 phr, filler agglomerates increased, volume fraction of rubber decreased and hence crosslink density decreased, leading to deterioration of properties. So a balanceable state of composite preparation demands EPDM to be filled with CB40 and 2.5 phr MBN. The mode of solvent transport moved from anomalous to fickian behavior on 5phr loading. As the filler loading increased further, transport mode tend to return back.

Table 5.9 Sorption data of EPDM-CB-MBN hybrid RNCs

Sample code	n	Diffusion coefficient, $D \times 10^{-7} (\text{cm}^2 \text{s}^{-1})$	Sorption Coefficient S	Permeation coefficient, $P \times 10^{-7} (\text{cm}^2 \text{s}^{-1})$	Crosslink density, $\nu \times 10^{-5} (\text{g mol/cc})$
CB40	0.5051	3.32	1.31	4.35	11.00
CB40+MBN _{2.5}	0.5155	2.95	1.24	3.66	12.30
CB40+MBN ₃	0.5128	3.01	1.24	3.74	12.25
CB40+MBN ₅	0.5030	3.05	1.24	3.78	12.08
CB40+MBN ₁₅	0.5449	3.00	1.19	3.57	10.30

Conclusions:

Surface treated barium sulphate proved to be a better candidate in partial replacement of carbon black in EPDM composites. It offered the benefit of minimizing hazardous carbon black, though at minimal levels, with ecofriendly filler. The synergistic effect of nano filler-carbon black dual filler loading on cure characteristics, mechanical properties and transport properties of the EPDM-CB-MBN hybrid RNCs were investigated. Fine dispersion of carbon black particles in the EPDM was partly achieved by mill mixing in the presence of MBN. The variation of cure rate constants (k) and the cure rate index (CRI) values with MBN loading for the EPDM-CB-MBN series registered superior results for a combination of CB40+MBN_{2.5}. The cure activation due to MBN, indicated by the higher CRI value of hybrid composites (compared to CB40) levelled off beyond 3 phr of loading. The filler dispersion analysis proved that α_f (Wolff's approach) increased with MBN loading indicating lower agglomeration in the matrix. These observations are in agreement with those obtained from Lee's approach. From strain sweep studies it was seen that when the nanofiller MBN is incorporated along with carbon black, in the cured state, the complex modulus is superior to that of carbon black alone filled systems. The proper dispersion of carbon black reduced energy consumption during mixing, and

improved mechanical properties of vulcanizates. Even 2.5 phr of MBN in combination with CB40 is enough to impart tensile strength superior to that of 50phr black in EPDM. For composite CB40+MBN_{2.5} the tensile strength marked an increment of 42.2% and 36% when compared to CB 40 and CB50 systems respectively. The dual filler network is far superior in imparting reinforcement, than CB alone filled systems. Elongation increased with filler loading, and was higher than CB40, CB50 systems indicating the lubricating action of modified MBN on EPDM networks, which enable polymer chains in easy slippage. At higher loadings tear strength and hardness improved but all other properties decreased and finally remained constant. When compared to EPDM-CB40, EPDM-CB40-MBN filled hybrid RNCs registered an overall increase of 19% in tear strength. It could be concluded that optimum CB-MBN ratio in EPDM to obtain equivalence with CB50 is CB 40:2.5 MBN. This combination indicates a balanceable state of saturation for the synergistic effect between CB and MBN in reinforcing EPDM. In comparison with EPDM/CB (100/40) the tensile strength, tear strength and abrasion resistance of hybrid RNC's were increased. Abrasion loss of hybrid RNC's decreased on loading of MBN upto 10 phr. Compression set was poor for EPDM hybrid RNCs. Nano filler-carbonblack combination assisted improved dispersion, as revealed by SEM images and the 3-D images of the superior composites. The retention of tensile strength and modulus indicated that the presence of MBN fillers imparted resistance to oven ageing marginally. TGA analysis also supported this fact. These fillers help to maintain the thermal stability of EPDM composites, though a superior resistance is not evidenced. With the incorporation of MBN, weight loss due to the EPDM degradation is still observed, but the relative intensity decreased. The incorporation of nano filler in combination with CB40 shifts the onset of degradation to a marginally higher temperature, though the temperature of maximum degradation remains the same. On comparison with EPDM-CB40, thermal behaviour of EPDM-CB40-MBN composites was slightly improved. With ageing, the tear strength decreased beyond 90% for CB filled composites, but for dual filler networks, the

deterioration was rather slow, indicating better thermal stability. MBN₁₅ composites showed lower rate of degradation than MBN₅ filled hybrid RNCs. To summarize, the rate of maximum degradation decreased from 1.04 to 0.98%/^oC with filler loading and modified nano filled systems in conjunction with CB have excellent thermal resistance. The degradation under inert atmosphere shows that MBN fillers could not improve thermal stability appreciably. Incorporation of 40phr of carbon black in EPDM manifested as reduction in diffusion coefficient by about 35%. A hybrid combination of this composite with even 2.5 phr of MBN improved diffusion resistance to 45%. In short, the composites with MBN 2.5 phr in combination with CB-40 offered better mechanical strength with marginally improved resistance to thermal degradation and toluene transport.

References

- [1]. Malas, C .K. Das; J. Mater. Sci., **2012**,47,2016.
- [2]. A.Botti, W.Pyckhout-Hintzen,D.Richter,V.Urbanand, E.Straube, J. Chem. Phys.,**2006**, 124, 174908.
- [3]. A.P.Meera, S.Said, Y.Grohensand, S.Thomas; J. Phys.Chem.C, **2009**, 113, 17997.
- [4]. J.Carretero-Gonzalez, H.Retsos,R.Verdejo, S.Toki, B. S.Hsiao, E. P.Giannelis, M. A.Lopez-Manchado; Macromolecules,**2008**, 41, 6763.
- [5]. A.Di Gianni, G. Colucci, A. Priola, L.Conzatti, M.Alessiand, P.Stagnaro; Macromol. Mater. Eng.,**2009**, 294, 705.
- [6]. A.Mohammad and, G.P.Simon; Rubber-Clay Nanocomposites, Woodhead Publishing Limited, CRC Press: Cambridge, **2006**.
- [7]. M.Arroyo, M.A. Lopez-Manchado ,B.Herrero;Polymer, **2003**, 44, 2447.
- [8]. P.C.Lebaron and,T.Pinnavaia, J. Chem.Mater., **2001**, 13, 3760.
- [9]. Z.Wangand,T. J. Pinnavaia; Chem. Mater., **1998**, 10, 3769.
- [10]. R.Sengupta, S.Chakraborty, S.Bandyopadhyay, S.Dasgupta, R.Mukhopadhyay, K.Auddyand, A. S. Deuri;Polym. Eng. Sci.,**2007**,47, 1956.
- [11]. G.Ramorino, F.Bignotti, S.Pandini,T.Ricco;Compos.Sci. Technol. **2009**, 69, 1206.
- [12]. M.Pramanik, S. K.Srivastava, B. K Samantaray and A. K.Bhowmick, J.Appl. Polym. Sci., **2003**, 87, 2216.
- [13]. Y.Konishiand, A.Cakmak; Polymer **2006**, 47, 5371.
- [14]. S.Praveen, P. K. Chattopadhyay, P.Albert, V. G.Dalvi, B. C.Chakraborty and S.Chattopadhyay;Compos. Part A: Appl. Sci. Manuf. **2009**, 40, 309.
- [15]. P. K.Chattopadhyay, U.Basuli ,S. Chattopadhyay; Polym.Compos., **2009**, 10.1002/pc.20866.
- [16]. K.C. Etika, L.Liu, L. A. Hess, J. C.Grunlan, Carbon, **2009**, 47, 3128.

- [17]. Q. X. Jia, Y. P. Wu, P. Xiang, X. Ye, Y. Q. Wang, L. Q. Zhang, *Polym. Polym. Compos.*, **2005**, 13, 709.
- [18]. C.M.Koo, S.O. Kim, I.J. Chung; *Macromolecules*, **2003**, 36, 2748.
- [19]. Y.Kojima, A.Usuki, M.Kawasumi, A.Okada, Y.Fukushima, T.Kurauchi, O.J.Kamigaito, *J. Mater. Res.*, **1993**, 8, 1185
- [20]. R.A.Vaia, S.Vasudevan, W.Krawiec, L.Scanlon, G.Lawrence, E.P.Ginnelx; *Adv Mater.*, **1995**, 7, 154
- [21]. J.X Li, J.Wu, C.M. Chan ; *Polymer*, **2000**, 41, 6935.
- [22]. S.Wang, Y.Hu, Z.Wang, T.Yong, Z.Chen, W.Fan; *Polym. Degrad. Stab.*, **2003**, 80, 157.
- [23]. E.P.Giannelis; *Adv. Mater.*, **1996**, 8, 29
- [24]. M.Alexandre and P.Dubois; *Mater. Sci. Eng.*, **2000**, 28, 1.
- [25]. E.P.Giannelis, R.Krishnamoorti, E.Manias; *Adv. Polym.Sci.*, **1999**, 138, 107.
- [26]. S.Praveen, P.K, Chattopadhyay, S.Jayendran, B.C.Chakraborty, S.Chattopadhyay; *Polym. Compos.*, **2010**, 31, 97
- [27]. L.Qu, G.Huang, P.Zhang, Y.Nie, G.Weng, J.Wu; *Polym. Int.*, **2010**, 59, 1397.
- [28]. Y.T.Vu, J.E.Mark, L.H. Pham, M.Engelhardt, *J. Appl. Polym.Sci.*, **2001**, 82, 1391
- [29]. P.Li, L.Yin, G.Song, J.Sun, L.Wang, H.Wang; *Appl. Clay Sci.*, **2008**, 40, 38.
- [30]. P.Schon, S.Dutta, M.Shirazi, J.Noordermeer, G.J.Vancso, *J. Mater.Sci.*, **2011**, 46, 3507.
- [31]. K.C.Guriya, D.K.Tripathy; *Rubber Compos. Process Appl.*, **1995**, 23, 193.
- [32]. H.Tan, A.I.Isayev, *J.Appl. Polym.Sci.*, **2008**, 109, 767.
- [33]. A.L.N. da Silva, M.C.G. Rocha, M.A.R. Moraes, C.A.R. Valente, F.M.B. Coutinho; *Polym .Test.*, **2002**, 21, 57.
- [34]. B.T. Poh, H.Ismail, E.H. Quah, P.L.Chin; *J. Appl. Polym. Sci.*, **2001**, 81, 47.

- [35]. F.S. Deghaidy; Egypt J. Sol., **2000**,23,167.
- [36]. J.B. Donnet;Rubber Chem. Technol., **1998**,71,323.
- [37]. J.D. Wang, Y.F. Zhu, X.W .Zhou, G. Sui, J.Liang;J. Appl. Polym. Sci., **2006**,100,4697.
- [38]. J.L.LebLANC;Prog. Polym. Sci., **2002**,27,627.

.....❧.....

ISOBUTYLENE ISOPRENE RUBBER - BARIUM SULPHATE NANOCOMPOSITES AND EFFECT OF NANOFILLER IN HAF-N330 FILLED IIR-HYBRID NANOCOMPOSITES

6.1 IIR- Barium sulphate nanocomposites

IIR-nano barium sulphate polymer composites (RNCs) using both unmodified and modified barium sulphate (BN, MBN) were prepared by mechanical mixing on a two roll mill. The cure characteristics, mechanical properties, thermal stability and mode of solvent transport through these elastomeric composites were evaluated. The amount of filler was varied from 0 to 15 phr and modified barium sulphate-MBN increased the rate of cure reaction. Another series of carbon black HAF-N330 filled hybrid composites with 50phr carbon black and varied amounts of nano filler MBN were prepared and compared with IIR-CB55 RC's. Thermal aging of IIR-MBN RNCs showed better retention of tensile strength, enhanced tear strength and modulus values at lower elongation at break indicating a synergistic influence of dual filler network to resist thermal aging. Characterization of the hybrid RNCs using AFM showed that there were changes in the morphology of the fracture surface with filler loading. The thermal stability of the RNCs improved with MBN concentration. The swelling studies were conducted on MBN-RNCs to estimate their superior behaviour and mechanism indicated a deviation from Fickian mode. CB systems followed Fickian mode. Overall enhancement resulted with IIR-MBN_{7.5} with 50phr carbon black as far as the swelling resistance and thermal stability were concerned; strength properties were retained similar to the gum series. The superior resistance of CB50 filled hybrid composites on comparison with CB55 to solvent and heat revealed synergistic influence due to formation of dual filler network.

Introduction

Normally, the type and concentration of fillers are found to greatly enhance vulcanisate properties of elastomers. Because of very small particle size, fillers like carbon black greatly enhance the stress-strain property and abrasion resistance. Butyl rubber, but has low affinity to carbon black due to low unsaturation and a maximum tensile strength is obtained only at a loading varied between 50-60 phr. Here tensile strength increases to a maximum value and further on decreases. Butyl rubber, a copolymer of isobutylene and isoprene contains less than 3% isoprene. Vulcanization [1] takes place at isoprene site involving allylic hydrogens i.e., polysulphidic crosslinks are attached at allylic positions. Number of S atom per crosslink is from 1 to 4 and these S-crosslinks have limited stability at elevated temperatures and can rearrange to form new crosslinks and lead to permanent set and creep. Due to steric constraints associated with the methyl group packing the chain dynamics of these elastomers are reduced significantly.

In the past few decades, researchers have been seeking new reinforcing fillers that are environment-friendly, inexpensive and readily available to partially replace CB. The replacement aims at cost reduction, on one hand and on the other synergy of different fillers might be obtained due to the complicated interactions through mixed network formation. These fillers like silica, kaolin, sepiolite etc. are inorganic in nature and hence incompatible with organic polymer matrices. Nano fillers like clays and CNT's have been incorporated into IIR to impart tailored properties like electrical conductivity improved aging resistances and rarely to act as reinforcement to the host matrix. In the present research work IIR which is a typical non-polar rubber with good aging properties and high impermeability to air was used as a base rubber matrix for the preparation of IIR-Barium sulphate nanocomposites. Barytes as well as elastomer-baryte composites are important radiopaque materials and find application as X-ray shields. Acid resistance offered by these materials is also important. Presently, two types

of barium sulphates one, nanofiller BN and other MBN were used for the study. The presence of peptizers like stearic acid has a limited role to play in improving the compatibility between CB and elastomers. The fillers were mixed with the bulk IIR matrix with sulphur as curing agent. The variation in the cure characteristics, morphology, mechanical properties, and thermal stability of the different nanocomposites had been analyzed and compared with each other and also with their respective controls. Swelling of polymer composites in solvents has become a major problem in application of polymer composites exposed to solvents of petroleum fraction and the study aims at handling the problem through nano barium sulphate and their hybrid composites with HAF. The sorption studies were carried out using toluene as solvent in order to assess the mode of solvent transport through these elastomeric composites. These studies were seldom conducted to assess the reinforcing properties of the composites than acid resistance and radiopacity. These properties have been dealt with in Chapter 7 & 8 respectively.

6.1 IIR-Barium sulphate nanocomposites

6.1.1 Preparation of rubber nanocomposites

Nano powders were synthesised via chemosynthetic pathway in presence of PVA (section 3.2.2) and modified using stearic acid (section 3.2.3). The nano barium sulphate powders obtained is hereafter referred to as BN and the modified compound as MBN and the filler loadings are represented as subscripts to this notation. The formulation for the preparation of the RNCs is given in Table 6.1 and that of HAF filled RNCs in Table 6.2.

Table 6.1 Compounding formulation for IIR–MBN/BN RNCs

Compounding ingredient	Phr MBN ₀ /BN ₀	Phr MBN ₁ /BN ₁	Phr MBN _{1.5} /BN _{1.5}	Phr MBN _{2.0} /BN _{2.0}	Phr MBN _{2.5} /BN _{2.5}	Phr MBN ₃ /BN ₃	Phr MBN ₅ /BN ₅	Phr MBN _{7.5} /BN _{7.5}	Phr MBN ₁₀ /BN ₁₀	Phr MBN ₁₅ /BN ₁₅
IIR	100.0	100.0	100.0	100.0	100.0	100.0	100.0	100.0	100.0	100.0
ZnO	4	4	4	4	4	4	4	4	4	4
Stearic acid	1.5	1.5	1.5	1.5	1.5	1.5	1.5	1.5	1.5	1.5
MBN or BN	0 0	1 1	1.5 1.5	2.0 2.0	2.5 2.5	3 3	5 5	7.5 7.5	10 10	15 15
Sulphur	1.5	1.5	1.5	1.5	1.5	1.5	1.5	1.5	1.5	1.5
TMTD	0.75	0.75	0.75	0.75	0.75	0.75	0.75	0.75	0.75	0.75
CBS	1.0	1.0	1.0	1.0	1.0	1.0	1.0	1.0	1.0	1.0

Table 6.2 Compounding formulation for IIR-CB-MBN hybrid RNCs

Compounding ingredient	Phr MBN ₀ /BN ₀	Phr MBN ₁ /BN ₁	Phr MBN ₂ /BN ₂	Phr MBN _{2.5} /BN _{2.5}	Phr MBN ₃ /BN ₃	Phr MBN ₅ /BN ₅	Phr MBN _{7.5} /BN _{7.5}	Phr MBN ₁₀ /BN ₁₀	Phr MBN ₁₅ /BN ₁₅
IIR	100	100	100	100	100	100	100	100	100
ZnO	4	4	4	4	4	4	4	4	4
Stearic acid	1.5	1.5	1.5	1.5	1.5	1.5	1.5	1.5	1.5
MBN	0	1	2	2.5	3	5	7.5	10	15
Sulphur	1.5	1.5	1.5	1.5	1.5	1.5	1.5	1.5	1.5
TMTD	0.75	0.75	0.75	0.75	0.75	0.75	0.75	0.75	0.75
CBS	1.0	1.0	1.0	1.0	1.0	1.0	1.0	1.0	1.0
6PPD	1	1	1	1	1	1	1	1	1
Paraffinic oil	15	13	13	13	13	13	13	15	15
HAF	55	50	50	50	50	50	50	50	50

6.1.2 Cure characteristics

The curing characteristics of all the vulcanizates are summarized in the Table 6.3 and 6.4. Using barium sulphate as filler, the nanocomposites with organically surface treated nano bariumsulphate did not register prominent influence on the cure characteristics.

Table 6.3 Cure characteristics for IIR–BN/-MBN RNCs

Filler loading (phr)	Minimum torque (dNm)		Maximum torque (dNm)		T ₁₀ (minutes)		T ₉₀ (minutes)	
	BN	MBN	BN	MBN	BN	MBN	BN	MBN
Sample code								
0	0.304	0.304	1.66	1.66	1.71	1.71	6.29	6.29
1.0	0.304	0.304	1.68	1.680	1.65	1.75	6.92	6.89
1.5	0.304	0.304	1.68	1.70	1.69	1.89	7.2	6.98
2.0	0.304	0.304	1.70	1.75	1.74	1.94	7.82	7.90
2.5	0.304	0.304	1.82	1.91	1.81	2.02	8.01	8.30
5.0	0.304	0.304	1.85	1.98	1.69	1.80	8.47	8.46
7.5	0.306	0.308	1.89	1.97	1.70	1.64	9.01	7.92
10	0.310	0.313	1.92	2.01	1.72	1.55	9.42	7.54
15	0.315	0.320	1.98	2.12	1.70	2.04	9.64	7.56

Table 6.4 Cure characteristics for IIR-CB-MBN hybrid RNCs

Filler loading (phr)	Minimum torque (dNm)	Maximum torque (dNm)	T ₁₀ (minutes)	T ₉₀ (minutes)
CB55	0.618	5.17	0.76	8.08
CB50	0.592	4.04	0.88	7.72
CB50+MBN _{2.0}	0.608	4.39	0.78	8.01
CB50+MBN _{2.5}	0.608	4.52	0.76	7.92
CB50+MBN _{3.0}	0.608	4.42	0.79	7.85
CB50+MBN _{5.0}	0.610	4.31	0.81	7.74
CB50+MBN _{7.5}	0.612	4.22	0.84	7.61
CB50+MBN ₁₀	0.601	4.16	0.89	7.45
CB50+MBN ₁₅	0.568	4.02	0.91	7.31

In the presence of organo treated nanofiller, both the cure time and scorch time increased with initial filler loading. Beyond a level it decreased, still the cure time was higher than gum. The effect being well registered at a filler

loading of 7.5 phr in the MBN series. This effect is essentially attributed to the carboxylate groups in the barium sulphate nano particles, which came from the organic surface treatment using stearic acid. Fatty acids are generally regarded as indispensable activators in conjunction with zinc oxide [2-4]. They solubilise the zinc oxide and the secondary effect is an increase in the amount of zinc sulphide produced. The zinc salts of fatty acids, which are a type of surfactant, also solublize insoluble accelerators to form the actual catalyst. One of the roles of the activators such as zinc carboxylates is to facilitate the opening of the elemental sulphur ring to form polysulphide ions, which increases the vulcanization rate but has little effect on the vulcanization efficiency. The effect is poor in butyl rubber since its amount of crosslinks is constant for a given set of vulcanization condition[5]. Unmodified nano filler hardly improves the cure characteristics of the rubber, probably due to a poor compatibility between the unmodified BN and hydrophobic polymer. Cure time increased with filler indicating hindrance of accelerator action. The D_{\min} values do not vary much with nano loading suggesting that the processability of the composite is not affected. The maximum torque increased indicating increase in modulus with filler loading.

6.1.3 Mechanical properties of IIR-MBN RNCs and Hybrid RNCs.

6.1.3.1 Mechanical properties of IIR-BN/MBN RNCs.

The tensile strength of butyl RNCs decreased with filler loading because of the poor ability of IIR elastomers to interact with fillers (Fig.6.1). The effect being severe with BN RNCs. But for MBN RNCs it could be seen that, the decrease in strength is marginal. A slight increase or rather a retention of tensile strength compared to gum composites can be observed with 7.5 phr MBN filled IIR's. Barium sulphate is used as extender and categorised as inert and hence is expected to reduce strength of IIR with no doubt. But the trends gave an otherwise result. This is attributed to the weak physical adsorption of MBN fillers on IIR surface via the peptising action of stearic acid coated fillers

during mixing and the cure activation (though minor here) during subsequent curing process. So it could be deduced that butyl rubber can be incorporated with barium sulphate fillers without much compromise of cure properties. A universal diluent barium sulphate can hence stay reinforcing on modification with stearic acid. Elongation at break decreased with loading and 50%, 200% and 300% moduli increased with filler loadings upto 7.5 phr for MBN RNCs (Fig. 6.2 and 6.3).

This indicates filler reinforcement with nano loading and for BN filled systems the trend was similar. Owing to their inertness, even at a filler loading of 5phr, the filler particles visibly showed reluctance to enter the matrix. This was observed as filler clusters in mixed composites on visual observation.

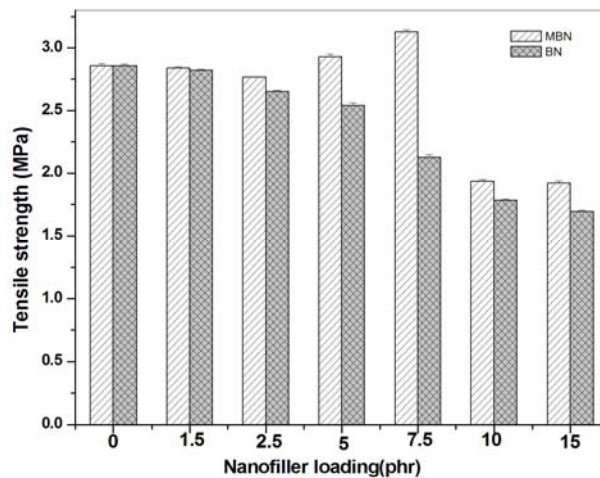


Figure 6.1 Variation of tensile strength with filler loading for IIR-RNCs

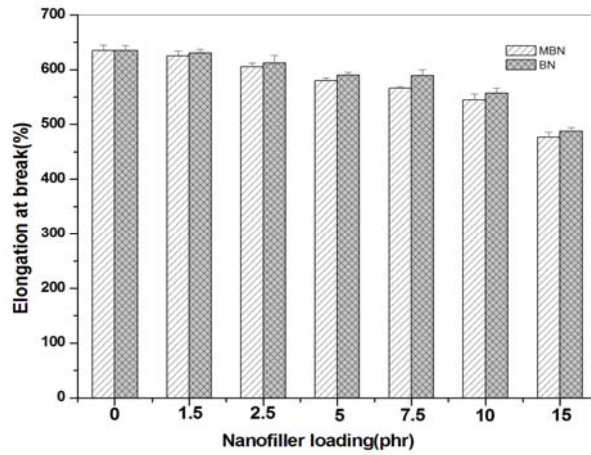


Figure 6.2 Variation of elongation at break with filler loading for IIR-RNCs

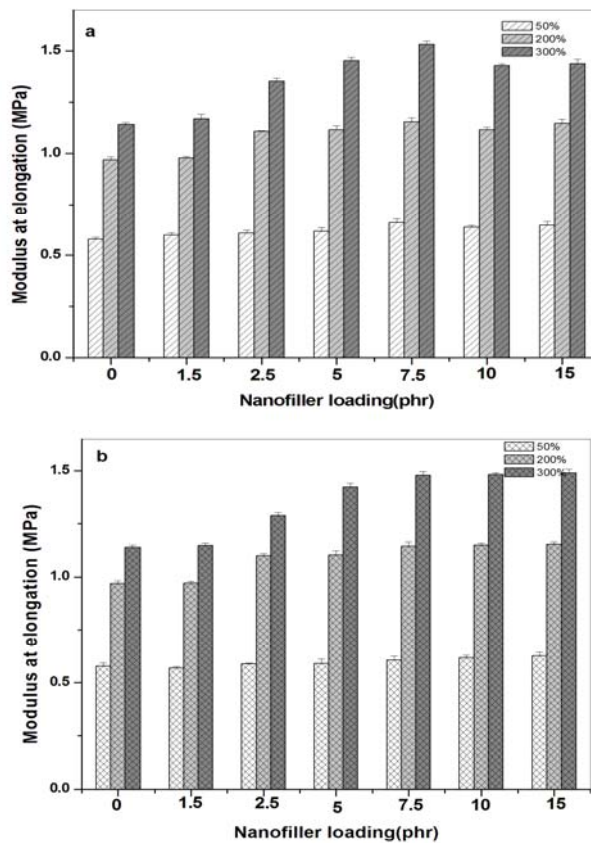


Figure 6.3 Variation of modulus at elongation with loading for a) MBN IIR RNCs, b) BN IIR-RNCs

6.1.3.2 Mechanical properties of IIR-CB-MBN hybrid RNCs.

The influence of hybrid filler systems on the properties of IIR composites is shown in Fig. 6.4 - Fig. 6.8 below. The compression set values decreased with nanofiller loading but the hybrid composites failed to register superior compression set compared to black alone filled IIR-CB composites. As far as the abrasion loss is considered the abrasion loss of hybrid RNCs decreased with increase in MBN loading and abrasion resistance was even better than CB RC's.

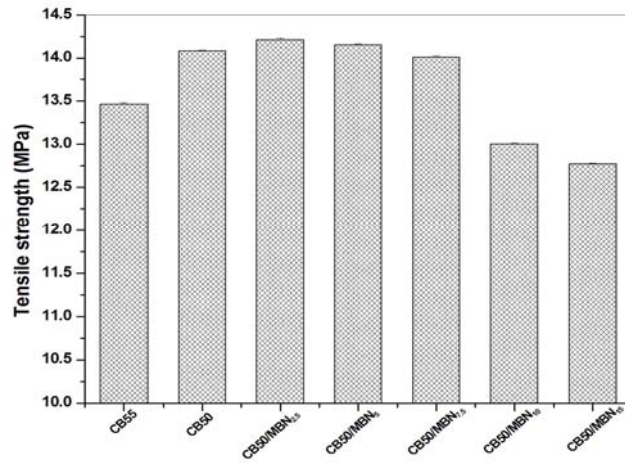


Figure 6.4 Variation of tensile strength with MBN loading in IIR-CB50 hybrid RNCs

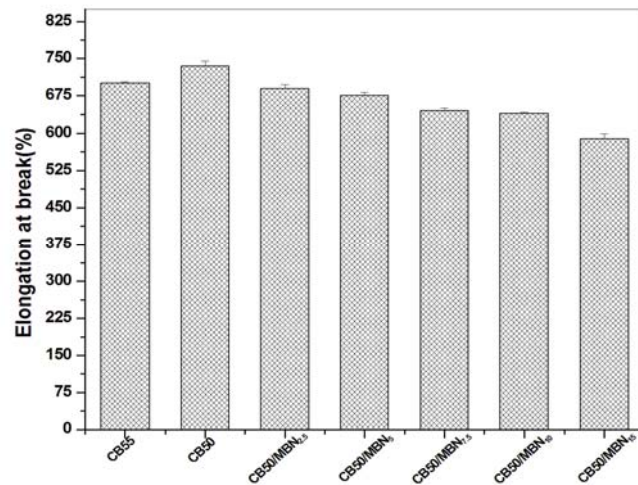


Figure 6.5 Variation of elongation at break with MBN loading in IIR-CB50 hybrid RNCs

The tear strength improved with fillers indicating enhanced obstruction posed by CB-MBN dual filler network on tear cracks initiated in IIR matrix. Hardness values indicated that the MBN filled hybrid RNCs yield comparable values with that of CB alone filled systems.

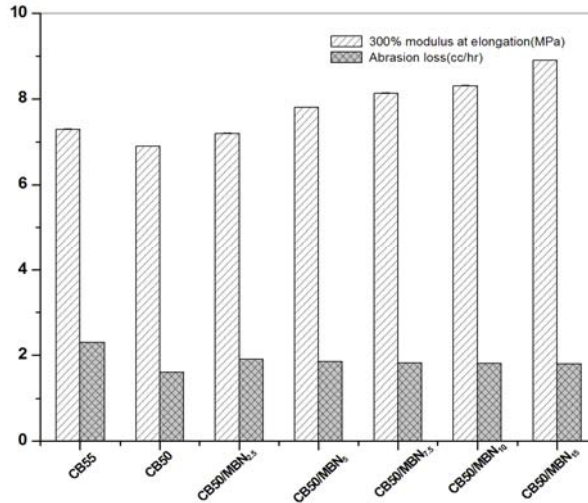


Figure 6.6 Variation of 300% modulus and abrasion loss with MBN loading in IIR-CB50 hybrid RNCs

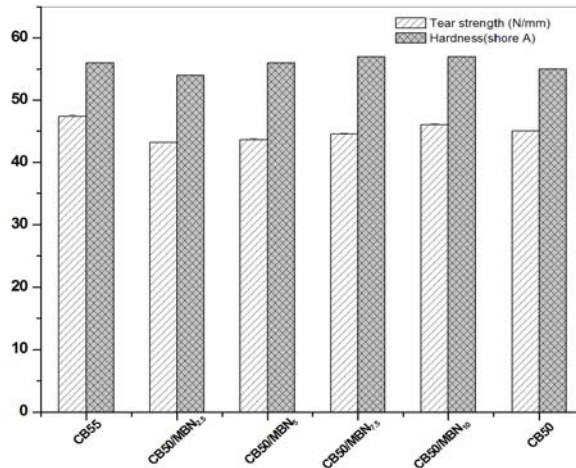


Figure 6.7 Variation of tear strength and hardness with MBN loading in IIR-CB50 hybrid RNCs

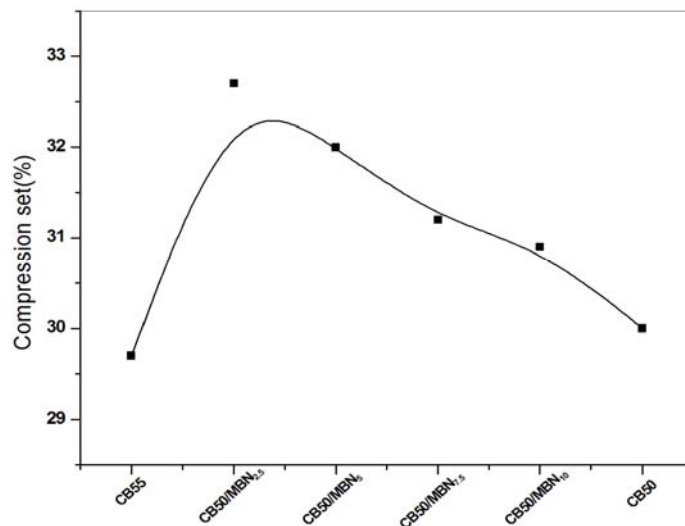


Figure 6.8 Variation of compression set (%) with MBN loading in IIR-CB50 hybrid RNCs

6.1.4 Thermal studies on hybrid systems: Thermal aging and TGA-analysis

The thermal studies were carried out on carbon black filled composites to assess the synergistic effect of MBN fillers in black filled IIR elastomer based composites. Owing to the resistance offered by reinforcement of elastomers by carbon black, the expected stability is high compared to non-black counter parts.

6.1.4.1 Thermal Aging

The retention of properties on thermal aging at 100° C is given in the Table 6.5. The graphical representations of the variation in tensile and tear properties are given in the Fig. 6.9-Fig. 6.11. During thermal aging, cross-link formation or cross-link breakage can take place or an existing cross-link may break and a stable linkage can be formed. It is observed that there is an initial increase in the tensile modulus after 48 hrs of aging at 100° C and after that there is a decline. The increase in modulus is due to the agglomeration of filler particles at higher temperature and due to increased cross links. The rate of crosslink formation depends on stability of composite and this additional crosslinks initially

increases the modulus and strength properties. On accelerated aging it leads to degradation of rubber. IIR has low level of unsaturation and hence is inherently stable to aging. Under the present state of study the composites offer better resistances upto 72hrs of aging at 100°C, with hybrid systems exhibiting superior properties than black alone filled composites. The data indicates the stabilisation of butyl with filler level of 7.5 phr. As far as the nano effect is concerned 95% retention in tensile strength and 80% retention in tear strengths are due to nano filler dispersion at 7.5 phr filled IIR-MBN RNCs, and is superior to CB55 system. The figure gives the exact variations in tensile and tear strengths on aging, where as Table 6.5 summarises data as retention in property compared to their unaged composites discussed previously.

Table 6.5 The retention of properties on thermal aging for IIR-CB-MBN hybrid RNCs

Filler loading (phr)	% retention in tensile strength		% retention in Elongation at break		%retention in 300% modulus	
	48 hrs	72hrs	48 hrs	72hrs	48 hrs	72 hrs
CB55	93	88	73	70	100	102
CB50	92	85	75	72	100	106
CB50+MBN _{2.5}	96	92	82	79	99	103
CB50+MBN ₅	96	94	85	79	98	102
CB50+MBN _{7.5}	96	95	88	80	100	106
CB50+MBN ₁₀	97	94	90	85	100	107

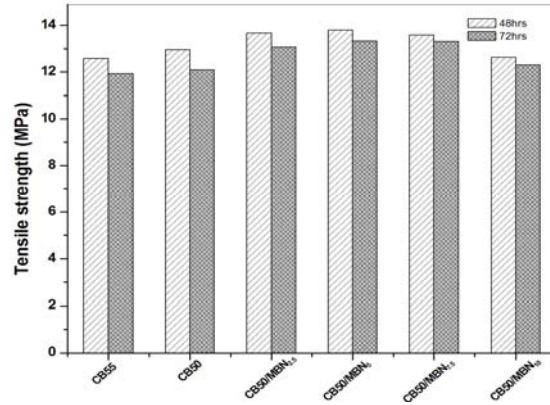


Figure 6.9 Tensile strength of IIR-CB-MBN hybrid RNCs on thermal aging.

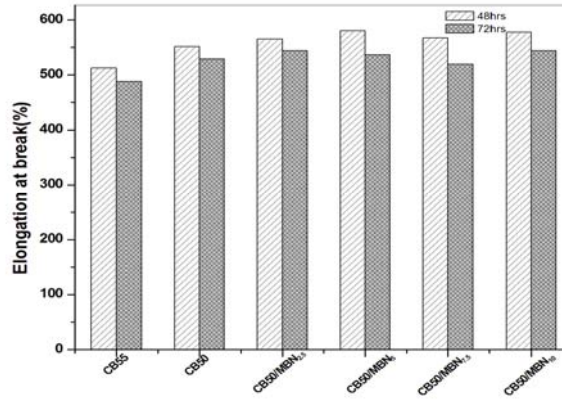


Figure 6.10 The elongation at break (%) of IIR-CB-MBN hybrid RNCs on thermal aging.

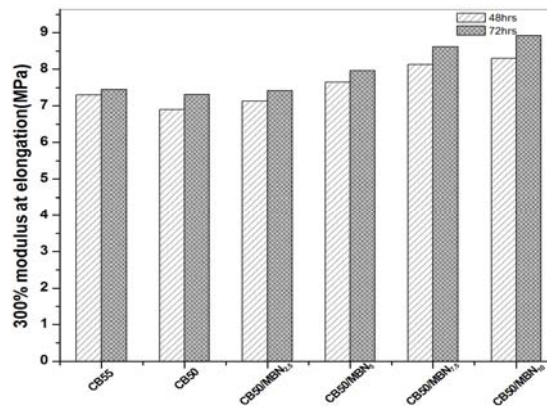


Figure 6.11 The 300% modulus of IIR-CB-MBN hybrid RNCs on thermal aging

6.1.4.2 TGA-analysis of IIR-MBN-CB hybrid nanocomposites

From the previous studies of composites we could conclude that MBN RNCs can exhibit better properties due to filler rubber interaction (marginal as IIR is too poor to be compatible with inorganic fillers) that exists in the composites which BN RNCs lack. So detailed thermal properties of MBN, MBN-CB hybrid RNCs have been carried out and discussed in forthcoming sections.

In the case of MBN filled IIR RNCs, cure rate is accelerated beyond 7.5 phr loading. The reason for the lower cure time (seen in former section) at higher loading is due to the increase in thermal transition of IIR in presence of MBN, which promotes the vulcanization process better than at other loadings. This modified barium sulphate has increased specific surface by surface treatment, which results in improved thermal transition, filler–filler and filler–matrix interactions. Within the composite system, there could be two paths of thermal transition. In one path, heat can pass from MBN-polymer-MBN flakes and in the other path through direct contact between the MBN spheroids. For IIR composites, due to poor filler compatibility both mechanisms are possible with second predominant. The TG curves of the MBN₀ and MBN_{7.5} hybrid rubber nanocomposites and CB50, CB55 series are shown in Fig. 6.12 and that of CB-MBN hybrid RNCs are shown in Fig. 6.13. From the TGA curves of MBN alone and black alone filled system it could be seen clearly that the CB55 system is the stablest at high temperatures. The detailed study (Fig. 6.13 and Table 6.6) of hybrid RNCs revealed that as the nanofiller loading increased and reached upto 7.5 phr the stability increased and on higher loading it was left unchanged. The thermal characteristics as estimated by TGA are presented in Table 6.6. The degradation behaviour of the materials could be clearly read from the Differential thermogravimetry (DTG) curves shown inset in Fig. 6.13. The temperature of onset of degradation (Ti), the temperature at which the rate of decomposition is maximum (Tmax), the peak degradation rate (Rmax) and the

decomposition temperature at 5% weight loss ($T_{-5\%}$) and 50% weight loss ($T_{-50\%}$) are given in Table 6.6. The IIR-CB50 composites gives a single degradation between 400 and 500⁰C and peak maximum at 431.78 ⁰C. With the incorporation of MBN, weight loss due to the IIR degradation is still observed, but the relative intensity decreased. The incorporation of nano filler in combination with 50CB shifts the onset of degradation to a marginally higher temperature, though the temperature of maximum degradation remains the nearly constant. As the nano loading increases a lowering in the rate of degradation is observed. On comparison with IIR-CB50, thermal behaviour of IIR-CB50-MBN composites has been slightly improved. CB50-MBN_{7.5} shows lower rate of degradation than CB55-MBN₀ filled hybrid RNCs. To summarize the rate of maximum degradation decreases from 22.93%/min (1.134%/ °C) of CB55 to 21 %/min (1.096%/ °C) with filler loading upto 7.5 phr and modified nano filled systems in conjunction with CB are having superior thermal stability when compared with CB alone filled systems. The thermal data shows that the temperature of 5% weight loss is lower for carbon black filled systems indicating loss of oil as processing aid from the composite. The maximum degradation and onset of degradation temperatures have increased in the range between 7-14 °C for CB filled composites.

Table 6.6 Thermal degradation data of selected IIR based RNCs and hybrid RNCs

Sample code	Ti(⁰ C)	Tmax (⁰ C)	T _{-5%}	T _{-50%}
MBN ₀	357.2	419.6	331.9	413.2
MBN _{7.5}	357.9	420.4	333.9	415.3
CB50	361.9	431.8	245.9	432.6
CB55	362.4	433.3	247.1	434.0
CB50+MBN ₅	363.0	433.8	248.1	434.2
CB40+MBN _{7.5}	364.3	434.1	249.3	434.9
CB40+MBN ₁₅	364.0	433.9	249.0	435.0

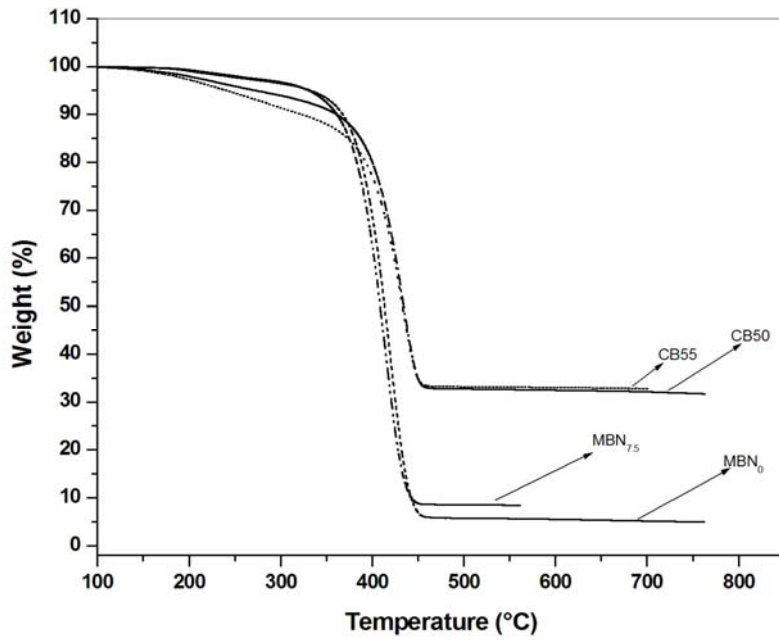


Figure 6.12 TGA traces of IIR-MBN₀&MBN_{7.5} RNC's and IIR-CB₅₀&CB₅₅ composites

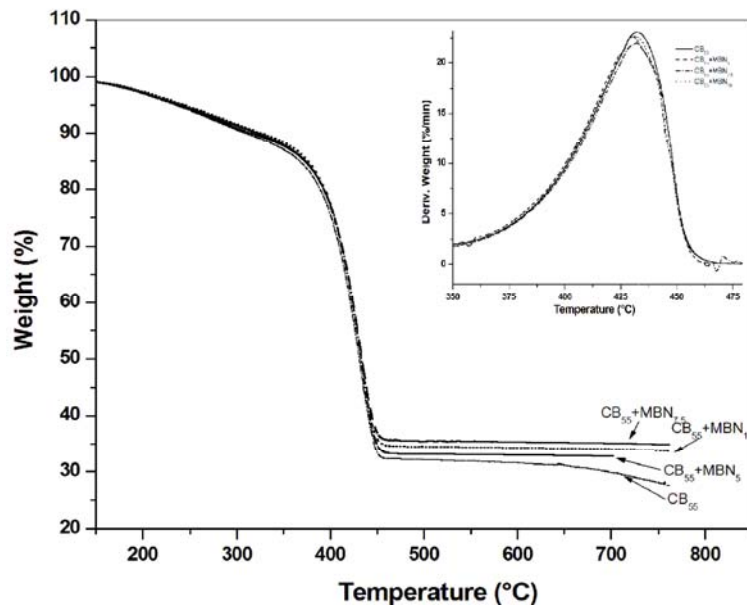


Figure 6.13 TGA traces and DTG (inset) traces of IIR-CB-MBN hybrid RNCs

The improvement of thermo oxidative resistance was attributed to three factors: (1) chemical activities of filler and polymer; (2) strong polymer–filler interactions; (3) uniform dispersion of fillers [5, 6]. CB and MBN are chemically inert and do not react, under the current test conditions. The dense polymer–filler networks hindered the access of degradation to the nanocomposites.

6.1.5 Cross link density and swelling studies of IIR-CB-MBN hybrid composites

The solvent sorption studies on the MBN filled RNCs and that of hybrid nanocomposites were done in toluene and the sorption curves are plotted in Fig.6.14. It is clear from the plots that as the filler loading increased the maximum solvent uptake of gum vulcanizates decreased. The effect being much more pronounced with nano filled rubber samples and enhanced with IIR-CB-MBN hybrid composites owing to the presence of dual network.

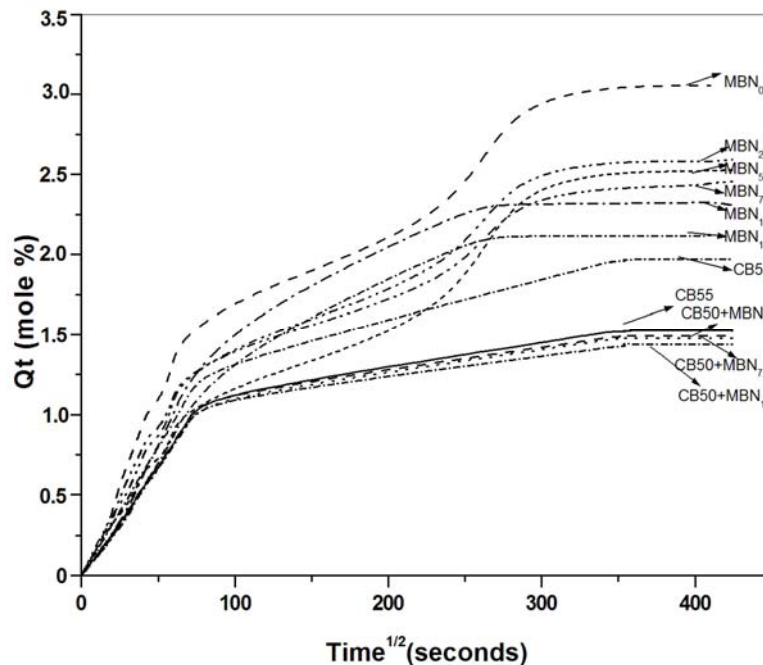


Figure 6.14 Sorption data of IIR-CB-MBN based hybrid RNCs

The diffusion coefficient, D for the samples are tabulated in Table 5.9. The diffusion coefficient varies dependent on solvent uptake, which shows a maximum for gum vulcanizates as seen in figure above. The changes in permeability and diffusivity of nanocomposites are conventionally explained as an outcome of strong filler-matrix interaction which restricts and limits the diffusion of toluene through entangled matrix-filler networks [7]. The permeation of toluene into a polymer membrane will also depend on sorptivity of penetrant in the membrane, the calculated values of sorption coefficient is given in Table 6.7. The net effect of both the phenomenon accounts for the permeation coefficient and values obtained are as seen in the same table. It is clear from the data that the permeability of nanocomposites decreased with nano filler content and was dominated by sorption. Moreover the black filled composites exhibits retention in strength and mechanical properties and a dramatic increment in the permeability. This may be attributed to the build up of filler network which leads to increase in filler volume fraction [8-12]. The incorporation of 55phr of carbon black in IIR reduces the diffusion coefficient by about 25 times. A hybrid combination of this composite with even 2.5 phr of MBN improves diffusion resistance i.e., the resistance to solvent permeation have been improved dramatically. The strength properties are retained at CB50+MBN_{7.5} filler loading, and the solvent transport was tremendously hindered with hybrid combination as seen from data below. This effect may be due to the presence of polar filler that enhances dispersion of carbon black fillers throughout the matrix forming a dual network; that restricts the flow of non-polar solvent through a non-polar matrix network. It could be seen that the solvent transport followed strictly fickian mode in CB and CB-MBN hybrid systems as shown from n value less than 0.5. The results indicated that in hybrid composites, the rate of diffusion of penetrant molecule is much less than the relaxation rate of the IIR polymer chains. Though the solvent transport decreased upto 15phr, filler agglomerates increased, volume fraction of rubber decreased and hence crosslink density decreased, leading to deterioration of propeties. A superior composite preparation demand IIR to be

filled with CB50+MBN_{7.5} to replace CB55 filled composites for applications demanding solvent resistance. The mode of solvent transport approached and remained in Fickian mode on increased MBN loading in the case of hybrid RNCs due to immobilization of rubber chain attributed to strong adsorptive force between rubber and filler [5]. For MBN RNCs, with increase in filler content transport mode started to deviate slightly from Fickian.

Table 6.7 Sorption data of IIR- MBN RNCs and IIR-CB50 hybrid RNCs

Sample code	N	Diffusion coefficient, $D \times 10^{-9} (\text{cm}^2 \text{s}^{-1})$	Sorption Coefficient, S	Permeation coefficient, $P \times 10^{-5} (\text{cm}^2 \text{s}^{-1})$	Crosslink density, $\nu \times 10^{-5} (\text{g mol/cc})$
MBN ₀	0.6908	57.70	2.82	16.30	9.0
MBN _{2.5}	0.5546	39.00	2.38	9.30	11.6
MBN ₅	0.5262	13.30	2.33	3.09	11.6
MBN _{7.5}	0.5170	9.25	2.26	2.09	11.3
MBN ₁₅	0.6100	10.70	2.12	2.28	10.4
CB55	0.3105	2.44	1.40	0.34	14.0
CB50	0.3099	2.22	1.33	0.29	14.9
CB50+MBN _{2.5}	0.3150	2.24	1.37	0.31	13.8
CB50+MBN ₅	0.3078	2.47	1.36	0.34	14.1
CB50+MBN _{7.5}	0.3030	2.75	1.24	0.34	14.5
CB50+MBN ₁₅	0.3149	3.00	1.19	0.36	13.9

6.1.6 Morphology of IIR-MBN-RNCs and IIR-CB-MBN hybrid RNCs

The AFM images of IIR RNCs containing 7.5 phr MBN is shown in figure below, the Fig. 6.15 a and b shows the 2-D and 3-D topographies of MBN 7.5 RNCs, c&d shows AFM images of IIR-CB50 RC's and figure e&f corresponds to that of IIR-CB50+MBN_{7.5}, hybrid RNCs. In first set of figures we could see uneven surface with high polymer fraction as seen from minimum

voids in 3-D topography. When black is filled then void regions increased indicating poor rubber–filler interaction, when hybrid systems are used void regions minimized from the level present in that of black alone filled composites.

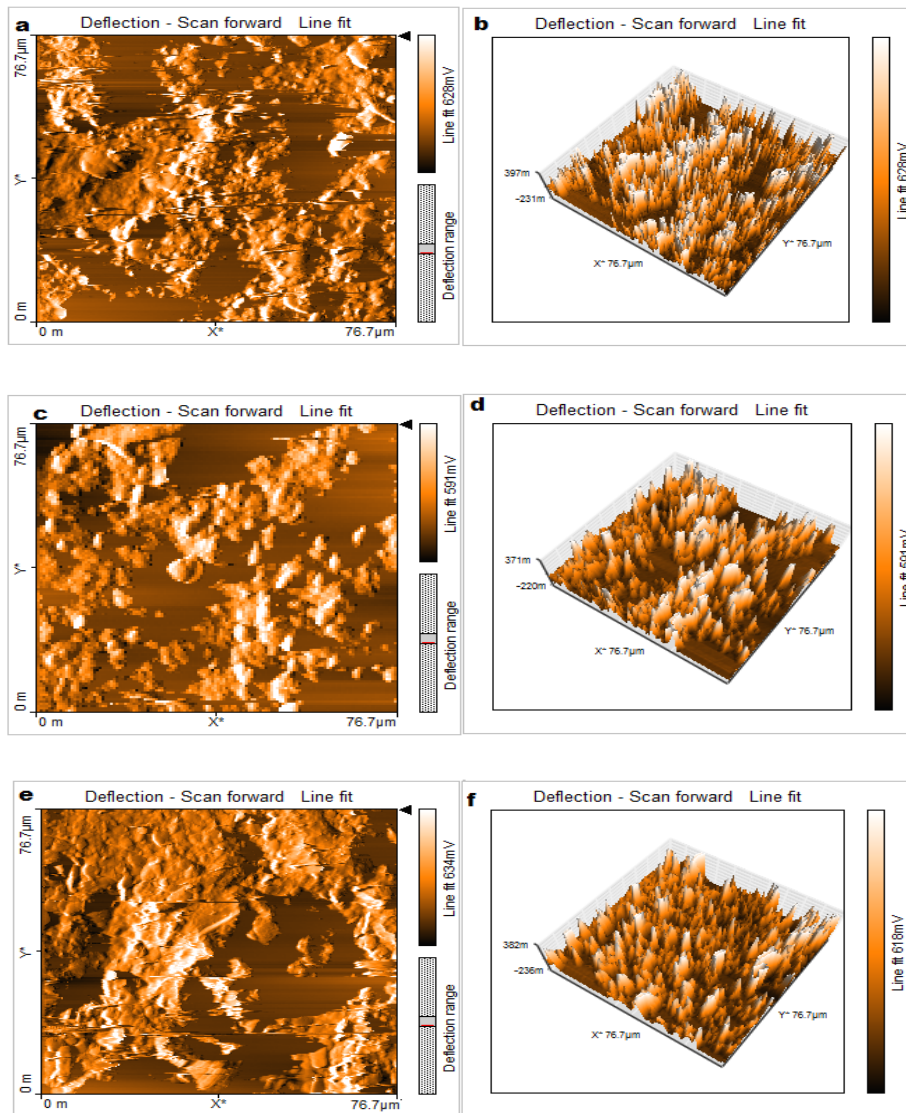


Figure 6.15 AFM images of a&b) IIR-MBN_{7.5} RNC, c&d) IIR-CB50, e&f) IIR-CB50+MBN_{7.5} hybrid RNCs

Conclusions

IIR-nano barium sulphate polymer composites (RNCs) using both unmodified and modified barium sulphate were prepared by mechanical mixing on a two roll mill. The strength properties appeared to remain unaffected by filler loadings and were retained at filler loading upto 7.5 phr. At higher loadings deterioration in property occurred. Thermal aging of IIR-MBN RNCs showed better retention of tensile strength and enhanced tear strength and modulus values at lower elongation at break indicating a synergistic influence of dual filler network. Almost 95% of the strength properties retained after oven aging at 100°C for IIR-CB-MBN RNCs after 72 hours. Characterization of the hybrid RNCs using AFM showed that there were changes in the morphology of the fracture surface with filler loading. The images revealed the non-uniform filler dispersion in IIR, which in turn was reflected in strength properties. The thermal stability of the RNCs improved with MBN concentration. IIR-CB50-MBN_{7.5} system exhibited excellent thermal stability as seen from TGA traces. The hybrid systems improved the maximum degradation temperature and increased the temperature at which degradation of IIR initiated normally. The swelling studies were conducted on MBN-RNCs to estimate their superior behaviour and mechanism indicated a deviation from fickian mode. CB systems followed fickian mode. Overall enhancement resulted with IIR- MBN_{7.5} with 50phr carbon black as far as the swelling resistance and thermal stability were concerned and strength properties were retained as same as that of the gum series. The superior resistance of CB50 filled hybrid MBN composites on comparison with CB55 to solvent and heat revealed synergistic influence due to formation of dual filler networks.

References

- [1]. M .Akiba, A.S. Hashim.;Prog.Polym.Sci., **1997**,22,475.
- [2]. F.W.Barlow; Rubber Compounding: Principles, Materials and Technique, 2nd edition, Marcel Dekker: New York, NY,**1993**.
- [3]. P.J. Fairclough, P.M.Swift;Rubber Developments,**1993**, 4,21.
- [4]. P.J.Wang ; J. Rubber Development., **1994**,47(¾),17.
- [5]. J.D.Wang, Y.F. Zhu, X.W. Zhou, G. Sui, J. Liang;J. Appl.Polym. Sci., 2006, 100, 4697.
- [6]. J.L Leblanc; Prog. Polym. Sci., **2002**,27,627.
- [7]. F.El-Tantawy,N.Dishovsky;J. Appl.Polym.Sci.,**2004**,91,2576.
- [8]. E.B. Spear;Colloid symposium monograph,**1923**,1,321.
- [9]. J.Crank; The mathematics of diffusion., 2nd Ed. Oxford: Clarendon Press, **1975**, 244.
- [10]. L.N.Britton,R .B. Ashman,T. M.Aminabhavi,P.E.Cassidy;J. Chem.Edn., **1988**, 65,368.
- [11]. S. Aprem, K.Joseph, A. P. Mathew,S.Thomas; J. Appl. Polym. Sci., **2000**, 78, 941
- [12]. R. S. Khinnava, and T. M. Aminabhavi;J. Appl. Polym. Sci., **1991**, 42, 2321.

.....❧.....

STUDIES ON SULPHURIC ACID CORROSION OF RUBBER- BARIUM SULPHATE NANOCOMPOSITES*

Section-a: Corrosion of Natural Rubber based RNCs

Section-b: Corrosion of EPDM based RNCs

Section-c: Corrosion of IIR based RNCs

‘Fluid resistance’ as far as rubber industry is concerned, is a term describing the extent to which a rubber product retains its original physical characteristics and ability to perform its barrier performances when exposed to oil, chemicals, water, organic fluids or any liquid which it is likely to encounter in actual service. Fluid resistance ‘tests’ rarely offer a direct correlation with actual service conditions, but still can quantify and provide a caution note regarding do’s and don’ts an anti-corrosive rubber design selector should keep in mind. In this chapter an attempt has been made to study the corrosion of NR, EPDM and IIR filled with commercial and nano barium sulphate and its combinations with HAF, in sulphuric acid of varied concentrations and the variations in strength properties are analysed and conclusions reached through three sections of studies.

* **Nisha Nandakumar**, Philip Kurian, “Effect of Chemical degradation on the Mechanical properties of Ethylene-propylene-diene (5-ethylidene-2-norbornene) terpolymer-BaSO₄ Nanocomposites” *Materials & Design*, **2013**, 43, 118.

* **A part of this work have been presented at:**

1. NishaNandakmar, PhilipKurian; National Seminar on Emerging trends In Nanotechnology, B.K.College for Women, Amalagiri, Kottayam-Sep. **2011**.
2. NishaNandakmar, PhilipKurian; International conference on Advances in Polymer Technology, Cochin University of Science and Technology, Kerala-Feb.**2010**.
3. NishaNandakumar, PhilipKurian; Advancements in Polymeric Materials, CIPET Bhubaneswar-Feb.**2010**.

Introduction

Prior to 1929, the rubber industry was hitherto engaged in technology development from eraser to tyre industry. With the advent of chemical industry more and more chemicals and corrosive substances came into use and hence the need for long lasting methods of protecting mild steel and concrete storage tanks, process vessels, mixers, reactors, agitators, pipelines, railroad tankers, ship tankers, etc. against corrosion became indispensable and the use of elastomers as construction material began to be recognized universally [1]. Rubber has wide latitude of properties gained by compounding and has ease of molding or being formed into any shape. In the pristine form, its strength, its bondability to metal substrates, its deformability, its resistance to attack by corrosive chemicals, its resistance to abrasion, its good electrical properties are noteworthy [2].

Rubber linings are passive fortification against corrosion of plant and equipment in chemical process industries. Apart from that, numerous applications demands the usage of rubber for flexible parts of significant machineries and structures like fuel cells in which a rubber portion of EPDM, acts as a membrane or anti corrosion coating. In these areas of applications, rubber acts as a sacrificial material reacting or unreacting with the corrosive media, diffusing the liquids or not diffusing, swelling by itself or not swelling, abrading or wearing by the particles, getting ozonised or oxidised: but still protecting the metal infrastructure beneath it, during its service under stressed environment. It is to be noted that there is no alternative material challenging the qualities of natural or synthetic rubbers for chemical resistance applications. The majority of rubber linings used has to withstand service conditions handling fertilizers and corrosive acids. The major component of most of these fertilizers is sulphuric acid. It is one of the most important products of the heavy chemical industry. Chamber acid and tower acid were the two concentrations of sulphuric acid produced by the lead chamber process, chamber acid being the acid produced in lead chamber itself (<70%) and tower acid being the acid recovered

from the bottom of the Glover tower[3,4]. The tower shell involved in sulphuric acid manufacture is generally carbon steel and a rubber lining is used to prevent the weak acid from attacking the carbon steel shell.

Most of the chamber acid is used in the production of mineral fertilizers. Sulphuric acid is used in the production of, for example, phosphoric, hydrochloric, boric, and hydrofluoric acids because of its ability to displace these acids from their salts. The service conditions demanding resistance to this acid is highly frequent and hence it is necessary to trace the behavior of rubber, if used as lining in this acid [5]. The present chapter deals with the study on the effect of acidic environment on the properties of elastomers selected NR, EPDM and IIR in general and in filled forms; and to monitor the role of nano BaSO₄ and carbon black on influencing the acid sorption and corrosion brought about. Barium sulphate, which is commonly referred to as barite, is used widely because of its high specific gravity, opaqueness to x-rays, inertness and whiteness [6]. Barite is one of the most important fillers used in the plastics, rubber and paint industries, and is also used in pharmaceutical formulations. It is found from literature that it has an ability to impart chemical resistance to the matrices in which it is filled. Investigations look forward to the action of nano barium sulphate in restricting corrosion and imparting resistances to various concentrations of sulphuric acid in their elastomer composites.

Section-a

**CORROSION OF NATURAL RUBBER BASED RNCs:
NATURAL RUBBER BARIUM SULPHATE COMPOSITES AND THEIR CORROSION IN
SULPHURIC ACID**

The aging of rubber products depends upon the environmental conditions during service and one reason for failure in many applications is with no doubt, chemical corrosion. In continuous process industry, machinery replacement is hard to achieve and the equipment life sustenance becomes vital. Even a weak solution of sulphuric acid can corrode a two-inch wall of steel in just 8 months as reported from literature. If direct contact of acid with metal can be avoided through a protective, acid resistant lining; the life of that equipment can be increased to a great extent. Though elastomeric lining is not the last word to cope with all corrosive and abrasive conditions, it can ensure a good role to play within. Natural rubber (NR) is known to exhibit numerous outstanding properties, and reinforcing fillers are unavoidably added into it in majority of the cases in order to gain the appropriate properties for specific applications. Incorporation of nano-particulates to a polymer matrix can enhance its performance, often to a dramatic degree, at the cost of two factors, the nature and the properties of the nanoscale filler [7]. This strategy yields high performance composites, when good dispersion of the filler is achieved and the properties of the nanoscale fillers are substantially different or better than those of the matrix [8, 9]. The enhanced properties of high performance nanocomposites may be mainly due to the high aspect ratio and/or the high surface area of the fillers [10], when good dispersion is achieved [11].

In this section, an investigation regarding the damage caused by acid to natural rubber containing barium sulphate and barium sulphate/carbon black - hybrid combination is done. Measurements of tensile strength and tear strength and crosslink densities have been made in order to quantitatively estimate the

extent of degradation at various stages of acid attack. The fracture surfaces of failed tensile and tear specimens have been investigated by means of SEM, both before and after acid aging and attempts have been made to correlate the changes in the surface topography with the extent of fall in mechanical properties as a result of acid corrosion. The weight changes associated with acid sorption was studied with rubber samples and metal inserts by immersion method.

7a.1 Natural rubber based composites

7a.1.1 Preparation of NR based composites

The NR based composites were prepared as described in sections 4.1.1 and 4.2.1. The compounding recipes used are given in the Table 4.1.

7a.1.2 Mechanical properties: Effect of acid concentration

Sulphuric acid causes deterioration of natural rubber vulcanizates through oxidation and digestion leading to pits and craters in the vulcanizates. Rate of degradation increased with acid concentration, and the time taken by the rubber matrix to disintegrate decreased. The effect of 0%, 25%, 50% and 75% acids were traced on unfilled rubber vulcanizates (BN_0) and the tensile strength was recorded following the acid aging up to 150 hours. From Fig. 7.1 it is seen that the vulcanizates completely degraded in 75% acid within a short span of 5 hrs, while 25% acid caused negligible degradation even after 150 hrs. In 25% acid concentration, tensile strength decreased by 18% indicating the low degradation rate at this concentration. When treated with 50% acid the tensile properties reduced to half its initial value, within 150 hrs. The analysis of this behavior and its influence on mechanical property demands the selection of one particular acid concentration for subsequent studies. So 50% acid was selected to measure the corrosion resistance of NR- filled and unfilled composites- in a laboratory scale within a short span of investigation.

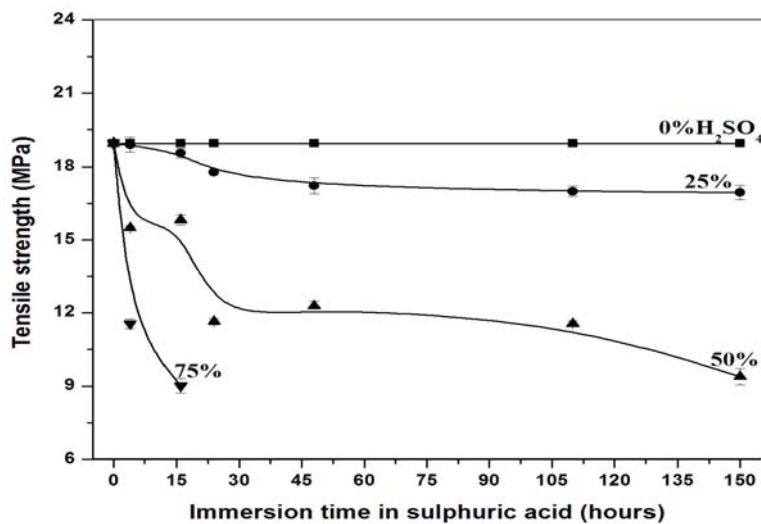


Figure 7.1 Effect of acid on mechanical properties of unfilled natural rubber vulcanizates

7a.1.3 Swelling test

Chemical reaction of rubber lining with the corrosive chemicals and acids causes deterioration, resulting in progressive damage to the lining unless the reaction is not allowed to continue further. Chemical resistant nature of rubber compounds can generally be obtained from change that rubber undergoes after immersion in liquids of varied concentrations. During immersion in a given liquid the surface layer of the rubber is attacked in the initial stages. The action of corrosive liquids such as acids, alkalis basically involves absorption, diffusion, permeation, extraction and chemical reaction. The absorption leads to swelling and increase in weight. Diffusion leads to percolation through pores. Permeation leads to leakage of fumes and gases. Extraction leads to reduction in weight. Chemical reaction either adds to the weight or degrades rubber depending upon the intensity and vigor of the reaction and also the conditions to which the reaction product is exposed. The leaching or extraction of certain chemical ingredients, especially the antioxidising agent from rubber has a significant role on useful life of lining. The international standard for immersion testing of rubber deal with change in weight of rubber samples when they are

immersed in corrosive liquids. The testing was carried out at 25° C and duration of the test according to specification BS ISO 1817(British) Rubber, vulcanized-Determination of effect of liquids, vary as follows: 24hrs, 48hrs, 96hrs, 168hrs and 30 days(Section 2.3.13.1).

The immersion test was carried out in the absence of direct sunlight at 25° C in order to avoid atmospheric oxidation and the volume of immersion solution was adequate to immerse the sample of rubber. The test pieces were buffed smooth after die cut from rubber lining. The changes in volume as well as weight of the test piece specimen after immersion, with respect to time were recorded. The test chemicals and reagents used in immersion test and the nature of attacks are given in Table 7.1.

Table 7.1 Modes of corrosion in aqueous sulphuric acid

Immersion test and the nature of attacks			
Name of chemicals present in medium	Nature	Density	Main type of attack on rubber
Water	Neutral	1.0	Diffusion
Sulphuric acid	Acidic	1.84	Diffusion

The samples for swelling in acid solution were die cut into round samples having 3 mm thickness and 20 mm diameter and were kept immersed in glass apparatus as shown in Fig. 7.2.

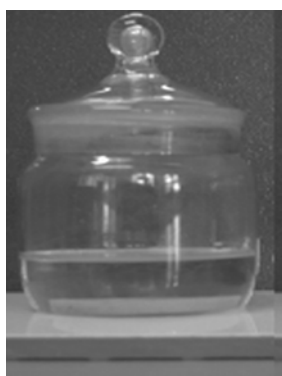


Figure 7.2 Immersion test in diffusion bottles

The samples were dipped in 0%, 25%, 50%, sulphuric acid solutions and weighed at regular time periods as per the specification demands. The surface acid was removed using Millipore de-ionized water. Weight increments were noted on an electronic balance and the corresponding remarks are summarized in Table 7.2.

Table 7.2 Immersion test results for natural rubber compounds

Sample name	Concentration of sulphuric acid used		Variation of weight % Over 28days	Grade
BN ₀	1	0	0.0	A
	2	25	1.98	B
	3	50	2.99	C
BN ₁	1	0	0.0	A
	2	25	1.98	B
	3	50	2.59	B
BN ₂	1	0	0.0	A
	2	25	1.00	A
	3	50	1.69	B
BN ₅	1	0	0.0	A
	2	25	0.90	A
	3	50	1.11	B
BN ₁₀	1	0	0.0	A
	2	25	1.34	B
	3	50	1.47	B
BN ₂₅	1	0	0.0	A
	2	25	1.30	B
	3	50	1.11	B
BN ₅₀	1	0	0.0	A
	2	25	0.0	A
	3	50	0.50	A
MBN ₁	1	0	0.0	A
	2	25	1.24	B
	3	50	1.98	B
MBN ₂	1	0	0.0	A
	2	25	0.90	A
	3	50	1.05	B
MBN ₅	1	0	0.0	A
	2	25	0.40	A

	3	50	0.78	A
MBN ₁₀	1	0	0.0	A
	2	25	0.0	A
	3	50	1.01	B
MBN ₁₅	1	0	0.0	A
	2	25	0.0	A
	3	50	0.36	A
MBN ₂₅	1	0	0.0	A
	2	25	0.0	A
	3	50	0.22	A
MBN ₅₀	1	0	0.0	A
	2	25	0.0	A
	3	50	0.25	A
CB30	1	0	0.0	A
	2	25	1.88	B
	3	50	3.10	C
CB30+MBN ₂	1	0	0.0	A
	2	25	0.83	A
	3	50	1.96	B
CB30+MBN ₅	1	0	0.0	A
	2	25	0.80	A
	3	50	1.62	B
CB30+MBN ₁₀	1	0	0.0	A
	2	25	0.68	A
	3	50	2.38	B
CB30+MBN ₁₅	1	0	0.0	A
	2	25	0.55	A
	3	50	1.51	B
CB30+MBN ₂₅	1	0	0.0	A
	2	25	1.70	B
	3	50	2.15	B
CB30+MBN ₅₀	1	0	0.0	A
	2	25	0.0	A
	3	50	0.12	A
CB40	1	0	0.0	A
	2	25	2.66	A
	3	50	3.60	C
C50	1	0	0.0	A
	2	25	0.0	A
	3	50	1.20	B

The compounds MBN₅, MBN₁₅, MBN₂₅, MBN₅₀, BN₅₀, C₅ and CB30+MBN₅₀ in 50% H₂SO₄ were graded 'A' under the analysis and the compound is eminently suitable to fit as lining for 50% sulphuric acid, the other compounds graded as 'B' can also reasonably be used but the carbon black filled composites with grade 'C' need to be used with brick lining to prevent corrosion of surface beneath it (ref. section 2.3.13.1).

7a.1.4 Retention of tensile and tear strength after acid immersion.

The mechanical properties of the mixes have been evaluated in Chapter 4 and SEM pictures are illustrated here to account for the extent of aging. The entire series used 50% dilute sulphuric acid as the immersion medium.

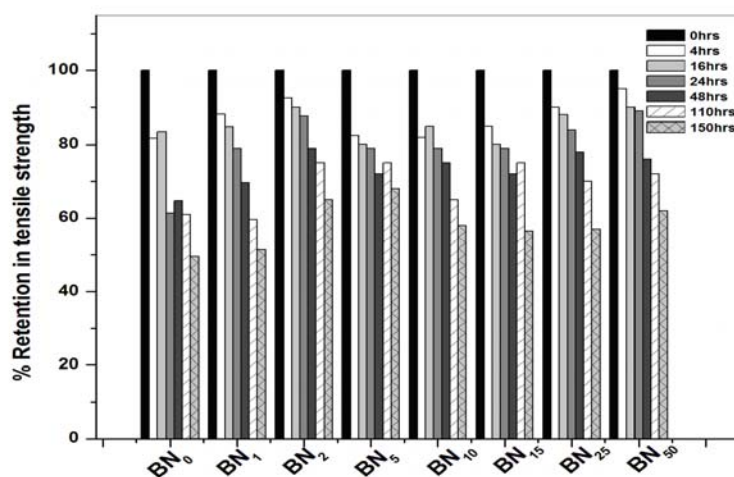


Figure 7.3a Percentage retention in tensile strength on acid aging- for BN filled RNCs upto 150hrs.

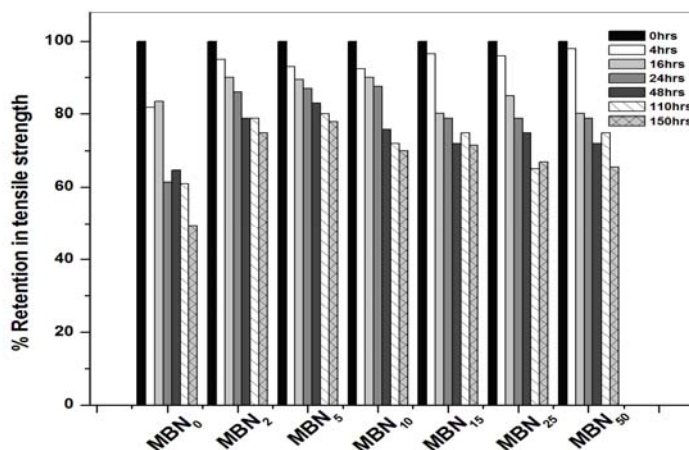


Figure 7.3b Percentage retention in tensile strength on acid aging - for MBN filled RNCs upto 150 hrs

On comparing the tensile property retention of BN, MBN and commercial BaSO₄ filled systems, it could be seen that the more stable systems are those RNCs filled with MBN, and nano filled systems excelled the heavily loaded commercial filled systems even at lower loading. The percentage retention in tensile strength of the natural rubber barium sulphate filled RNCs and their hybrid combinations with carbon black revealed a number of interesting facts. The behavior of various composites i.e., BN, MBN, CB+MBN filled composites and their comparison plots are shown in figure 7.3.a.b.c.d respectively. It could be seen from the graphs that as the nano loading increased, the stability against acid corrosion or, say retention of tensile strength was high, compared to that of the unfilled composites. After 150 hrs only 44% of the strength of unfilled composites were retained in 50% acid solution, whereas 58-63% of the strength of BN- RNCs retained after 150 hrs. Moreover at higher loadings the effect was not much pronounced and retention reached a saturation point beyond 15 phr and all the nano filled systems showed better retention on acid corrosion which rated around 60% in almost all the filled systems.

The tensile and tear properties on acid immersion exhibited more or less same trend for all the three sets, and the MBN RNCs turned out to be better choice for acid resistant material. For the MBN filled RNCs it could be seen that the retention

in tensile strength is above 65% for MBN₅- RNC and as the loading increased the retention in strength remained more or less constant and the fact is, 5 phr nano could provide property retention equivalent to 50 phr loading in both the cases. Another important fact is that the investigation of remaining immersion liquid showed that at nano level loading the solution clarity was maintained even after 150 hrs in MBN filled systems indicating the uniform dispersion and strong rubber-filler bonds. In 50 phr loaded composite the colour of solution started to turn reddish, indicating presence of filler leach outs, showing the presence of filler portion that failed to wet the composite and hence loosely adsorbed to it.

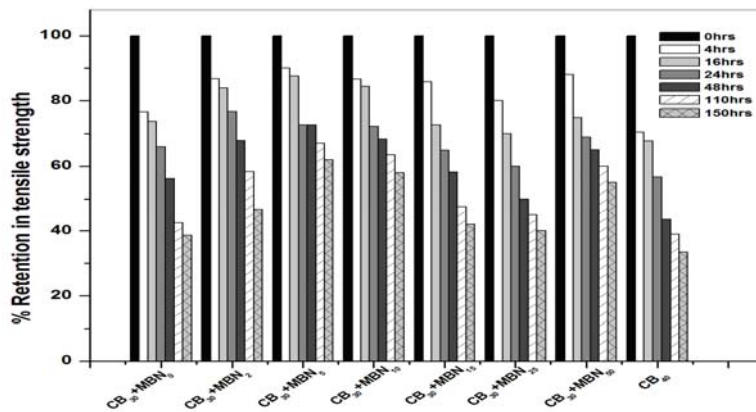


Figure 7.3c Percentage retention in tensile strength on acid aging for CB+MBN filled RNCs upto 150 hrs

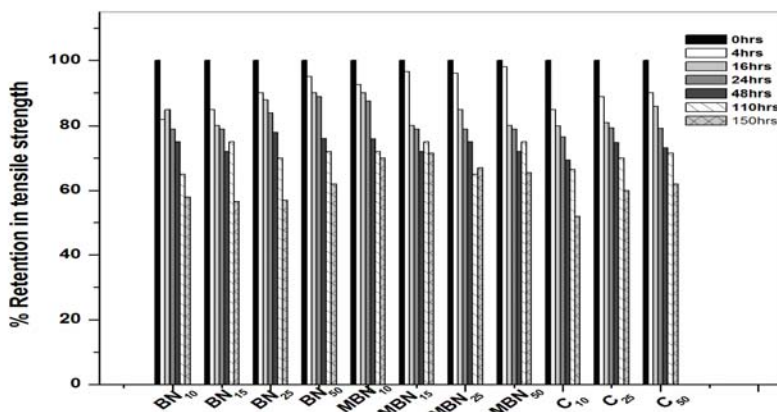


Figure 7.3d Percentage retention in tensile strength on acid aging upto 150 hrs: comparison plot of all the fillers with commercial BaSO₄

On investigating corrosion in hybrid nanocomposites it could be seen that black filled composites are poor candidates to fit severe acid environments as can be seen from nearly 65% degradation of tensile strength in CB40 system. The tear strength retention exhibited similar trends and the studies also revealed that the hybrid combination of black with nano barium sulphate at 5phr or above strengthens the compound to resist corrosion on acid immersion and retains around 60% of its strength (Fig. 7.4a-7.4d). The drawback of all these systems from industrial aspect is the colouration of immersion system indicating leaching of compounded fillers during acid attack (fraction of fillers which failed to form strong bonds with matrix polymer).

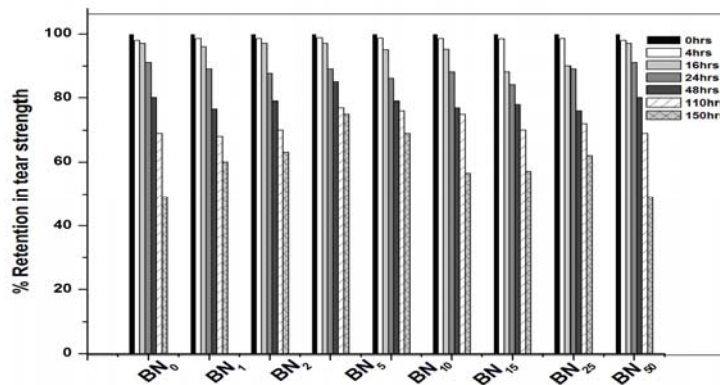


Figure 7.4a Percentage retention in tear strength on acid aging for BN filled RNCs upto 150 hrs

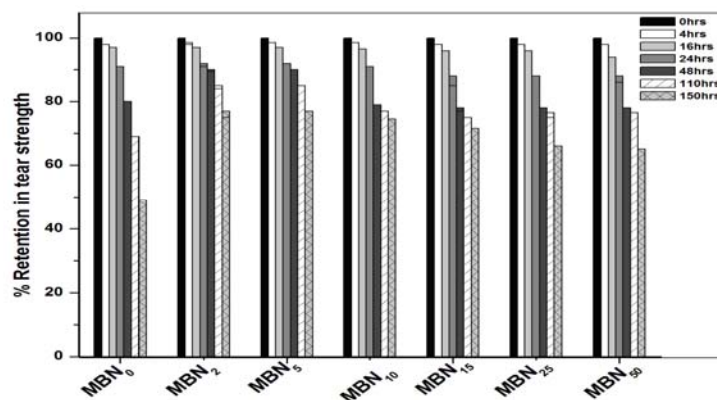


Figure 7.4b Percentage retention in tear strength on acid aging for MBN filled RNCs upto 150 hrs

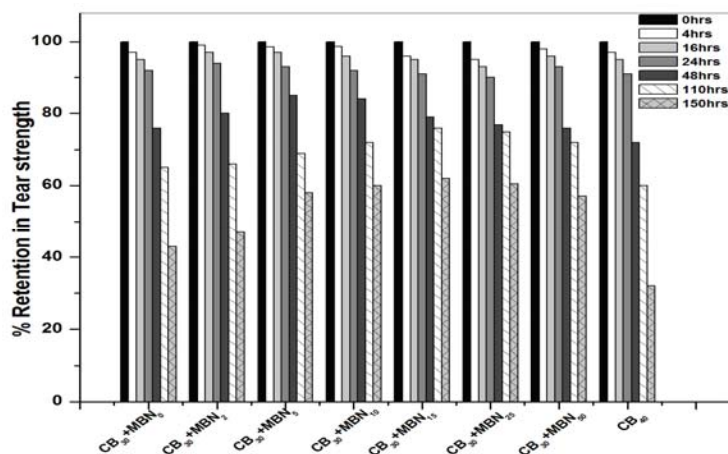


Figure 7.4c Percentage retention in tear strength on acid aging for CB+MBN filled RNCs upto 150 hrs

7a.1.5 Tests for acid resistance using rubber sheets adhered to Mild steel samples

Rubber covered metal strips (metal inserts of mild steel) were made for studying the acid resistance of these selected rubber samples by bonding natural rubber to mild steel (MS) sheets using chemlok 205 as primer and adhesive chemlok 220 as cover coat and cured at 150 °C. The samples were prepared accordingly (ref. section 2.3.13). The rubber covered MS samples of 5cm x 5cm were kept immersed in 50% acid solution and the percentage weight is not considered alone but it is combined with the area of the sample as well as the number of days of immersion (of 12, 40, 80 days) are recorded and referred to as 'g'. The days are recorded as 'D'. The surface areas of the samples are noted before commencing the test and this is referred to as m². From the data collected a graph is plotted with g/m² vs D.

For a good quality rubber lining compound to be used the curve should be as near to the x-axis as possible, i.e., it should have a low slope. Similarly, for the same quality of rubber lining the curve will exhibit a rise in the beginning but later on, it should fall off rapidly. These were proposed by Andritz-Ruthner

company and it can be noted here that Ruthner has not specified any references but only comparative data can be obtained for a given series of rubbers.

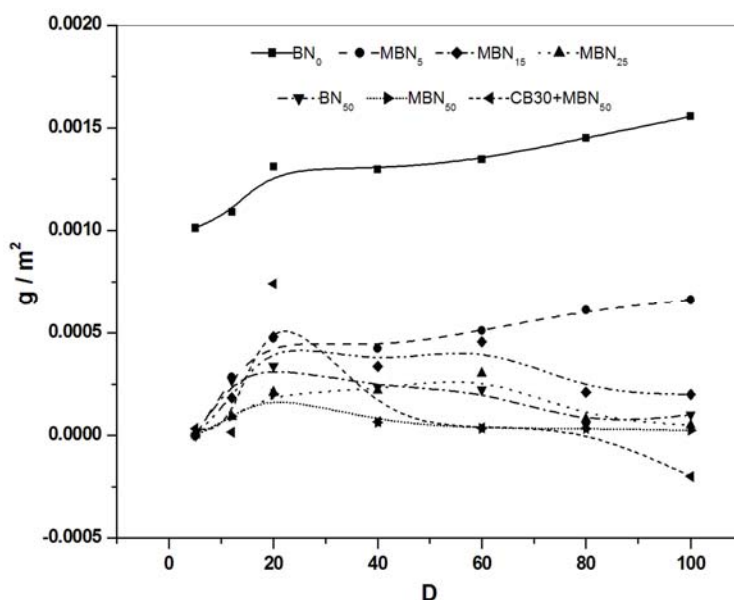


Figure 7.5 Plots for acid resistance of various MS inserts covered by natural rubber composites- MBN₅, MBN₁₅, MBN₂₅, MBN₅₀, BN₅₀ and CB30+MBN₅₀ in 50% H₂SO₄

These plots (Fig. 7.5) for all the composites MBN₅, MBN₁₅, MBN₂₅, MBN₅₀, BN₅₀, CB30+MBN₅₀ (that were graded ‘A’ by previous analysis) revealed were very interesting, the unfilled rubber covered MS specimens showed an increase in g/m² as the number of days increased, and showed no signs of approaching the vicinity of x-axis. This indicated that the compound is unsuitable for rendering protection from 50% sulphuric acid to MS specimens. In the case of modified barium sulphate samples, it could be seen that as filler loading increased the curves which started from a lower point of the graph rose initially and as days passed it started sloping downward approaching x-axis indicating more stabilization in acidic environment. Same is the case with BN-RNCs but resistance offered is lower than that of MBN’s. The carbon black filled systems showed an increase in weight percent indicating absorption of

acid during initial period. This was followed by sudden drop leading to negative values. This indicated that the lose in weight of rubber samples is due to corrosion and it is supported by the red colouration of acid used for immersion over the 100 days of immersion test. All the non-black composites left acid without discolouration and the weight change normalized over 40 days to 100 days of immersion test. These plots confirm that MBN is better in arresting acid percolation through NR composites when compared to their black filled counter parts and BN composites.

7a.1.6 Interpretation of acid corrosion in terms of surface relief features of RNCs as observed in a SEM

The mechanical properties as revealed in Chapter 4 part a & b, showed that MBN filled systems had better properties compared to unmodified nano filler i.e., BN filled systems and the CB30+MBN₅ system also exhibited synergistic effect of hybrid fillers. The study on percent retention of tensile properties again indicated the superior properties and synergistic effect in MBN filled vulcanizates. The explanations to the facts mentioned in the former section are confirmed with SEM photographs and the novel surface features appearing over specimens as a result of corrosion. The retention in tensile property studied, revealed that, MBN₅ system is showing better retention and the hybrid system exhibited lower but superior behavior when compared to black alone filled systems. As seen from the Fig. 7.6, SEM fractograph of unfilled-unaged vulcanizate indicates the presence of randomly oriented tear lines. The bright regions on the fracture surface are characteristics of a strain crystallized matrix undergoing rupture at high strains [12]. Once the sample is aged, there is a considerable drop in strength properties and SEM image has reduced tear lines and an image of the same sample at higher magnification as shown in Fig. 7.6c shows that, acid corrosion creates vacuoles and these relief features act as crack propagators and increases the ease of rupture, which supports the reason for reduced tear lines in image 7.6b.

The image 'c' in the same Figure corresponds to MBN₅ filled system which has a number of curved tear lines and these parabolic lines are signs of higher strength, and the acid aging corrodes rubber leading to blister formation which reduces strength to a small extent only, and still the rubber has tear lines indicating stability.

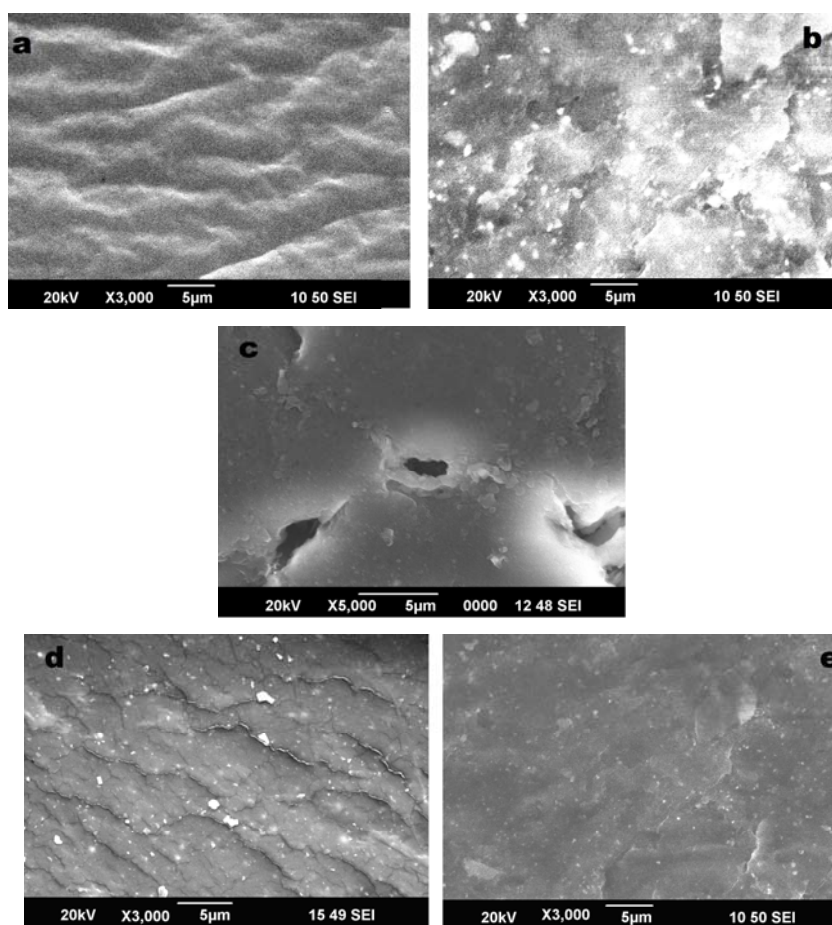


Figure 7.6 a)SEM of tensile fracture surface of unfilled unaged mix, BN₀ indicating randomly arranged tear lines b) BN₀ aged in 50% acid c)BN₀ aged, image at higher magnification indicating voids and fissures with reduced tear lines d)MBN₅ RNC unaged e)MBN₅ RNC aged

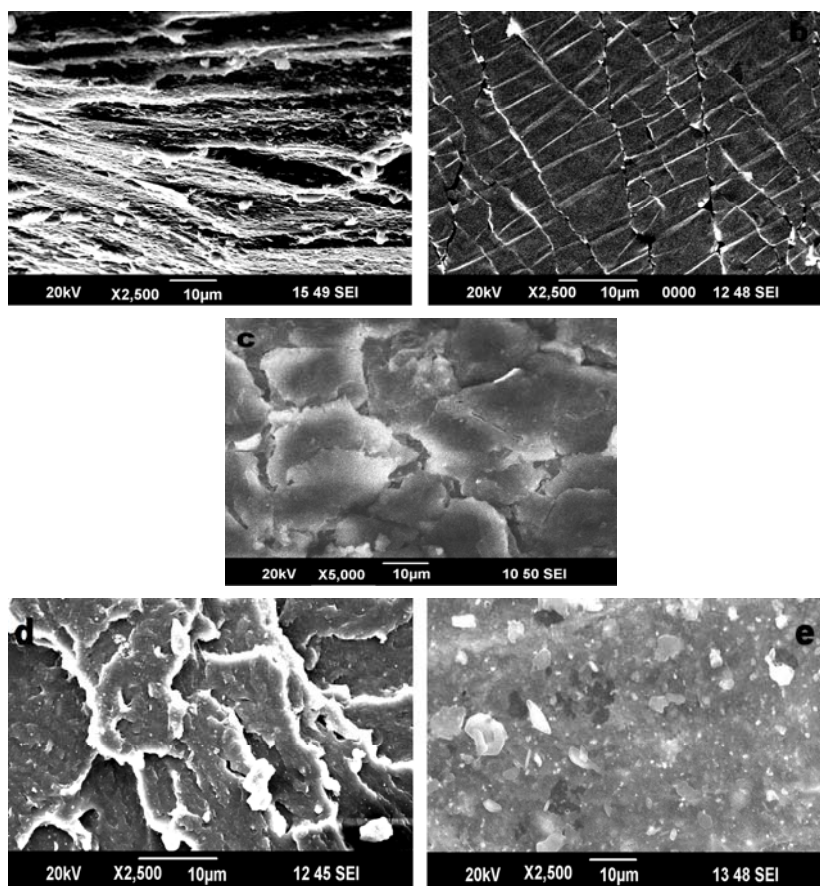


Figure 7.7 a) SEM of tensile fracture surface of black filled unaged mix CB30 indicating randomly arranged tear lines b) acid aged CB30 c) image of acid aged CB30 at higher magnification d) Image of CB30+MBN₅ e) Image of acid aged CB30+MBN₅

In the case of 30 phr black filled systems the unaged images shows parabolic tear lines indicating stability which is lost on aging as seen from figures 7.7 c&d (higher magnification clearly shows void formation leading to instability), and hence a drop in tensile properties results. On the other hand in hybrid system randomly oriented tear lines indicating high degree of stability is minimized on acid aging, but to a small extent and hence only a low drop in properties results for the hybrid system. The SEM images of same sample after acid corrosion for 150 hrs indicate the presence of blisters on fracture surface and on the main fracture path. The formation of void regions owes to liberation

of gaseous products formed as a result of side reactions occurring during corrosion.

Conclusions:

Natural rubber composites could not withstand acid concentrations higher than 50% and is rapidly degraded. The mechanical properties after acid aging, and SEM pictures illustrated the extent of aging. The entire series used 50% dilute sulphuric acid as the immersion medium. When treated with 50% acid the tensile properties reduced at a moderate rate and a marked reduction of tensile to half its initial value within 150 hrs was observed. This acid concentration proved to be better immersion medium to study resistance of NR; filled and unfilled composites in a laboratory scale within a short span of investigation. As the concentration of acid is increased, the rate of degradation also increased but the time taken by the rubber matrix to disintegrate decreased. Sulphuric acid causes deterioration of natural rubber vulcanizates through oxidation and digestion leading to pits and craters in the vulcanizates.

As the nano loading increased, the stability against acid corrosion also increased on comparison with unfilled composites. The mechanical strength showed 58% retention in BN, MBN- RNCs over 150 hrs in 50% acid where as only 44% of the strength retained in unfilled system. Retention reached a saturation point beyond 15 phr and all the nano filled systems showed better retention on acid corrosion which rated around 60% in almost all the filled systems. On investigating corrosion in hybrid nanocomposites black filled composites proved as poor candidates to fit severe acid environments and corrosion resulted in 65% degradation of tensile strength in CB40 system. Hybrid combination of black with nano barium sulphate at 5phr and above strengthened the compound to resist corrosion on acid immersion and retained 60% of its mechanical strength. The immersion tests conducted on metal inserts and round rubber specimens supported the findings and the strength deteriorations are evidenced as craters and vacuoles in SEM micrographs. The

metal insert immersion test showed that as nano filler loading increased the g/m^2 vs D plots approached x-axis indicating stabilization in acidic environment. The drawback of all the black filled systems from industrial aspect is the colouration of immersion system due to leaching of compounded fillers during acid attack, whereas the white composites showed no signs of leachouts or discolourations. The SEM images of same sample after acid corrosion for 150 hrs indicate the presence of blisters on fracture surface and on the main fracture path. The formation of void regions owes to liberation of gaseous products formed as a result of side reactions occurring during corrosion. The filled system has a number of curved tear lines and these parabolic lines are signs of higher strength, and the acid aging corrodes rubber leading to blister formation which reduces strength to a small extent. Nano filled systems are better materials to resist a concentration of 50% sulphuric acid and black filled systems are applicable only at very dilute concentrations of acid.

Section-b

CORROSION OF EPDM BASED RNCs:

**ETHYLENE PROPYLENE DIENE RUBBER-BARIUM SULPHATE COMPOSITES AND THEIR
CORROSION IN SULPHURIC ACID.**

Ethylene-propylene-diene terpolymers(EPDM) are elastomers with a saturated backbone which makes them resistant to weathering[13]. During industrial services demanding EPDM based construction films, membranes or linings, the surface of the elastomer is degraded under the weathering conditions like radiation, heat, ozone[14-18]chemical media[19]etc. These aspects deteriorate the surface as well as bulk properties of the elastomer. It is important that one understands the extent of chemical degradation and changes occurring on structure and performances of EPDM under such environments. Numerous reports have been published so far on EPDM degradation and stability; majority of which emphasized mainly on both thermal and irradiative aging. Only a few reports have focused on chemical degradation of EPDM in aggressive aqueous environments. Tan. et al.[20] studied mechanical stability of EPDM in a PEM fuel cell environment containing acid solutions and Wang et al. [21,22] investigated the in-situ epoxidation of ethylene propylene diene rubber by performic acid. There is a substantial literature discussing the degradation of EPDM on acid exposure. Few results concerning the degradation in nitric acid and influence of media on mechanical properties were reported. Acidic solutions are often encountered by rubber goods during exposure. Sulphuric acid is a major component in PEM fuel cell to which EPDM gaskets are exposed during service life. So an investigation of the behavior of EPDM vulcanizate to acid helps to engineer maintenance free products and increase their service life. Mitra et al. investigated the chemical degradation of uncross-linked rubber in 20% Cr/H₂SO₄ environment; which caused loss of bulk properties. They investigated the chemical degradation of pure, peroxide cured as well as the sulphur cross linked EPDM composites. An interesting application field of this rubber is as a seal for

the submerge pump. During service, the seal surface comes in contact with water containing several salts under acidic or basic condition. It has been found often that these seals fail to perform to the expected level due to deterioration, and these realms need systematic investigations and remedial steps [19,20].

BaSO₄ is one of the chemically inert fillers known for its ability to impart acid resistance to polymers. Having its size reduced to nano scale the efficiency increase. BaSO₄ filled polymer systems have been widely studied by researchers; but rather less research regarding their application to polymer matrix has been reported [23-24]. Filler combinations are often used so that an adequate balance of properties can be achieved, along with good characteristics [25]. Present work is the first of its kind dealing with degradation due to acids in EPDM-BaSO₄ nano composites.

In our present work the focus is on role of nano barium sulphate in imparting resistance to sulphuric acid, when incorporated into the EPDM matrix. EPDM-BaSO₄ nano composites having nano concentration varied were compounded and vulcanised and their cure characteristics were determined. FTIR spectroscopy was used for monitoring the emergence of new functionalities upon degradation. Using SEM, surface topographical changes were monitored. The effect of degradation on mechanical properties of matrix was measured as retention in mechanical properties and influence of nano barium sulphate was analysed. Crosslink density of the degraded samples at different time of exposure in acids was determined to estimate the influence of acid attack on crosslink formed. In this section time dependent degradation of the gum vulcanizates of Ethylene propylene Diene(EPDM) and EPDM-Barium sulphate nano composites with and without HAF in sulphuric acid were studied. Impact of degradation on the mechanical properties of these composites was also evaluated. Gum compounds and nanocomposites cured were subjected to an aggressive acidic medium, i.e., an aqueous solution of sulphuric acid (H₂SO₄). The changes in functional groups were monitored using Fourier transform infrared spectroscopy (FTIR).

7b.1 EPDM based composites

7b.1.1 Preparation of EPDM based composites

The EPDM based composites were prepared as described in sections 5.1.1 and 5.2.1. The compounding recipes used are shown in Table 5.1.

7b.1.2 Mechanical properties: Effect of acid concentration

Sulphuric acid causes deterioration of EPDM vulcanizates through oxidation and digestion leading to pits and craters in the vulcanizates. The EPDM contains 4.5% ENB as diene facilitating vulcanization sites and these ENB sites (discussed in forth coming sections) are highly susceptible to such kind of attacks. As the concentration of acid is increased, the rate of degradation increases and the time taken by the rubber matrix to disintegrate decreases. Analysis of the behavior demands the selection of one particular acid concentration for subsequent studies.

For this purpose the effect of 0%, 25%, 50%, 60% and 70% acids were traced on unfilled rubber vulcanizates BN₀ and the tensile strengths were recorded following the acid aging for upto 15 weeks. At 25% and 50% acid strength, tensile strength showed an increasing trend(35% and 75% respectively) upto 15 weeks of analysis and the rate of increase was higher in concentrated acid. This is shown in the Fig. 7.8. This increase is on account of the crosslink formation during exposure to acid which is a direct indication of degradation of EPDM.

An anomalous behavior was seen for EPDM in 60% acid. At the initial stages of aging tensile strength increased, but from the 7th to the 15th week, property deterioration took place and tensile strength reduced to half its initial value. This extra ordinary behavior had some interesting informations to share with the researcher's realm. At a still higher concentration (above 70%) the graph showed a decreasing trend from the very beginning. This is a direct

indication of degradation of EPDM. Even after 5 weeks of aging there was 50% loss in tensile strength and this led to the conclusion that EPDM is unfit for such concentrated environments. Thus an acid concentration of 60% was selected to measure the corrosion resistance of EPDM, filled and unfilled composites in a laboratory scale within a relatively short span of investigation.

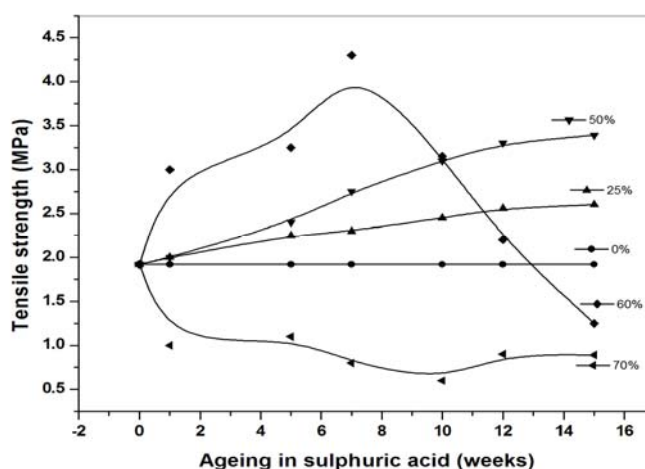


Figure 7.8 Effect of acid on mechanical properties of EPDM vulcanizates

7b.1.3 Swelling test

1. Immersion test

The international standard for immersion testing of rubber deal with change in weight of rubber samples when they are immersed in corrosive liquids. The testing was carried out The change in volume as well as weight of the test piece specimen after immersion ,with respect to time is (Table 7.3) recorded: The general effect of corrosive liquids involves absorption, diffusion, permeation, extraction and chemical reaction. Here, for EPDM, another probability is the increase in crosslink or breaking up of crosslinks on aging. This is due to the presence of double bond in ENB, which is not a part of main chain. Diffusion leads to percolation through pores and the chemical reaction either adds to the weight or

degrades rubber depending upon the intensity and vigor of the reaction and also the conditions to which the reaction product is exposed.

Table 7.3 Immersion test results for EPDM compounds

Sample name	Concentration of sulphuric acid used		Variation of weight % Over 28days	Grade
BN ₀	1	0	0.0	A
	2	50	0.78	A
	3	60	1.34	B
BN ₂	1	0	0.0	A
	2	50	0.76	A
	3	60	1.37	B
BN _{2.5}	1	0	0.0	A
	2	50	0.75	A
	3	60	1.21	B
BN ₅	1	0	0.0	A
	2	50	0.65	A
	3	60	1.15	B
BN ₁₀	1	0	0.0	A
	2	50	0.64	A
	3	60	1.13	B
BN ₂₅	1	0	0.0	A
	2	50	0.55	A
	3	60	0.91	A
BN ₅₀	1	0	0.0	A
	2	50	0.25	A
	3	60	0.50	A
MBN ₁	1	0	0.0	A
	2	50	0.76	A
	3	60	1.31	B
MBN ₂	1	0	0.0	A
	2	50	0.74	A
	3	60	1.27	B
MBN ₅	1	0	0.0	A
	2	50	0.73	A
	3	60	1.13	B
MBN ₁₀	1	0	0.0	A
	2	50	0.65	A

MBN ₁₅	3	60	1.13	B
	1	0	0.0	A
	2	50	0.48	A
	3	60	1.08	B
MBN ₂₅	1	0	0.0	A
	2	50	0.31	A
	3	60	0.97	A
MBN ₅₀	1	0	0.0	A
	2	50	0.22	A
	3	60	0.50	A
CB40	1	0	0.0	A
	2	50	-3.20	C
	3	60	-7.25	D
CB40+MBN ₂	1	0	0.0	A
	2	50	-2.74	B
	3	60	-7.60	D
CB40+MBN ₅	1	0	0.0	A
	2	50	-2.74	B
	3	60	-7.50	D
CB40+MBN ₁₀	1	0	0.0	A
	2	50	1.47	B
	3	60	4.38	D
CB40+MBN ₁₅	1	0	0.0	A
	2	50	1.33	B
	3	60	3.90	D
CB40+MBN ₂₅	1	0	0.0	A
	2	50	1.49	B
	3	60	3.95	D
CB40+MBN ₅₀	1	0	0.0	A
	2	50	2.00	B
	3	60	6.00	D
CB50	1	0	0.0	A
	2	50	-5.00	B
	3	60	-10.50	D
C50	1	0	0.0	A
	2	50	0.27	A
	3	60	0.65	A

The RNCs of MBN and BN, C₅₀ exhibited similar behavior in 50, 60% acids, still MBN filled EPDM composites exhibited superior behavior owing to its increased bondability with matrix polymer. But at higher acid percentages,

the compatibility between matrix and filler is not much advantageous. All that matters is the presence of passive filler barium sulphate in the diffusion path of acid through rubber which nullifies the attack of acid on elastomers by creating networks that pose hinderance to acid flow in matrix. All the 50 phr filled MBN, BN, C;(modified, unmodified and commercial barium sulphate fillers) composites are good protective linings against 60% acid and all other lower compositions of barium sulphate alone filled composites are reasonably good and hence graded as B. The CB filled systems are poor shields and cannot be recommended for 60%acid linings and show decrease in weight with time indicating filler leach outs and were graded D under the analysis. These compounds are suitable to fit as lining for 50% sulphuric acid along with brick lining only. The hybrid combinations are graded as B at higher barium sulphate loadings and hence can reasonably be used to prevent corrosion of surface beneath it(ref. section 2.3.13.1). The immersion tests are based on few number of days of immersion and provide limited data.

2. Tests for acid resistance using rubber sheets adhered to Mild steel samples

Rubber covered metal strips (metal inserts of mild steel) were made for studying the acid resistance of these selected rubber samples by bonding natural rubber to mild steel(MS) sheets using chemlok205 as primer and adhesive chemlok 238 as cover coat and cured at 150 °C. The samples were prepared accordingly(ref. section 2.3.13). The rubber covered MS samples of 5cm x 5cm were kept immersed in 60% acid solution and the percentage weight is not considered alone but it is combined with the area of the sample as well as the number of days of immersion(of 12, 40, 80 upto 100 days) are recorded and referred to as 'g'. The days are recorded as 'D'. The surface areas of the samples are noted before commencing the test and this is referred to as m². From the data collected a graph is plotted with g/m² vs D (Fig. 7.9)

For a good quality rubber lining compound to be used the curve should be as near to the x-axis as possible, i.e., it should have a low slope.

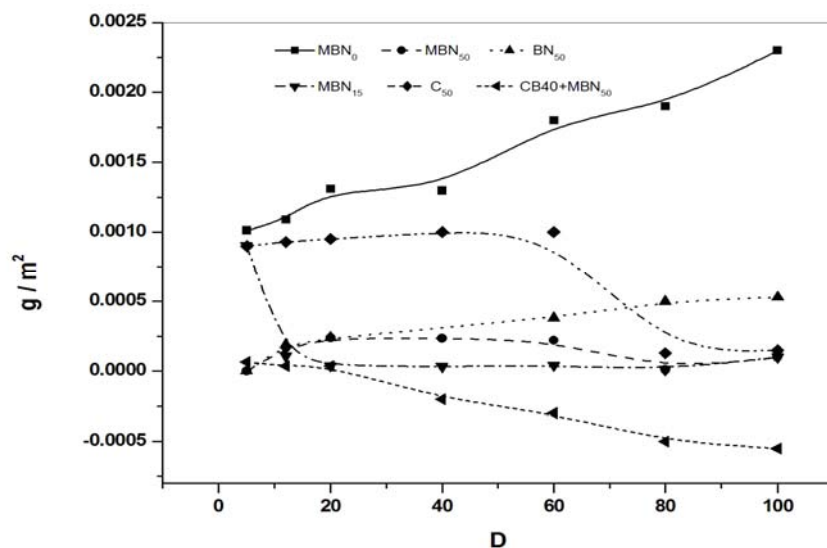


Figure 7.9 Plots for acid resistance of various MS inserts covered by EPDM composites- MBN₀, MBN₁₅, MBN₅₀, BN₅₀, C₅₀ CB40+MBN₅₀ in 60% H₂SO₄

The results discussed were for superior systems as seen from Table 7b.1 and results showed that for the prescribed period of time MBN₀ showed a constant increase in weight and whereas 50 phr filled MBN and BN showed only slight increase in weight and graph remained in the vicinity of x-axis; where as commercial filler incorporated composites showed initial increase, which remained constant upto 60 days and started approaching x-axis which indicate filler (from agglomerates due to incompatibility of filler and rubber) pullouts from composites due to acid attack. MBN₁₅ systems showed initial decrease in weight per surface area indicating an initial absorption later on the graph indicates that after initial absorption, the rubber-passive filler network hindered further intake of acid and swelling remained constant. Though the plots for CB40+MBN₅₀ was at the closest vicinity of x-axis, the fact that the weight of composite is getting reduced indicates that the composite is dissolving in acid

and it is not an indicative of stabilisation as stated earlier by Andritz and Ruthner.

7b.1.4 Studies on the influence of acidic environment on physical properties of MBN RNCs.

The studies on variation of tensile strength (Fig. 7.10(a-d)) on acid aging for 15 weeks in 60 percentage concentrated sulphuric acid followed a dramatic trend. All the samples had their tensile strengths increased upto 7 weeks. The samples showed a large increase in tensile strength on 7th week of aging. On further aging these EPDM based composites decreased in strength and eventually reached their lowest values at 15th week of aging. Observing the trend it is clear that all the composites including the unfilled composites retained more than 65% of their strength properties on aging, and MBN 15phr filled system possessed even 90% retention indicating arrest of corrosion by MBN networks existing well dispersed in the rubber matrix. The initial trend of large increase in tensile strength indicates the occurrence of a particular mechanism involving new crosslink formation which demands much investigation. Black filled composites and hybrid composites are poor choices as seen from (Fig. 7.10c) for 60% acid aging situations and hybrid ones with higher MBN loading exhibited enhanced efficiency in withstanding corrosion. The black filled composites lost more than 70% of their strength properties and yielded to acids, MBN filled hybrid black composites retained nearly 53% of their strength, still they are unsuitable for acid linings as revealed from immersion test. The 50 phr filled samples performed superior in immersion tests and their retention in strength was well around 55-60% which is a reasonably good result as far as lining is concerned, the nano filled composites, especially that of MBN exhibited excellence in resistance compared to commercial bariumsulphate filled composites.

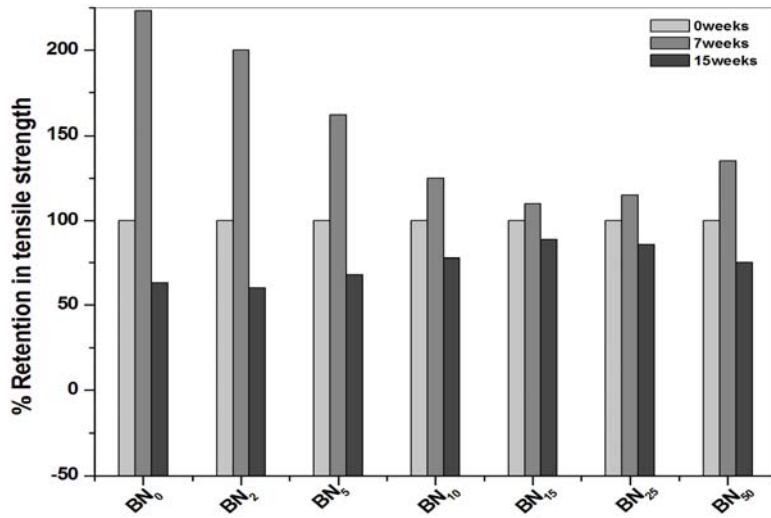


Figure 7.10a Percentage retention in tensile strength on acid aging upto 15 weeks in 60% acid for BN filled RNCs

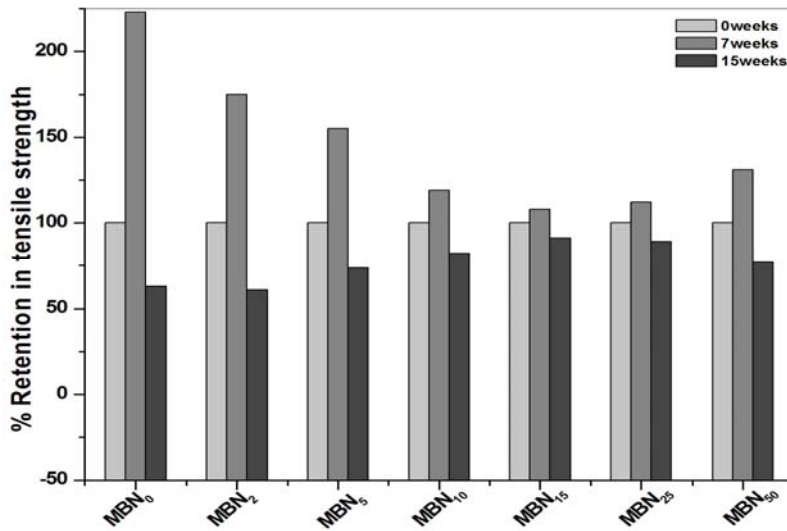


Figure 7.10b Percentage retention in tensile strength on acid aging upto 15 weeks in 60% acid for MBN filled RNCs

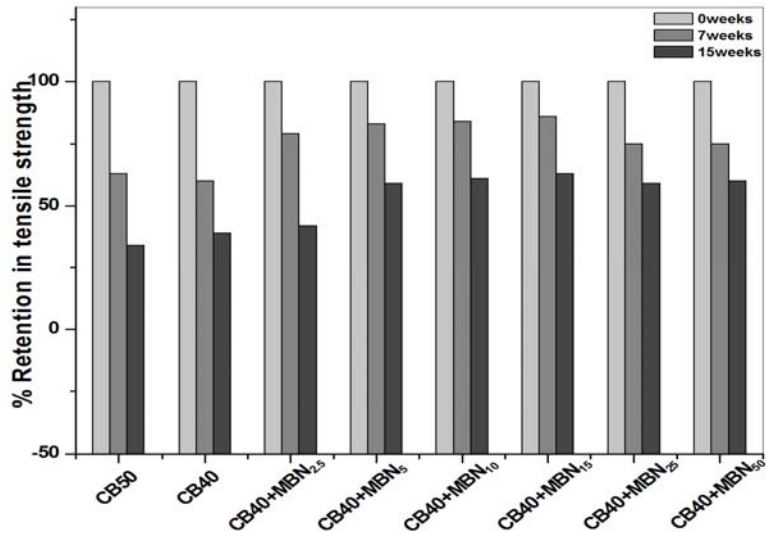


Figure 7.10c Percentage retention in tensile strength of NR-CB-MBN filled hybrid RNCs on acid aging upto 15 weeks in 60% acid

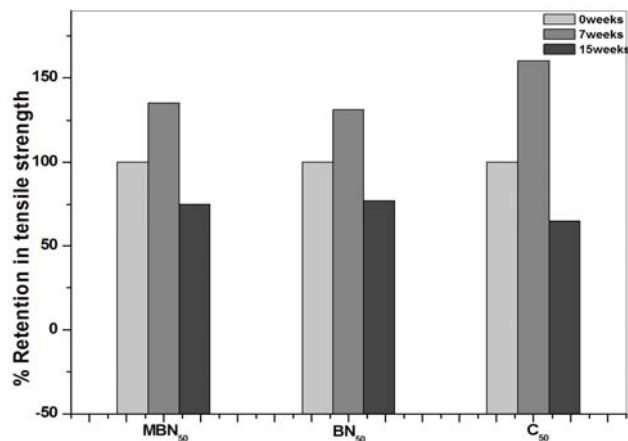


Figure 7.10d Percentage retention in tensile strength of 50 phr BN, MBN, C filled RNCs on acid aging upto 15 weeks in 60% acid

7b.1.5 Effect of 60% sulphuric acid on crosslink density and mechanical properties of composites MBN₀ and MBN₁₅

Figures 7.11a-7.11d gives the variation in crosslink densities, tensile strength, % elongation at break and 100 % modulus of EPDM composites MBN₀ (unfilled) and MBN₁₅ (15 phr modified nanobarium sulphate filled).

Effect on crosslink densities:

The crosslink densities of the samples exposed to acid for 0, 5, 7, 10, 12, 15 weeks respectively were obtained by swelling in toluene after acid aging in 60% sulphuric acid. The trend followed in crosslink density is shown in Fig. 7.11a. For MBN₀, crosslink density increased rapidly by 40% upto 7 weeks and afterwards it showed a minor decrease upto 12 weeks and reached its maximum on 15th week.

In MBN₁₅ the crosslinking phenomenon was not rapid as the graph states. The crosslink density increased slightly upto 7 weeks and there after it decreased and attained a minimum at 15th week indicating slow cross-link formation due to acid aging.

This variation in crosslink density can be explained as follows; when rubber samples are exposed to aqueous acid, decrosslinking due to hydrolysis of crosslink [17] sites is the prime process causing chemical degradation. In MBN₁₅ this decrease is manifested slightly, but in MBN₀ this is not visible, instead a rapid shoot up of crosslink density is visualized and this owes its origin from the fast formation of newer recombination products of oxygenated species. In MBN₀ no kind of fillers or filler networks pose hindrance to diffusion of acid through the matrix and hence the matrix is highly prone to corrosion (possible mechanisms discussed later). As the period of aging increased (15 weeks) crosslinking and decrosslinking reactions proceeded depending on stability of composites and for unfilled EPDM the corrosion is severe leading to high CLD. FTIR data and mechanism supports the explanation(in forth coming sections). The chemistry behind the crosslinking and decrosslinking can be explained as follows.

In a vulcanised rubber matrix, a mixture of different types of crosslinks are formed eg., polysulphidic, disulphidic, monosulphidic, along with some cyclic sulphur structure. In a typical sulphur cured rubber, the bond dissociation energy

of polysulphidic crosslinks (C-S_x-C) is ~120kJ/mol, disulphidic linkages (C-S-S-C) is ~ 240 kJ/mol and monosulphidic linkages (C-S-C) is ~270 kJ/mol [20]. This indicates that polysulphidic bonds will undergo acid induced hydrolysis faster than disulphidic and monosulphidic linkages in a chemical degradation environment. Such a hydrolysis of different kinds of crosslinks due to chemical degradation caused by acid exposure possibly change CLD over time. On aging over 7 weeks this decrosslinking and subsequent recombination may be responsible for rise in CLD. Soon after this, on continued aging; CLD in acid medium attains a plateau region for MBN₁₅ where as no such effect was seen in MBN₀.

It is possible that in MBN₀ some physical deentanglements as well as chemical modifications leading to stable network formation are equally responsible. Eg; transformation of polysulphidic linkages into disulphidic and monosulphidic linkages [14] which might have led to increase in CLD. So the increase in CLD for MBN₀ after 7-15 weeks is because of the fact that, chemically weaker crosslinks undergo acid induced hydrolysis, faster than relatively stabler crosslinks. On increasing exposure time, more and more stable crosslinks remain in the system and this causes increase in CLD. The observed trend and FTIR data in next confirms our postulation[14]. To sum up, the aggressiveness of the exposure medium is reduced in the presence of added nano barium sulphate. The nano filler due to its passiveness and smaller size entered the matrix and minimised to a better extent decrosslinking, and prevented recombinations. The nano filler arrests acid transport by creating passive networks over a pretty long period of time.

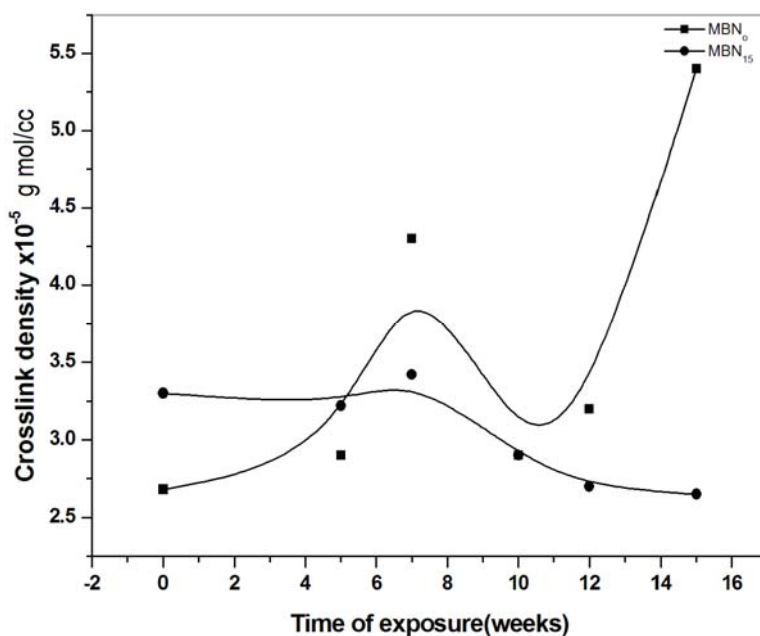


Figure 7.11a Variation in crosslink density of MBN₀ and MBN₁₅, EPDM-RNCs on acid aging for 15 weeks

Effect on mechanical properties:

The trend observed in crosslink density is reproduced with mechanical properties from the property retention graph itself (discussed in 7b.4). It is seen that all the composites showed a sharp increase in strength properties on aging upto 7 weeks, and a decrease on 15 weeks of subsequent aging. The trends exhibited can be clearly explained on comparing the data of two model systems one MBN₀ and another one MBN₁₅. Tensile strength of a vulcanizate is a complex function of chemical nature of crosslinks and crosslink density [15]. It increased with increase in crosslink density up to a maximum and there after decreased with further increase in CLD. This is because the tensile strength is dependent on the number of efficient network chains. When the crosslink density is too high, the average molar mass of the rubber chain between two successive crosslink points decreases and the mobility of the chain segment is restricted, which limits the orientation of the network chains and then results in the decrease of the tensile strength. The hydrolysis of crosslinks (as evidenced by

FTIR 7b.5) changes the optimum level of crosslink density, which facilitates an increase in the tensile values upto 7 weeks of exposure, afterwards with increase in CLD ; tensile decreases. The reduction in tensile strength was about 65% in MBN₀ upto 15 weeks aged whereas in MBN₁₅ the tensile strength is retained 90% even after 15 weeks of exposure.

From Figures 7b-7d it could be seen that in MBN₀, % retention of elongation at break increases for 7 weeks of aging and started decreasing upto 12 weeks of exposure. Again it increased over 15 weeks of aging in 60% acid. Owing to the chemical degradation, when the crosslink density is too high, the mobility of the chain segment is restricted, which limits the orientation of the network chains and then results in decrease of % elongation at break, on further degradation rubber chain mobility increases, and hence this anomalous behaviour exhibited in %elongation at break. In MBN₁₅ elongation at break is found to decrease with aging which indicates that the filler restricts mobility of chain segment. The increase in modulus is reflected from decrease in elongation due to stiffening on aging.

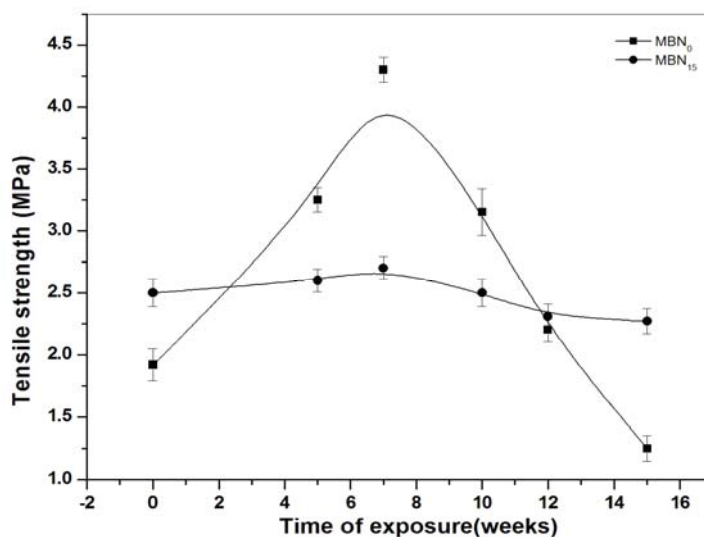


Figure 7.11b Variation in tensile strength of MBN₀ and MBN₁₅ EPDM-RNCs on acid aging for 15 weeks

All these trends firmly confirm that decrosslinking through hydrolysis of crosslinks is the primary reaction in sulphuric acid degradation upto 7 weeks and beyond the period the species formed combine to form new crosslinks which causes an increase in crosslink density [15], (these explanations are well supported by FTIR).

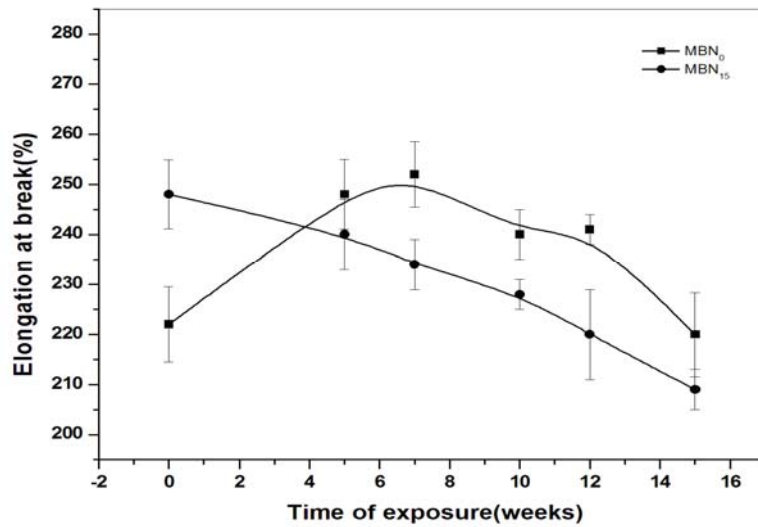


Figure 7.11c Variation in %elongation at break of MBN₀ and MBN₁₅ EPDM-RNCs on acid aging for 15 weeks

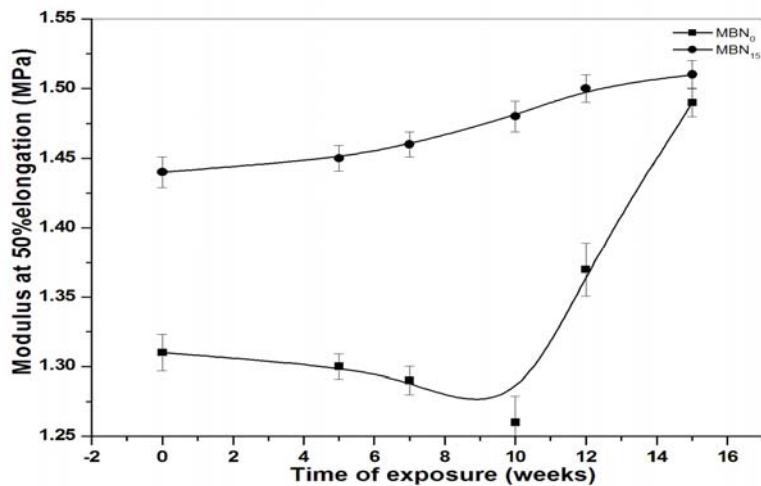


Figure 7.11d Variation in 100%modulus of MBN₀ and MBN₁₅ EPDM-RNCs on acid aging for 15 weeks

7b.1.6 FTIR analysis:

Emergence of neo-functionalities on aging upto 15 weeks as evidenced from Infrared spectroscopy

FTIR analysis were performed on MBN₀ and MBN₁₅ samples after exposure to aggressive 60 % SA (sulphuric acid) over a time period of 15 weeks. Initial spectra of both were identical with minor differences in the region around 1200-1000cm⁻¹. The correspondance between the spectrum and vibration modes, here and in the rest of the paper was obtained from the hand book [16].

The IR spectra obtained for samples aged over different periods showed important changes in the region of (a) hydroxylated products (b) carbonylated products (c) deformation vibrations and are depicted in Figures 7.12a, b, c respectively.

A group of new bands emerges in the spectra as a result of chemical degradation by acid at 3200-3600 cm⁻¹ due to hydroxylated products. It is evident from FTIR results that as aging period increased, peaks around 3600cm⁻¹ started to broaden in MBN₀ whereas in MBN₁₅ no such broadening is seen upto 12 weeks. This broadening is due to the increase in the functional groups such as alcohols, carboxylic acids and peroxides. After 12 weeks the hydroxyl species increased as indicated by broadening of peaks in MBN₁₅.

The formation of alcohol is again substantiated from formation and increase in peak between 778-760 cm⁻¹. The peak at 1400 cm⁻¹ stands for O-H bend in tertiary alcohol, all these data obtained from FTIR region evidences that, the primary process is decrosslinking via hydrolysis [7]. It is also evident that the degradation rate is lowered in the presence of nano filler since degradation products are peaking only after 15 weeks of aging. In the carbonyl region, in MBN₀ we encountered maxima at 1775, 1735(-C=O, aldehydes), 1728(-C=O, ketones), 1695, 1675, 1650 cm⁻¹ (α , β unsaturated carbonyls), 1590(carboxylates), in MBN₁₅ the peaks are seen at 1775, 1735, 1728, 1695, 1650, 1598 cm⁻¹ but with narrower peak areas, indicating rarity of species [16].

Much pronounced difference is observed in the deformation vibration region. In MBN₀ for first five weeks of aging, peaks are not identifiably broadened, whereas after that time period new bands emerged indicating accelerated aging. A group of new bands at 1550 (COO⁻, carboxylates), 1198/1120 (C-O-C, from ester, ether/S-O from sulphur-oxygen adduct), 1045/990 (C-C-O, C-O-C from ethers, esters and carboxylate salts), 1400 (O-H bending in tertiary alcohols, which is due to attack of acid on ENB double bond). The peak at 779 cm⁻¹ (hydroxyl), a decrease in band at 808 and increase at 871,909 cm⁻¹ confirms the attack of acid on C=C, leading to the formation of vinyl unsaturation.

In MBN₁₅, deformation vibration peaks are observed at 1550 (carboxylates,COO⁻), 1400(O-H bending in tertiary alcohols, which is due to attack of acid on ENB double bond), 1250, 1140/990 (C-C-O), 900, 767 cm⁻¹ (O-H), 900 cm⁻¹ (for disappearance of double bond). The peak areas are narrow compared to MBN₀ and only few peaks appeared upto 12 weeks (MBN₁₅-12w). Certain new peaks (narrow) emerged on aging after 15 weeks (MBN₁₅-15w), which shows that degradation is slow upto 15 weeks in the presence of nano BaSO₄. The entire FTIR analysis evidenced the fact that in the presence of nanofillers, formation of new functionalities are arrested to a better extent than in its absence, and hence improve the degradation resistance of rubber.

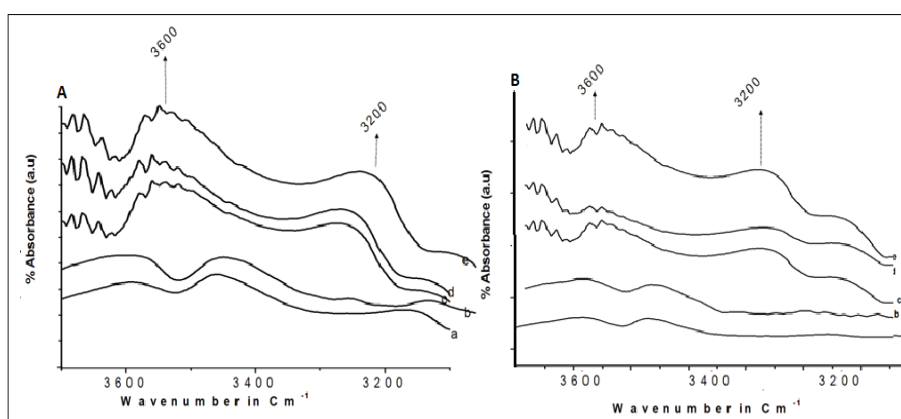


Figure 7.12.a: Hydroxyl region of A) MBN₀, B) MBN₁₅
(in Figure, a=0, b=5, c=7, d=10 and e=12 weeks of acid aging in 60% sulphuric acid)

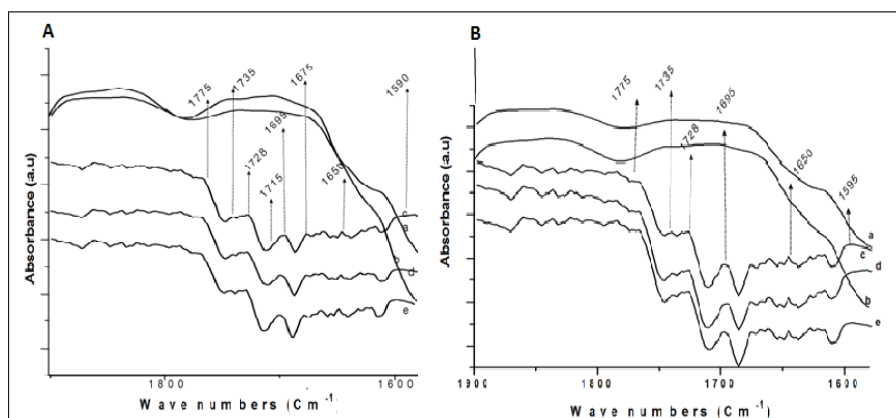


Figure 7.12.b: Carbonyl region of A) MBN₀, B) MBN₁₅
(in Figure; a=0, b=5, c=7, d=10, e=12 weeks of acid aging in 60% sulphuric acid)

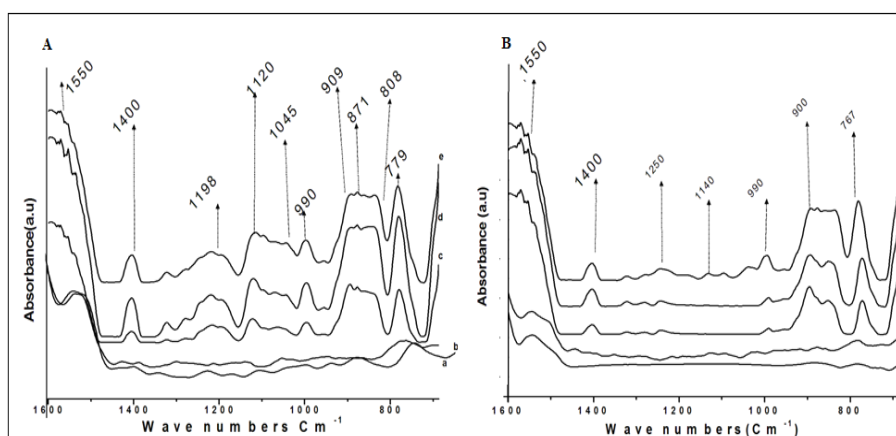


Figure 7.12.c: Deformation vibration region of A) MBN₀, B) MBN₁₅
(in figure; a=0, b=5, c=7, d=10, e=12 weeks of acid aging in 60% sulphuric acid)

7b.1.7 Proposal of a plausible mechanism for attack of acid on EPDM, supported by IR and mechanical studies

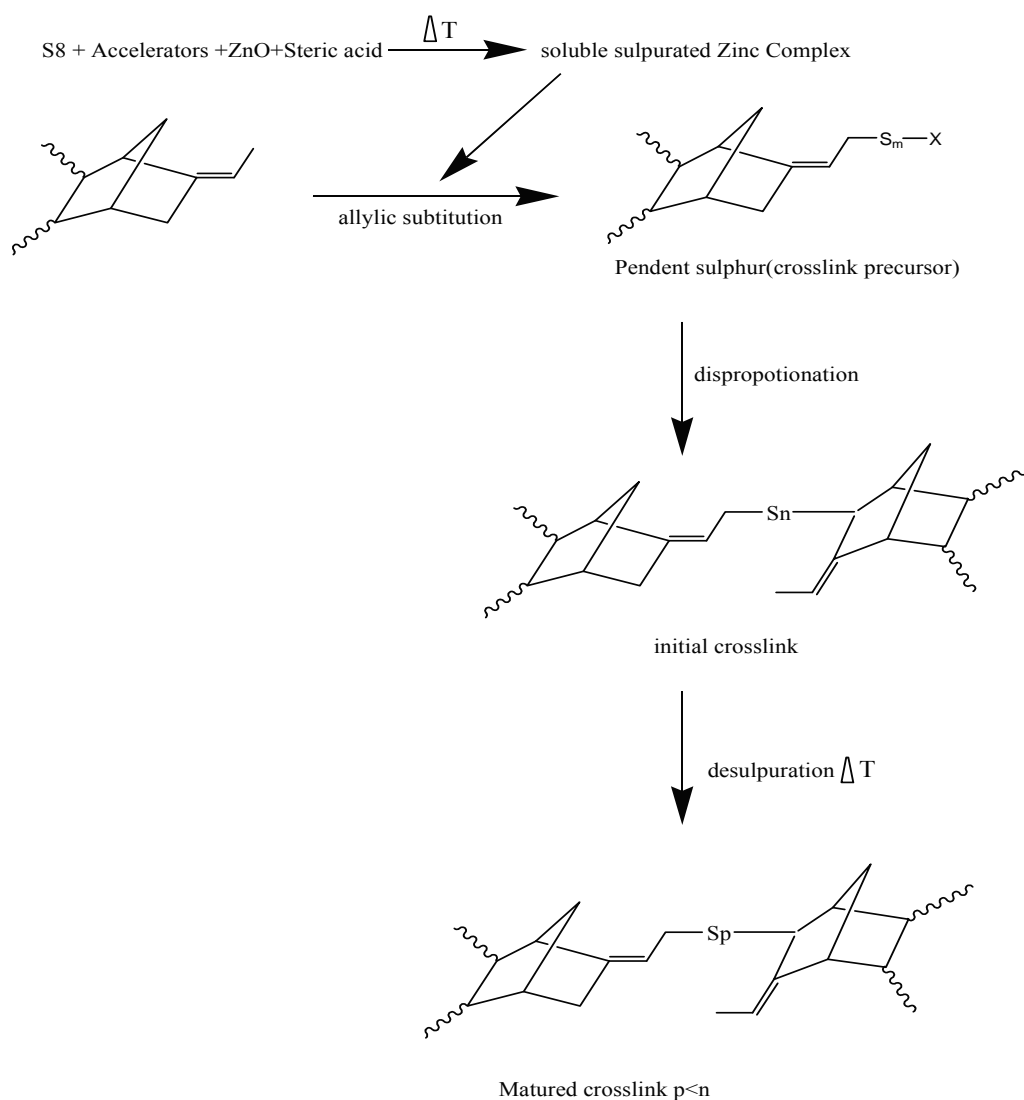
From FTIR analysis the major species and neo functionalities emerged during degradation of EPDM in 60% acid were isolated and a mechanism reasonable with findings and mechanical properties proposed. The two major attacking species in sulphuric acid solution is H_3O^+ and HSO_4^- and the presence of C=C not fully consumed in crosslink formation provides site for acid attack and results in formation of oxygen containing species OH, C=O, COOH. They

can undergo recombination to form ester or ether linkages as shown in schemes. The mechanism tried gives an idea about reactions, species responsible for degradation and these reactions may compete throughout the process [17].

The plausible mechanism can be stated and correlated with analytical data as follows; the hydrolysis of crosslinks is evidenced from decrease in crosslink density and increase in modulus at 50 %elongation. The emergence of hydroxyl, carbonyl and carboxylic acid peaks in IR owes to acid attack on C=C bond of ENB in EPDM. The mechanism predicts recombination of oxygenated species on prolonged exposure, which is evidenced by C-O-C bond in IR and variation in mechanical properties together with, increase in crosslink density. The surface degradation is sufficiently strong to affect bulk properties.

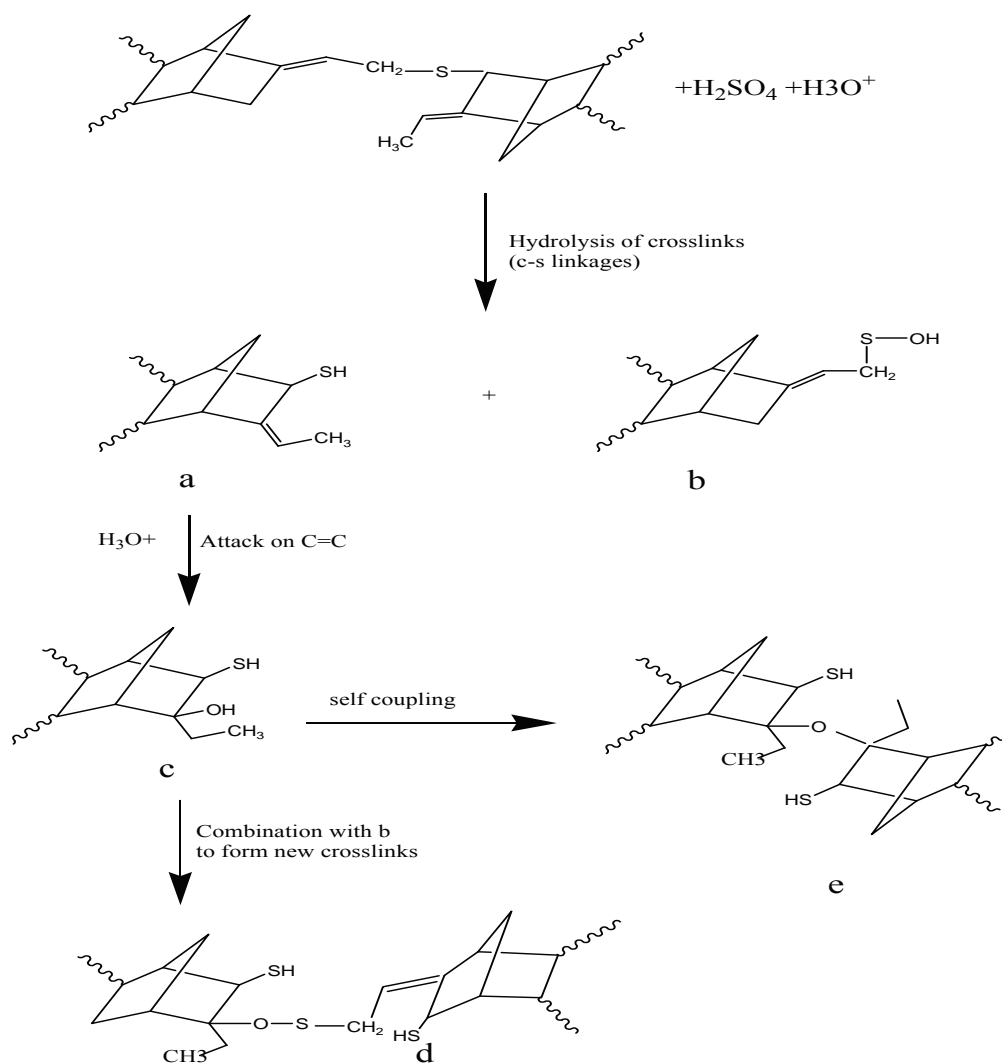
Mechanism of sulphur crosslink formation in EPDM-ENB :

Mechanism of sulphur crosslink formation in EPDM-ENB [18-19]

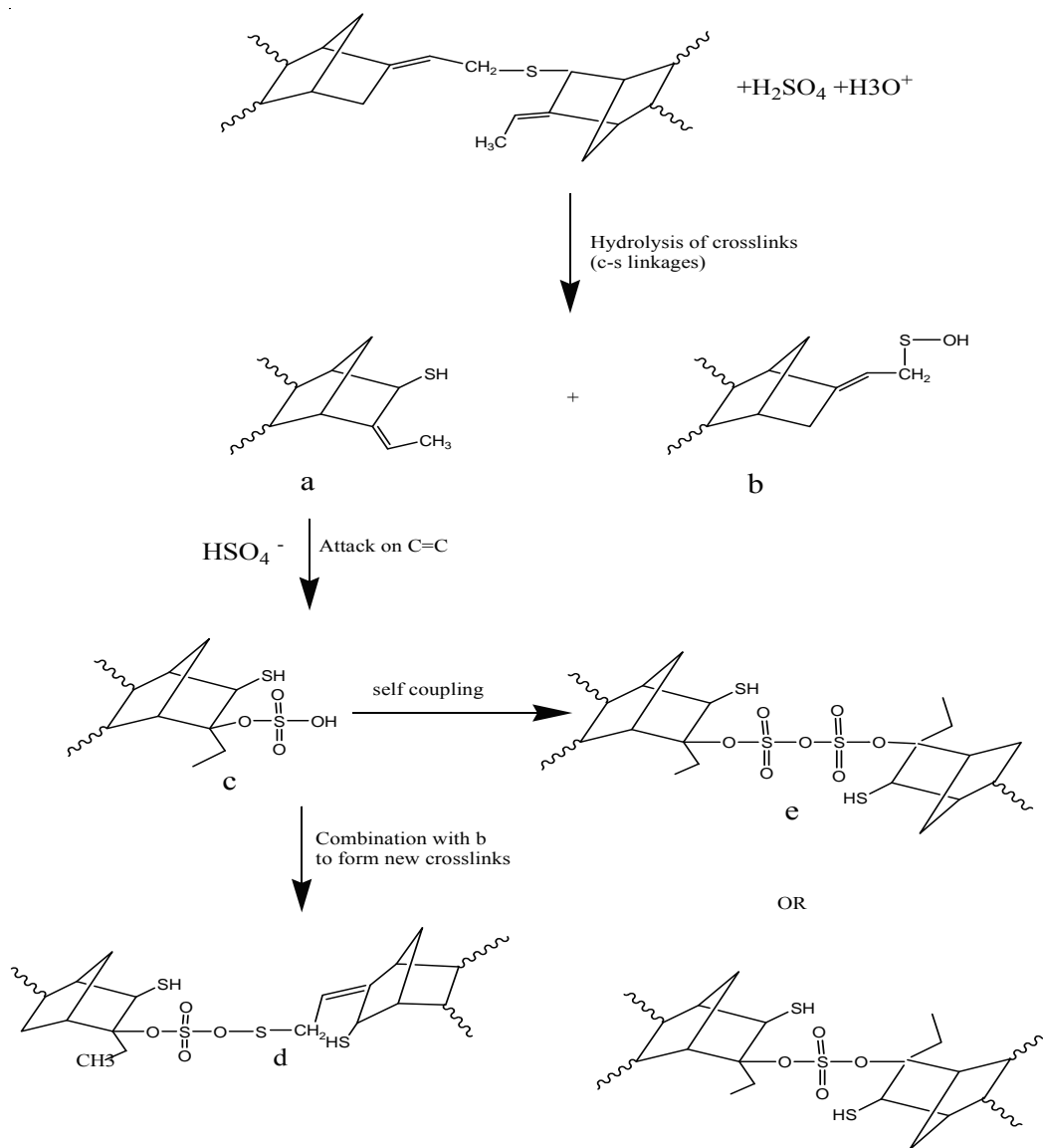


Degradation Mechanism Proposed:

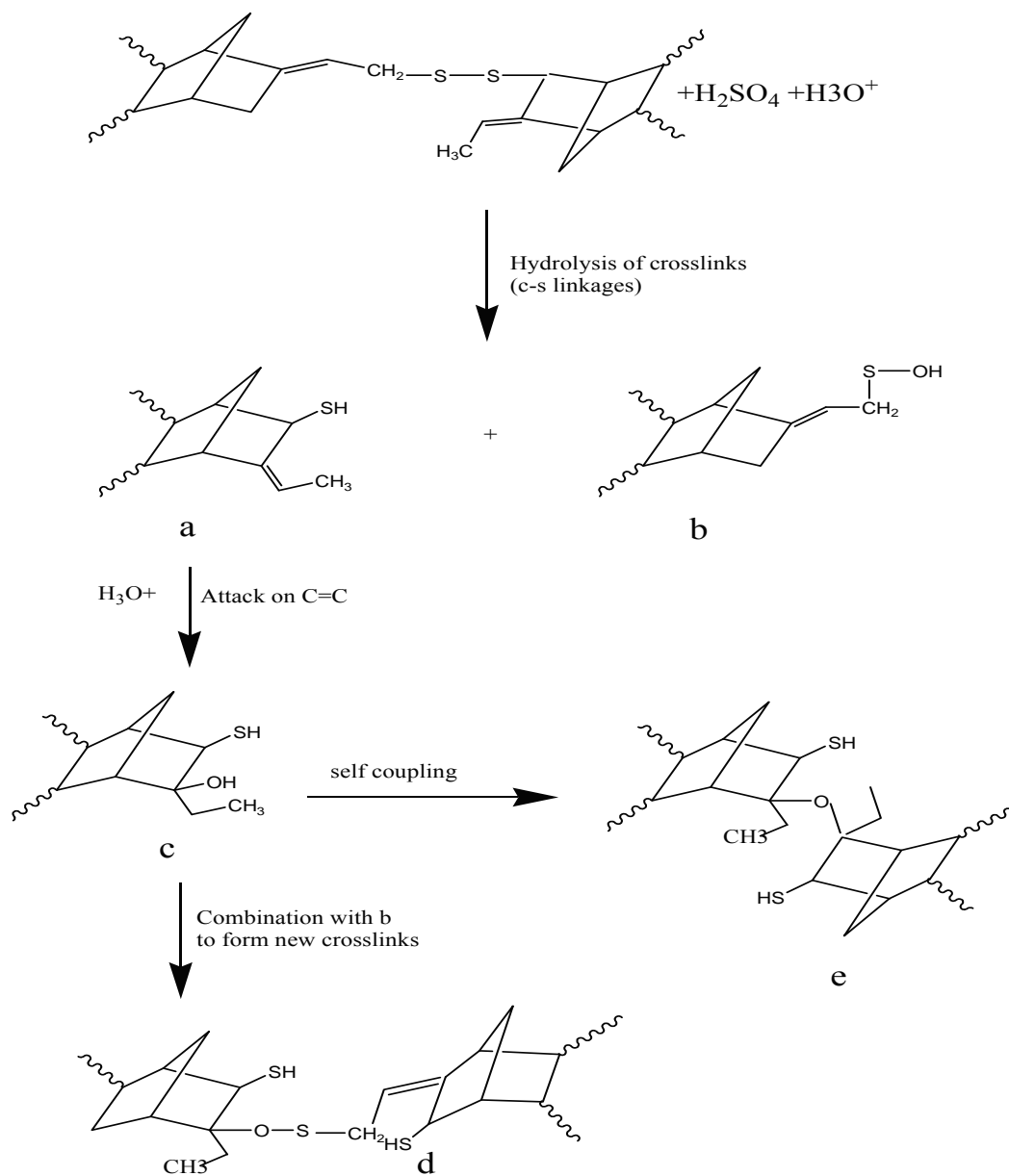
Scheme.1 Attack on Monosulphidic crosslinks
Scheme :1a H₃O⁺ attack



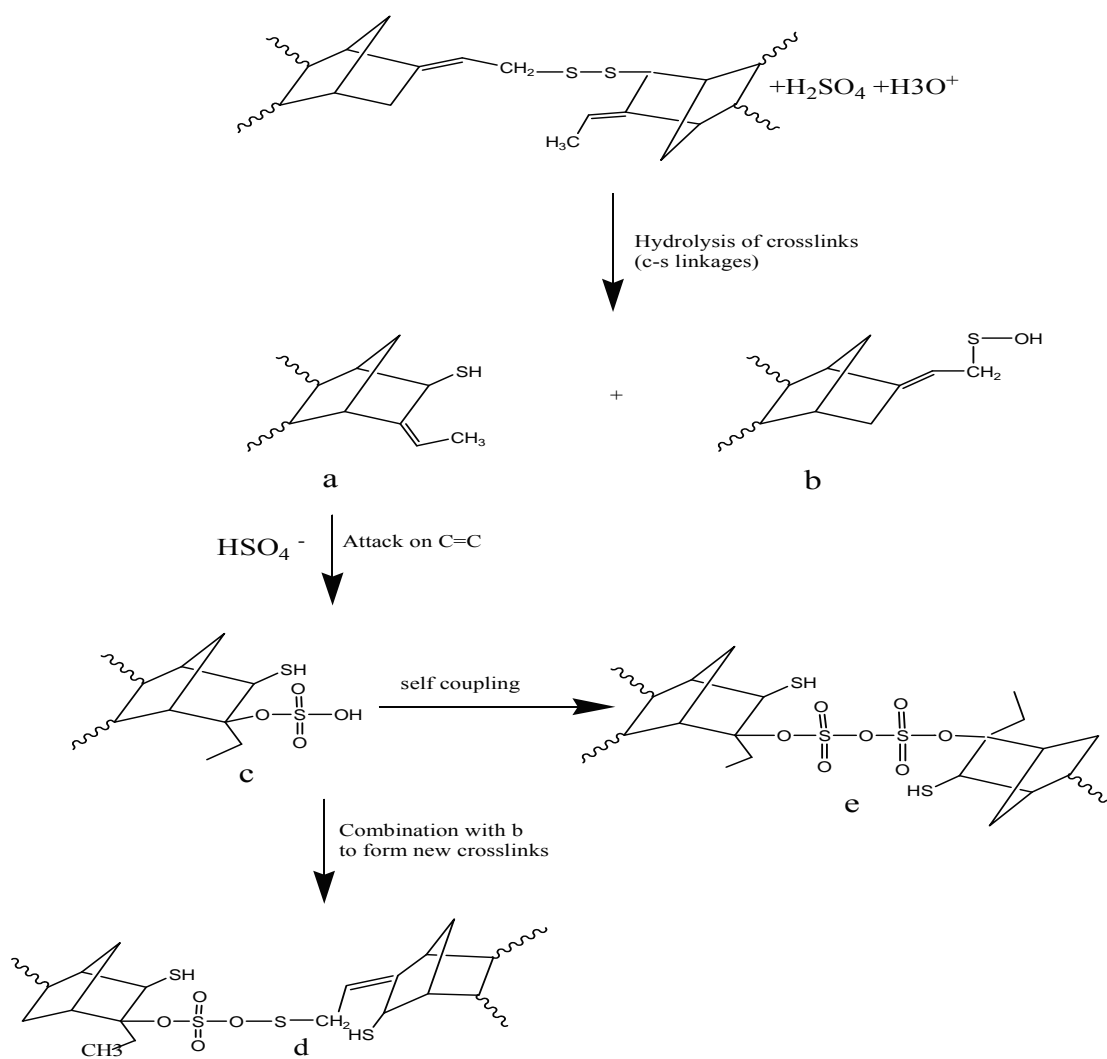
Scheme:1b attack by HSO_4^-



Scheme 2. Attack on Disulphidic/polysulphidic sulphur crosslinks
Scheme:2a attack of H₃O⁺



Scheme 2b: attack by HSO_4^-



7b.1.8 Interpretation of acid corrosion in terms of surface relief features of MBN RNCs as observed in SEM

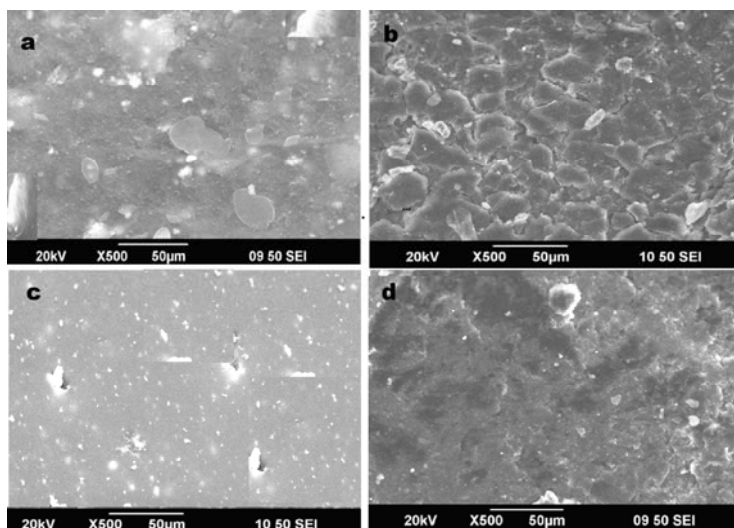


Figure 7.13 SEM images of MBN₀ (a) before aging, b) after aging and MBN₁₅ [c] before aging, d) after aging to compare changes taking place in morphology on aging over 15 weeks

In the case of 15 phr MBN filled systems the unaged images shows stability which is lost on aging as seen from figures 7.13b, 7.13d and hence a drop in tensile strength results, on 15 weeks of aging, crack initiation is observed. On the other hand in pure EPDM, stability is highly minimized on acid aging indicated by cracks formed all over the rubber samples, hence sharp drop in properties results for MBN₀ (Fig. 7.13a,b) system. The SEM images of same sample after acid corrosion for 15 weeks indicate the presence of blisters on fracture surface and on the main fracture path. The formation of void regions owes to liberation of gaseous products formed as a result of side reactions occurring during corrosion. The deterioration of properties are hence justified by morphological features in rubber SEM images.

Conclusions

EPDM composites could withstand acid concentrations of 60% and is having stability upto 15 weeks of acid aging and the aging resistance can be improved by increased loadings of nano barium sulphate fillers. The mechanical properties after acid aging, as the tensile, tear strengths determined and SEM pictures illustrated the extent of aging. The entire series used 60% dilute sulphuric acid as the immersion medium. The trends of tensile strength variation indicated a probability of decrosslinking and crosslinking reactions on acid immersion. This acid concentration proved to be better immersion medium to study resistance of EPDM; filled and unfilled composites in a laboratory scale within a short span of investigation.

As the nano loading increased, the stability against acid corrosion increased on comparison with unfilled composites. The maximum mechanical strength retained shows that 91% retention in MBN-RNCs over 15 weeks in 60% acid where as only 65% of the strength retained in unfilled system. Retention reached a saturation point beyond 15 phr and all the nano filled systems above this showed better retention on acid corrosion. On investigating corrosion in hybrid nanocomposites black filled composites proved as poor candidates to fit severe acid environments and corrosion resulted in degradation of CB40 system. Hybrid combination of black with nano barium sulphate at 5phr and above strengthened the compound to resist corrosion on acid immersion and retained 60% of its mechanical strength, but still degradation of rubber as indicated by weight loss is an indication of severe corrosion of rubber filled with carbon black. The immersion tests conducted on metal inserts and round rubber specimens supported the findings and the strength deteriorations are evidenced as craters and vacuoles in SEM micrographs. The metal insert immersion test showed that in nano filled systems the g/m^2 vs D plots approached x-axis indicating stabilization in acidic environment. The drawback of all the black filled systems from industrial aspect is the colouration of immersion system due

to leaching of compounded fillers during acid attack, whereas the white composites showed no signs of leachouts or discolorations. Nano filled systems are better materials to resist a concentration of 60% sulphuric acid and black filled systems are applicable only at very dilute concentrations of acids. FTIR analysis of model samples indicated cross linking and decrosslinking reactions and a number of recombination products of species generated during acid attack on EPDM. A mechanism was successfully proposed on the basis of IR of aged samples and corresponding mechanical properties to explain corrosion in pure EPDM and its slowing down in the presence of nano filler.

Section-c

**CORROSION OF IIR BASED RNCs:
ISOBUTYLENE ISOPRENE RUBBER-BARIUM SULPHATE COMPOSITES AND THEIR
CORROSION IN SULPHURIC ACID**

In this section, an investigation regarding the damage caused by acid to IIR containing barium sulphate, barium sulphate and carbon black-hybrid combination is done. Measurements of tensile strength and modulus have been made in order to quantitatively estimate the extent of degradation at various stages of acid attack. The fracture surfaces of failed tensile specimens have been investigated by means of SEM, both before and after acid aging and attempts have been made to correlate the changes in the surface topography with the extent of fall in mechanical properties as a result of acid corrosion. The weight changes associated with acid sorption was studied with rubber samples and metal inserts by immersion method.

7c.1 Isobutylene Isoprene rubber based composites

7c.1.1 Preparation of IIR based composites

The IIR based composites were prepared as described in sections 6.1.1 and 6.1.2. The compounding recipes used are shown in Table 6.1 and 6.2.

7c.1.2 Mechanical properties: Effect of acid concentration

As the concentration of acid is increased, the rate of degradation increases and the time taken by the rubber matrix to disintegrate decreases and the analysis of the behavior demands the selection of one particular acid concentration for subsequent studies. For the purpose the effect of 0%, 50%, 60% and 75% and 80% acids were traced on unfilled rubber vulcanizates MBN₀ and the tensile strength was recorded following the acid aging upto 15 weeks.

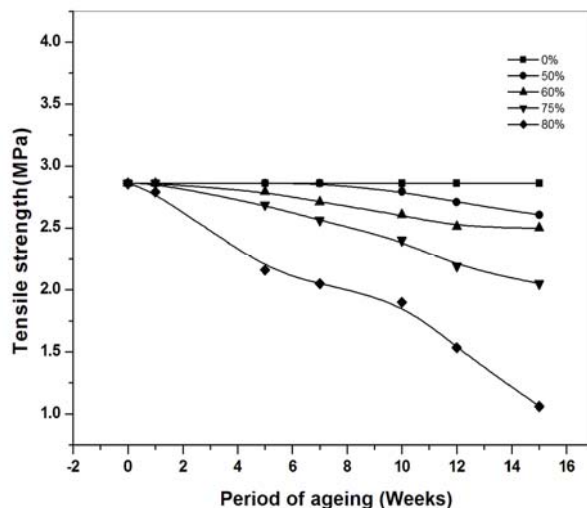


Figure 7.14 Variation in tensile strength of unfilled IIR vulcanizates with aging in sulphuric acid

It can be seen from Fig. 7.14 that the vulcanizates degraded in 80% acid beyond 8 weeks and lost 62 % of its strength on 15 weeks of aging, whereas in the 75% acid it exhibited negligible degradation around 25% even after 15 weeks of aging and the composites showed better stability in 50, 60% of sulphuric acids respectively. Only less than 12% of property was lost on acid aging even after 15 weeks. When treated with 75% acid the tensile properties reduced at a moderate rate, without severe degradation enabling us to trace the trend in degradation over the short time of investigation. In 80% acid, a marked reduction of tensile strength to less than half its initial value within 5 weeks could be observed. So 75% acid concentration was selected to measure the corrosion resistance of IIR; filled and unfilled composites in a laboratory scale within a limited span of investigation.

7c.1.3 Immersion tests

1. Swelling test

The chemical reaction of rubber lining with the corrosive chemicals and acids causes deterioration, resulting in progressive damage to the lining unless the reaction is not allowed to continue further. The international standard for

immersion testing of rubber deal with change in weight of rubber samples when they are immersed in corrosive liquids (Table 7.4). The testing was carried out at 25° C and duration of the test according to specification BS ISO 1817(British Rubber, vulcanized-Determination of effect of liquids, vary as follows: 24hrs, 48hrs, 96hrs, 168hrs, 30 days (Section 2.3.13.1).

Table 7.4 Immersion test results for IIR compounds

Sample name	Concentration of sulphuric acid used		Variation of weight % Over 28days	Grade
BN ₀	1	50	0.0196	A
	2	60	0.0458	A
	3	75	1.3354	B
	4	80	3.0361	D
BN _{2.5}	1	50	0.0570	A
	2	60	0.1621	A
	3	75	1.5678	C
	4	80	3.1213	D
BN ₅	1	50	0.0200	A
	2	60	0.0490	A
	3	75	1.3740	B
	4	80	2.2361	B
BN _{7.5}	1	50	0.0120	A
	2	60	0.0330	A
	3	75	1.0410	B
	4	80	2.0923	B
BN ₅₀	1	50	0.0080	A
	2	60	0.0100	A
	3	75	0.8800	A
	4	80	1.0300	A
MBN _{2.5}	1	50	0.0450	A
	2	60	0.1321	A
	3	75	1.3280	B
	4	80	3.0710	C
MBN ₅	1	50	0.0441	A
	2	60	0.1021	A
	3	75	1.3090	B
	4	80	3.0512	C

MBN _{7.5}	1	50	0.0412	A
	2	60	0.1000	A
	3	75	1.2900	B
	4	80	3.0433	C
MBN ₁₀	1	50	0.0412	A
	2	60	0.1000	A
	3	75	1.2900	B
	4	80	3.0342	C
MBN ₁₅	1	50	0.033	A
	2	60	0.087	A
	3	75	1.0023	B
	4	80	3.0265	C
MBN ₅₀	1	50	0.0030	A
	2	60	0.0090	A
	3	75	0.5800	A
	4	80	1.0091	B
CB55	1	50	0.1179	A
	2	60	0.5200	A
	3	75	13.87	D
	4	80	25	D
CB50+MBN _{2.5}	1	50	0.371	A
	2	60	0.6710	B
	3	75	11.25	D
	4	80	21	D
CB50+MBN ₅	1	50	0.2971	A
	2	60	0.5710	B
	3	75	9.24	D
	4	80	19	D
CB50+MBN ₁₀	1	50	0.260	A
	2	60	0.5312	A
	3	75	8.5	D
	4	80	16	D
C50	1	50	0.025	A
	2	60	0.059	A
	3	75	1.59	B
	4	80	4	D

2. Tests for acid resistance using rubber sheets adhered to Mild steel samples

Rubber covered metal strips (Metal inserts of mild steel) were made for studying the acid resistance of these selected rubber samples by bonding IIR to Mild steel sheets using chemlok 205 as primer and adhesive chemlok 238 as cover coat and cured at 150 °C. The samples were prepared accordingly (ref. section 2.3.13). The rubber covered MS samples of size 5cm x5cm were kept immersed in 50% acid solution and the percentage weight was not considered alone but it is combined with the area of the sample as well as the number of days of immersion. The weight of 12,40,80 days were recorded and referred to as ‘g’. The days were recorded as ‘D’. The surface areas of the samples are noted before commencing the test and this was referred to as m². From the data collected a graph was plotted with g/m² vs D (Fig. 7.15).

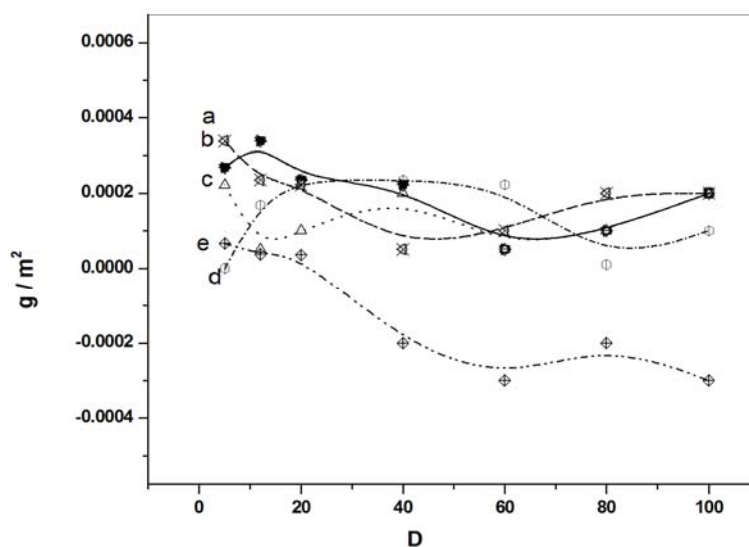


Figure 7.15 a)MBN_{7.5}, b)BN₁₅, c)MBN₁₅, d)MBN₅₀, e) CB50+MBN₁₀ IIR composites covered MS plates in 75% acid

For a good quality rubber lining compound to be used the curve should be as near to the x-axis as possible, i.e., it should have a low slope. Similarly, for the same quality of rubber lining the curve will exhibit a rise in the beginning but

later on, it should fall off rapidly. These were proposed by Andritz-Ruthner company and it can be noted here that Ruthner has not specified any references but only comparative data can be obtained for a given series of rubbers. All the MBN composites turned to be good in resisting acid flow to the MS sheets as seen from the closeness of curve to x-axis. For the MBN filled composites the weight change was feeble over 100 days of study. For black filled MBN10 composites weight loss occurs due to leach out of carbon black as indicated by negative weight change. The results went hand in hand with immersion tests.

7c.1.4 Retention in mechanical properties on acid aging

The retention of tensile strength and 50% modulus are the factors of prime importance as far as butyl rubber composites in acid contact are concerned. A minimum requirement for a better lining is at least retention of 50% of its strength and modulus at 50%. The figures 7.16 to 7.18 indicated that the gum vulcanizates resist acid degradation with low ease on its own; but the presence of passive fillers improves their tensile strength by nearly 10% at a filler level of 15phr and as it increased to 50 phr the stabilization increased and BN, MBN exhibited similar behaviours in acid and were better than CB50. MBN exhibited a minor superior stabilization as seen from better retention in aging after 15 weeks acid aging. The 50% modulus increased rapidly for IIR and IIR-CB composites and finally degraded after 15 weeks of aging. The presence of at least 15 phr of MBN or BN improved retention of 100% indicating stabilization.

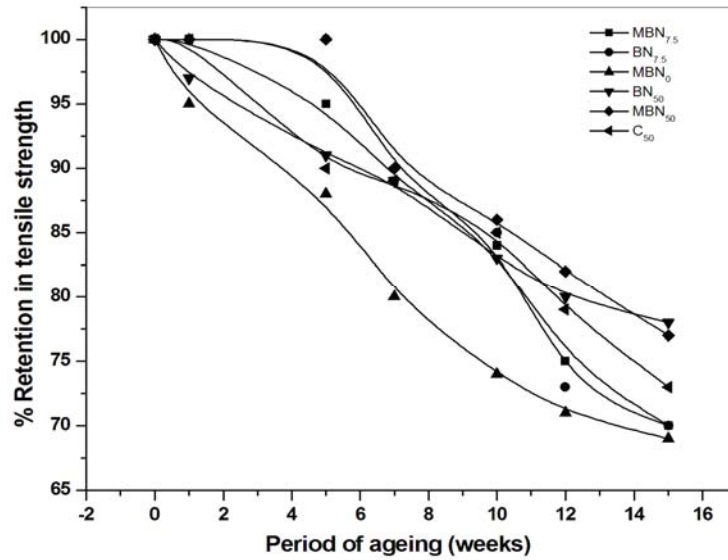


Figure 7.16 Percentage retention in tensile strength of MBN, BN RNCs on acid aging in 75% acid for 15 weeks

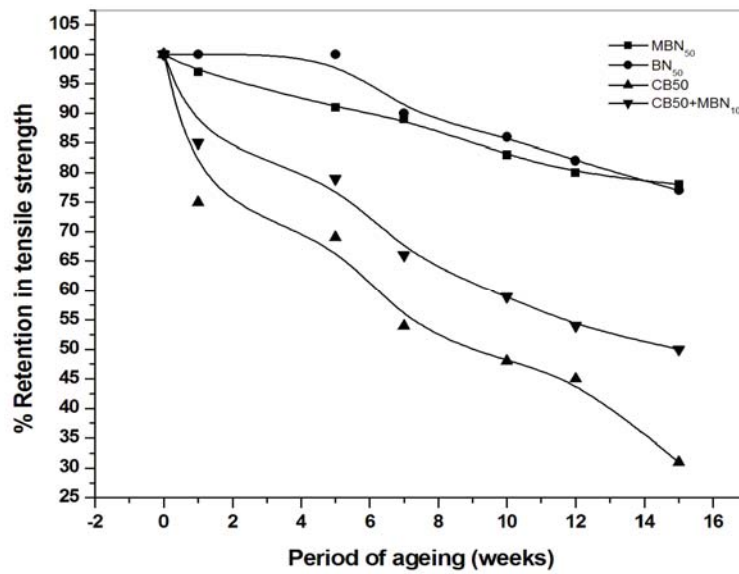


Figure 7.17 Percentage retention in tensile strength of MBN₅₀, BN₅₀, CB50 and CB50+MBN₁₀ RNCs on acid aging in 75% acid for 15 weeks

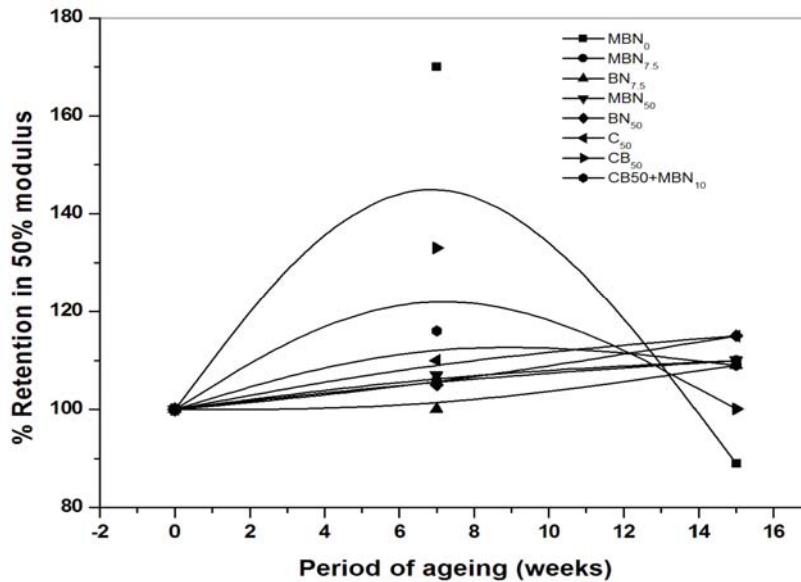


Figure 7.18 Percentage retention 50% modulus of MBN, BN RNCs on acid aging in 75% acid for 15 weeks

7c.1.5 Influence of acid degradation on composite morphology

The SEM photographs of MBN₀ and MBN₁₅ are given below in Fig. 7.19. Even the presence of 15 phr of the filler restricted acid corrosion by creating acid passive rubber filler networks leading to blocks to the crack propagation in RNCs of IIR, whereas from SEM photos of IIR vulcanizates it is clear that the morphology is cracked on acid immersion for 15 weeks.

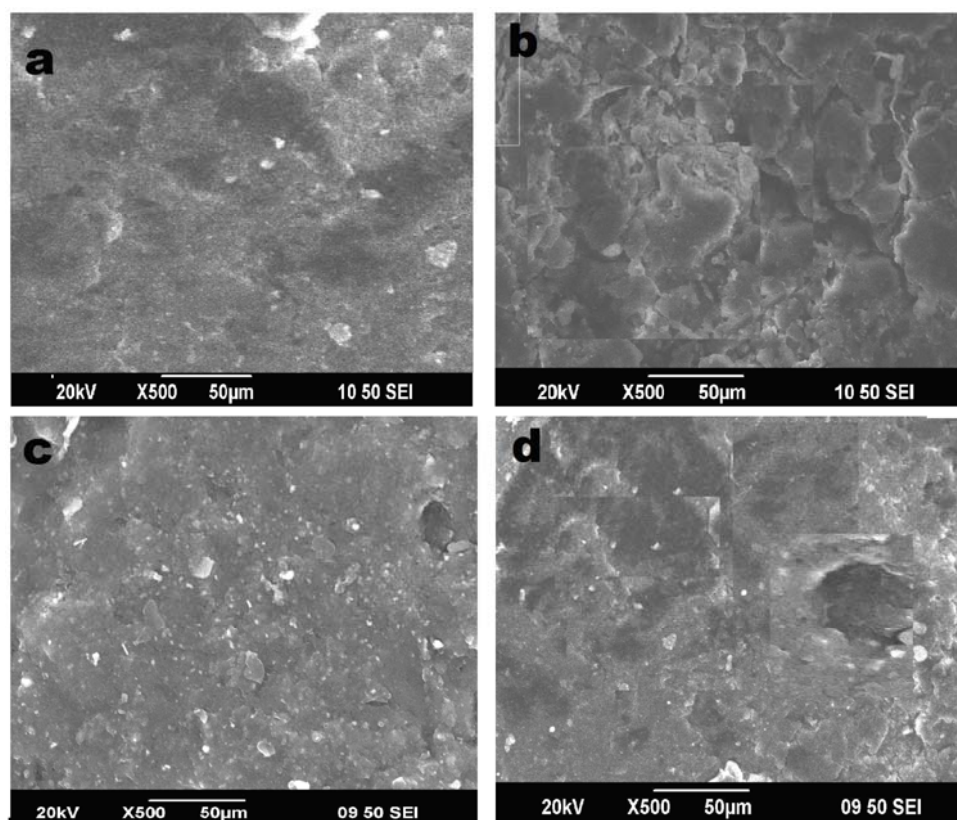


Figure 7.19 SEM photographs 1. a) IIR-MBN₀(pure), b)aged for 15 weeks 2. c) IIR-MBN₁₅(pure) d)aged for 15 weeks in 75% sulphuric acid.

Conclusions

Butyl rubber withstands upto 75% acid concentrations and 80% acid deteriorated the strength properties. Marked reduction of tensile to less than half its initial value within 5 weeks could be observed. So 75% acid concentration was used to measure the corrosion resistance of IIR; filled and unfilled composites in a laboratory scale within a limited span of investigation. All the BN and MBN composites yielded better properties where as black filled ones lost their strength within 5weeks aging. Immersion tests and SEM morphologies evidenced resistance offered by MBN fillers.

References

- [1]. Protective lining by the protective lining applicators-a subdivision of the rubber manufacturers association, Rubber manufacturers association , Washington DC.**1975**
- [2]. M. L.Berins,;Plastics Engineerig Handbook of the Society of Plastics Industry Inc Chapman &Hall, NY. **1991**
- [3]. "The Columbia Encyclopedia".http://www.encyclopedia.com/topic/sulphuric_acid.aspx . **2008**
- [4]. "Sulphuric acid". Encyclopedia Britannica,**1911**,26, 65.
- [5]. V.C.Chandrasekharan;Rubber as a construction material for corrosion protection, Scrivener,MA, **2010**.
- [6]. E. Joselevich, I. Willner; J. Phys. Chem.,**1994** ,98,7628.
- [7]. Manias, Evangelos; Nature Mater.,**2007**,1.
- [8]. Y. Mai, Z. Yu, Y. Mai, Z. Yu. ed. Polymer Nanocomposites. Woodhead Publ. "*Polymer-Clay Nanocomposites*", T. J. Pinnavaia, G. W. Beall (eds.), Wiley, **2006**.
- [9]. U. Arimitsu; K.Masaya; Y.Kojima; A.Okada,T. Kurauchi, O.Kamigaito; *J. Mater. Res.*, **1993**, 8, 1174.
- [10]. N.M.Mathew, A.K.Bhowmick, B.K.Dhindaw, S.K.De; *J.Mater.Sci.*, **1982**,17, 2594.
- [11]. J.A.Riedel, R.VanderLaan, Ethylene Propylene Rubbers.In The Vanderbilt Rubber Handbook,R.T.Vanderbilt co:Newyork;**1973**, 13 ed.,123.
- [12]. A.Rivaton, S.Cambon, J.L.Gardette; *Polym. Degrad. Stab.*, **2006**,91,136.
- [13]. R.S. Rajeev, S.K.DE, A.K.Bhowmick, B.John;*Polym. Degrad. Stab.*, **2003**,79;449.
- [14]. N.S.Tomer, R.P.Delorf singh, J.Lactose;*Polym. Degrad. Stab.*, **2007**,92,457.

- [15]. H.Guirginca, T.Zaharescu, A.Meghea; Polym. Degrad.Stab., **1995**, 50, 45.
- [16]. N.Grassie; Developments in polymer degradation-6.London:Elsevier Applied Science; [chapters3and7] ,**1985**.
- [17]. S.Mitra, S.Ghanbari-Siahkali, P.Kingshott, H.K.Rehmeier, H.Abildgaard, K.Almdal; Polym. Degrad. Stab, **2006,91,69**.
- [18]. A.Rivaton, S.Cambon, J.L.Gardette;Nuclear Instruments and Methods in Phy. Res. B, **2005**, 227,343.
- [19]. S.Mitra, S.Ghanbari-Siahkali, P.Kingshott, H.K.Rehmeier, H.Abildgaard, K.Almdal; Polym Degrd Stab, **2006**, 91, 81.
- [20]. J.Tan, Y.J.Chao, H.Wang, J.Gong, J.W. Vanzee; Polym. Degrad. Stab. **2009**, 94, 2072.
- [21]. X .Wang, H .Zhang, Z .Wang, B.Jiang; Polymer, **1997**,38,540
- [22]. K.Wang, J.S.Wu, Ye.L.Zeng, Compos.Part-A Appl.S. ., **2003,34,1199**.
- [23]. M.Akiba, AS.Hashim;Prog. Polym. sci., **1997**, 22,475.
- [24]. S.M. Clarke, F.Elian, E.M. Terentjev; Eur.Phy.JE Soft Matt., **2000**,2,335.
- [25]. D.Lin-Vien,N.B,colthup,W.G.Fateley,J.G.Grasseli,The Handbook of Infrared &Raman characteristics of organic molecules, Academic Press,Newyork.**1991**

.....❧.....

APPLICATION OF ELASTOMER - BARIUM SULPHATE COMPOSITES AS RADIOPAQUE POLYMERS*

EVALUATION OF RADIOPAQUE OF ELASTOMER-BARIUM SULPHATE COMPOSITES OF NR, EPDM AND IIR USING CLINICAL X-RAYS

8.1 Introduction

8.2 Radiopaque polymers & radiopacity: The role of polymers in X-ray shielding

8.3 Radiopacity and radiopacifiers

8.4 State-of-the art research

Part-a: Studies on the Effect of MBN and BN on the X-Ray Opacity of Natural Rubber

Part-b: Studies on the Effect of MBN and BN on the X-Ray Opacity of Ethylene-Propylene-Diene Rubber.

Part-c: Studies on the Effect of MBN and BN on the X-Ray Opacity of IIR Composites

A series of Barium sulphate-elastomer composites were produced on a laboratory scale, using unmodified and modified barium sulphate fillers having particle size in the nanometre range (BN and MBN). The radiopacity studies at the operating voltage range of medical X-rays (40-100kVp) on the as prepared composites based on NR, EPDM and IIR were carried out. The visibility of rubber samples under X-rays were satisfactory at thickness of 6mm and the elastomer composites exhibited maximum homogeneity in opacity at 40kVp and 5mAs. As the energy of X-rays increased homogeneity in X-ray opacity decreased and opacity diminished beyond 80kVp. The optical density and half-value layer decreased with filler content, whereas the attenuation coefficient of the composites increased with filler loading. The EPDM- MBN filled RC's exhibited better opacities than any other elastomer composite under study and their performances were marginally higher, still; comparable with that of NR-RC's. NR filled with all varieties of barium sulphate fillers exhibited better opacities at loadings under investigation, whereas IIR based RC's rendered poorer opacities under X-rays when compared to NR and EPDM. The maximum value of attenuation coefficient, 1.24cm^{-1} and that of HVL-0.56 cm were obtained with EPDM-MBN₁₅₀. These composites had the least optical density, 0.14 indicating highest radiopacity among all the elastomers composites and turned out to be a better opacifier on comparison with lead shield of 0.1mm thickness. All the elastomer composites having particles in the nanometre range, provided radiopacity higher than composites with commercial fillers. The optical density measurements and hence the calculated attenuation coefficients were supported by radiographic image analyses. The capacity of these fillers to offer opacity as revealed from the studies showed an order corresponding to decreasing surface activity, i.e., MBN>BN>>BC. The radiographic results and mechanical properties when correlated revealed that MBN filled elastomers due to their better ability to get adhered to host matrix helped to impart better opacity than inert BN, BC fillers which rather bonded loosely to the matrix and hence failed to impart such properties to polymers.

* **NishaNandakumar**, PhilipKurian; "Eco-friendly Nanofilled Natural polymer as Novel X-ray shields for Clinical X-rays" International Seminar on New Horizons in Chemistry, Saint Josephs College Irinjalakuda, Thrissur Sep. 2013.

8.1 Introduction

In the space of a century, diagnostic radiology have urbanized considerably to the point of becoming indispensable and incontrovertible tool in all medical specialities [1]. Radiation shielding apparels are commonly used to protect medical patients and X-ray workers from exposure to direct and secondary radiation during investigative imaging in hospitals, clinics and dental offices. In these environments, typical peak X-ray energy spectrum is from 40 to 120 kVp. The photoelectric effect tremendously dominates energy transfer and absorption in this region. Apart from their performance as X-ray shields, another area of application of radiopaque polymers is their ability to allow non-destructive imaging under X-rays. It offers a non-destructive technique for non-invasive evaluation of the performance of a polymeric material used in complicated applications as in tunnel linings beneath sea, tank linings, inner covers and seals, inner tubes of tyres and in various applications. The various realms of X-ray encounter in day to day life are shown in Fig. 8.1 [2].

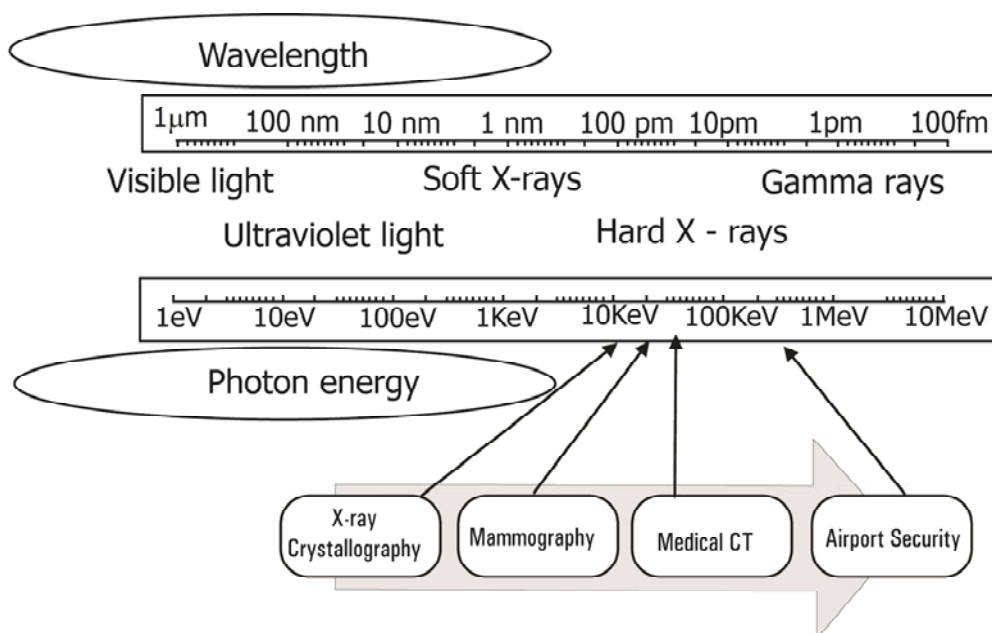


Figure 8.1 Various realms of X-ray encounter in day to day life.

X-ray shielding demands opacity of employed polymers to X-rays where as in X-ray imaging simple visibility is all that is needed. Now days radiation protection materials are applied in aerospace fields for various astronaut in-cabin and out-cabin clothes for space walks, for which a mixture of opacifier additives are used to provide high efficiency of protection. Radiopacity is an indispensable property which renders the devices visible under fluoroscopy or X-ray imaging and has diverse fields of applications as catheters, dental tools, surgical tools and radiation shields. Being denser, these radiopaque materials appear lighter on an X-ray image and this provides the contrast needed to accurately locate or position the device inside the body during critical procedures in surgical applications in the medicinal therapeutic realms. Polymers in general being radiolucent, additives are incorporated in to them for being imaged by X-ray, these fillers called radiopacifiers, attenuate energy differently and provide the contrast in an X-ray radiograph. The type and amounts of radiopaque additives used and the thickness of sample will affect the image contrast and sharpness. In radiopaque elastomers, the purpose of elastomer component is to act as a bonding agent, i.e., to bond the metal particles to form a composite material. The impermeability of a shielding material is proportional to its density and in the light of this concept, lead has been historically used but with health and environmental concerns [3, 4] Lead has good absorbing abilities for radiation with energies higher than 88 (the absorption energies for the K electron shell of Pb is 88 KeV) kilo electron volts (keV) or 3–40 keV, but they weakly absorb radiation with energies between 40–88 keV. This energy region is therefore marked as ‘lead feeble absorbing area’ [4]. The X-ray generated by a general medical tube voltage commonly lower than 130 kVp is in the range starting from and operating mainly at 40kVp, so this is the regular region of X-ray potential used for medical diagnosis. Using lead as radiation shield in this region is thus defective [4-6]. Consequently, the research for lead free radiation material is attracting much interest and some explorations have been conducted to substitute them. In particular, some elements, such as copper, tin, iodine, and barium have been investigated because

their total mass absorption coefficients exceed that of lead for wavelengths longer than 0.141\AA and shorter than the critical absorption wavelength for the K electron shell in these elements [7]. However, the absorption energies for the K electron shell of these elements are 9.0, 29.2, 33.2, and 37.4 keV, respectively. The absorption energy of the K-shell electron of the lighter lanthanides fall in the same range but are not cost effective being rare earths [8-10]. Moreover a major shortcoming of lead is its toxicity. The lead contamination is a serious menace to be faced during the shield preparation, service life and even after disposal after its service life since it pollutes the soil of the landfills and consequently the air and water in which it is disposed. Moreover it is highly toxic to living tissues and enzymes and children are at high risk to hazardous lead poisoning [11].

Fine powders can exhibit inimitable electrical/optical characteristics compared to bulk materials, since surface features are no longer negligible to volume characteristics in this system [12]. Barium sulphate has been integrated into resins to form electrically insulating composites with X-ray attenuation properties and is also applied in the bio mineralization and molecular recognition realms of research [1, 13-16]. Barium sulphate powder is also used in some polymer system as fillers and they are relatively highly sinterable which is very important for preparation of BaSO_4 ceramic. These barium sulphate filled elastomeric composites need to be prepared at higher filler loadings in order to meet the specific requirements. Though the commercial filler in elastomers fail to maintain the properties of polymers, they offer superior opacity and resistance to acids and radiations. Now days, nano materials gained a great deal of attention in both scholarly and industrial research. Fine particle dimensions and narrow size distribution are often important while engineering ceramic materials

8.2 Radiopaque polymers & radiopacity : The role of polymers in X-ray shielding

Polymers are generally radiolucent. Usually the X-rays are absorbed well by dense materials i.e., heavy atoms such as barium and lead. Though rubber is

effective against most beta radiation they cannot be detected by X-ray imaging techniques because they mainly contain the elements such as carbon, hydrogen, oxygen, nitrogen and in some cases elements like silicon. These organic materials containing higher numbers of hydrogen atoms in a given volume such as poly isoprene, synthetic polymers etc., acts as an exceptional base material for X-Ray shielding [17]. However these are susceptible to damage by ionizing radiation than ceramics and metals. Consequently, polymers exhibit relatively low electron density, which render them radiolucent. Sharp images can be obtained only from those materials that are having very high electron density [18, 19]. The common practice for introducing radiopacity is via incorporation of radiopaque fillers. Fillers such as barium sulphate, zirconium oxide, bismuth halides are incorporated to polymers or supporting matrices in order to achieve the necessary X-ray contrast once exposed. Radiopaque materials are widely applied in constructing shields effective in absorbing radiations. The shields could be in a number of different shapes as blocks, plates, rods, pellets etc. One of the major problems these materials have to face is their incompatibility with the polymer matrix. The probability of leaching into the body fluid over long periods of time often affects the physical and mechanical properties of the implant adversely. This can affect the stability of the implant and induce toxicity of metal ions.

8.3 Radiopacity and radiopacifiers

In order for a matrix polymer or compound to absorb radiation, it should contain a radiopaque additive. Radiopacifiers are the substances added to a polymer matrix to impart radiopacity. Radiopacity is now considered as an advantageous property of implants used in surgery as it follows the post operative assessment of the fate of the implant using X-ray radiography [20]. Radiopacity is widely approved as a property of all intra oral materials used in dentistry. Elastomeric impression materials, endodontic sealers, posts and restorative materials, direct filling restorative materials and resin cement luting agents are all radiopaque. The drawback of most of these materials except

barium compounds is their toxicity. Table.8.1 shows opacifiers used in radiopaque materials.

Table 8.1 Elements incorporated into some commercial radiation shielding materials

ELEMENT	ATOMIC NO.	Density (g/cm ³)	K absorption edge (keV)
Cadmium (Cd)	48	8.65	26.7
Indium (In)	49	7.31	27.9
Tin (Sn)	50	7.30	29.2
Antimony (Sb)	51	6.69	30.5
Cesium (Cs)	55	1.87	36.0
Barium (Ba)	56	3.5	37.4
Cerium (Ce)	58	6.66	40.4
Gadolinium (Gd)	64	7.90	50.2
Tungsten (W)	74	19.3	69.5
Lead (Pb)	82	11.36	88.0
Bismuth (Bi)	83	9.75	90.5

8.4 State-of-the art research

The need to maintain elasticity of rubber is of paramount importance under any serious and severe environmental conditions. The same is the requirement for a radiopaque shield. A number of researchers have investigated the significance of elastomers as matrices in radiation protection field. In order to make these matrices fit under service facing radiation corrosion, opacifier incorporation is essential. Polymers could be rendered opaque to X-rays by blending them with radiopacifiers as barium sulphate, tantalum, heavy metal salts as barium bromide, bismuth halides, uranyl nitrate etc. Several different approaches are available in literature for the incorporation of opacifier into polymers of which chelation of opacifier into appropriate polymer ligand is novel. Another approach is to covalently bond a radiopaque agent i.e., a dye to polymer only if the matrix in study is a polymer containing reactive functional group. In the literature it is reported by Cabasso et al. [21] about polymers and monomers that can solubilise heavy metal salts such as barium halides, bismuth halides, uranyl nitrate and lanthanides. Polymer salt complexes of bismuthtribromide and uranyl nitrate with acrylated polyphosphonates [22] have

been synthesized, where the phosphoryl group act as a strong coordinating site to the metal ion. Complexes with polymers containing carbonyl groups have also been synthesized. Barium and zinc acrylates have been reported as radiopacifier and it can be copolymerized with methyl methacrylate [23]. However they are ionic in nature and hence lead to significant absorption of water leading to slow hydrolysis of polyacrylates resulting in loss of the opacifying atoms. Transparent, hard materials were obtained by co-polymerizing MMA and Styryl diphenyl bismuth at 65°C with benzoyl peroxide as initiator [24, 25]. Permanent incorporation of chemical into the polymer structure is a remedial step to avoid the loss by leaching of the heavy metal X-ray contrast agent in any kind of solvent. Matching copolymerization could be obtained with other monomers as styrene or other vinyl monomer [26]. McCaffrey et al. studied the attenuating properties of several types of Pb based and non-Pb radiation shielding materials and a correlation was made of radiation attenuation, materials properties, calculated spectra and ambient dose equivalent [27]. Shielding materials on other hand need a formulation for large scale application for which traditional mill/machinery based preparation is acceptable. Elastomeric as well as plastic materials have been used for matrix application as seen in literature. Lead is the most common shielding material used to protect against X-rays. Ramakrishna et al. prepared Pb-NR composites as X-ray shields, lead-natural rubber composites have been produced on a laboratory scale, and their X-ray shielding abilities were manipulated. The effect of antioxidants on the physical, mechanical and aging properties of the composites were investigated [28]. Rubber composite materials were prepared using styrene-butadiene-rubber as matrices and incorporating with carbon black and PbO₂ for X-ray shielding [29].

Multilayer elastomeric material filled with radiation-attenuating compounds were patented to attenuate radiations using radiopaque filler free of lead using bismuth, tungsten, barium, iodine, Tin and their mixtures in the form of metal oxides or salts. The elastomers used were natural rubber, polybutadiene, polyisoprene,

polyurethane, polychloroprene, silicone rubber, SBR, SBS, isoprene/isobutene such as butyl, and blends [30, 31]. A silicone-based rubber was patented as electrically insulating X-ray shielding device in which the electrically insulating X-ray shielding oxide or nitride particles as cerium, erbium, ytterbium, or some combination were dispersed [32]. Mohammed et al. in their research prepared SBR composite materials using PbO_2 and TiO_2 as fillers and their X-ray opacity was quantified [33]. For the first time, a series of $\text{Gd}(\text{AA})_3/\text{NR}$ (natural rubber) gadolinium composites for X-ray shielding were prepared by an in-situ reaction method. Occurrence of the in situ polymerization of $\text{Gd}(\text{AA})_3$ in composites during peroxide vulcanization of NR markedly improves the dispersion level of the shielding phase by the great reduction of $\text{Gd}(\text{AA})_3$ particle size and the formation of small sized poly- $\text{Gd}(\text{AA})_3$ from the matrix. The X-ray shielding properties of all composites apparently increase with the increase of the degree of dispersion of $\text{Gd}(\text{AA})_3$ [34].

Elastomeric materials alone are not used in shield construction. The versatile radiopacifier triphenylbismuth forms miscible and often optically transparent blends of high radiopacity with a wide range of polymeric materials including polystyrene, polyvinylchloride, polyalkenes, polyacrylates and epoxy resins. Low molecular weight iodine compounds in transparent plastic materials and toys provide improved X-ray contrast. Incorporation of elements of high atomic mass to increase the average electron density and specific gravity of polymers is done in many ways. The radiopaque polymers may be in the form of blends, polymer salt complexes and polymerization products of radiopaque monomers [35-37].

In the present chapter we have reported the preparation of rubber composites with surface modified (MBN) and unmodified (BN) nano barium sulphate at different loadings. The exposure period was selected to be 5mAs from anode heat rating charts for a given kVp. The X-ray attenuation properties of these nano composites were measured at 40kV applied potential for 5mAs

using a clinical X-ray and compared with rubber barium sulphate composites and lead shield standard. In the present study 0.1mm thick lead sheet was used for comparison, since it is the apt thickness used commercially to shield X-ray voltages from 50-80kVp[38-40]. The effects of thickness of rubber sample on radiographs were compared at constant potential of X-ray. The radiographs of nanocomposites were recorded at different applied potentials (40, 50, 60, 80 kVp) for 5mAs. The transmittance percentage of X-rays were accounted in terms of optical density, which indicates the darkening of X-ray caused by passage of radiation through the radiographic film escaping the rubber samples kept as filters in their path. Natural rubber, EPDM and IIR were selected as representative elastomers to form a matrix support to the opacifier and to track the effect of nano filler in these three elastomers. The work also aims at accounting the relation between opacity and rubber-filler interaction. The study aims to assess the performance of fillers in varied elastomer matrices rather than concentrating much into the mechanistic details and stabilities of irradiated elastomers.

Part-a

STUDIES ON THE EFFECT OF MBN AND BN ON THE X-RAY OPACITY OF NATURAL RUBBER

From literature, it is clear that higher amount of opacifier is required for good radiopacity. Generally, most of the fillers used are micron sized particles and hence have poor compatibility with rubber matrix. Therefore it will be difficult to homogeneously disperse these inorganic compounds into the rubber matrix, especially for high loading. The poor dispersion and interfacial interaction leads to poor mechanical properties of rubber composites. The large size of the dispersed phase, in addition to inhomogeneous dispersion, is assumed to limit the shielding performance of the dispersed phase, probably because of the presence of micro-local, micro-non filled rubber parts and the lowering of the probability of interaction between the filler phase and X-ray. In order to improve dispersion surface treatment is a widely acceptable technique. The control of particle size, morphology and crystalline structure of the particles during preparation process is essential to achieve key properties for the appliances. The synthesis and characterisation of barium sulphate nano materials have been reported in chapter.3 of this thesis. The modification of inert surface is also done to enable dispersion. In this section a detailed study on the radiopacity of natural rubber compounded with prepared nano barium sulphate both modified (surface treated) and unmodified is reported. Natural rubber has been selected for this part of work owing to its better mechanical properties, availability and cost effectiveness that make NR applicable to all fields of industrial, medical and automotive sectors of engineering materials. Attempts focus on preparing an X-ray attenuator from a bio polymer and eco-friendly, non-toxic filler. Keeping in mind the plentiful potential of radiopacifiers, we prepared radiopaque polymers from NR through incorporation of nano barium sulphate. The study looks forward to apply it as a non-Pb attenuator for X-rays in the region ranging from

40-80kVp particularly effective at 40kVp which is the normal operating regime of clinical X-rays.

8a.1 Experimental Methods

8a.1.1 Materials used.

- 1) Natural Rubber
- 2) Compounding ingredients like activator, accelerator, curative and antioxidant.
- 3) MBN, BN as radiopacifier
- 4) Lead shield (0.2mm), precipitated barium sulphate for comparing the opacities, the details of all of these materials used are given in chapter 2.

8a.1.2 Radiopacity Studies

Radiopacity of different systems were studied using a general clinical X-ray instrument at 40 kV energy and 5mAs current. In this technique, the radiation from X-ray tube is transmitted through the material and reaches the film. After processing the film (the radiograph) the negative image is obtained, which on developing yields X-ray photographs. The filled radiopaque NR vulcanizates samples were compression moulded to circular specimens and used for radiopacity studies.

8a.1.2.1 Determination of Optical density

The term optical density refers to the degree of blackening of the film. The degree of blackness is directly related to the intensity of radiation. The measurement of blackness is called photographic density or optical density (OD)(section 2.3.13.1).

8a.1.2.2 Determination of attenuation coefficient

The attenuation coefficient of the sample was calculated using the equation as seen in section (section 2.3.13.2).

8a.1.2.3 Determination of Half-value-layer (HVL)

HVL is the absorber thickness required to reduce the intensity of the original beam by one half. The product of the linear attenuation coefficient and half value layer is equal to 0.693(section 2.3.13.3). HVL measures the intensity of a beam.

8a.1.3 Preparation of NR-opacifier composites.

The compounds as per the formulations given in Table 8.2 were mixed on a two roll mill size (15 x 33 cm) and were kept for 24 hrs for maturation. The compounds were moulded in an electrically heated hydraulic press at 150^o C at a pressure of 200 kg/cm² up to respective optimum cure times obtained from RPA. When the amount of opacifier is increased, it becomes very difficult to compound. The amount of radiopacifier was limited to loadings upto 150 phr for ease of compounding. The sheets were cut into dumb bell shape to measure the tensile properties and circular discs to measure radiopacity.

8a.2 Results and discussion

8a.2.1 X-ray Analysis of Natural rubber based radiopaque compound.

8a.2.1.1 X-ray radiographs of samples at constant potential.

The X-ray (obtained using a collimator) photographs of Natural rubber-Barium Sulphate samples with 50 phr concentrations of BaSO₄-MBN, BN and BC can be seen from Fig. 8.1. The radiographs were obtained at an applied potential of 40kVp and 5mAs. It is observed that the visibility of NR-MBN₅₀ is higher than NR-BN₅₀ which is very much greater than NR-BC₅₀ which may be attributed to the effective interaction of matrix and filler and uniform filler dispersion assisted by the presence of modifier. Fig. 8.2 illustrates the effect of increasing filler loading on the X-ray visibility of composites. From Fig. 8.2 it is clear that the radiopacity of NR vulcanizates increased with increase in radio opacifier loading. Even lower loadings of MBN can impart opacity to NR matrix. The Fig. also shows that the radiopacity is higher for NR vulcanizates with 50 phr MBN having particles in the nanometre range, which is comparable with composite containing 150 phr of BC. In the low energy level, radiopacity of a material is mainly reliant on photoelectric effect.

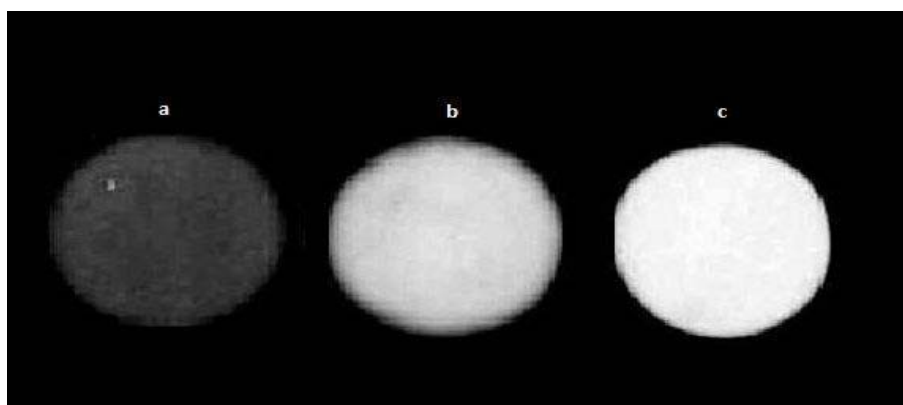


Figure 8.1 X-ray photographs of rubber composites filled with 50 Phr barium sulphate obtained using collimator: a.NR-BC₅₀, b.NR-BN₅₀, c.NR-MBN₅₀

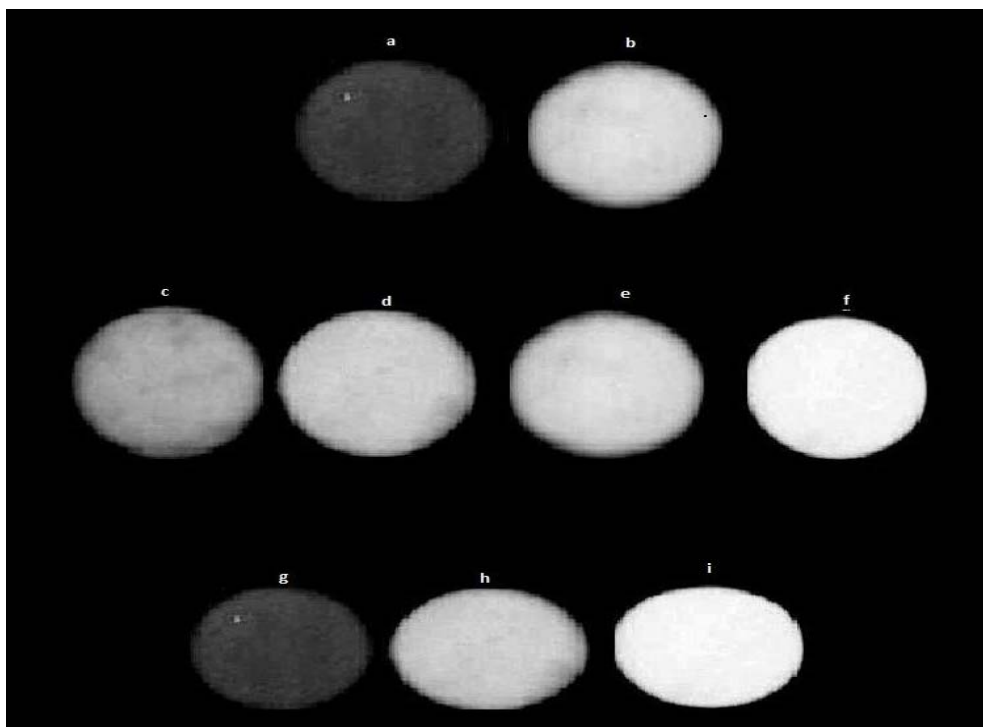


Figure 8.2 X-ray photographs of rubber composites with various filler loadings
a)NR-BN₂₅, b)NR-BN₅₀, c)NR-MBN₁₀, d)NR-MBN₁₅, e)NR-MBN₂₅,
f)NR-MBN₅₀, g)NR-BC₅₀, h)NR-BC₁₀₀, i)NR-BC₁₅₀

8a.2.1.2 Effect of thickness of rubber samples on visibility under X-rays.

Radiopacity of the sample depends on the electron density of the material. Fig. 8.3 shows the positive print of X-rays of samples with varying thickness from 0.77mm to 12mm of NR-MBN₅₀ composite. It shows that the radiopacity varies with thickness of the samples. At a thickness of 0.77mm the radiopacity is very low that, the visibility range is poor. The visibilities of rubber samples are satisfactory only when the thickness is above 6mm. It is clear from the Fig.8.3 that the samples with higher thickness give better radiopacity. At higher thickness, the concentration of the opacifier is high and hence the electron density also increases. When radiopacity increases, the darkening decreases and hence the optical density decreases.

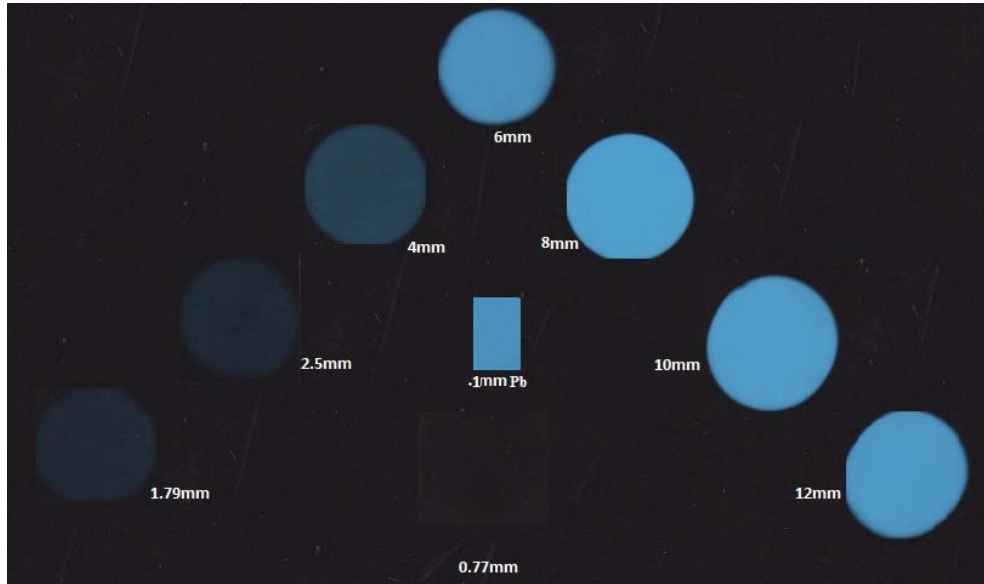


Figure 8.3 Positive prints of X-ray radiographs of rubber samples NR-MBN₅₀ with thickness varied.

8a.2.1.3 Effect of changing applied voltage on visibility of the composites

The Fig. 8.4 shows the photographs obtained by X-rays at different higher energy levels of MBN₅₀. It could be seen that as the energy level increases the opacity is reduced, the effect being more homogeneous at low energy levels of 40, 50 kVp. The decrease in radiopacity at high energy levels is due to increase in penetration of the rays into the sample. The effect is well supported by optical density measurements [38].

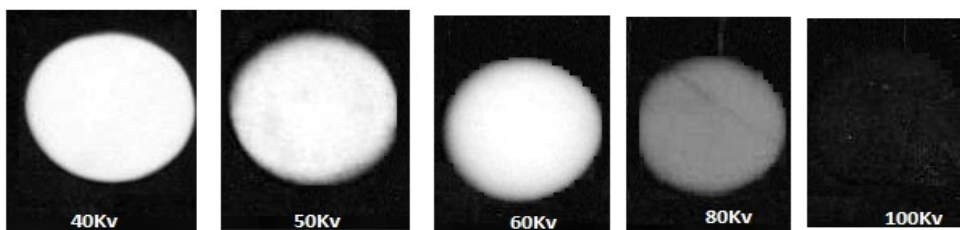


Figure 8.4 Effect of changing energies on the visibility of the composites

8a.2.2 Optical density and linear attenuation coefficient with filler loading

The variation of optical density with amount of filler is shown in graph 8.5.a. When the amount of radiopacifier in the rubber matrix increases the optical density decreases, as it is inversely related to radiopacity. Attenuation is the reduction in the intensity of an X-ray beam as it traverses matter by either the absorption or deflection of photons from the beam. Attenuation coefficient is a measure of the quantity of radiation attenuated by a given thickness of an absorber, specifically referred to as linear attenuation coefficient. The HVL is the absorber thickness required to reduce the intensity of the original beam by one half. The variation of optical density with amount of filler at 40kVp, 5mAs is shown in graph as in Fig. 8.5. The OD values are numerated in Table 8.3. When the amount of radiopacifier in the NR matrix increases the optical density decreases, as it is inversely related to radiopacity. The lead shielder (0.1mm thick lead sheet is used commercially to shield X-ray from 50-80kVp and hence elastomers composites were compared with 0.1mm Pb) had an optical density of 0.169 and Natural rubber control sample had an OD value 1.29 and the optical density 'I' of the back ground was 2.40; at this operating conditions, which can be compared with elastomer based composites at higher loadings. The linear attenuation coefficient increased with filler loading and the higher the value of attenuation coefficient, the better will be the radiopacity. The determination of HVL is a commonly used method in calculating barrier requirements for diagnostic installations. It is the thickness of a specific substance that, when introduced into the path of beam of radiation, reduces the exposure rate by one half [39-41].

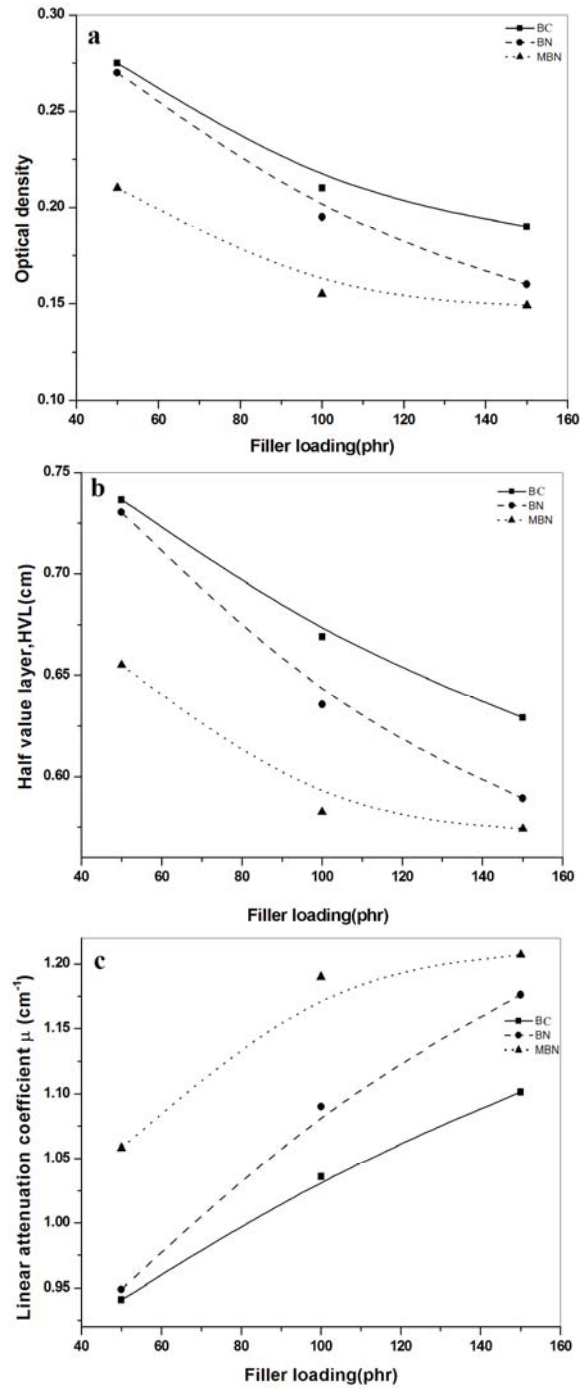


Figure 8.5. a) Optical density b) Linear attenuation coefficient c) Half -value layer of NR-BaSO₄ based rubber composites.

Table 8.3. Various parameters determining X-ray attenuation at an operating voltage of 40kV and 5mAs.

Sl.No:	Sample code	OD	μ (cm ⁻¹)	HVL (cm)
1.	NR-BC ₅₀	0.275	0.9409	0.7365
2.	NR-BC ₁₀₀	0.221	1.0358	0.6690
3.	NR-BC ₁₅₀	0.190	1.1015	0.6292
4.	NR-BN ₅₀	0.270	0.9488	0.7304
5.	NR-BN ₁₀₀	0.195	1.0902	0.6357
6.	NR-BN ₁₅₀	0.160	1.1761	0.5892
7.	NR-MBN ₅₀	0.210	1.0580	0.6550
8.	NR-MBN ₁₀₀	0.155	1.1900	0.5824
9.	NR-MBN ₁₅₀	0.149	1.2070	0.5741

From Fig.8.5 it could be seen that for all NR based RCs the optical density and HVL values decreased with filler loading whereas the linear attenuation coefficient increased. NR-MBN₅₀ had opacity values comparable with that of NR-BC₁₅₀, and NR-MBN₁₅₀ had better radiopacity among all the composites. The BN filled composites have opacities that falls intermediate to that of MBN, BC filled natural rubber composites. The X-ray attenuation data is summarized in Table 8.3.

8a.2.3 Physical properties

Most of the applications met by NR demands retention of physical properties without much deterioration of filler incorporation and so tensile strength of natural rubber filled systems have significance. The physical properties (Fig. 8.6) of various systems indicated the dilution effect of adding higher loadings of radiopaque filler in rubber. These higher filler loadings will lead to loss of strain induced crystallization in NR. Nano sized particles BN, MBN showed better property at loadings of 50 phr, with best properties observed in MBN systems.

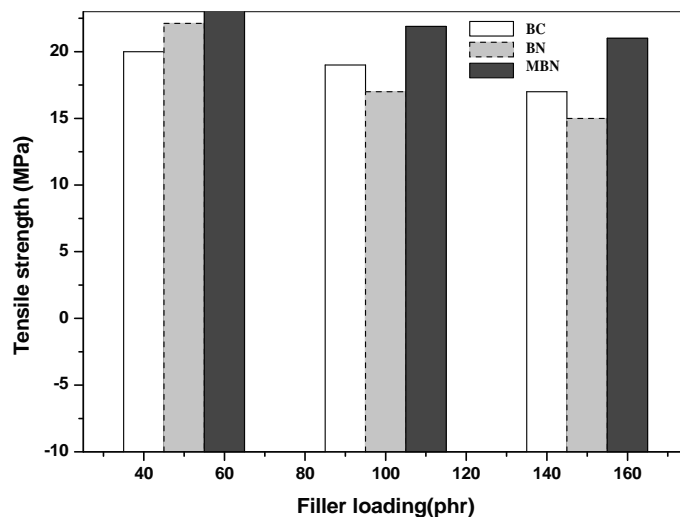


Figure 8.6 Tensile strength of various mixes

The dilution effect leading to loss of property is diminished in the presence of modification which assists dispersion at higher loadings. Improved rubber filler interactions should; and has contributed well into reinforcement and hence opacity to X-rays; the fact being well proved from the opacity studies.

Conclusions

Barium sulphate-natural rubber composites were produced on a laboratory scale, using unmodified and modified barium sulphate fillers having particle size in the nanometre range (BN and MBN). These natural polymer-eco-friendly filler based composites can be used as a non-Pb X-ray attenuator in the realm of medical X-ray examination. The radiopacity studies at the operating voltage range of medical X-rays (40-100kVp) on the as prepared composites based on NR were carried out. The visibility of rubber samples under X-rays were satisfactory at thickness of 6mm and the elastomer composites exhibited maximum homogeneity in opacity at 40kVp and 5mAs. The optical density and half-value layer decreased with filler content, whereas the attenuation coefficient of the composites increased with filler loading. NR filled with all varieties of barium sulphate fillers exhibited better opacities at loadings under investigation.

NR barium sulphate composites turned out to be a better opacifier on comparison with lead shield of 0.1mm thickness. All the elastomer composites having particles in the nanometre range, provided radiopacity higher than composites with commercial fillers. The optical density measurements and hence the calculated attenuation coefficients were supported by radiographic image analyses. NR-MBN₅₀ had opacity values comparable with that of NR-BC₁₅₀ and the maximum value of attenuation coefficient-1.207cm⁻¹ and that of HVL-0.5741cm were obtained with NR-MBN₁₅₀. The ability of MBN to get adhered to the host matrix made it a better candidate as radiopaque filler compared to BN and BC. The inert BN, BC fillers which, rather bonded loosely to the matrix failed to impart superior properties to the host polymer.

References:

- [1] H. Chen, M.M Rogalski and J. N. Anker; Phys. Chem. Chem. Phys., **2012**,14, 13469.
- [2] <http://www.discoveriesinmedicine.com/To-Z/X-ray-Machine.html#ixzz2JugKcpKi>
- [3] J. W. Owens, L. G. Butler, C. Dupard-Julien, K. Garnes, Mater. Res. Bull.,**2001**, 36, 1595.
- [4] L. Liu, L. Q. Zhang, S. H. Zhao, J. Rare Earth, **2002**, 20, 241.
- [5] Liu.L,He.L,Yang.C,Zhang.W,Jin.R,Zhang,L.,Macromol.Rapid Commun., **2004**,25,1197.
- [6] A Guide to the use of Lead for Radiation Shielding, Lead Industries Association, Inc.NY**2001**
- [7] W.W. Edward; The Massachusetts General Hospital, Boston, Mass., A Corporation of Massachusetts, US patent 3514 607,**1970**.
- [8] J. H. Hubbell, Int. J. Appl. Radiat. Isot. **1982**, 33, 1269.
- [9] H. Ebel, R. Svagera, M. F. Ebel, A. Shaltoutz, J. H. Hubbell;X-Ray Spectrom.,**2003**, 32, 442.
- [10] L.Liu, L.Zhang, S.Hu, S.Wen, Z.Wei; US Patents US2012/0012793 A1, **2012**,
- [11] [11a] H. Akira, N. Kazuyuki,K. Hisataka; Matsushita Electric Industrial Co., Ltd., Osaka, Japan, US 4 203 886 ,**1980**.
[11b] J. Q.William, A. L.Paul, Bechtel BWXT Idaho, LLC, Idaho Falls, Id,US 6 166 390,**1998**.
- [12] El Samy and M.shall; Nanotechnology, Molecularly designed materials, ACS Symposium Series 622, Washington DC, Chapter 5, p.79, **1996**
- [13] H.Bala, W. Fu, J. Zhao, X. Ding ,Y. Jiang et al.;Colloids Surfaces A:Physicochem. Eng. Aspects, **2005**,252,129.
- [14] J.Unsworth,B.A. Lunn, P.C. Innis, J.Mater. Sci. Lett., **1993**, 12,132.

- [15] S. Mann, Nature, **1993**, 365, 499.
- [16] B.R. Heywood and S.Mann; Adv. Mater., **1994**, 6, 9.
- [17] NR-PB Referral guidelines for imaging. Radiation Protection. Italy: European Commission [Online], **2000**. Available at [.http://europa.eu.int/comm/environment/radprot/118/rp-118-en.pdf](http://europa.eu.int/comm/environment/radprot/118/rp-118-en.pdf).
- [18] H.H.Candler; J.Biomed. Mater. Res.,**1971**,5, 342,
- [19] D.W.Xia, J.J.Smith; Poly.Sc.Poly.Lett.Ed, **1984**,22,617.
- [20] D.C.Watts and J.F. McCabe; J.Dent, **1999**,27, 73.
- [21] I.Cabasso, J.Smid and S.K.Salmi; J. Appl. Polym.Sci.,**1990**,41 ,3025.
- [22] I.Cabasso, J.Smid, A.Obligin , S.R.Rawls U.S Pat.Filed Oct **1986**.
- [23] E.C.Combe; J. Dent. Res., **1971**,50, 668.
- [24] F.Mottu, D.A.Rufenacht , E.Doelker; Invest.Radiol., **1999** ,323.
- [25] D.F Williams,R.Roaf; Implants in surgery,W.B saunders,London **1973**,p.132
- [26] M.Castillo, J.Yillalobos ,J.Walker.; United States Patent, 6,077,880,June 20, **2000**
- [27] J. P. McCaffrey, H. Shen, B. Downton, E. Mainegra-Hing; Med. Phys., **2007**,2, 34.
- [28] Ramakrishna et al.; Mater. Sci. Technol., **1986**, 2.
- [29] Madani , A.I. Abd-El Hafez ; Particle Phy. Insights ,**2010**,3 ,9.
- [30] Hatanaka et al.; Radiation shielding,US patent 20077274031 ,**2007**.
- [31] P.Sonntag, R. Krikorian,P, Hoerner;Multilayer elastomeric material filled with radiation-attenuating compounds,preparation method and uses thereof ,US patent,US20080182093A1,**2008**.
- [32] T. S. Parker,J. E. Burke Electrically insulating X-ray shielding devices in an X-ray tube US patent 20120106713,**2012**
- [33] M.H.Al-Maamori, O.H. Bodairy, N. A. Saleh, Nat. Appl. Sci., **2012**, 3, 3.

- [34] L.Liu, L. He, C. Yang, W. Zhang, R.Guang Jin, L.Q. Zhang; *Macromol. Rapid Commun.* **2004**, 25, 1197.
- [35] M.Castillo, J.Yillalobos and .J.Walker; United States Patent, 6,077,880, June 20 **2000**.
- [36]. V.S Nisha, R.Joseph; *Rubber Chem. Tech.*,**2006**,79,1.
- [37] Wikipedia – The free encyclopedia-**2012**.
- [38] J.H. Hubbell;Photon cross-section,attenuation coefficient from 10Kev to 100Gev,Washington,DC,U.S.NBS,Handbook 29,**1969**
- [39] S.C. Buschong;Development of radiation protection in diagnostic radiology,Cleveland,CRC press,**1973**
- [40] E.J. Hall;Radiobiology for the radiologist.Hagerstown,MD,Harper and Row,**1973**.
- [41] Recommendations on limits for exposure to Ionising radiation .National council on Radiation Protection and Measurements,7910 Woodmont ave, Bethesda, MD28814.NCRP report no:91,**1987**.

Part-b

STUDIES ON THE EFFECT OF MBN AND BN ON THE X-RAY OPACITY OF ETHYLENE PROPYLENE DIENE RUBBER.

Ethylene-propylene-diene terpolymers (EPDM) represents a class of elastomers with a saturated backbone which makes these materials resistant against weathering [1, 2]. During outdoor applications the rubber surfaces have to face weathering conditions such as radiation [3], heat [4, 5], ozone [6] chemical media [7,8] etc., which can deteriorate its surface properties and results in loss of bulk properties. EPDM rubbers, because of their excellent resistance to degradation and easiness to accept large amounts of fillers coupled with electrical insulation properties, are widely used in wire and cable coatings. An example would be cables in nuclear power plants which may be exposed to elevated temperatures and gamma irradiation. These conditions are known to cause their aging and consequently the degradation over time. Aging by gamma irradiation of crosslinked EPDM elastomers has been studied for unfilled rubbers [1-5]. Chain scissions and crosslinking mechanisms have been evidenced, depending on the irradiation conditions and on the polymer formulation. These raw elastomers can be tailored to meet specific requirements by incorporation of fillers. Nevertheless, fillers can influence the degradation mechanism. They themselves can act as opacifiers by blocking these radiations or they can modify the polymer degradation by trapping radicals or degradation by-products which can interact with intermediate chemical species involved in the matrix degradation. They can also be degraded and led to the formation of supplementary degradation by-products, which can interact with the matrix degradation process. Moreover, whether they are still inert or not during the matrix degradation, this matrix degradation can induce a modification of the filler-matrix interaction: this may have consequences in the reinforcement efficiency of the filler, and therefore be involved in the consequences of the degradation in the overall properties of the composite.

EPDM has been selected for this part of work owing to its better weathering resistances and affordability of high filler loadings and to utilise its

imparted opacity to all fields of industrial, medical equipment and automotive sectors of engineering materials. Barium sulphate widely known for its radiopacity has been incorporated into EPDM to develop radiopaque rubbers. The influence of fillers such as barium sulphate on the rubbers and then its consequences on the mechanical properties have been scarcely investigated. In this section a detailed study on the radiopacity of EPDM rubber compounded with barium sulphate both modified and unmodified is reported. Keeping in mind the plentiful potential of radiopaque material, an attempt is made to prepare radiopaque polymers suiting clinical X-ray fields, out of EPDM rubber through incorporation of these fillers. When radiopacity is imparted to these materials then it will be a new vista to the era of high voltage insulators with radiopacity. The materials find applications in X-ray tube housing and cables and wires used in X-ray exposed regions specifically that of medical industry.

8. b. 1 Experimental

8. b. 1. 1. Materials Used

- 1) Ethylene propylene diene rubber
- 2) Compounding ingredients like activator, accelerator, curative and antioxidant.
- 3) MBN, BN as radiopacifier
- 4) Precipitated barium sulphate for comparing the opacities. The details of all these materials used is given in chapter 2.

8.b.1.2 Preparation of EPDM -opacifier composites.

The compounds as per the formulations given in Table 8.4 were mixed on a two roll mill size (15 x 33 cm) and were kept for 24 hrs for maturation. The compounds were moulded in an electrically heated hydraulic press at 160° C at a pressure of 200 kg/cm² up to respective optimum cure times obtained from RPA. The amount of radiopacifier was limited to 150 phr for ease of study. The sheets were cut into discs to measure radiopacity. (Section 2.3.13)

8b.2 Results and discussion

8b.2.1 X-ray Analysis of Ethylene Propylene Diene rubber based radiopaque compound.

8.b.2.1.1 X-ray radiographs of samples at constant potential.

The X-ray (obtained using a collimator) photographs of EPDM-Barium Sulphate samples with 50 phr concentrations of BaSO₄-MBN, BN and Barium sulphate can be seen from Fig.8.7. The radiographs were obtained at an applied potential of 40kVp and 5mAs. It is observed that the visibility of EPDM-MBN₅₀ is higher than EPDM-BN₅₀ which is much better than EPDM-BC₅₀. Fig.8.8 illustrates the effect of increasing filler loading on the visibility of composites. From Fig. 8.8 it is clear that the radiopacity of vulcanizates increases with increase in radiopacifier loading. Even lower loadings of MBN can impart opacity to EPDM matrix. The Fig. also shows that the radiopacity is higher for EPDM vulcanizates with 50 phr nano MBN which is nearly equal to composite containing 150 phr of precipitated barium sulphate(BC). In the low energy level, radiopacity of a material is mainly reliant on photoelectric effect.

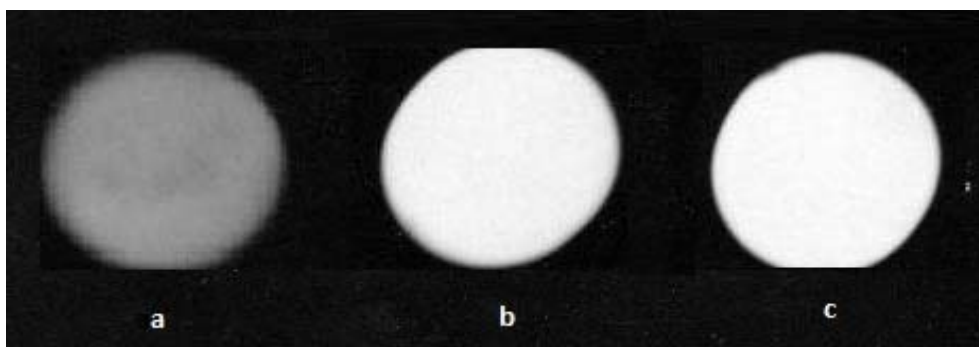


Figure 8.7 X-ray photographs of 50 Phr filled rubber composites obtained using collimator. a. EPDM-BC₅₀ b. EPDM -BN₅₀, c. EPDM -MBN₅₀

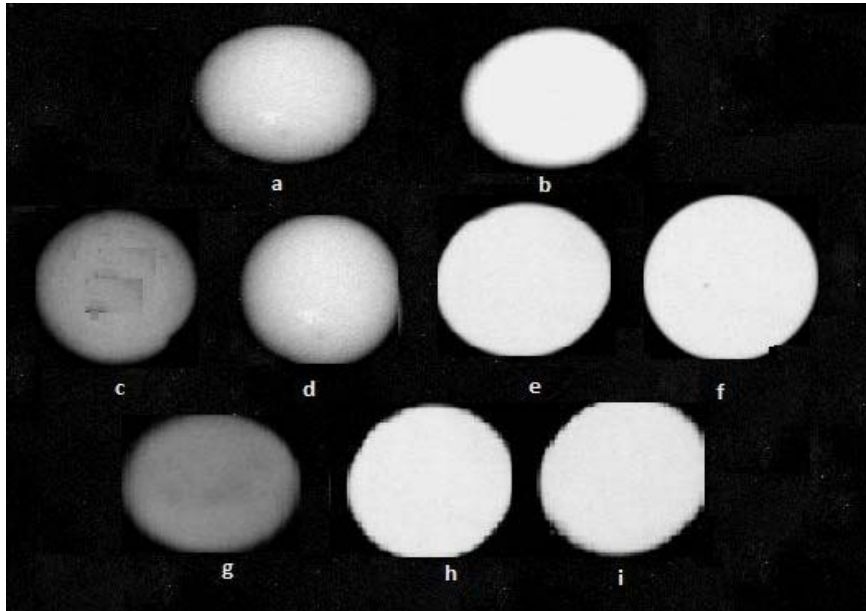


Figure 8.8 X-ray photographs of Rubber composites with various filler loadings. a. EPDM BN₅₀ ,b. EPDM -BN₁₀₀ ,c.EPDM-MBN₁₅ d. EPDM- MBN₂₅ f.EPDM-MBN₅₀, EPDM-MBN 100 g.EPDM-BC₅₀ , h.EPDM-BC₁₀₀, i.EPDM-BC₁₅₀

8b.2.1.2 The effect of sample thickness

The opacity varied more or less as seen in Fig.8.4 for NR composites

8b.2.1.3 Effect of changing applied voltage on visibility of the EPDM composites.

The Fig. 8.9 shows the photographs obtained by X-rays at different higher energy levels. It could be seen that as the energy level increases the opacity is reduced, the effect being more homogeneous at low energy levels of 40,50,60 kVp. The decrease in radiopacity at high energy levels is due to increase in penetration of the rays into the sample and also K-edge value of barium sulphate. This effect is well supported by optical density measurements.

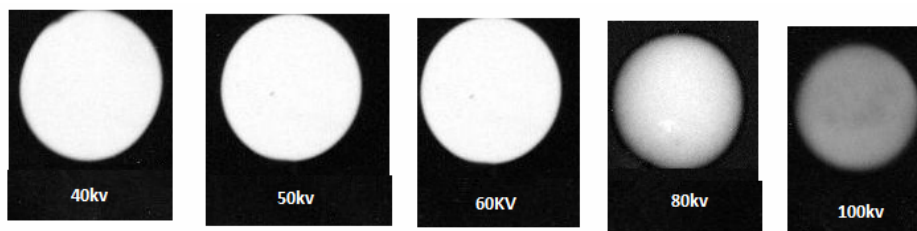


Figure 8.9 Effect of changing energies on the visibility of the composites

8b.2.2 Optical density(OD) and linear attenuation coefficient (μ)of the composites

The variation of optical density with amount of filler at 40kVp, 5mAs is shown in graph as in fig 8.10. The OD values are numerated in Table 8.5. When the amount of radiopacifier in the EPDM matrix increases the optical density decreases, as it is inversely related to radiopacity. The lead shielder had an optical density of 0.169 and EPDM rubber control sample had an OD value 1.313 and the optical density 'T' of the back ground was 2.40 at this operating conditions. For commercial barium sulphate (BC) and unmodified nano barium sulphate (BN) powders the variation in optical density was more or less similar; but on incorporation of modified nano powders the OD values decreased drastically. Since filler loading varies similarly in all the three cases, this sharp change is the result of improved rubber-filler interaction in MBN composites, compared to the dilution effect of BN, BC's. The influence of higher loadings in EPDM RC's on tensile strength is less investigated since all applications involving EPDM demands its weathering resistances rather than mechanical strengths. The linear attenuation coefficient increased with filler loading and the higher the value of attenuation coefficient, the better will be the radiopacity. The HVL value also decreased on increased loading and results being best with MBN loaded RC. A detailed portrayal of these facts is as below:

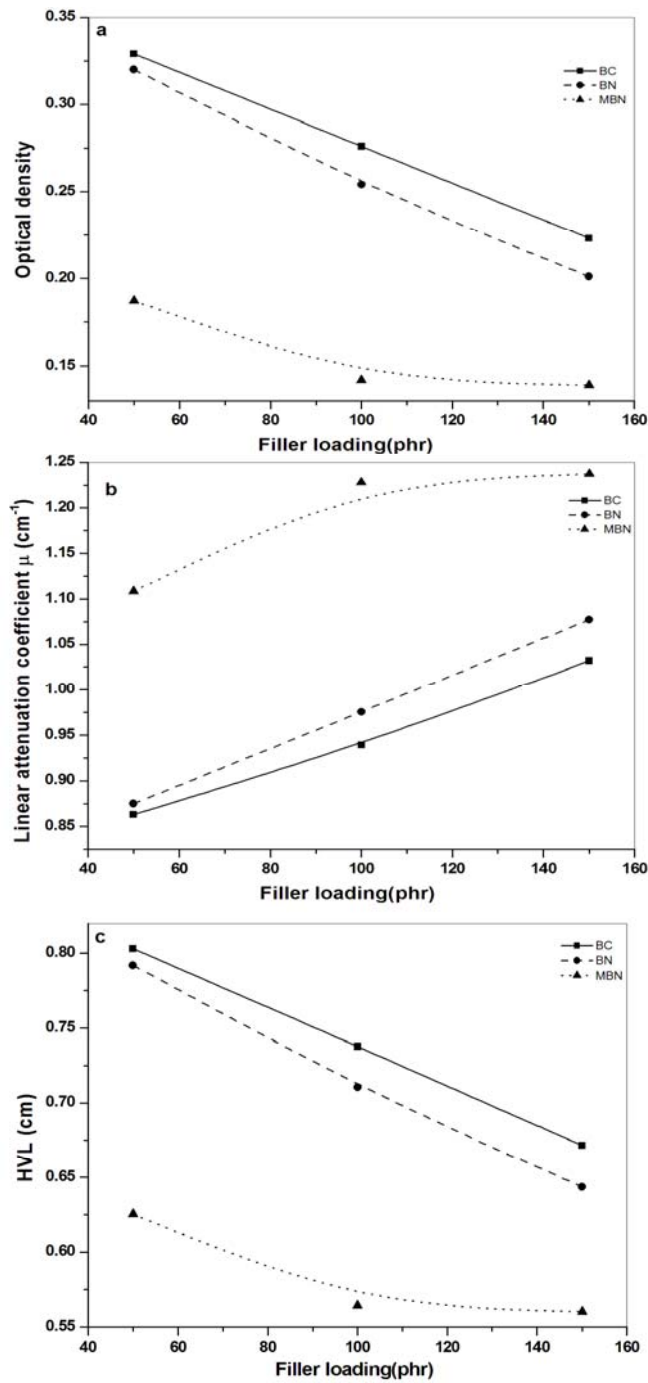
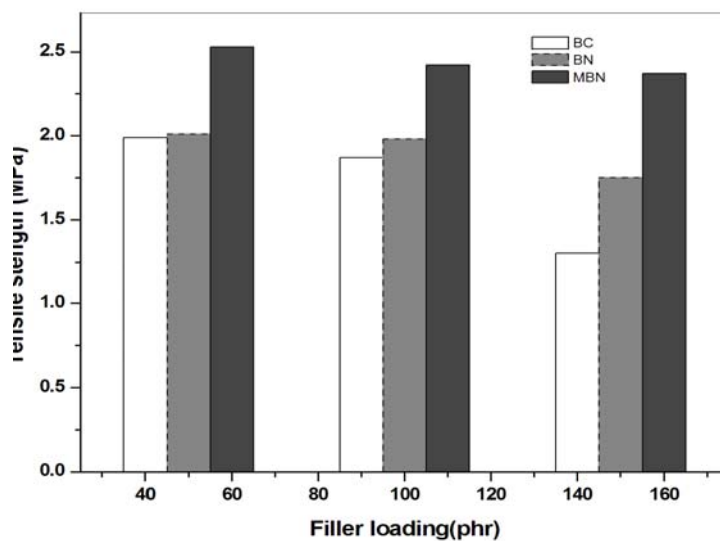


Figure 8.10 a) optical density b) linear attenuation coefficient c) The half -value layer of EPDM-BaSO₄ based Rubber Composites.

Table 8.5 Various parameters determining X-ray attenuation at an operating voltage of 40kV and 5mAs.

Sl.No:	Sample code	OD	$\mu(\text{cm}^{-1})$	HVL(cm)
1.	EPDM-BC ₅₀	0.329	0.8630	0.8030
2.	EPDM-BC ₁₀₀	0.276	0.9393	0.7378
3.	EPDM-BC ₁₅₀	0.223	1.0319	0.6716
4.	EPDM-BN ₅₀	0.320	0.8751	0.7919
5.	EPDM-BN ₁₀₀	0.254	0.9754	0.7105
6.	EPDM-BN ₁₅₀	0.201	1.0770	0.6434
7.	EPDM-MBN ₅₀	0.187	1.1084	0.6252
8.	EPDM-MBN ₁₀₀	0.142	1.2279	0.5644
9.	EPDM-MBN ₁₅₀	0.139	1.2372	0.5601

8b.2.3 Physical property:**Figure 8.11. Tensile strength of various mixes**

The determination of tensile strength revealed that, dilution effect predominates at higher loading. Unfortunately, EPDM rubber shows poor tensile strength because of its low degree of unsaturation and the position of the unsaturation being not in the polymer backbone [11]. A frequent application met by EPDM demands environmental resistances without much deterioration on filler

incorporation. So tensile strength of natural rubber filled systems has significance. The physical properties of various systems indicated minor dilution effect of adding higher loadings of radiopaque filler in rubber. Nano sized particles showed better property at loadings of 50 phr, with better property observed in MBN systems. The dilution effect leading to loss of property is diminished in the presence of modification which assists dispersion at higher loadings and nearly 95% of strength is retained. Improved rubber filler interactions have contributed well into reinforcement and hence the opacity to X-rays.

Conclusions

Barium sulphate-EPDM composites were produced on a laboratory scale, using unmodified and modified barium sulphate fillers having particle size in the nanometre range (BN and MBN) and compared with commercial precipitated barium sulphate (BC). These elastomer-eco-friendly filler based composites can be used as a non-Pb X-ray attenuator in the realm of medical X-ray examination. The radiopacity studies at the operating voltage range of medical X-rays (40-100 kVp) carried out showed that the visibility of rubber samples under X-rays were satisfactory at thickness of 6mm and the elastomer composites exhibited homogeneity upto 80kVp with maximum at 40kVp and 5mAs. The optical density and HVL decreased with filler content, whereas the attenuation coefficient of the composites increased with filler loading. The results showed that the opacity highly depended on dispersion level of fillers assisted by modifier treatment. The dispersion level of the shielding phase in the elastomers improved with reduction of particle size of barium sulphate (BN, MBN) and X-ray shielding properties of all the composites apparently increase with increase in dispersion degree of filler in (MBN) composites. EPDM with all varieties of barium sulphate fillers exhibited better opacities at loadings under investigation and turned out to be better opacifier on comparison with lead shield of 0.1mm thickness. All the elastomer composites having particles in the nanometre range, provided radiopacity higher than composites with commercial fillers. The optical

density measurements and hence the calculated attenuation coefficients were supported by radiographic image analysis. EPDM-MBN₅₀ had opacity values comparable with that of BC₁₅₀. But of all the composites EPDM MBN₁₅₀ composites attained best results with an attenuation coefficient of 1.24cm⁻¹ and HVL of 0.56cm. The capacity of these fillers to offer opacity showed an order MBN>>BN>BC corresponding to decreasing surface activity. The radiographic results and mechanical properties revealed that, inspite of the dilution effect at higher filler levels, MBN filled elastomers due to their better ability to get adhered to host matrix helped to provide higher effectiveness in opacity than inert BN, BC fillers which rather bonded loosely to the matrix and hence failed to impart such properties to the host polymer.

References:

- [1] J.A.Riedel, R.VanderLaan, Ethylene Propylene Rubbers.In The Vanderbilt Rubber Handbook,R.T.Vanderbilt co:New york;**1973**, 13 ed.,123.
- [2] A.Rivaton, S.Cambon, J.L.Gardette; Polym. Degrad. Stab., **2006**,91,136.
- [3] R.S.Rajeev,S.K.DE,A.K.Bhowmick,B.John;Polym.Degrad.Stab.,**2003**,79; 449.
- [4] N.S.Tomer, R.P.Delorf singh, J.Lactose;Polym. Degrad. Stab., **2007**;92,457.
- [5] H.Guirginca, T.Zaharescu, A.Meghea; Polym. Degrad.Stab.,**1995**,50,45.
- [6] N.Grassie; Developments in Polymer Degradation-e 6.London:Elsevier Applied Science; [chapters3and7] ,**1985**.
- [7] S.Mitra, S.Ghanbari-Siahkali, P.Kingshott, H.K.Rehmeier, H.Abildgaard, K.Almdal; Polym. Degrad. Stab.,**2006**,91,69.
- [8] A.Rivaton, S.Cambon, J.L.Gardette;Nuclear Instruments and Methods in Physics Research B, **2005**, 227,343.
- [9] N.Celette, I.Stevenson, L.David, J.Davenas, G.Vigier, G.Seytre; Nuclear Instruments and Methods in Physics Research B, **2001**, 185,305.
- [10] E.Planes, L.Chazeau, G.Vigier, Fournier; J.Polymer,**2009**,50 ,4028.
- [11] M. Morton, Ed., Rubber Technology; Van Nostrand Reinhold, NewYork, **1987**,3

Part-c

STUDIES ON THE EFFECT OF MBN AND BN ON THE X-RAY OPACITY OF IIR COMPOSITES.

Among the various elastomers available for barrier applications, the most well-known and widely applied materials are isobutylene-isoprene copolymer, commonly-called butyl rubber, and its derivatives [1-2]. Butyl rubber is reported to have very low permeability to gases or liquids [3-4]. Often reinforced with particulate fillers or fibers, butyl rubber and its derivatives are utilized in personal protective clothing (including gloves and coveralls) as well as pneumatic tire liners. These peculiarities make IIR applicable to all fields of industrial and automotive sectors of engineering materials [5]. Keeping in mind the plentiful potential of radiopaque material, an attempt was made to prepare radiopaque polymers from IIR through incorporation of nano barium sulphate. Imparting opacity to IIR finds application in industrial barrier formularies and in tyre industry. The present investigation aims at imparting opacity to compounded IIR, following a basic formulary and to find the level and type of filler loading responsible for rendering it opaque under X-rays without much compromise in physical strength.

8.c.1 Experimental

8.c.1.1 Materials Used

- 1) IIR
- 2) Compounding ingredients like activator, accelerator, curative and antioxidant.
- 3) MBN, BN as radiopacifier
- 4) Lead shield, precipitated barium sulphate for comparing the opacities, The details of all of these materials used are given in chapter 2.

8.c.1.2 Preparation of IIR-opacifier composites.

The compounds as per the formulations given in Table 8.6 were mixed on a two roll mill size (15 x 33 cm) and were kept for 24 hrs for maturation. The compounds were moulded in an electrically heated hydraulic press at 170^o C at a pressure of 200 kg/cm² up to respective optimum cure times obtained from RPA. When the amount of opacifier was increased, it became very difficult to compound. The amount of radiopacifier was limited to 150 phr for ease of compounding. The sheets were cut into dumb bell shape to measure the tensile properties and discs to measure radiopacity.

8c.2 Results and discussion.

8c.2.1 X-ray Analysis of IIR based radiopaque compound.

8c.2.1.1 X-ray radiographs of samples at constant potential

The X-ray (obtained using a collimator) photographs of IIR-Barium Sulphate samples with 50 phr concentrations of BaSO₄-MBN, BN and Barium sulphate can be seen from Fig. 8.12. The radiographs were obtained at an applied potential of 40 kVp and 5mAs. It is observed that the visibility of IIR-MBN₅₀ is higher than IIR-BN₅₀ which is very much greater than IIR-BC₅₀ which may be attributed to the interaction of matrix and filler and filler dispersion. Fig. 8.13 illustrates the effect of increasing filler loading on the visibility of composites. From Fig. 8.13, it is clear that the radiopacity of vulcanizates increases with increase in radiopacifier loading. Lower loadings of MBN can impart opacity to IIR matrix. The Fig. 8.12 also shows that the radiopacity is higher for IIR vulcanizates with 50 phr nano MBN which is nearly equal to composite containing 150 phr of BC. In the low energy level, radiopacity of a material is mainly reliant on photoelectric effect. Again a minimum of 100 phr filler is needed to impart opacity in the case of IIR composites as seen from attenuation data.

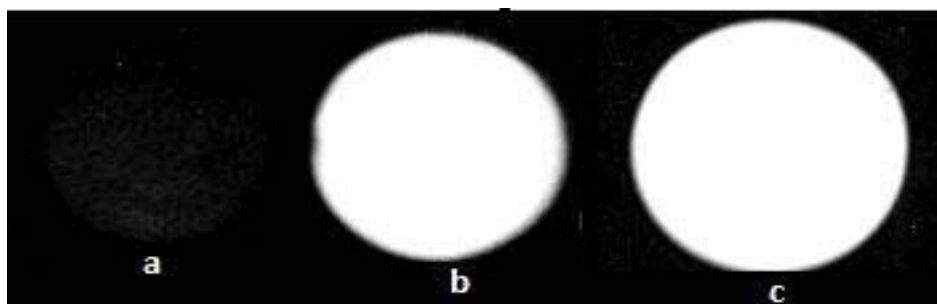


Figure 8.12 X-ray photographs of 50 Phr filled rubber composites obtained using collimator a.IIR-BC₅₀, b.IIR-BN₅₀, c.IIR-MBN₅₀

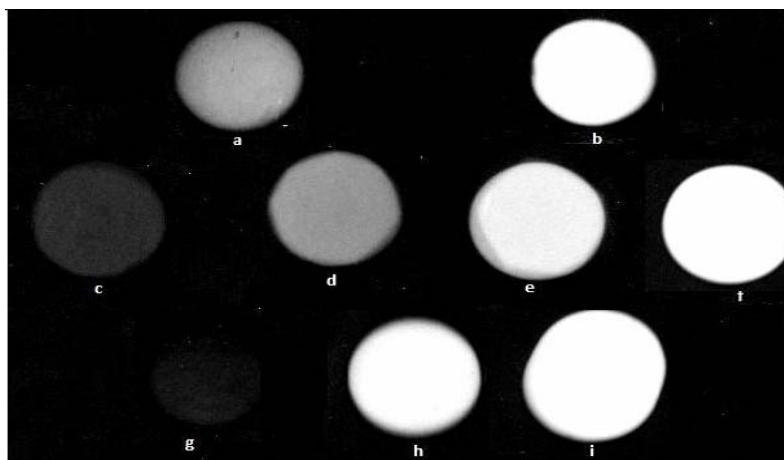


Figure 8.13 X-ray photographs of Rubber composites with various filler loadings. a. IIR-BN₅₀ ,b. IIR-BN₁₀₀ ,c. IIR-MBN₁₅ d. IIR- MBN₂₅ e. IIR-MBN₅₀,f. IIR-MBN₁₀₀g. IIR-BC₅₀, h. IIR-BC₁₀₀, i. IIR-BC₁₅₀

8c.2.1.2 The effect of sample thickness

The comparative opacity varied more or less as seen in Fig. 8.4part 1

8c.2.1.3 Effect of changing applied voltage on visibility of the composites

The Fig. 8.14 shows the photographs obtained by X-rays at different higher energy levels. It could be seen that as the energy level increases the opacity is reduced, the effect being more homogeneous at low energy levels of 40 kVp. The decrease in radiopacity at high energy levels is due to increase in penetration of the rays into the sample. 40-50 kVp range of X-rays give homogeneous radiographs and above that visibility diminishes drastically. The effect is well supported by optical density measurements.

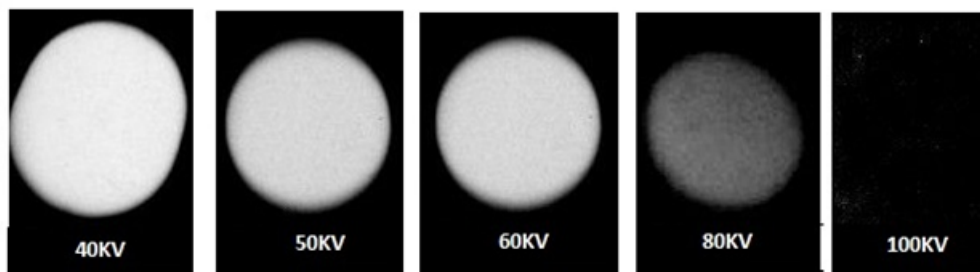


Figure 8.14 Effect of changing energies on the visibility of the composites .

8c.2.2 Optical density(OD) and linear attenuation coefficient (μ)of the composites

The OD values are numerated in Table 8.7. When the amount of radiopacifier in the IIR matrix increases the optical density decreases, as it is inversely related to radiopacity. The lead shielder had an optical density of 0.169 and IIR rubber control sample had an OD value 1.363 and the optical density 'I' of the back ground was 2.40 ;at this operating conditions, which can be compared with elastomer based composites at higher loadings. For commercial barium sulphate (BC) and unmodified nano barium sulphate (BN) powders the variation in optical density was more or less similar; but on incorporation of modified nano powders the OD values decreased drastically. Since filler loading varies similarly in all the three cases, this sharp change is the result of improved rubber-filler interaction in MBN composites, compared to the dilution effect of BN, BC. The linear attenuation coefficient increased with filler loading and the higher the value of attenuation coefficient, the better will be the radiopacity. HVL decreased on increased loading and results being best with MBN loaded RC's. A detailed portrayal of these facts are shown in following Table 8.7and graphs (Fig. 8.15)

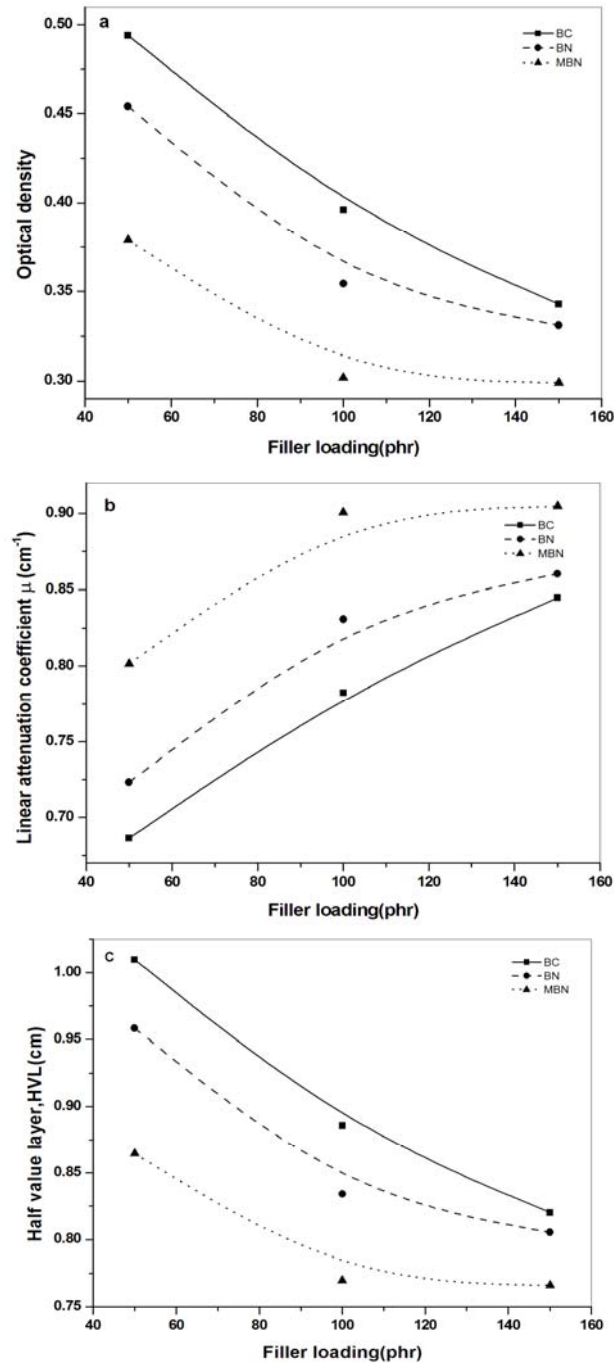


Figure 8.15. a) optical density b) linear attenuation coefficient c) The half - value layer of IIR-BaSO₄ based Rubber Composites.

Table 8.7 Various parameters determining X-ray attenuation at an operating voltage of 40kV and 5mAs

Sl.No:	Sample code	OD	$\mu(\text{cm}^{-1})$	HVL(cm)
1.	IIR-BC ₅₀	0.494	0.6865	1.0095
2.	IIR-BC ₁₀₀	0.396	0.7825	0.8856
3.	IIR-BC ₁₅₀	0.343	0.8449	0.8202
4.	IIR-BN ₅₀	0.454	0.7236	0.9583
5.	IIR-BN ₁₀₀	0.354	0.8307	0.8342
6.	IIR-BN ₁₅₀	0.331	0.8604	0.8055
7.	IIR-MBN ₅₀	0.379	0.8016	0.8646
8.	IIR-MBN ₁₀₀	0.302	0.9005	0.7696
9.	IIR-MBN ₁₅₀	0.299	0.9045	0.7661

8c.2.3 Physical Properties

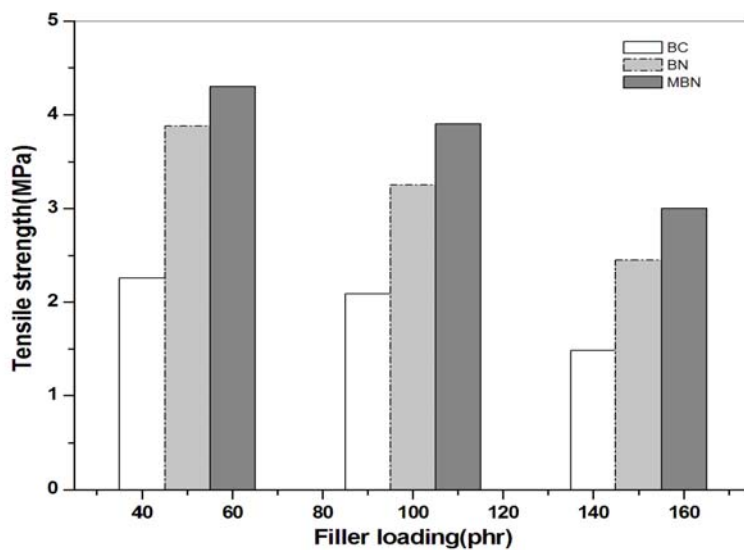


Figure 8.16 Tensile strength of various mixes

From the period of mill mixing onwards, the incompatibility of filler BC was manifested in the form of flaky powders on the filled butyl mix surfaces, where as no such appearances were observed in BN, MBN mixes. The influence

of higher loadings in IIR RC on tensile strength is less investigated since all applications involving IIR demands its impermeability to air, X-ray and acid resistances rather than mechanical strength. The poor wettability due to increased filler loading not only failed to impart strength to IIR, but also deteriorated its properties. Nano sized particles BN, MBN showed better property at loadings of 50 phr, the effect being predominant with MBN systems. This may be attributed to better physical bonding and dispersion of filler into rubber, in the absence of chemical compatibility. The dilution effect leading to loss of property is manifested strongly even in the presence of modification at all levels of loading and hence the opacity to X-rays.

Conclusions

Barium sulphate-IIR composites were produced on a laboratory scale, using unmodified and modified barium sulphate fillers having particle size in the nanometre range (BN and MBN) and compared with commercial precipitated barium sulphate (BC). These elastomer-eco-friendly filler based composites enable them to be visible under X-ray examinations, though not effective as non-Pb X-ray attenuator in the realm of medical X-ray examination. The radiopacity studies at the operating voltage range of medical X-rays (40-100 kVp) showed that the visibility of rubber samples under X-rays were satisfactory at thickness of and above 6mm. The elastomers composites exhibited better homogeneity in opacity at 40 kVp and 5mAs and opacity remained homogeneous only upto 60 kVp. The optical density and half-value layer decreased with filler content, whereas the attenuation coefficient of the composites increased with filler loading. The opacity of composites appears to be dependant on dispersion level of fillers to a small extent. The dispersion level of the shielding phase in the elastomers improved with reduction of particle size of barium sulphate (BN, MBN) imparting it better shielding properties. All the elastomer composites having particles in the nanometre range, provided radiopacity better than composites with commercial fillers. The optical density measurements and hence

the calculated attenuation coefficients were supported by radiographic image analyses. IIR-MBN₅₀ had opacity values comparable with that of BC₁₀₀. But of all the composites IIR-MBN₁₅₀ composites attained the best results with an attenuation coefficient of 0.90 cm⁻¹ and HVL of 0.77 cm. The least OD value found was with this composite, corresponding to a value of 0.30 which falls far above that of lead shielder 0.17. The capacity of these fillers to offer opacity as revealed from the studies showed an order corresponding to decreasing surface activity, i.e., MBN>BN~BC. The ability of MBN to get adhered to host matrix accounts for its better performance.

References:

- [1]. H. Chen, M.M Rogalski ,J. N. Anker; Phys. Chem. Chem. Phys., **2012**, 14, 13469.
- [2]. W. S. Penn, Maclaren and Sons, Ltd, London; Synthetic. Rubber. Technol.,**1960**,1.
- [3]. W. J. Roff, J. R. Scott, J. Pacitti; Handbook of CommonPolymers, Butterworth & Co. Ltd., London,**1971**.
- [4]. P. A. Schweitzer;Corrosion Resistance of Elastomers, Marcel Dekker, Inc., New York **1990**,39.
- [5]. G. J. Van Amerongen;J. Polym. Sci., **1950**,5, 307.

.....*✍*.....

SUMMARY AND CONCLUSIONS

In recent decades researchers have been seeking new reinforcing fillers for elastomers, which are environment friendly, inexpensive and can act as reinforcement. Elastomeric composites with special properties are highly important owing to their flexibility and readiness to be transformed into any shape of choice, simple or complex. Barium sulphate is widely used as filler in polymer industry and it possesses two inherent characteristics that could be transferred to an elastomer matrix once filled within. Among its strengths, one is its inherent resistance to chemicals especially acids and other one is its ability to be rendered opaque to radiations. The former property depends basically on the polymer characteristics initially and can be enhanced by incorporation of barium sulphate, where as the latter property is solely imparted by the filler and varies depending on fillers particle size and modifications. In the realm of acid resistant linings and radio opaque shields flexibility is of prime importance and the traditional materials used are rigid lead based materials or lead filled composites at too heavy loadings. Owing to its high density resulting in massive materials the portability is tedious and linings are uncomfortable for real time applications. A survey of literature reveals that the reports on delicate elastomeric composites are scarce.

In the present work the reinforcement owing to incorporation of MBN and BN fillers is explored in elastomer matrices as natural rubber, EPDM and IIR. The nano fillers MBN and BN were incorporated into these matrices alone and in combinations with HAF-N330, to impart strength properties to the base polymer and to assess the formation of dual filler network. Enhancements in properties due to formation of dual networks were expected. Apart from nano

effect the influence of higher loadings of activated fillers on radiopacity and acid resistances also registered a significant output.

Nano barium sulphate was prepared in the presence of PVA and the prepared nano composites were modified using alcoholic solution of stearic acid. The surface treatment and size reduction were revealed from SEM, TEM morphologies and IR analysis. The prepared BN and MBN were used to fabricate composites based on elastomers NR, EPDM and IIR by proper compounding on a two roll mill followed by moulding.

Compared to BN, MBN was effective in increasing the cure rate. This was supported by cure kinetics studies and the cure reaction followed first order kinetics. The filler dispersions studies with all the matrices except IIR, revealed that MBN and BN got well dispersed in NR, EPDM matrices at lower loadings. At higher loadings agglomeration occurred. The tensile strength studies revealed that NR-MBN₂ system exhibited maximum reinforcement as far as mechanical properties were considered. The tensile strength registered an increment of 31 % in NR and in EPDM, same state of loading gave an increment of 35 % (i.e., in EPDM- MBN₂ system). For IIR composites though there is a marginal rise in tensile strength for 7.5 phr filled composites the effect is less pronounced. The compression set values were deteriorated with nano loading which is an expected result for elastomers with nano loading. The solvent resistance of these composites indicated that, the transport mode of toluene through NR and IIR followed strong deviation from Fickian mode, whereas in EPDM composites the mode lie close to Fickian mechanism, still it is anomalous. The uniform dispersion at lower loadings and agglomeration at higher ones were evidenced from SEM and AFM images.

Hybrid RNCs of all the elastomers were fabricated and amount of carbon black varied depending on the reinforcement offered by HAF-N330 in different matrices. The carbon black filled composites prepared were NR-CB40, EPDM-CB50 and IIR-CB55. The hybrid RNCs were prepared in order to assess the role of modified nano barium sulphate, MBN in improving the dispersion and in turn the mechanical properties of rubber-CB-MBN hybrid RNCs. The MBN loadings were varied in small levels from 0 to 15 phr and the base polymer had reduced carbon black filler level, the combinations used in various elastomers were NR-CB30 +MBN, EPDM-CB40+MBN, IIR-CB50+MBN.

This recipe was followed to assess the influence of MBN on incorporability of CB into matrix. The results reveal that in NR at a filler level of CB30+MBN₅ better mechanical properties were observed and the properties were superior to that of CB40 and CB30 alone systems. The solvent transport mode was anomalous, but the presence of dual filler network enhanced solvent resistances and diffusion reduced by about 40%. So 5phr MBN can successfully replace 10 phr black from NR, with superior mechanical properties and thermal stabilities as revealed from TGA and aging analysis. The Wolff's parameter and Lee's parameter evidenced enhanced dispersion of CB-MBN dual networks in NR.

In EPDM based composites EPDM-CB40 and EPDM-CB40+MBN were fabricated. It could be seen that the influence of dual filler networks on enhancing properties of EPDM is much more effective than the effect in NR, for EPDM being a weak matrix. CB40+MBN_{2.5} (40 phr carbon black and 2.5 phr MBN) showed enhancement in tensile properties by 42 %, 36 % superior to CB40, CB50 systems respectively. The dual networks could not enhance the properties like compression set. It could improve the thermal stability to a minor extent by improving the onset of degradation. Tmax values were left unchanged. The same result was reconfirmed in oven ageing as indicated by better retention

of properties. This filler loading CB40+MBN_{2.5} implemented the nano effect on EPDM-CB systems.

The IIR-CB-MBN filled systems failed to register a synergistic effect as far as the mechanical properties are concerned. Still a marginal increase in properties were observed for CB50-MBN_{7.5} system and is comparable with CB55 system. The synergistic influence of dual filler networks are implemented in IIR as an improvement in resistance to thermal aging and resistance to solvent transport. The transport mode in IIR composites followed a fickian pattern. Synergy in IIR is manifested as thermal and solvent resistances. The 2-D, 3-D AFM images supported the formation of dual network as indicated from minimal voids on surfaces in hybrid RNC's of all composites.

Application of barium sulphate in imparting acid resistance to an elastomer is significant as far as the need for application of rubber lining as passive fortification against plant protection is concerned. Elastomers offer an additional benefit of being flexible than the traditional lead sheets used as acid resistant linings.

NR is seldom used in contact with environment demanding corrosion protection against concentrated acids. Studies revealed that pure NR, can withstand only 150 hours of corrosion atmosphere with stability retained. The behaviour and retention of properties, in NR on ageing are revealed from SEM images. The mechanical strength showed 58 % retention in BN, MBN- RNCs over 150 hrs in 50 % acid, where as only 44 % of the strength is retained in unfilled system. There is drastic destruction of morphology in ageing and CB filled system lost 65 % of their strength in acid. The immersion tests also supported it and white composites even at lower loadings can fit well in acid concentrations of 50 %. Black composites but gets disintegrated readily.

The acid resistance studies on EPDM based RNCs revealed that in 60 % acid, the rubber exhibited anomalous behaviour. The behaviour when tracked indicated emergence of new functionalities in EPDM. For all the nano filled systems above 5phr, 60 % acid is the maximum acid strength that could be withstood by EPDM. Hybrid RNC's yielded to environment even at lower acid concentrations. The results were confirmed by immersion test results and IR, SEM analysis.

Butyl rubber based nanocomposites exhibited high degree of stability in acid upto 70 % concentration, with hybrid systems became unstable.

Barium sulphate can act as a replacement for Pb based materials in clinical X-ray field, since its K-edge is such that it screens radiations from 37 kVp to 60 kVp which is the normal energy range used for whole body X-ray imaging. Barium sulphate-natural rubber composites were produced on a laboratory scale, using unmodified and modified barium sulphate fillers having particle size in the nanometre range (BN and MBN). These natural polymer-eco-friendly filler based composites can be used as a non-Pb X-ray attenuator in the realm of medical X-ray examination. The radiopacity studies at the operating voltage range of medical X-rays (40-100 kVp) in the as prepared composites based on NR were carried out. The visibility of rubber samples under X-rays were satisfactory at thickness of 6mm and the elastomer composites exhibited maximum homogeneity in opacity at 40 kVp and 5 mAs. The optical density and half-value layer decreased with filler content, whereas the attenuation coefficient of the composites increased with filler loading. NR filled with all varieties of barium sulphate fillers exhibited better opacities at loadings under investigation. NR barium sulphate composites turned out to be a better opacifier on comparison with lead shield of 0.1mm thickness. All the elastomer composites having particles in the nanometre range, provided radiopacity higher than

composites with commercial fillers. The optical density measurements and hence the calculated attenuation coefficients were supported by radiographic image analyses. NR-MBN₅₀ had opacity values comparable with that of NR-BC₁₅₀ and the maximum value of attenuation coefficient-1.207cm⁻¹ and that of HVL-0.5741cm were obtained with NR-MBN₁₅₀. The ability of MBN to get adhered to the host matrix made it a better candidate as radiopaque filler compared to BN and BC. The inert BN, BC fillers which, rather bonded loosely to the matrix failed to impart superior properties to the host polymer.

Barium sulphate-EPDM composites were produced on a laboratory scale, using unmodified and modified barium sulphate fillers having particle size in the nanometre range (BN and MBN) and compared with commercial precipitated barium sulphate (BC). The optical density and HVL decreased with filler content, whereas the attenuation coefficient of the composites increased with filler loading. The results showed that the opacity highly depended on dispersion level of fillers assisted by modifier treatment. The dispersion level of the shielding phase in the elastomers improved with reduction of particle size of barium sulphate (BN, MBN) and X-ray shielding properties of all the composites apparently increased with increase in dispersion degree of filler in (MBN) composites. EPDM with all varieties of bariumsulphate fillers exhibited better opacities at loadings under investigation and turned out to be better opacifier in comparison with lead shield of 0.1mm thickness as seen from lower OD values. All the elastomer composites having particles in the nanometre range, provided radiopacity higher than composites with commercial fillers. EPDM-MBN₅₀ had opacity values comparable with that of BC₁₅₀. But of all the composites EPDM MBN₁₅₀ composites attained best results with an attenuation coefficient of 1.24cm⁻¹ and HVL of 0.56cm. The capacity of these fillers to offer opacity showed an order MBN>>BN>BC corresponding to decreasing surface activity. The radiographic results and mechanical properties revealed that, inspite of the dilution effect at higher filler levels, MBN filled elastomers due to their better

ability to get adhered to host matrix helped to provide higher effectiveness in opacity than inert BN, BC fillers which rather bonded loosely to the matrix and hence failed to impart such properties to the host polymer.

Barium sulphate-IIR composites were produced on a laboratory scale, using unmodified and modified barium sulphate fillers having particle size in the nanometre range (BN and MBN) and compared with commercial precipitated barium sulphate (BC). The elastomer composites exhibited better homogeneity in opacity at 40 kVp and 5mAs and opacity remained homogeneous only upto 60 kVp. The optical density and half-value layer decreased with filler content, whereas the attenuation coefficient of the composites increased with filler loading. The opacity of composites appears to be dependant on dispersion level of fillers to a small extent. The dispersion level of the shielding phase in the elastomers improved with reduction of particle size of barium sulphate (BN, MBN) imparting it better shielding properties. All the elastomer composites having particles in the nanometre range, provided radiopacity better than composites with commercial fillers. IIR-MBN₅₀ had opacity values comparable with that of BC₁₀₀. But of all the composites IIR-MBN₁₅₀ composites attained the best results with an attenuation coefficient of 0.90 cm⁻¹ and HVL of 0.77cm. The least OD value found was with this composite, corresponding to a value of 0.30 which falls far above that of lead shielder 0.17. The capacity of these fillers to offer opacity as revealed from the studies showed an order corresponding to decreasing surface activity, i.e., MBN>BN~BC. The ability of MBN to get adhered to host matrix accounts for its better performance.

Future prospects of these studies involves, fabrication of nanocomposites based on other synthetic rubbers. Various intrusive phenomena taking place at the inter phase of the polymer and filler, polymer-polymer and filler-filler interfacial areas need to be revealed clearly. The synergism of these fillers with carbon black have been revealed, much light could be shed on synergy between silica and nano BN, MBN. There is ample scope for carrying out the possibility

of its application in real time X-ray shields and prepare a high range combination of elastomers and opacifiers to use as shields to X-rays, apart from barium sulphate. Possibilities also exist in using MBN as a component of X-ray shields using mixture of opacifiers to scan entire region of disastrous X-rays. The highlights of the results and the composites exhibiting the best properties are summarised in table 9.1 below.

Table 9.1: Summary of Highlights in the Conclusions derived.

Matrix	NR	EPDM	IIR
<i>Nanocomposite exhibiting superior strength and thermal properties</i>	MBN ₂	MBN ₂	MBN _{7,5}
<i>Hybrid RNC vs. CB RCs exhibiting superior strength and thermal properties</i>	CB30+MBN ₅	CB40+MBN _{2,5}	CB50+MBN _{7,5}
<i>Solvent transport in hybrid RNC's</i>	40 % enhanced Solvent resistance'; Anomalous solvent transport	45 % enhanced Solvent resistance; Anomalous solvent transport	23% enhanced Solvent resistance; Fickian transport
<i>Acid resistance</i>	RNC's good to with stand 50 % H ₂ SO ₄ /Hybrid RNCs destabilised in 25 % acid	RNC's good to with stand 60 % H ₂ SO ₄ /Hybrid RNCs destabilised in 50 % acid	RNC's good to with stand 75 % H ₂ SO ₄ /Hybrid RNCs destabilised in 60 % acid
<i>Radiopacity</i>	NR-MBN150 best opacifier of NR-RNCs	EPDM-MBN150 best elastomer opacifier	IIR-MBN150 best of IIR-RNCs but poor elastomer opacifier
<i>OD compared with OD=0.17 of Pb</i>	0.1490<0.17 ;better opacifier than Pb	0.1390<0.17 ;best opacifier than Pb	0.2990>0.17 ;poor opacifier than Pb
<i>HVL</i>	0.5741	0.5601	0.7661

.....*✂*.....

Abbreviations and Symbols

ASTM	American Society for Testing and Materials
BaSO ₄	Barium sulphate
CaCO ₃	Calcium carbonate
CNT	Carbon nano tube
CS	Crystallite size
DNA	Deoxy ribonucleic acid
TiO ₂	Titanium dioxide
CVD	Chemical Vapour Deposition
DMA	Dynamic Mechanical Analysis
DSC	Differential Scanning Calorimetry
FTIR	Fourier Transform Infrared
PVA	Polyvinyl alcohol
SEM	Scanning Electron Microscopy
EDAX	Energy dispersive X ray analysis
SWNT	Single walled carbon nanotube
TGA	Thermo gravimetric analysis
ZnO	Zinc oxide
ACN	Acrylonitrile content
AFM	Atomic Force Microscopy
BR	Butadiene rubber
B-IIR	Bromobutyl rubber
CB	Carbon black
CPE	Chlorinated polyethylene
CR	Chloroprene rubber
CRI	Cure Rate Index
DBP	Dibutyl phthalate
DTG	Derivative thermogravimetry
EM	Electron Microscopy
ENR	Epoxidised natural rubber
EPDM	Ethylene propylene diene monomer
EPR	Ethylene propylene rubber
EV	Efficient vulcanization
HAF	High abrasion furnace
IIR	Isoprene isobutylene rubber

IR	Infrared spectroscopy
ISAF	Intermediate super abrasion furnace
M100	Modulus at 100% elongation
MA	Maleic anhydride
MA-g-EPDM	Maleic anhydride-grafted -EPDM
MBTS	Mercaptobenzothiazyl disulphide
MWCNT	Multi walled carbon nanotubes
NBR	Nitrile rubber
NMR	Nuclear Magnetic Resonance
NR	Natural Rubber
PEO	Poly (ethylene oxide)
phr	Parts per hundred rubber
PUR	Polyurethane rubber
SAXS	Small-angle X-ray Scattering
SBR	Styrene-butadiene rubber
SEM	Scanning Electron Microscopy
SMR L	Standard Malaysian rubber latex
SRF	Semi reinforcing furnace
TEM	Transmission Electron Microscopy
TS	Tensile strength
XNBR	Carboxylated nitrile rubber
XSBR	Carboxylated styrene-co-butadiene rubber
ENB	5-Ethylidene-2-norbornene
HD	1, 4-Hexadiene
DCPD	Dicyclopentadiene
MBT	Mercaptobenzothiazole
DPG	Diphenyl guanidine
FKM	Fluoroelastomers
PTFE	Polytetrafluoroethylene
CCl ₄	Carbon tetrachloride
HF	Hydrogen fluoride
Ca(OH) ₂	Calcium hydroxide
PbO ₂	Litharge (Lead oxide)
MT	Medium thermal
SiC	Silicon carbide
GC	Gas chromatography

SANS	Small-angle neutron scattering
IBR	Isoprene–butadiene rubber
ISAF	Intermediate super abrasion furnace black
D	Diffusivity
TS	Tensile strength
CFCs	Chlorofluorocarbons
CO	Carbon monoxide
UV	Ultraviolet
MU	Mooney unit
ATH	Aluminium hydroxide
CBS	N-Cyclohexyl-2-benzothiazolesulfenamide
TMTD	Tetramethylthiuram disulfide
ZDEC	Zinc diethyldithiocarbamate
VGC	Viscosity gravity constant
CaO	Calcium oxide
PEG	Polyethylene glycol
ADC	Azodicarbonamide
MEK	Methyl ethyl ketone
RPA	Rubber Process Analyser
EB	Elongation at break
RF	Radio frequency
MPa	Mega pascal
ML	Mooney viscosity -large rotor
SE	Shielding effectiveness
XRD	X-ray diffraction analysis
POSS	Polyhedral oligomeric silsesquioxane
E	Apparent degradation activation energy
dB	Decibels
R	Universal gas constant
%	Percentage
ΔT	Temperature change
Pa	Giga Pascal
kJ/mol	Kilo Joule per mole
mm/min	Milli meter per minute
kJ/mol	Kilo Joule per mole
N/mm ²	Newton per millimetre square

cm	Centimeter
cm ⁻¹	Centimeter inverse
cm ³	Centimeter cube
μm	Micrometer
Mw	Molecular weight
MPa	Mega Pascal
m ² g ⁻¹	Meter square gram inverse
nm	Nanometer
T _g	Glass transition temperature
wt %	Weight percentage
°C	Degree Celsius
ΔG _{mix}	Gibb's free energy of mixing
ΔH _{mix}	Enthalpy of mixing
ΔS _{mix}	Entropy of mixing
T	Absolute temperature
δ	Solubility parameter of the polymer
χ'	Interaction parameter
D _{min}	Minimum torque
D _{max}	Maximum torque
T ₁₀	Scorch time
T ₉₀	Optimum cure time
G'	Storage modulus
G''	Loss modulus
G*	Complex modulus
V _r	Volume fraction of rubber
M _s	Mass of solvent sorbed
M	Molar mass of solvent
M _p	Mass of polymer
Q	Ratio of swollen weight to original weight
W ₁	Weight of the sample before swelling
W ₂	Weight of the sample after swelling
M _c	Number-average molecular weight between crosslinks
F	Weight fraction of insoluble components
A ₀	Weight of the absorbed solvent corrected for the Swelling increment

ρ_r	Density of rubber
ρ_s	Density of the solvent
GHz	Gega hertz
α	Decomposed fraction
η_r	Relative viscosity
M_r	Relative modulus
m_f	Mass of filler in the compound
α_f	Specific constant for the filler
T_i	Onset degradation temperature
$T_{-5\%}$	50% weight loss temperature
$T_{-50\%}$	5% weight loss temperature
r	Correlation coefficient
S/cm	Siemens per centimeter
' λ '	Wavelength of X ray
' β '	Full width at half maximum of diffraction peak (FWHM)
' Θ '	Angle corresponding to the peak
d	Average size of crystallites
π	pi
MBN	Organically modified nano barium sulphate
BN	Unmodified nano barium sulphate
BC	Commercial barium sulphate
RC	Rubber composites
RNC	Rubber nanocomposites
μ	Linear attenuation coefficient
OD	Optical density
HVL	Half-value layer
mAs	milli ampere seconds
Gd(AA) ₃	Gadolinium acrylate
kVp	kilo volt potential
keV	kilo electron volts

List of Publications

Journal Publications

1. **Nisha Nandakumar**, Philip Kurian; “Chemosynthesis of Monodispersed Porous BaSO₄ Nano-Powder by Polymeric Template Process and its Characterisation” *Powder Technology*, Volume 224, 2012, p51-56.
2. **Nisha Nandakumar**, Philip Kurian; “Effect of Chemical degradation on the Mechanical properties of Ethylene-propylene-diene (5-ethylidene-2-norbornene) terpolymer-BaSO₄ Nanocomposites” *Materials & Design*, Volume 43, 2013, p 118-124.
3. **Nisha Nandakumar**, Philip Kurian; “Natural rubber as X-ray attenuator for Clinical x-rays: Analysis of Radiopacity in Natural rubber-Nano Bariumsulphate based Composites for Medical applications”. *Journal of Materials Chemistry B*, (under review).
4. Ajalesh B Nair, **Nisha Nandakumar** and Rani Joseph; Ethylene-propylene-diene (5-ethylidene-2-norbornene) terpolymer/aluminium hydroxide nanocomposites: Thermal, mechanical and flame retardant characteristics. *Composites Part B: Engineering* (under review)
5. **Nisha Nandakumar**, Philip Kurian; “Synergistic effect of Nano Bariumsulphate-Carbonblack Hybrid Filler networks in Ethylene propylene diene Rubber” *Journal of Applied Polymer Science* (to be communicated)
6. **Nisha Nandakumar**, Philip Kurian; “Degradation of Natural and Synthetic polymers in Artificial Acidic environment and Influence of Acid on Mechanical properties and Morphological characteristics” (to be communicated)

Conference papers

1. **Nisha Nandakumar**, Philip Kurian; “Eco-friendly Nanofilled Natural polymer as Novel X-ray shields for Clinical X-rays” International Seminar on New Horizons in Chemistry, Saint Josephs college Irinjalakuda, Thrissur Sep. 2013.
2. **Nisha Nandakumar**, Philip Kurian; “Effect of Carbonblack and Bariumsulphate on the Thermo-chemical resistance of Natural rubber Composites” International Rubber Conference, Kovalam, Trivandrum Oct. 2012

3. **NishaNandakumar**, PhilipKurian; “Synergistic effect of Carbonblack and BaSO₄ on Properties of Natural rubber Composites” Scientia-2012, NSAP, Mahathma Gandhi University College of Engineering, Muttom, Thodupuzha, Idukki Sep. 2012. (*best Paper award*)
4. **NishaNandakumar**, PhilipKurian; “Durability of Naturalrubber - Bariumsulfate Composites exposed to Acidic environment”, National Seminar on Emerging trends In Nanotechnology, B.K.College for Women, Amalagiri, Kottayam-Sep. 2011.
5. **NishaNandakumar**, PhilipKurian; “Investigation of acid sorption characteristics in EPDM- BaSO₄ Nano composites” International conference on Advances in Polymer Technology, PS&RT, Cochin University of Science and Technology, Kerala-Feb.2010.
6. **NishaNandakumar**, PhilipKurian; “Influence of Nano heavy metal sulphate on mechanical properties and swelling characteristics of EPDM composites” Advancements in Polymeric Materials, CIPET Bhubaneswar-Feb.2010.
7. **NishaNandakumar**, PhilipKurian; “Synthesis of Spheroidal BaSO₄ Nano particles and its Characterisation.” National Seminar on Quantum Chemistry and Nano Techniques - SNM College Maliankara, Ernakulum Nov. 2009.
8. **NishaNandakumar**, Binsy.V; “Studies of Surface acid properties of Mixed ligand Complexes of Cobalt(II), Nickel (II), Copper(II), Heterogenised over Zirconia” National Seminar on Advancements in Chemistry”, Mercy College Palakkad-Dec.2008.

.....❧.....